CIVIL ENGINEERING STUDIES
Structural Research Series No. 581

UILU-ENG-93-2004

ISSN: 0069-4274

SEISMIC RESPONSE OF TILT-UP CONSTRUCTION

By

James W. Carter III
Neil M. Hawkins
and
Sharon L. Wood

A Report to the
National Science Foundation
Research Grant BCS 91-20281

Department of Civil Engineering
University of Illinois at Urbana-Champaign
Urbana, Illinois

December 1993

50272-101

REPORT DOCUMENTATION PAGE	1. REPORT NO. UILU-ENG-93-2004	2.	3. Recipient's Accession No. -

4. Title and Subtitle

Seismic Response of Tilt-Up Construction

5. Report Date
December 1993

6.

7. Author(s)

James W. Carter III, Neil M. Hawkins, and Sharon L. Wood

8. Performing Organization Report No.
SRS 581

9. Performing Organization Name and Address

University of Illinois at Urbana-Champaign
Department of Civil Engineering
205 North Mathews Avenue
Urbana, Illinois 61801

10. Project/Task/Work Unit No.

11. Contract(C) or Grant(G) No.
BCS 91-20281

12. Sponsoring Organization Name and Address

National Science Foundation
4201 Wilson Boulevard, Room 545
Arlington, Virginia 22230

13. Type of Report & Period Covered

14.

15. Supplementary Notes

16. Abstract (Limit: 200 words)

Tilt-up construction is an economical method of constructing low-rise industrial and commercial buildings. However, the structures are susceptible to seismic damage. The seismic response of tilt-up construction is reviewed in this report. Construction techniques are described, design procedures are summarized, the results of previous experimental and analytical research are compared, and observed damage during recent earthquakes is discussed. The measured response of three tilt-up buildings in California is also presented.

17. Document Analysis a. Descriptors

Low-Rise Buildings, Precast Concrete Wall Panels, Roof Diaphragms, Connections, Earthquakes, Design Provisions, Observed Damage, Measured Seismic Response

b. Identifiers/Open-Ended Terms

c. COSATI Field/Group

18. Availability Statement	19. Security Class (This Report) UNCLASSIFIED	21. No. of Pages 224
—	20. Security Class (This Page) UNCLASSIFIED	22. Price

(See ANSI-Z39.18)

OPTIONAL FORM 272 (4-77)
Department of Commerce

SEISMIC RESPONSE OF TILT–UP CONSTRUCTION

LIST OF TABLES

LIST OF FIGURES

1. INTRODUCTION

Tilt–up construction is an efficient and economic method for constructing low–rise structures which has become popular throughout the United States. Wall panels in tilt–up structures are cast horizontally at the construction site, rather than in a prefabrication plant or on–site in vertical forms. Tilt–up construction derives its name from the process of "tilting" the wall panels up into their final vertical position. Once in place, the panels are connected to one another using pilasters, steel plates, or splicing "chord" steel at the roof level, so as to form a structurally continuous wall system. The panels are then connected to the foundation using cast–in–place "dowel–type" connections [80]. Finally, the roof is attached to the walls through ledger beams attached to the panels.

Tilt–up construction offers certain advantages to contractors when compared with conventional cast–in–place walls or precast wall sections shipped to the site [3]. Tilt–up walls are usually cast horizontally on the floor slab, therefore, form costs are low only the edges of the wall need to be formed. Further, both compaction of the concrete and preparation of special surface finishes are easier when panels cast horizontally rather than vertically. Also, transportation costs and restrictions on panel size and configuration due to vehicle limitations are virtually eliminated when the panels are cast on site [70]. Generally, tilt–up walls are only handled once (when they are tilted into place) during the construction process [30]. Consequently there is less chance of damage to a tilt–up wall panel, as compared to the use of conventional precast elements, which must be handled at least twice. Tilt–up panels can also function as shear walls [70] thereby eliminating the need for perimeter bracing and reducing overall building costs.

There are, however, several distinct disadvantages to tilt–up construction. Some of its constructibility advantages are lost if the structure is located on a relatively confined site. Operations are difficult if the area of the floor slab that is free of utilities and can be used to cast panels is less than 6,000 ft^2, or if the width of the building is less than 50 ft. Generally it is not cost–effective to construct these small structures using tilt–up panels [31]. Uncongested, non–urban sites are desirable for tilt–up construction because adequate room is needed for casting the panels and to allow movement of the crane used to erect the panels.

Tilt–up construction is cost–effective if a proposed building is one– to two–stories in height and has a relatively simple configuration (meaning the structure is built with perpendicular corners and has large–area offsets, if offsets are desired). Examples of simple configurations are structures with rectangular, L–shaped, or H–shaped plan geometries. Structures with small–area offsets, although favored for aesthetic reasons, may increase the cost significantly and can lead to less reliable seismic response calculations.

1.1 Past Seismic Performance

During the 1964 Alaska earthquake and the 1971 San Fernando earthquake, typical damage in tilt–up structures included partial collapse of roof sections due to failure of the panel–to–roof connections and collapse of wall panels following failure of the panel–to–roof and panel–to–panel connections [32,41,55]. As a consequence of the structural behavior during those earthquakes, building code provisions were revised in an effort to improve the seismic performance of tilt–up construction [75,76,77]. The response of tilt–up construction during the 1987 Whittier Narrows and 1989 Loma Prieta earthquakes showed that some improvements had been achieved. However, the degree of damage to some tilt–up buildings in the 1987 and 1989 earthquakes was still unacceptable [10,35,69].

The seismic performance of tilt–up construction is closely linked to the connection details. The designer of tilt–up structures is faced with a difficult task of detailing each connection to provide the stiffness required to resist service loads within permissible deflection limits while also ensuring that each connection has sufficient ductility, energy–dissipation capacity, and stability to survive seismic loads. The connections must also accommodate the expansion and contraction of structural elements due to temperature, creep, and shrinkage [21].

1.2 Research Needs

In the two decades since the San Fernando earthquake, considerable efforts have been made to improve the seismic performance of tilt–up construction. Building code provisions have been revised [63]; lateral–load tests on slender walls have been performed [52] and the results led to the adoption of new design procedures for tilt–up wall panels [5]; in–plane bending tests have been conducted on a variety of diaphragms representing typical roof construction [1,23,43,44,45,72,74]; analytical models have been developed to calculate the overall response of tilt–up structures to seismic loadings [1,4,6,7,8,12,53,54]; and isolated tilt–up panels have been subjected to simulated earthquake loading [6,7,28]. The results of these investigations have led to an improved understanding of the behavior of tilt–up structures during strong ground motion.

However, the performance of tilt–up construction in recent earthquakes demonstrates that additional research is needed if seismic damage is to be reduced to acceptable levels. There have been no tests of complete tilt–up systems and attempts to validate analytical models of tilt–up construction using the measured response of buildings during recent earthquakes have been limited. Physical testing has consisted only of tests on single panels and isolated diaphragms. There have been few tests to measure the capacity and ductility of typical connections used in tilt–up buildings. Finally, there are a large number of existing tilt–up structures that have details which do not satisfy current building code regulations. Repair and rehabilitation procedures must be developed to reduce the seismic vulnerability of these structures.

1.3 Objective and Scope

This report is intended to summarize existing information about the seismic performance of tilt–up construction. The scope of the report is limited to traditional, tilt–up structures in which concrete wall panels are cast horizontally. No attempt is made to interpret the response of tilt–up frame structures.

This report is divided into seven chapters. Chapter 2 describes the influence of construction techniques on the design of tilt–up structures. Design considerations for the wall panels, the roof diaphragm, and the critical connections used in tilt–up construction are discussed in Chapter 3. In Chapter 4, the results of previous experimental tests of tilt–up wall panels and roof diaphragms, and previous analytical studies are summarized. Acceleration histories recorded during recent earthquakes measured in three tilt–up buildings in California are evaluated in Chapter 5. Chapter 6 summarizes the damage observed in tilt–up structures following the 1964 Alaska, the 1971 San Fernando, the 1987 Whittier Narrows, and the 1989 Loma Prieta earthquakes. Results are summarized in Chapter 7.

1.4 Acknowledgements

This report was completed with the assistance of graduate students Gregory J. Lakota and Fernando S. Fonseca. Funding for this study was provided by the National Science Foundation, under Grant BCS–9120281, for which the cognizant NSF program official was Dr. Henry J. Lagorio and subsequently is Dr. M.P. Singh. Opinions and findings expressed in this report do not necessarily reflect those of the sponsor.

2. CONSTRUCTION OF TILT–UP STRUCTURES

Most important developments related to the design and construction of tilt–up structures may be traced to innovations in the field. Tilt–up was first used in the early 1900's as an efficient method for fabricating durable concrete wall panels used in military structures [13]. Contractors found that the quality of concrete panels cast horizontally and tilted into place exceeded that of traditional cast–in–place walls. Until the 1960's, tilt–up construction was used almost exclusively for one and two–story warehouses and industrial structures where economical, quick construction was emphasized [24]. During the past 30 years, increased attention has been placed on aesthetics, and the uses for tilt–up structures now include office buildings, shopping centers, and other commercial buildings. Construction techniques have been continually refined as the market for tilt–up structures has continued to expand.

Typical techniques for fabricating and erecting the tilt–up wall panels and roof diaphragms are reviewed briefly in the following sections. The influence of these construction techniques on the design of tilt–up structures is also discussed.

2.1 Wall Panel Construction

Knowledge of fabrication and erection techniques for tilt–up panels is required to proportion the panels effectively. Although the panel height is determined by the architect, panel weight, and therefore width and thickness, is often limited by the capacity of the crane used during construction. Stresses induced in the panels during lifting must also be considered during design [79]. Cables are attached to connections cast in the wall panels at the pick points (Fig. 2.1) and used by the crane to lift the panels from a horizontal to a vertical position. Improper placement of the pick point can result in extensive cracking of the panel during tilting.

Other factors considered in design include panel fabrication, positioning of the crane at the site, and the lifting schedule. The proposed building floor plan, panel dimensions, and the architectural treatments to the exterior panel surface must be considered to ensure that panel fabrication and erection are completed efficiently and economically [46]. For example, the outside face of the wall panels is typically cast against the floor slab. The crane is then attached to the inside face of the panel and the panels are positioned from inside the building (except when erecting the last few panels) [46]. This procedure prevents excessive head swing from the top of the panel and provides excellent traction for the crane when it operates on the floor slab (Fig. 2.2). Hence, the panel erection process influences the proportioning and fabrication of the wall panels and the design of the building foundation.

Special attention must be paid to the design of concrete panels. Variations in width should be minimized and attention paid to large openings in order to ensure structural integrity and maintain serviceability after the panels have been lifted into place [10,35,78]. The openings should be located so as not to interfere with

the load path within the panel (Fig. 2.3). It is desirable that openings be placed so as not to intercept panel joints (Fig. 2.4), because differential movements between panels can cause doors to stick or windows to break [78]. However, piers must be of sufficient size to resist shear forces, and an arrangement with panel joints through the openings may be more desirable based on strength considerations.

Care must also be taken to ensure the serviceability of connections within the structure. Roof framing members should not be connected to the walls at the panel–to–panel joints in order to accommodate thermal expansion of the panels (Fig. 2.5) [78]. Thermal effects are an important consideration for panel–to–panel connections, because very stiff connections can cause cracking and eventual degradation of the panels [78].

2.2 Roof Construction

Roof construction for tilt–up and other low–rise buildings consists of the assembly of three structural elements: the framing members, the roof skin, and the fasteners. In the interest of minimizing project costs, roofs are usually constructed to serve both as an outer protective covering for the building and as a structural diaphragm to resist lateral loads. Wood and steel are often used as the roofing elements in tilt–up buildings, with plywood–sheathed roofs being the most common form of roof construction in the western U.S. (Fig. 2.6). Metal deck roofs are often used in the eastern U.S.

Building performance is often directly related to the choice of fasteners in the roof system [57]. Because vertical loads on the roof of a typical low–rise building are relatively small compared with lateral loads from wind or earthquakes, the capacity of the roof is proportional to the amount, distribution, and shearing resistance of the fasteners.

2.2.1 Wood Diaphragms

A typical plan view of a plywood diaphragm is shown in Fig. 2.7. Glued–laminated (glulam) beams run in the transverse direction of the building and are connected to the tilt–up wall panels and interior columns. Sawn purlins span between the glulam beams, and are overlain by a skin of plywood. Nails are used to connect the structural members.

Wood roofs designed to resist large lateral loads should be constructed as blocked rather than unblocked systems [33]. In a blocked roof, framing members are located around the entire perimeter of each 4x8–ft plywood panel in the roof diaphragm (Fig. 2.8) [57]. Blocking prevents buckling of the plywood under lateral loads. The shear capacity of a blocked roof is 1.5 to 2 times the strength of a similar unblocked diaphragm [57]. However, if the design shears are low, which might occur if the proposed building is not designed to resist earthquake loads, an unblocked diaphragm is probably the most cost efficient choice.

Panelized roof systems are often used to minimize the cost of constructing a wood diaphragm. Panel sections are fabricated on the ground from purlins and blocking members overlain with sheets of plywood

(Fig. 2.9). The grids are then lifted into position and connected to glulam beams and purlins already in place. Speed of construction is the primary advantage of this technique: an experienced crew of five workers can fabricate up to 20,000 ft^2 per day [33].

2.2.2 Metal Deck Diaphragms

Truss girders and steel joists typically serve as the main structural members in metal deck diaphragms (Fig. 2.10). Where shear is transferred from the diaphragm to the walls, a perimeter steel angle ledger is typically used as a shear collector, as shown in Section A–A of Fig. 2.10. In situations where diaphragm–to–wall connections are embedded steel plates or steel framing members, typical connections are as shown in Sections B–B, C–C, and D–D. The metal decking typically consists of ribbed members that are either puddle–welded, screw fastened, or pin–attached to the framing members.

Similarly to blocking in a wood diaphragm, buckling of the roof skin is prevented by installing channel or Z– or C–type metal deck members transverse to the ribs at each panel end (Fig. 2.11). Metal decking is typically 20–ft long and spans 2 to 3 joists. Therefore, placing these "blocking" elements every second or third joist provides a mechanism for transferring large shears within the diaphragm.

2.2.3 Composite Diaphragms

Composite diaphragms usually comprise a metal deck diaphragm, as discussed in Section 2.2.2, overlaid with a layer of concrete. The concrete fill acts as a global buckling mechanism for the metal deck diaphragm skeleton.

3. DESIGN OF TILT–UP STRUCTURES TO RESIST LATERAL LOADS

During design, the wall panels located around the perimeter of tilt–up buildings are typically assumed to form a box which resists the horizontal and vertical loads. The use of load–carrying members around the perimeter of the structure increases the available area in the building by eliminating the need for internal bracing. When a uniformly distributed horizontal load is applied at the roof level, the roof diaphragm acts as a deep beam (Fig. 3.1): the interior roofing members represent the web and the perimeter chords represent the flanges (members BF and CG in Fig. 3.1). Similarly to a plate girder, the diaphragm web is designed to resist the in–plane shear forces and the flanges are proportioned to resist the axial forces developed due to bending [3].

Shear forces developed in the diaphragm are transferred to the end walls and are then carried as horizontal shear into the foundation. Chord reinforcement, located in the panels at the elevation of the diaphragm or in the edge of the diaphragm itself, restrains the out–of–plane deflections of the tilt–up panels which result from the in–plane deformations of the diaphragm.

Tilt–up systems represent an economical alternative to metal–clad or masonry buildings in the competitive environment of low–rise commercial and industrial structures. In order to reduce the total cost of a building, the effort spent on design of tilt–up systems is usually minimized [15]. Maximum advantage is taken of standardized design procedures and minimum building code requirements. Although this approach provides a quick and inexpensive method for proportioning tilt–up wall systems, it is only reliable for regular, rectangular buildings with few openings in the wall panels or offsets in the perimeter. More sophisticated analytical methods may be required for the design of buildings with irregular geometries.

Design of a tilt–up system involves the proportioning of three components: the tilt–up wall panels, the horizontal diaphragm, and the primary connections (those between the wall panels and the diaphragm, between adjacent wall panels, and between the wall panels and the foundation). Methods used to design these structural elements and factors affecting component performance are discussed in the following sections.

3.1 Wall Panels

The provisions of the Uniform Building Code [77] govern the design of tilt–up wall panels in most regions of high seismicity in the U.S. Panels must have sufficient strength to resist moments and axial forces due to the factored vertical and lateral loads, and must have sufficient stiffness to control deflections under service loads. Because slender walls may develop significant out–of–plane deflections, P–Δ moments must be considered when evaluating both panel strength and stiffness.

Individual wall panels are typically modelled as uniformly–loaded, simply–supported beams (Fig. 3.2). The midspan deflections corresponding to the cracking moment, Δ_{cr}, and nominal flexural capacity, Δ_n, may be approximated as:

$$\Delta_{cr} = \frac{5\ M_{cr}\ h^2}{48\ E_c\ I_g} \tag{3.1}$$

$$\Delta_n = \frac{5\ M_n\ h^2}{48\ E_c\ I_{cr}} \tag{3.2}$$

where M_{cr} is the cracking moment of the panel, M_n is the nominal flexural capacity of panel, h is the distance between supports, E_c is Young's modulus for concrete, I_g is the moment of inertia corresponding to gross sections, and I_{cr} is the moment of inertia corresponding to fully cracked sections.

The UBC limits midspan deflections under service loads, Δ_s, to [77]:

$$\Delta_s \leq \frac{h}{150} \tag{3.3}$$

where Δ_s is calculated assuming a linear variation of displacement between the cracking moment and the nominal capacity:

$$\Delta_s = \Delta_{cr} + \frac{(\ M_s - M_{cr}\ )}{(\ M_n - M_{cr}\ )}\ (\ \Delta_n - \Delta_{cr}\ ) \tag{3.4}$$

where M_s is the maximum moment in the wall under service loads.

Typically, the provisions of UBC Section 2336 are used to determine the design lateral forces for the wall panels. The specified lateral force for design is [77]:

$$F_p = Z\ I\ C_p\ W_p \tag{3.5}$$

where F_p is the lateral force resisted by the panel, Z is the seismic zone factor, I is the importance factor, C_p is defined as 0.75 for exterior walls, and W_p is the weight of the panel. For a building located in seismic zone 4 with an importance factor of 1, the design lateral force is equal to 30% of the panel weight.

The UBC design procedure [77] is based on the results of a series of lateral load tests conducted by the ACI–SEASC Task Committee on Slender Walls [16]. Twelve tilt–up wall panels, with slenderness ratios ranging from 30 to 60, were tested during this investigation. The test configuration is shown in Fig. 3.3. The Task Committee found that previous design procedures [81], which assumed that the entire wall panel was fully cracked, overestimated mid–panel deflections. An iterative approach for estimating deflections was proposed where the panel midspan deflection is calculated using Eq. 3.6 based on the magnitude of the midspan moment under service loads and the midspan moment is determined using Eq. 3.7 which includes the influence of P–Δ effects (Fig. 3.4).

$$\Delta = \begin{cases} \dfrac{5\,M\,h^2}{48\,E_c\,I_g} & M < M_{cr} \\ \dfrac{5\,M_{cr}\,h^2}{48\,E_c\,I_g} + \dfrac{5\,(M - M_{cr})\,h^2}{48\,E_c\,I_{cr}} & M_{cr} < M < M_y \end{cases} \tag{3.6}$$

$$M = \frac{w\,h^2}{8} + \frac{P_p\,\Delta}{2} + P_o\,\Delta + \frac{P_o\,e}{2} \tag{3.7}$$

where w is the lateral load, Δ is the midspan deflection, M is the midspan moment, M_y is the yield moment for the panel, P_p is the weight of the panel, P_o is the applied vertical load at the top of the panel, and e is the eccentricity of the applied load, P_o.

The design procedures in the UBC and Task Committee report are based on the following assumptions:

- A wall panel behaves as a uniformly–loaded, simply–supported member: maximum moments and deflections occur at midspan and the horizontal displacement of the top of the panel relative to the base is ignored.
- The panel cross–section is constant over the height of the panel.

Many common tilt–up structural configurations do not satisfy the conditions implied in the design procedures. Under seismic loading, the roof of a tilt–up structure moves relative to the base violating the assumed simply–supported boundary conditions, concentrated loads are transferred to the panel at intermediate points along the panel height in buildings with multiple stories, and panels are frequently cast with large openings causing variations in the moment of inertia over the height of the panel. Proportioning of panels with openings for seismic loads appears to be the most important of these concerns. Damage was observed in panels with openings following the 1987 Whittier Narrows [10,35] and 1989 Loma Prieta [69] earthquakes.

3.2 Diaphragms

A diaphragm transfers lateral forces from one lateral–load resisting system to another. In the process of transferring these forces, the energy dissipated by the flexible diaphragm can reduce the magnitude of the forces that the other structural elements must resist. In tilt–up structures the roof is typically the primary diaphragm, however, vertical diaphragms, such as those used to subdivide the structure or to compensate for wall offsets, may also be found in tilt–up construction. In the following sections, emphasis is placed on horizontal diaphragms.

Horizontal diaphragms in tilt–up structures are typically designed to be flexible and may sustain sizeable in–plane deformations when subjected to lateral loads. As shown in Fig. 3.1, the horizontal shear developed in the diaphragm is resisted by the transverse walls which must transfer that shear to the foundations. Continu-

ity within the diaphragm and between the diaphragm and the transverse wall is dependent upon the strength and deformation capacity of various connections. Four general criteria must be satisfied [73]:

- Connections between adjacent sections of the roof (e.g. BIKC and IJLK in Fig. 3.1) must restrain relative horizontal deflections.
- Connections between the roof framing members and the diaphragm skin must prevent buckling of the skin.
- Connections between the diaphragm and the lateral–load resisting walls must be sufficient to transfer the diaphragm shear (e.g. connection between roof panel BIKC and wall panel ABCD in Fig. 3.1).
- Connections between the sections of the diaphragm and the diaphragm chord (e.g. chords BF and CG in Fig. 3.1) must be sufficient to transfer the shear resulting from out–of–plane bending of the longitudinal wall panels.

Connection details vary depending upon the materials used to construct the diaphragm. Factors influencing the design and behavior of wood and metal–deck diaphragms are discussed in the following sections. Metal–deck diaphragms generally provide more stability, stiffness, and resistance to environmental effects than wood diaphragms. Experience has shown that panel–to–roof connections in tilt–up structures with metal deck diaphragms perform better under severe loading than panel–to–roof connections in tilt–up structures with plywood diaphragms. However, connections between roof elements in a metal deck do not perform as well as those in plywood diaphragms under the same conditions. Regardless of connector performance, the materials used for diaphragm construction are usually chosen to minimize the initial cost of construction.

3.2.1 Diaphragm Strength and Stiffness

The distribution of forces from the diaphragm to the tilt–up wall panels depends on the stiffness of the diaphragm [3]. As shown in Fig. 3.5(a), forces are distributed in proportion to the tributary area supported by the wall panels in buildings with flexible diaphragms. In contrast, forces are distributed in proportion to the relative stiffness of the wall panels (Fig. 3.5(b)) in buildings with rigid diaphragms. ACI Committee 551 [3] classifies diaphragms according to the shear stiffness (Table 3.2) and reports that most plywood and metal–deck diaphragms may be considered to be semi–flexible (Fig. 3.5(a)). Composite and concrete diaphragms are typically semi–rigid or rigid (Fig. 3.5(b)).

According to one school of thought, a rigid diaphragm is beneficial for lateral–load resistance because the out–of–plane deflections in the wall panels are reduced [42,50,73]. However, flexible diaphragms and flexible roof–to–wall connections provide a mechanism for energy dissipation which reduces the magnitude of the forces transmitted to the perimeter walls [71].

(a) Wood Diaphragms

Historically, plywood diaphragms have been the most common type of diaphragm used in tilt–up construction on the West Coast. The allowable shear strength of various plywood diaphragm configurations is summarized in Table 3.1 [77]. The results of monotonic experimental tests [23,43,44,45,72,74] sponsored by the American Plywood Association in the 1950's and 60's form the basis for these design provisions. The nominal shear strength of plywood diaphragms is typically 3 to 4 times the allowable shear stress for design [57].

The UBC requires that the in–plane deformations of the diaphragm must not exceed the deflection limits of the supporting elements [76]. The following equation was developed from tests by Countryman [23] and is suggested by the American Plywood Association [57] for calculating deflections in single–layered, plywood sheathed diaphragms under service loads:

$$d = \frac{5vL^3}{8EAb} + \frac{vL}{4Gt} + 0.094\,Le_n + \frac{\Sigma\,(\Delta_c\,X)}{2b} \tag{3.8}$$

where d is the maximum deflection of the diaphragm, in.; v is the diaphragm shear, lb/ft; L is the diaphragm length, ft; b is the diaphragm width, ft; A is the cross–sectional area of the chord, in.^{2}; E is the elastic modulus, psi; G is the shear modulus, psi; t is the effective thickness of the plywood; e_n is the deformation of the nails, in.; Δ_c is the slip in the individual chords, in.; and X is the distance between the support and the splice, ft.

The four components of Eq. 3.7 correspond to deflection due to diaphragm bending, deflection due to diaphragm shear, deflection due to slip of the individual nails, and deflection due to slip at the chord splices, respectively. Representative values of fastener slip, e_n, are summarized in Table 3.3. The individual chord splice slip, Δ_c, has not been quantified in any of the building codes or design recommendations and is usually assumed based on data from relevant tests or engineering judgement. When the flange chord is steel reinforcing bar or steel angle ledgers as in concrete tilt–up construction, the splice slip component is reduced to the minimal effect of web–flange shear transfer between the perimeter chord and the boundary diaphragm elements [34].

(b) Metal–Deck Diaphragms

Guidelines for the design of metal–deck diaphragms are published by the Steel Deck Institute [47,48]. The results of experimental tests conducted at West Virginia University [49] form the basis for these provisions.

As shown in Fig. 3.6, the panel length for metal–deck sheets typically corresponds to 2 or 3 times the purlin spacing. Connections between the corrugated decking and the supporting members are shown schematically in Fig. 3.7. The strength of the diaphragm is typically controlled by failure of the connections in

the metal deck or local buckling of the metal–deck panels [48]. Nominal diaphragm strengths for each mode of failure are summarized in Table 3.4. Three conditions must be evaluated to determine the shear strength of a diaphragm that is limited by the connections: failure of the structural connections between the metal deck and the supporting members along the edge of the diaphragm (Fig. 3.8), failure of the structural and sidelap connections (connections between adjacent metal–deck panels) in an interior panel (Fig. 3.9), and failure of the corner fasteners (Fig. 3.10) [48].

The deflection of a metal–deck diaphragm is larger than the deflection of a comparable, continuous plate of uniform thickness because the metal–deck diaphragm is made from individual sheets of finite width that are joined at discrete points along the edges [49]. Stress fields are discontinuous within the metal–deck diaphragm due to these gaps leading to larger displacements. The corrugations in the metal deck are susceptible to warping at the ends of the panels, which also increases the deformations.

Studies of metal–deck diaphragms [49] have identified four phenomenon that must be considered when calculating diaphragm deflections: shear displacement of the diaphragm, end warping of the deck panels, slip at the interior sidelap connections, and slip of the supporting system of purlins and edge beams. An underlying assumption in this approach is that the shear stiffness of the metal deck is small compared with the flexural stiffness. Therefore, only shear deformations are considered [47].

The displacement due to pure shear (Fig. 3.11(a)) may be calculated as [48]:

$$\Delta_s = \left(\frac{P\ a}{L}\right) \frac{2\ (1 + \nu)}{E\ t}\ \frac{s}{d} \tag{3.9}$$

where Δ_s is the pure shear displacement, in.; P is the applied diaphragm load, kip; a is the diaphragm width, ft; L is the diaphragm length, ft; ν is Poisson's Ratio; E is Young's Modulus, ksi; t is the thickness of the deck element, in.; d is the corrugation pitch, in.; and s is the developed flute width, in. (Fig. 3.7(b)).

Unless the corrugated deck elements are restrained, an extra component of deflection results from warping (Fig. 3.11(b)). This component of displacement is derived from treating the corrugation as a beam on an elastic foundation and leads to rather cumbersome expressions for warping displacement. However, warping constants, D_n, are tabulated in the Steel Deck Institute manual [48] for common deck panels so detailed calculations are unnecessary.

The influence of fastener and support slip are included in the coefficient C [48]:

$$C = \frac{E\ t}{w}\ S_f \left(\frac{24L}{2a_1 + n_p a_2 + 2n_s S_f/S_s}\right) \tag{3.10}$$

where S_f is the structural connection flexibility, in./kip; S_s is the sidelap connection flexibility, in./kip. The terms a_1, a_2, n_s, and n_p are related to the number and arrangement of the fasteners, and are defined in

Table 3.4. Fastener strengths and flexibilities are defined in Table 3.5 and discussed in Section 3.2.2. The slip coefficient, C, decreases with an increase in the number and stiffness of the fasteners, or with an increase in the thickness of the metal deck.

The shear displacement, warping constant, and slip coefficient are combined to give the total deflection of a diaphragm subjected to a load P as follows [48]:

$$\Delta_t = \Delta_s + (\phi D_n + C)\frac{P\ a}{E\ t\ L} \tag{3.11}$$

where Δ_t is the diaphragm deflection, in. and the factor ϕ reflects the influence of purlin spacing on warping. Values of ϕ are tabulated in Ref. 48 and range from 1.0 for deck sheets that span over two or three purlins to 0.58 for deck sheets that span over eight purlins.

The shear stiffness, expressed in kip/in., of a metal deck diaphragm may be calculated as [48]:

$$G' = \frac{E\ t}{2.6\ \frac{s}{d} + \phi D_n + C} \tag{3.12}$$

(c) Composite Diaphragms

When additional stiffness is required in a metal–deck diaphragm, the decking is often over–lain with concrete. In concrete composite diaphragms, the shear strength is dependent upon the type of concrete used. Nominal strengths are presented in Table 3.6 for composite diaphragms with structural and insulating concretes.

The shear stiffness of concrete composite decks may be derived from Eq. 3.12. The concrete fill prevents warping of the corrugated elements and the stiffness of the concrete fill must be considered [48]:

$$G' = \frac{E\ t}{2.6\ \frac{s}{d} + C} + 3.5\ d_c\ (f_c')^{0.7} \tag{3.13}$$

where d_c is the depth of the concrete cover above the top corrugations, in. and f_c' is the specified compressive strength of the concrete, psi.

3.2.2 Diaphragm Fasteners

(a) Wood Diaphragms

The fasteners used within the framing elements of a wood roof diaphragm can be broken down into three categories [71]: nails, staples, and adhesives. Nails are by far the most common mechanical fastener in wood diaphragm construction and are produced with either plain or mechanically deformed shanks. Nail pull–out was a common cause of roof failures in low–rise buildings in the 1971 San Fernando earthquake [55] and at

that time most nails had plain shanks. By inducing deformation in the nail shank, an increase in the nail's pull–out resistance occurs, along with a decrease in the required depth of penetration for the nail to achieve resistance. Therefore deformed shank nails are now recommended for use in high seismic zones.

The pull–out strength of nails with lengths between ¾ and $1^1/_8$ in. and various deformed shanks are compared with 6d common nails in Fig. 3.12 [20]. In general, nails with helical threads provide more strength and create a stiffer connection than nails with annular threads [71]. The size of the nail head is also important [71]. A large nail head gives a larger bearing area and therefore more resistance against the nail pulling through the diaphragm skin. Splitting of the plywood skin was also a common mode of roof failure in the 1971 San Fernando earthquake [55].

Staples are the second most common type of fasteners in plywood diaphragms. Staples are not as variable in geometry as nails. They have such general classifications as "slender" or "thin" and "stout" or "fat" [71]. It is considered better practice to use many slender staples than a few stout staples because slender staples cause less splitting of the plywood and can be driven with lighter tools. Staples can be used in place of nails in order to control plywood splitting or when a small fastener spacing is required.

Two types of adhesives are used in diaphragm construction: rigid adhesives and mastic adhesives. Rigid adhesives use staples or nails only to hold the wood in place until the adhesive has set [71]. Mastic adhesives, however, resist service loads with the help of fasteners, and at large loadings the load is carried solely by the fasteners while the mastic adhesive acts to reduce the amplitude of the deflection [71]. Although adhesives provide strong and durable connections, their use is not widespread because of their relatively high cost.

(b) Metal–Deck Diaphragms

The fasteners used for connections within metal–deck diaphragms can be divided into three categories: welds, screws, and power–driven pins [47]. Each type of fastener exhibits higher strength and stiffness when the connection is between the metal deck and a structural member (structural connections) than when the connection is between deck sheets (sidelap or stitch connections). The fastener strength and flexibility of structural connections will be denoted as Q_f and S_f, while the fastener strength and flexibility of sidelap connections will be denoted as Q_s and S_s. The strength and flexibility of common connectors are presented in Table 3.4 [48].

Welded connections are the most common in metal decks due to the speed of construction [47]. The strength of puddle welds without washers depends on the thickness of the metal deck, the diameter of the weld, and the strength of the base material. Problems can occur if the amperage is too high during welding leading to burn–through of the upper layer of deck, or if the amperage is too low there may be improper fusion into the bottom layer [47]. When thin deck sheets (less than 0.028 in.) are used a the diaphragm, weld washers

are recommended because they act as a heat sink and control the size of the hole [48]. The strength of a welded connection with weld washers is related to the thickness of the deck, the diameter of the hole in the washer, and the electrode strength. The strength of welded sidelap connections is taken to be 75% of the comparable strength of structural welded connections. Welded connection flexibility is usually small compared with the flexibility of other types of fasteners because the slip around the welds is relatively small and limited primarily to distortion of the deck element around the weld [48].

The equations for strength and flexibility of screwed connections are based on experimental data using No. 12 and No. 14 screws and apply to both self–drilling and self–tapping types of screws [47]. For structural connections, the strength is controlled by the thickness and yield stress of the decking. Strength depends on deck thickness and screw diameter for sidelap connections.

Power–driven pins are shafts, which may be slightly tapered, that are driven through the deck elements. Holes are not pre–drilled. The strength of structural connections depends on the type of pin and the thickness of the deck, while the strength of sidelap connections depends only on the thickness of the deck.

3.2.3 Design of Non–Rectangular Diaphragms and Diaphragms with Openings

Due to the inherent flexibility of roof diaphragms in tilt–up buildings, large deflections are expected under lateral loads. Consequently, tilt–up buildings with irregular plans may experience large incompatibilities in displacements between adjoining sections of diaphragm near reentrant corners or near stairwells attached to the roof (Fig. 3.13(a) and 3.14(a)). The concentration of displacements generates large shear forces and has the potential to cause structural damage [14]. In order to resist these shear forces, the diaphragm must be designed with structural members that "collect" the force and transfer it to the vertical wall panels. These collector elements, called drag struts, receive the diaphragm force in shear and then "drag" the force back to the vertical elements by anchorage [14]. Figures 3.13(b) and 3.14(b) show that the addition of drag struts has divided the diaphragm into smaller rectangular diaphragms [14], and the displacements at reentrant corners and stairwells are compatible with the surrounding structural elements.

Rather than provide structural elements to resist the high shear forces developed at the reentrant corners and stairwells, efforts can be made to eliminate these forces altogether by avoiding displacement incompatibilities at reentrant corners and stairwells as shown in Fig. 3.13(c) and 3.14(c). By not attaching the wall panels to the roof in these areas, displacement incompatibilities at critical locations no longer exist. The unattached walls and stairwells will deflect as solitary units without affecting the global diaphragm response.

Smaller rectangular diaphragms within a global non–rectangular diaphragm are called "subdiaphragms," and are subject to the same code provisions and constraints as a typical diaphragm [34]. Specifically, all sub-

diaphragms must be sized such that they conform to the maximum diaphragm aspect ratios given in Table No. 25–I of the UBC (Table 3.7) [77].

High local shears that may be present in a diaphragm with openings must also be considered. Local shears are typically considered by analyzing the diaphragm as a Vierendeel truss [74] as shown in Fig. 3.15. The shear and bending forces along and across critical sections of the diaphragm must be calculated to determine if the surrounding framing members have sufficient capacity to resist the amplified bending and shear forces located in the vicinity of the opening. It is important to provide blocking members around the perimeter of all openings and to provide a positive direct connection between the blocking and the surrounding framing elements.

3.3 Connections in Tilt–Up Systems

Selecting appropriate connections is the most important aspect of designing tilt–up buildings to resist earthquake loads. The capacity and ductility of the connections will determine whether or not a structure performs satisfactorily during an earthquake. The connections in a tilt–up structure can be divided into three types: panel–to–foundation connections; panel–to–panel connections; and panel–to–roof connections.

3.3.1 Panel–to–Foundation Connections

Typical panel–to–foundation connections are shown in Figs. 3.16 and 3.17 [40,55,80]. The Uniform Building Code [77] requires that connections between precast walls and the supporting member must resist a tensile force in lb of at least $50*A_g$ where A_g is the cross–sectional area of the wall in in.^{2}. Most designers do not provide a physical connection between the tilt–up panel and the foundation as specified by the UBC because in many instances the weight of the panel counteracts any uplift forces. Rather, a dowel connection between the panel and floor slab is typically provided. If lateral loads are expected to produce uplift forces in the tilt–up panels, then designers typically will provide one of the following types of connections: (1) physical connection between tilt–up panel and foundation (which in most instances is #4 bars at 4 ft on center), or (2) sufficient panel–to–panel connections to constrain the in–plane walls to behave as one monolithic shear wall. This monolithic behavior increases the resisting moment of the shear wall which counteracts the applied moment from the lateral forces producing uplift. Currently, many engineers are trying to remove UBC provision 2615(i)3B which would allow designers to decide if panel–to–foundation connections are needed.

3.3.2 Panel–to–Panel Connections

Panel–to–panel connections have changed significantly during the past 30 years. In the 1960's continuous, cast–in–place pilasters were often used to connect panels (Fig. 3.18(a)). Another common detail was to provide connections at six to eight foot intervals along the height of the wall (Fig. 3.18(b)). However, in recent construction, a single continuous chord is typically provided at the roof level around the perimeter of

the building [10,80], with no other connections between panels, except at the corners of the building (Fig. 3.19). The perimeter chord provides a restraint that holds the tilt-up building together, so that it functions as a unit under seismic loading. Designers recommend restricting panel-to-panel connections to the single continuous chord in order to eliminate degradation of connections due to temperature and shrinkage effects. Also, some designers believe that the increased amount of structural damping due to fewer panel-to-panel connections more than compensates for the decreased lateral resistance that results from using less connections [80].

Pilaster connections are not common in new construction because the pilasters produce stress concentrations at the connected panel edges, as a result of out-of-plane deflections, and they restrain movement due to shrinkage and temperature effects [10].

3.3.3 Panel-to-Roof Connections

In tilt-up construction, the critical connection for seismic loading is usually the connection between the roof diaphragm and the concrete tilt-up wall panel. Panel-to-roof connections must be designed to resist forces normal and parallel to the plane of the panel. Inadequacies of these connection have been the cause for many partial roof and panel collapses during the past three decades. The 1964 Alaska earthquake and the 1971 San Fernando earthquake gave clear evidence that the use of the popular wood ledger connection, as shown in Figs. 3.20 and 3.21 [77], must be restricted to regions of low seismic risk and should be replaced by some type of joist anchor in high seismic risk zones (Fig. 3.22) [25].

Wood ledger connections were found to be susceptible to three failure mechanisms: the ledger was placed in cross grain bending by seismic lateral loads which resulted in the wood ledger splitting along the bolt line; the bearing stresses of the nails in the plywood-to-ledger connection caused the nails to shear through the plywood; and the force on the nails resulting from tension in the plywood overcame the pull-out resistance of the ledger.

In 1976, the UBC [75] introduced four new code provisions to avoid these problems (Fig. 3.23). Those provisions are reproduced in Appendix A. Section 2310 specifies a direct connection between the wall and diaphragm capable of resisting at least 200 lb per lineal foot of wall. Section 2312(j)2D requires continuous ties between diaphragm chords to anchor these forces. Section 2312(j)3A prohibits the use of toe nails, nails subjected to withdrawal, or wood framing used in cross-grain bending or cross-grain tension in all seismic zones except zone 1. Section 2312(j)3C draws attention to the need to have exterior panels able to accommodate structural movements resulting from both lateral forces and temperature changes. These provisions have remained essentially unchanged through the 1991 edition of the UBC [77].

As specified in Section 2310 of the UBC, the panel–to–roof connection must resist a minimum anchorage force of 200 lb per lineal foot of wall. This provision rarely controls in tilt–up construction, however. Consider, for example, a tilt–up warehouse with a plywood roof diaphragm constructed in California during the early 1970's. The panel height is likely to be greater than 17 ft. The design force for the panel, F_p, is calculated using Eq. 3.5 where the zone factor is taken to be 0.4, the importance factor is taken to be 1.0, and C_p is taken to be 0.75 [77]. This leads to a design lateral force for the panel of $0.3W_p$ where W_p is the weight of the panel. However, the UBC states that when designing the connections in the middle half of the building, C_p must be multiplied by 1.5 for flexible diaphragms. If the tilt–up panel is modelled as a simply–supported member, then the connection force between the foundation and the panel is the same magnitude as the connection force between the panel and the diaphragm, $0.225W_p$. Assuming a minimum panel thickness of 5½ in., the weight of the panel is 1170 lb/ft, and the connection between the panel and the diaphragm must be designed to resist 265 lb/ft, which is greater than the specified minimum strength. Therefore, the minimum anchorage force of 200 lb/ft should be considered to be a lower bound in tilt–up construction.

The unsatisfactory performance of many panel–to–roof connections indicated that continuous ties were needed between diaphragm chords to distribute horizontal forces within the diaphragm and that direct, positive connections were needed for anchorage of the diaphragm to the panels. Because the use of continuous ties from one end of a diaphragm to the other was highly inefficient, the concept of subdiaphragms was introduced (Fig. 3.23). A series of small "diaphragms" within the total diaphragm were used to transfer anchorage forces to the wall from the diaphragm interior. For the 16x64–ft subdiaphragm EFGH in Fig. 3.23, the longitudinal purlins serve as ties, if the purlins are connected directly to the wall (Fig. 3.22, 3.24, and 3.25) and are made continuous over the interior glulam beams (Fig. 3.26). If, however, the purlins do not frame into the side walls, as is the case for some existing construction, then a retrofit can be made by introducing ties into the 8x16–ft subdiaphragm HIJK (Fig. 3.23) by metal straps or rods, as shown in Figs. 3.28, 3.29, 3.30, and 3.27, to create the continuous tie connection. In the transverse direction, the continuous tie can be provided by connecting the glulam beams directly to the tilt–up wall as shown in Fig. 3.31. The subdiaphragm concept, therefore, simultaneously fulfills the provisions for continuous ties between diaphragm chords and for closely–spaced ties for walls with negligible bending resistance between anchors.

Several varieties of "direct" connections of plywood sheathing and roof joists to the wall panel reinforcement, as seen in Figs. 3.22, 3.28, 3.29, 3.30, 3.31, have been used. The advantages and disadvantages of each of those connections are listed below each figure [25]. Connections used to retrofit the wood ledger in Fig. 3.20 and 3.21 to provide better anchorage of the framing members to the wall panel by providing a "direct connection" are shown in Figs. 3.24, 3.25, 3.27. Such schemes were used to repair and upgrade roof–to–wall connections after the 1971 San Fernando and 1987 Whittier Narrows earthquakes.

After the 1971 San Fernando Earthquake, building codes also placed limits on plywood thickness [75]. For the details shown in Fig. 3.23, plywood was to be at least $^5/_{16}$-in. thick for sub-purlins (studs) placed 16 in. on center and at least $^3/_8$-in. thick for studs placed 24 in. on center. These limits on plywood thickness were implemented to reduce the likelihood of nail shearing through the plywood.

The influence of shrinkage in wood diaphragm elements must be considered when evaluating the durability of panel-to-roof connections. Shrinkage in sawn lumber framing members may be approximated as $^1/_{32}$ in. shrinkage per 1 in. of width or depth as the member progresses from the green to the dry state [25]. Glulam beams can be expected to shrink $^1/_{16}$ in. per foot of depth for every 3% moisture loss. This restraint could lead to pull-out of the fasteners connecting the embedded strap to the plywood, or degradation of the ledger due to cross-grain tension splitting along the bolt line.

3.4 Summary

Typical design procedures for tilt-up construction treat a building as a series of individual components, rather than a structural system. The diaphragm is designed as a simply-supported shear beam to transfer lateral forces into the end walls, and the wall panels are designed as slender columns, pinned at both ends, to resist gravity and lateral loads. Code-specified forces are often used to design the critical connections.

4. SUMMARY OF PREVIOUS INVESTIGATIONS OF THE SEISMIC BEHAVIOR OF TILT–UP CONSTRUCTION

Since the 1971 San Fernando earthquake, engineers throughout the U.S. have studied the seismic response of many types of buildings, and developed design provisions to improve the performance of new construction. In Southern California, emphasis was placed on reducing the seismic risk of unreinforced masonry and tilt–up buildings. These types of construction have sustained significant structural damage during recent earthquakes and represent a large portion of the inventory of existing, low–rise, industrial buildings.

Much of the work related to tilt–up construction has been conducted by researchers at Agbabian Associates [4,5,6,8,7,9,10,11,12,27,28], where analytical modelling procedures have been developed based on the results of experimental tests. Analytical models of tilt–up systems have also been developed at Dames and Moore [53,54].

Experimental tests of diaphragms subjected to cyclic loads have been conducted by Agbabian/Barnes/ Kariotis (ABK) [1] and researchers at the University of British Columbia [26], the University of California [84,85], Stanford University [83], and Washington State University [39]. The ABK tests represent the most extensive investigation with tests of full–scale plywood, wood–sheathed, and metal deck diaphragms. However, a detailed description of the results has not been published [2].

The results of these experimental and analytical studies are summarized in this chapter. Diaphragms are discussed in Section 4.1, tilt–up wall panels are discussed in Section 4.2, and analytical models for complete tilt–up systems are summarized in Section 4.3.

4.1 Cyclic Response of Diaphragms

During a design–level earthquake, the types of roof diaphragms used in most tilt–up structures are expected to experience nonlinear response. The nature of this response is extremely sensitive to the types of connections used within the diaphragm and to the actual material properties of the diaphragm components, which are highly variable. Most of the experimental research to date has focused on the behavior of wood diaphragms, because wood diaphragms have been used almost exclusively in Southern California and the Pacific Northwest during the past 20 years. The results of five experimental investigations of the cyclic response of wood diaphragms and panels are summarized in Section 4.1.1. Data from individual connections and complete diaphragms are presented. The limited data from cyclic tests of metal–deck diaphragms are described in Section 4.1.2. Methods for modelling diaphragms are discussed in Section 4.1.3. Analytical representations of the diaphragms range from using several nonlinear spring elements to special–purpose finite–element models with individual nail elements.

This section is not intended to summarize all experimental and analytical work related to diaphragms. Only investigations that involve cyclic loading are discussed. The paper by Peterson [56] contains a comprehensive review of the literature related to wood diaphragms.

4.1.1 Experimental Tests of Wood Panels and Diaphragms

The first phase of many investigations of the behavior of plywood diaphragms and panels is devoted to understanding the response of the individual nailed connections. The measured response of nails connecting plywood and framing members is shown in Fig. 4.1. The data shown in Fig. 4.1(a) were obtained by cycling the connection to a given force level [39], while the connection shown in Fig. 4.1(b) was cycled between given displacement levels [26]. In both cases, the stiffness of the connection decreased as the amplitude of the displacement increased, and the connection exhibited a region of extremely low stiffness as the applied load passed through zero. Once the connection was pushed into the nonlinear region of response, specimens would experience larger displacements when pushed to the same nominal force level (Fig. 4.1(a)) and specimens pushed to a specified displacement would resist lower forces as the number of loading cycles increased (Fig. 4.1(b)).

Five experimental investigations in which complete diaphragms or panels were subjected to load reversals are summarized in Table 4.1. Young and Medearis [83], Zacher and Gray [84,85], Itani and Falk [39], and Dolan [26] evaluated the response of plywood, gypsum board, and waferboard panels, while ABK [1] and Itani and Falk [39] investigated the behavior of plywood, lumber–sheathed, and gypsum board diaphragms. The general shape of the measured hysteretic response of complete diaphragms closely resembles the behavior of the individual connections (Fig. 4.2). The force–displacement curves are pinched, diaphragm stiffness decreases with increasing displacement, and diaphragm stiffness decreases as the number of inelastic loading cycles at a constant displacement or force level increases.

Young and Medearis [83] found that 20 cycles at the nominal design level did not influence the capacity of the wall panel nor the nonlinear force–displacement response. This observation was confirmed in small–scale panel tests by Yasumura and Sugiyama [82] where panels were subjected to 50 cycles at $\pm 60\%$ of the strength of nominally identical specimens tested monotonically. Accumulated damage was observed in tests when the panels were subjected to loading cycles of $\pm 80\%$ of the capacity [82].

Young and Medearis [83] also estimated viscous damping factors from their test results. During load cycles at the nominal design level, damping values of 0.07 and 0.10 were calculated for panels with one and two layers of plywood, respectively. Polensek [58] identified damping factors between 0.07 and 0.11 from low–amplitude, free–vibration tests of plywood floor systems. Itani and Falk [39] also estimated damping coefficients from free–vibration tests (Fig. 4.3). At a displacement level of 0.1 in., damping factors in the plywood diaphragm specimens were between 0.1 and 0.15. Equivalent damping factors increased to more

than 0.20 when the displacement level was increased to 0.6 in. As indicated in Fig. 4.3(b), the displacement levels used in both free–vibration tests did not cause significant nonlinear response in the diaphragms.

The ABK diaphragm tests were designed to evaluate a number of practical concerns such as the influence of blocking, roofing materials, and retrofit nailing on the response of diaphragms [1]. Table 4.2 contains a summary of the primary experimental variables in these tests. Each diaphragm was subjected to a series of quasi–static load reversals and earthquake motions in real time. Schematic drawings of the diaphragm test specimens are shown in Fig. 4.4. Comparisons of the quasi–static and dynamic response of diaphragm D are shown in Fig. 4.2(c) and (d). The average initial stiffness inferred from the low–amplitude quasi–static tests of all diaphragms are reported in Table 4.2.

Data obtained during the dynamic, earthquake simulations indicate that diaphragm response remains nearly linear up to accelerations of approximately 0.1g [1]. Beyond 0.1g, the nonlinear characteristics of the diaphragm may be observed. Researchers noted that roofing material initially added stiffness to the diaphragm, however, the roofing material separated from the diaphragm when the accelerations reached approximately 0.2g [1].

Zacher and Gray [84,85] compared the behavior of panels connected with nails and staples, and evaluated the influence of over–driving the fasteners. The results indicated that stapled panels do behave satisfactorily, however the nailed panels were able to resist larger displacements before failure. Panels with nails over–driven by $^1/_8''$ failed in a brittle manner at displacements that were less than 75% of the displacement capacity of similar panels in which the nail heads did not break the plywood veneer. The displacement capacity of panels with staples was also reduced when the staples were over–driven, however, the failure mode was not as abrupt as observed for the nailed connections.

4.1.2 Experimental Tests of Metal–Deck Diaphragms

As indicated in Table 4.2, metal–deck diaphragms were also tested as part of the ABK investigation [1]. The measured response of diaphragm R is shown in Fig. 4.5. Response during the quasi–static tests (Fig. 4.5(a)) is similar to that of plywood diaphragms. The metal–deck diaphragm displayed a pinched hysteresis curve and the effective stiffness decreased with increasing displacement. It is difficult to make conclusions about the cyclic force–displacement response of metal–deck diaphragms from the dynamic data (Fig. 4.5 (b)).

4.1.3 Analytical Models of Diaphragms

The measured data described in Section 4.1.1 form the basis for the analytical representations of diaphragms discussed in this section. In all cases, the nonlinear features of the analytical models were scaled

from available experimental data. No procedures are available to estimate the nonlinear response of a diaphragm given the nominal design properties discussed in Chapter 3.

In the late 1970's, Adham and Ewing [11] developed an analytical model where eight inelastic spring and damper assemblies were used to model wood diaphragms (Fig. 4.6). Diaphragm properties scaled from the monotonic tests performed by Tissel [74] were combined with the linear hysteresis rules shown in Fig. 4.7. The calculated frequencies of plywood and lumber sheathed diaphragms ranged from 2.8 to 11.5 sec. which is considerably larger than those inferred by Blume and Rea from full–scale, non–destructive tests of wood diaphragms in school buidlings [17,18,62].

Following the ABK tests [1], Adham [4] refined the hysteresis model for plywood diaphragms. A second–order curve was selected to model the force–deflection envelope of the diaphragm (Fig. 4.8(a)):

$$F(e) = \frac{F_u\, e}{\frac{F_u}{K_1} + |e|} \tag{4.1}$$

where $F(e)$ is the force in the spring, e is the deformation of the spring, F_u represents the strength of the diaphragm, and K_1 is the initial diaphragm stiffness. When the diaphragm is subjected to cyclic loading, the hysteresis rules defined in Fig. 4.8(b) are used to control the response. Based on the observed response of the ABK diaphragms, the unloading stiffness, K_2, was assumed to be equal to the initial diaphragm stiffness, K_1, and the force level used to define slip at low applied loads, F_1, was taken to be ten percent of the strength of the diaphragm, F_u. Values of the critical parameters, K_1, K_2, F_u, and F_1, for an arbitrary plywood diaphragm are calculated from the experimental data using the scaling rules listed below [4]:

$$K_i = \frac{L'D}{LD'} K_i' \tag{4.2}$$

$$F_i = \frac{D}{D'} F_i' \tag{4.3}$$

where L is the length and D is the width of the diaphragm section under consideration, and the following parameters were taken from the ABK test results [1]:

L' = length of diaphragm section in test = 20 ft
D' = width of diaphragm section in test = 20 ft
K_1' = observed initial stiffness of diaphragm in test = 324 kip/ft
K_2' = observed reloading stiffness of diaphragm in test = 324 kip/ft
F_u' = observed strength of diaphragm in test = 32 kip
F_1' = observed strength at which diaphragm stiffness increases during cycling = 3.2 kip

During the NSF–sponsored TCCMAR program, the ABK tests [1] were re–evaluated and the diaphragm hysteresis model was revised to include strength degradation at large displacements and variation of the un-

loading stiffness with the level of deformation [9,36,29]. The force–deflection envelope and hysteresis rules for the revised model are shown in Fig. 4.9. The unloading stiffness, K_u, was defined as:

$$K_u = K_1 \left(\frac{e_y}{e_{\max}}\right)^{\gamma} \tag{4.4}$$

where e_y represents the yield deformation and is defined as $^1/_3\, F_u/K_1$, e_{max} is the maximum deformation of the diaphragm during previous loading cycles, and γ is assumed to be 0.2 for wood diaphragms. Viscous damping was ignored in the revised diaphragm model (Fig. 4.6), the hysteretic damping was considered to be sufficient. Calculated and measured displacement response of diaphragm N are compared in Fig. 4.10 during one of the later earthquake simulations [9].

Itani and Falk [39] and Dolan [26] developed special–purpose finite–element codes to analyze the response of plywood diaphragms and panels. The researchers used similar modelling techniques: framing members were represented using linear beam elements, the plywood sheathing was modelled with linear plane–stress or shell elements, and nonlinear spring elements were used to model the nailed connections between the framing and sheathing. Special gap elements were used in both investigations to allow adjacent sheets of plywood to separate, but not overlap. Dolan [26] used similar bi–linear elements to represent the connections between framing members, while Itani and Falk [39] used hinged connections to attach all framing members.

The general nature of the calculated response in both investigations was governed by the choice of nonlinear nail element. Data from connection tests (Fig. 4.1) were used to develop envelope curves for the nailed connections (Fig. 4.11). Approximately 100 connections were tested in each investigation. Itani and Falk [39] chose a power curve to represent the data,

$$F_{con} = a_1 \Delta^{a_2} \tag{4.5}$$

while Dolan [26] used a three–parameter model,

$$F_{con} = (P_o + K_2 |\Delta|)\left(1 - e^{-\frac{K_o|\Delta|}{P_o}}\right) \tag{4.6}$$

where F_{con} is the force resisted by the connection, Δ is the displacement of the connection, and a_1, a_2, P_o, K_o, and K_2 are constants whose values were determined from the experimental data using a curve fitting technique.

– Both finite–element models were used successfully by the researchers to reproduce their experimental results (Fig. 4.12).

4.2 Cyclic Response of Tilt–Up Wall Panels

Agbabian Associates conducted a series of dynamic tests on tilt–up wall panels in the early 1980's [6, 8, 7, 28]. The experimental setup for these tests is shown in Fig. 4.13. Three wall panels were tested. Key parameters of the experimental program are summarized in Table 4.3. Two load cells, 1 displacement transducer, and 9 velocity transducers were used to measure the response of the panels. Displacements and accelerations along the height of the panel were later calculated from the velocity data.

These experiments were closely linked to the analytical modeled described in Section 4.3. Researchers calculated the transverse response of a representative tilt–up building at the top of the longitudinal wall panels using the 1940 El Centro and 1971 Castaic (San Fernando) earthquake records. This calculated response was then used as the input motion at the top of the wall panel, and the ground motion was used to drive the base of the panel (Fig. 4.13). Response was calculated for tilt–up buildings with rigid and flexible diaphragms.

Each wall panel was subjected to a series of 9 or 10 earthquake simulations. The effective peak ground acceleration was increased from 0.2g to 0.4g in the later tests. By the end of the testing sequence, all panels had experienced inelastic response. The El Centro ground motion, combined with a rigid diaphragm, proved to be the most severe test of the panels. The maximum acceleration and displacement response of the panels, inferred from the measured velocity data, is shown in Fig. 4.14. The amplitude of the displacements increased as the panels were subjected to more loading cycles and sustained structural damage (Fig. 4.15).

The distributions of accelerations and displacements closely resembled the first mode shape of a panel that is pinned at both ends (Fig. 4.14). The researchers, therefore, concluded that the response of the panel at mid–height should govern the design, and that using fully cracked sections for panel design was a conservative assumption [6, 8, 7]. Distributions of moments were also calculated along the panel height (Fig. 4.16). Although the distribution of moments did not correspond to the expected first mode shape, the researchers concluded that design procedures for walls were appropriate because the magnitude of the calculated moments was less than those calculated using the ACI–SEASC recommendations for slender walls [81].

4.3 Analytical Models of Tilt–Up Systems

In the early 1980's, Adham [4] developed an analytical model for tilt–up construction that was based on an earlier representation of unreinforced masonry buildings [11]. Considering the representative tilt–up building shown in Fig. 4.17, the following assumptions were made:

- Earthquake motion in the transverse direction of the building was considered to be critical.
- Only half of the building was analyzed due to symmetry (Fig. 4.17(c)).
- The roof diaphragm was modelled as a deep shear beam using four inelastic springs (Fig. 4.17(d)). Hysteresis rules for the inelastic springs are defined in Fig. 4.8.

- The transverse wall panels were assumed to be rigid. Therefore, ground motion was assumed to be transmitted to the roof without amplification at the end of the building (Fig. 4.17(d)).
- The longitudinal wall panels were assumed to deform primarily in out–of–plane bending. Linear beam elements were used to represent these panels (Fig. 4.17(d)).
- The response of the two longitudinal walls was assumed to be the same. Therefore, a single set of beam elements could be used to model the longitudinal walls (Fig. 4.17(e)).

A total of 23 nodes, 4 inelastic springs, and 18 linear beam elements were used to model the 300′ by 150′ warehouse shown in Fig. 4.17(a) [6]. The model did not include any type of connection between adjacent longitudinal wall panels. A viscous damping factor of 5% was used for the beam elements, and two damping factors (0.07% and 10%) were used for the nonlinear springs. The model was subjected to a scaled version of the N69W component of the motion recorded at Castaic during the 1971 San Fernando earthquake.

Calculated acceleration response at the top and mid–height of the center longitudinal wall panel is shown in Fig. 4.18 and 4.19 for the lightly–damped and moderately–damped models, respectively. In both cases, the amplitude of the response is greater at mid–height of the panel than at the top. The amplitude of the accelerations at the roof exceeded those at the ground by a factor of 1.4 for the moderately–damped model and 2.6 for the lightly–damped model. This result implies that the connection forces between the wall panels and the roof exceed those between the wall panels and the foundation. The calculated acceleration response of the center of the roof was used as the driving function at the top of the panel for the experimental tests described in Section 4.2 [6, 8, 7, 28].

Distributions of the calculated accelerations and moments along the height of the center longitudinal wall panel are shown in Fig. 4.20. Unlike the experimental data, the distribution of calculated moments resembled the first mode shape of a pinned–pinned beam.

In the late 1980's, researchers at Dames and Moore used a similar model to represent the seismic response of tilt–up buildings [53, 54]. The idealized building and analytical models for linear and nonlinear analyses are shown in Fig. 4.21. The transverse walls were assumed to be rigid and the longitudinal walls were modelled using beam elements. The diaphragm was assumed to deform in shear. Initially, linear elements were used to model the diaphragm and longitudinal wall panels. Bi–linear models were later adopted to evaluate the influence of member nonlinearity on structural response.

A 200′ by 200′ building was subjected to the S69E component of the 1952 Taft ground motion. The initial stiffness of the diaphragm was varied such that the natural period of the diaphragm ranged form 0.25 to 2.0 sec. Viscous damping factors of 5% and 10% were used. The calculated anchorage forces between the diaphragm and longitudinal walls exceeded 50% of the weight of the wall panels for the majority of the condi-

tions considered (Fig. 4.22). The magnitude of the forces was not reduced significantly in the nonlinear analyses. Because panel–to–roof connections typically have limited ductility, the researchers concluded that linear analyses were appropriate for tilt–up construction [53,54].

The distribution of shear forces in the diaphragm is shown in Fig. 4.23. The results indicate that shear forces do not decrease linearly with distance from the end walls. Proposed shear distributions for design are also indicated in Fig. 4.23.

Following the 1987 Whittier Narrows earthquake, researchers at Agbabian Associates revised their analytical model to reflect the observed damage in tilt–up buildings and to take advantage of the improved modelling capabilities developed as part of the TCCMAR research program [29]. The modelling of three actual buildings is described in Ref. 9. In all three cases, the nature of the analytical model is considerably different from the earlier analyses [4,6]. For earthquake motion in the transverse direction, the following changes were made:

- The longitudinal walls are not included in the analyses, because their contribution to the stiffness of the building was considered to be negligible.
- The transverse wall panels were modelled using linear beam elements.
- Nonlinear springs were used to represent the soil supporting the transverse wall panels. Panel uplift could be evaluated with these elements.

A warehouse in Hollister, California (discussed in Chapter 5 of this report) was analyzed to demonstrate the performance of the revised nonlinear model for diaphragms (Fig. 4.9). The analytical model of the 300′ by 100′ warehouse is shown in Fig. 4.24 for earthquake motion in the transverse direction. The concrete wall panels were assumed to be uncracked in the analysis. The stiffness of the plywood diaphragm was inferred from the results of the ABK tests [1] using the scaling procedure defined in Eq. 4.2 and 4.3. The diaphragm stiffness was subsequently increased by a factor of 3 to account for the roofing material and insulation [9].

The response of this building during the 1986 Morgan Hill earthquake was recorded as part of the California Strong Motion Instrumentation Program [38]. Comparisons of the calculated and measured displacement at the center of the diaphragm, relative to the top of the transverse walls, are shown in Fig. 4.25. The general nature of the measured response is well–represented by the analytical model.

A 165′ by 544′ warehouse in Downey, California and a 294′ by 452′ building in Whittier, California (Fig. 4.26) were analyzed as part of an investigation of tilt–up performance during the 1987 Whittier Narrows earthquake [9]. Both buildings were located less than 10 miles from the epicenter. The Downey building sustained minor structural damage during the earthquake, while no damage was observed in the Whittier building [9].

Analytical models of the Downey and Whittier buildings for ground motion in the transverse direction are shown in Fig. 4.27 and 4.28, respectively. The models included a more–detailed representation of the transverse walls than was used to analyze the Hollister building and nonlinear springs were included beneath the transverse walls in the Downey building to model the soil. The response of the longitudinal walls was not modelled explicitly, however, the response of the longitudinal wall panels was evaluated by subjecting an isolated panel to the calculated diaphragm accelerations and the input ground motion.

Although the response of these buildings was not recorded during the Whittier earthquake, the ground motion was recorded at six sites within 15 miles of the epicenter, and both buildings were inspected thoroughly after the event. Therefore, the performance of the analytical model was evaluated by comparing the extent of structural damage predicted using the analytical model and damage observed following the earthquake.

The results of the analyses of the Downey building agreed with the observed damage. For transverse ground motion, panel uplift was calculated to occur in the west and interior walls. When the building was subjected to longitudinal ground motion, the calculated forces between the diaphragm and the longitudinal wall panels exceeded the strength of the connections. Evaluation of the longitudinal wall panels subjected to transverse ground motion indicated that the dynamic moments were less than the cracking load for the panels. The calculated damage in the panel–to–foundation and panel–to–roof connections was observed following the earthquake, and cracking of the wall panels was not observed.

The correlation between calculated and observed damage in the Whittier building was not as good. The analyses indicated damage in the panel–to–roof connections, distress in the diaphragm along the south wall of the building, and extensive cracking of the longitudinal wall panels, when the building was subjected to transverse ground motion. None of this damage was observed in the structure. The researchers believed that the skewed wall panels along the south end of the building may have led to problems modelling the diaphragm, and that the ground motion measured approximately 1.2 miles from the building was not representative of the motion at the site.

4.4 Summary

As indicated in this chapter, the seismic response tilt–up construction has been studied extensively in the past 15 years. Analytical models for calculating the seismic response of plywood diaphragms and tilt–up buildings have been summarized. However, little guidance is available for the engineer interested in performing independent calculations. The response of tilt–up buildings is closely linked to the nonlinear characteristics of the diaphragms. All the researchers scaled experimental data to obtain the parameters used in their analyses. The link between the design equations discussed in Chapter 3 and the analytical models is missing.

Therefore, the influence of variations in the diaphragm, such as the type or spacing of the fasteners or the thickness of the plywood, on the structural performance can not be evaluated.

The seismic response of tilt-up construction is also related to the performance of the structural connections between the roof and wall panels, adjacent wall panels, and wall panels and the foundation. With the exception of the study by Adham et al. [9] where the panel-to-foundation connections were modelled, connections are not considered in the analytical models discussed. Although most damage observed after an earthquake has been attributed to failure of the connections, the current analytical models can not be used to evaluate the required strength and ductility of these critical elements.

5. MEASURED STRONG–MOTION RESPONSE OF TILT–UP BUILDINGS

Acceleration response histories have been recorded in tilt–up buildings during several recent earthquakes as part of the California Strong Motion Instrumentation Program [37,38,59,60,61,66,67]. The physical characteristics of three buildings for which data are available are summarized in Table 5.1. Two of the buildings, the Hollister and Redlands warehouses, represent traditional tilt–up construction. The one–story structures are rectangular in plan, have relatively few openings in the tilt–up panels, and are used primarily for storage. The Milpitas industrial building, on the other hand, represents the recent trend of using tilt–up wall panels in multi–story commercial buildings. The first story in this building is used as a warehouse and the second for offices. Every wall panel has openings for windows or doors.

The seismic response of each of the structures will be summarized in the following sections. Generalizations about the dynamic behavior of tilt–up buildings will also be presented.

5.1 Hollister Warehouse

A view of the north–east corner of the Hollister warehouse is shown in Fig. 5.1 and the floor plan is shown in Fig. 5.2. Six–in. thick tilt–up panels are used throughout the building, with the exception of four 7–in. panels at the north and south ends of the longitudinal walls. Cast–in–place pilasters are used to connect adjacent wall panels. Cambered, glulam beams, ranging in depth from 22½ in. to 28½ in. with a width of 5 1/8 in., run in both the longitudinal and transverse directions of the building (Fig. 5.3). The beams are supported by a single line of 8–in. standard pipe columns. The roof is formed from a grid of 4x14 and 4x10 purlins at 8 ft on center with 2x4 stiffeners at 2 ft on center, overlain by ½–in. structural plywood. Blocking was provided throughout the diaphragm. The plywood is covered with 2–in. styrofoam insulation, 1–in. fesco board, and roofing material.

Typical reinforcement in the wall panels consists of a single layer of #4 bars spaced at 12 in. on center in each direction (Fig. 5.4). Two #9 bars form the chord in the longitudinal walls and a single #5 bar is used in the transverse walls. Chord reinforcement from adjacent panels was overlapped and welded.

The building was designed with nine openings in the tilt–up walls: four overhead doors for truck access and five doors for personnel (Fig. 5.5). Two #5 bars were typically placed in the wall panels next to the openings.

Records from thirteen strong–motion instruments were obtained during the 1984 Morgan Hill, 1986 Hollister, and 1989 Loma Prieta earthquakes. Five instruments recorded the ground motion, four monitored transverse motion at the roof, three recorded longitudinal motion at the roof, and one instrument monitored the out–of–plane response of a longitudinal wall panel at midheight. Instrument locations are indicated in Fig. 5.6 and summarized in Table 5.2. Horizontal ground acceleration histories recorded at the base of the warehouse are shown in Fig. 5.7 for the three earthquakes. Corresponding linear response spectra are presented in Fig. 5.8.

Acceleration histories are shown in Fig. 5.9, 5.10, and 5.11 for the Morgan Hill, Hollister, and Loma Prieta earthquakes, respectively. The following observations were made from the acceleration response:

- The amplitudes of the transverse accelerations at the center of the roof (channel 4) and the top of the longitudinal wall (channel 5) were approximately 3 times greater than the corresponding ground accelerations (channel 7). The out–of–plane motion at midheight of the center longitudinal wall panel (channel 6) exceeded the ground accelerations by a factor of approximately 2.5.
- The longitudinal accelerations at the center of the roof (channel 11) were observed to be amplified by a factor of 1.5 to 2 relative to the longitudinal ground acceleration (channel 13).
- In–plane accelerations measured at the top of the walls (channels 2 and 3 for transverse motion and channels 10 and 12 for longitudinal motion) were essentially the same as the accelerations recorded at the base of the walls (channel 7 for transverse motion and channel 13 for longitudinal motion). No appreciable amplification of the in–plane ground motion was observed at the roof.

Normalized Fourier amplitude spectra of the acceleration response histories are shown in Fig. 5.12, 5.13, and 5.14. A summary of the predominant frequency for each channel is presented in Table 5.2.

- Similarly to the acceleration histories, the Fourier amplitude spectra indicate that the frequency content of the in–plane wall response is essentially the same as the corresponding ground motion.
- Out–of–plane response at the center of the walls and response at the center of the diaphragm was similar and may be used to identify the fundamental natural frequency of the structure. In the transverse direction, the natural frequency was approximately the same during the Morgan Hill and Hollister earthquakes, ranging from 1.6 to 1.7 Hz. The natural frequency decreased to 1.10 Hz during the Loma Prieta earthquake. The decrease in structural stiffness observed during the Loma Prieta earthquake is consistent with the increased amplitude of the response and observed damage following the earthquake [67].
- The Fourier amplitude spectra from out–of–plane motion at midheight of the longitudinal wall panels (channel 6) indicate amplification of response between 3 and 5 Hz. However, the out–of–plane response of the panels is dominated by the transverse behavior of the building.
- Longitudinal structural frequencies are not easily identified from the Fourier amplitude spectra. The relative frequency content was essentially the same as the ground motion for frequencies less than 2 Hz. Maximum amplification at the center of the roof occurred between 6 and 7 Hz.

The digitized data provided by the California Department of Conservation included displacement histories which were obtained by integrating the corrected acceleration response. Displacement response at the base of the structure and the center of the roof is shown in Fig. 5.15. The longitudinal displacement of the roof was essentially the same as the north–south ground displacement. Amplification of the transverse displacements at the center of the roof may be observed.

The displacement of the structure relative to the ground may be interpreted as an indication of damage during an earthquake. However, due to the nature of the numerical integration process, the magnitude of the relative displacement response must be considered to be approximate. Differences between the integrated structural displacement records and the integrated ground displacement are shown in Fig. 5.16, 5.17, and 5.18 as the "unfiltered" relative displacement records. It was observed that the predominant frequency of the

ground motion tended to dominate the calculated relative displacement response, especially for the transverse response recorded at the top of the transverse end walls and the longitudinal response. The relative displacement records were filtered in the frequency domain, in an attempt to remove the noise attributable to the ground motion. Details of the filtering procedure are described in Appendix B. The filtered relative displacement records for the Hollister warehouse are also shown in Fig. 5.16, 5.17, and 5.18. Calculated maximum relative displacements are summarized in Table 5.3 for the unfiltered and filtered records. The following trends may be observed:

- The relative displacement records in the transverse direction at the center of the building (channels 4, 5, and 6) were not significantly affected by the filtering process. Maximum relative displacement variations were typically within ±15% for the unfiltered and filtered records, which is consistent with the error expected for numerical integration of acceleration records [68]. The primary difference between the unfiltered and filtered records, was that the filtered relative displacement records tended to oscillate about zero displacement, while the unfiltered records oscillated about the ground displacements.

- The character of the relative displacement records in the transverse direction at the end of the building (channels 2 and 3) were dramatically changed by the filtering process. In many cases, the maximum relative displacement from the filtered records was less than one–half of the maximum relative displacement from the unfiltered records. Due to the significant change in the amplitude and frequency content of the relative displacement records at the top of the transverse walls, the relative displacement records for channels 2 and 3 were considered to be unreliable.

- Longitudinal relative displacement records (channels 10, 11, and 12) were also dominated by the ground displacements. The amplitude of the longitudinal relative displacements was larger at the center of the roof than along the longitudinal walls. However, the relative displacement records for channels 10, 11, and 12 were considered to be unreliable.

- The transverse relative displacements of the roof sustained by the Hollister warehouse during the Loma Prieta earthquake were an order of magnitude larger than the relative displacements of the roof during the Morgan Hill and Hollister events. The maximum relative roof displacement in the transverse direction during the Loma Prieta earthquake was on the order of 1% of the building height.

- The out–of–plane displacements at the top of the longitudinal wall panel were consistently larger than the response at midheight of the panel.

5.2 Redlands Warehouse

The east elevation of the Redlands warehouse is shown in Fig. 5.19 and the floor plan is shown in Fig. 5.20. The building is divided nearly in half by a non–bearing stud partition wall. Panels south of the fire wall are 22–ft wide and panels north of the fire wall are 20–ft wide. Panels along the transverse sides of the building are 22½–ft wide. All panels are 7–in. thick. Pilasters are used to connect adjacent panels.

Cambered glulam beams span between the longitudinal walls (Fig. 5.21). The ½–in. plywood sheathing is supported by 4x14 purlins at 8–ft on center and 2x4 rafters at 2–ft on center. All four openings in the perimeter walls (two overhead doors and two personnel doors) were located in the east, longitudinal wall (Fig. 5.22).

Structural response during the 1986 Palm Springs, 1992 Landers, and 1992 Big Bear earthquakes was recorded at 12 locations. Three instruments recorded ground motion, five recorded transverse response at the roof, three recorded longitudinal response at the roof, and one recorded the out–of–plane response of a longitudinal wall panel at midheight. Instrument locations are indicated in Fig. 5.20 and summarized in Table 5.4. Horizontal ground acceleration histories recorded at the base of the warehouse are shown in Fig. 5.24 for the Palm Springs earthquake. Corresponding linear response spectra are presented in Fig. 5.25. Digitized data are not yet available from the Landers and Big Bear earthquakes.

Acceleration histories are shown in Fig. 5.26, 5.27, and 5.28 for the Palm Springs, Landers, and Big Bear earthquakes, respectively. Observations from the acceleration response are summarized below:

- The maximum transverse acceleration response was measured at the quarter–point of the longitudinal walls (channel 5) during the Palm Springs and Landers earthquakes, indicating that the non–bearing fire wall and overhead door openings in the longitudinal wall influenced the dynamic response of the structure. During the Big Bear earthquake, maximum transverse accelerations were recorded at the center of the longitudinal wall (channel 4). This change in behavior indicates that the stiffness of the fire wall decreased during the Big Bear event, however, no information on observed damage is available.

- The amplitude of the transverse accelerations at the roof (channels 3 and 5) were 3 to 5 times the amplitude of the transverse ground acceleration (channel 12). The out–of–plane accelerations at midheight of the center longitudinal wall panel (channel 2) were approximately 2.5 times the magnitude of the transverse ground accelerations.

- The magnitude of longitudinal accelerations at the center of the transverse walls at the roof level (channel 9) were amplified by a factor of approximately 3 relative to the longitudinal ground accelerations (channel 11).

- The in–plane acceleration response at the top of the longitudinal (channels 8 and 10) and transverse (channels 6 and 7) walls was approximately the same as the corresponding ground accelerations (channel 11 in the longitudinal direction and channel 12 in the transverse direction).

Normalized Fourier amplitude spectra for the Palm Springs earthquake acceleration records are shown in Fig. 5.29.

- The fundamental transverse natural frequency of the warehouse was observed to be 2.6 Hz. The fundamental natural frequency in the longitudinal direction was 3.2 Hz.

- The Fourier amplitude spectra for in–plane wall response were essentially the same as those for the corresponding ground acceleration records.

Integrated displacement response at the base of the structure and the center of the roof is shown in Fig. 5.30. The longitudinal displacement of the roof was essentially the same as the north–south ground displacement. The transverse response of the roof may be observed in the east–west absolute displacement record.

Unfiltered and filtered relative displacements for the Redlands warehouse are shown in Fig. 5.31. Calculated maximum relative displacements are summarized in Table 5.5 for the unfiltered and filtered records. The following trends may be observed:

- The relative displacement records in the transverse direction at the center of the building (channels 2, 3, 4, and 5) were not significantly affected by the filtering process. Roof–level relative displacements at the quarter–point of the longitudinal wall (channel 5) exceeded those at the center of the longitudinal wall (channel 3), indicating that the fire wall influenced structural response.
- The character of the relative displacement records in the transverse direction at the end of the building (channels 6 and 7) were dramatically changed by the filtering process. The relative displacement records for channels 6 and 7 were considered to be unreliable.
- Longitudinal relative displacement records recorded on the top of the longitudinal walls (channels 8 and 10) were also dominated by the ground displacements. The relative displacement records for channels 8 and 10 were considered to be unreliable. Longitudinal relative displacements recorded at the top of the south transverse wall (channel 9) were not significantly influenced by filtering. The amplitude of the longitudinal relative displacements measured by channel 9 were approximately one–fifth of the transverse relative displacements recorded by channel 5.
- The maximum relative roof displacement sustained by the Redlands warehouse during the Palm Springs earthquake was less than 0.1% of the building height.
- The out–of–plane displacements at the top of the longitudinal wall panel were consistently larger than the response at midheight of the panel.

5.3 Milpitas Industrial Building

The north–west corner of the two–story Milpitas industrial building is shown in Fig. 5.32 and the floor plans are shown in Fig. 5.33. The tilt–up panels are typically 24–ft wide with window openings at both the first and second story levels (Fig. 5.34). Panel thickness varies between 16 in. along the panel edges to 8 in. above and below the windows. Chord reinforcement is located at the second floor and roof levels and is welded between adjacent panels.

Eighteen, structural steel tube columns are used to carry the vertical floor and roof loads. The columns are arranged in a 24x30–ft grid. Deep, open web steel girders span in the longitudinal direction of the building at the second floor level. Open web steel joists span between the girders in the transverse direction and support a metal deck and a 2½–in. concrete slab. Puddle welds were used to connect the metal deck to the joists and girders. The pitched roof is supported by glulam beams running in the transverse direction. The roof diaphragm consists of ½–in. plywood sheathing with 2x4 joists and 6x16 purlins.

Thirteen instruments recorded the response of the building during the 1988 Alum Rock and 1989 Loma Prieta earthquakes. Instrument locations are shown in Fig. 5.35 and summarized in Table 5.6. Five instruments recorded the ground motion, the transverse building response was monitored by three instruments at the roof and three at the second floor, and the longitudinal building response was recorded by one instrument at the roof and one at the second floor. Horizontal ground acceleration histories recorded at the base of the building are shown in Fig. 5.36 for the two earthquakes. Corresponding linear response spectra are presented in Fig. 5.37.

Measured acceleration records are shown in Fig. 5.38 and 5.39 for the Alum Rock and Loma Prieta earthquakes, respectively. Observations are noted below:

- The maximum transverse accelerations recorded at the center of the longitudinal walls at the roof level (channel 4) were approximately 3 times greater than the maximum transverse ground accelerations (channel 9). Maximum transverse accelerations recorded at the second floor level (channel 7) were approximately 25% greater than the transverse ground accelerations.
- The in–plane response of the transverse walls measured at both the roof and second floor levels (channels 3, 5, 6, and 8) was essentially the same as the transverse ground acceleration (channel 7).
- The magnitude of the longitudinal acceleration response, measured at the center of the transverse walls (channel 11 at the roof and channel 12 at the second floor), exceeded the transverse acceleration response at both the roof (channel 4) and second floor level (channel 7) during both earthquakes. Amplification factors, relative to the base, exceeded 4 for longitudinal acceleration response at the roof and were approximately 1.6 at the second floor level.

The corresponding Fourier amplitude spectra are shown in Fig. 5.40 and 5.41. The predominant natural frequencies are between 3.5 and 5 Hz in the transverse direction and between 4.5 and 5.5 Hz in the longitudinal direction. The frequency signature is less pronounced in the data from the 1988 Alum Rock earthquake.

Integrated displacement histories are shown in Fig. 5.42. The amplitude of the ground displacement is an order of magnitude larger during the Loma Prieta earthquake than during the Alum Rock earthquake. As a result of the large ground displacements during the Loma Prieta earthquake, the relative displacements of the structure are not significant. Relative displacements at the roof may be observed in both the longitudinal and transverse directions during the Alum Rock earthquake however.

Unfiltered and filtered relative displacements for the Milpitas industrial building are shown in Fig. 5.43 and 5.44. Calculated maximum relative displacements are summarized in Table 5.7 for the unfiltered and filtered records. The following trends may be observed:

- The signal–to–noise ratios for the relative displacements in the Milpitas industrial building were smaller than those observed for the Hollister and Redlands warehouses. Therefore, the reliability of all the relative displacement data must be questioned.
- The relative displacement records from all channels during the Loma Prieta earthquake were significantly affected by the filtering process.

- Only two channels of relative displacement data during the Alum Rock earthquake appear to be insensitive to filtering: channels 4 and 11, which represent the transverse and longitudinal response at the center of the roof. The maximum relative displacement of the roof was less than 0.05% of the height of the building.

5.4 Summary

The measured response of three tilt–up buildings during seven recent earthquakes in California has been presented. Although the structural systems used in the three buildings differ, the following generalizations about the seismic response of tilt–up construction may be made:

- Transverse accelerations were observed to be amplified by a factor of approximately 3 between the base and the center of the roof. The measured out–of–plane response at midheight of the longitudinal wall panels was amplified relative to the ground accelerations. However, maximum amplification was observed at the roof level.
- The magnitude of the amplification of the longitudinal accelerations appeared to be dependent upon the aspect ratio and structural characteristics of the building. Amplification factors ranged from 1.5 in the Hollister warehouse to 4 in the Milpitas industrial building.
- In–plane acceleration response of the transverse walls at the roof level was essentially the same as the corresponding ground motion. The magnitudes of the acceleration histories were not amplified appreciably, and the frequency content of the signals was nearly identical.
- Displacement of the roof relative to the ground was more pronounced in the transverse than the longitudinal building response. Maximum out–of–plane displacements at the roof level were approximately twice those measured at the midheight of the panel.
- Non–bearing partition walls and openings in wall panels may influence the behavior of tilt–up construction. Maximum transverse acceleration response was observed at the quarter–point of the longitudinal walls in the Redlands warehouse.

6. OBSERVED PERFORMANCE OF TILT–UP CONSTRUCTION DURING EARTHQUAKES

Investigations of the performance of individual tilt–up structures during the 1964 Alaska, the 1971 San Fernando, the 1987 Whittier Narrows, and the 1989 Loma Prieta earthquakes are summarized in this chapter. Typical types of damage are listed in Table 6.1, along with an indication of the frequency. The observed behavior of tilt–up construction during the four earthquakes is summarized in Sections 6.1 through 6.4. Section 6.5 contains some general observations.

6.1 The 1964 Alaska Earthquake

The 1964 Alaska earthquake damaged tilt–up structures at the Elmendorf Air Force Base and provided the first evidence of the potential seismic vulnerability of this type of construction [32]. The Elmendorf Warehouse suffered the worst structural damage in the area: three of five bays collapsed. The plan view of the building is shown in Fig. 6.1 and typical roof framing and concrete fire wall details are shown in Fig. 6.2. Adjacent structures of different forms of construction sustained only minor damage, implying that the cause of the collapse was not the magnitude of the earthquake (M_L=8.3–8.6) but rather the structural system used in the warehouse.

Following the earthquake, investigators identified the likely cause of failure to be pullout of the anchor bolts from the tilt–up concrete walls. The anchor bolts connected the wall panels to the steel frame and plywood roof diaphragm. This failure mechanism could have been prevented by installing ties in the concrete column to confine the anchor. Brittle failure of the steel reinforcement in concrete columns and of the welds connecting the cross bracing in the fire walls to the steel roof framing members was also observed [32]. These connections were unable to develop the full strength of the structural members, suggesting problems related to insufficient connection ductility, as well as connection strength.

6.2 The 1971 San Fernando Earthquake

Major structural damage was observed in tilt–up warehouses located in the Sylmar Industrial Tract and San Fernando Industrial Tract following the 1971 San Fernando earthquake. Studies of eight tilt–up buildings are reported in Ref. 41 and 55. Collapse of the roof or wall panels was observed in four of these structures.

Most of the failures were attributed to inadequate connection details between the plywood diaphragm, the ledger beams, and the tilt–up panels (Fig. 3.20). Three modes of failure occurred at this interface:

- plywood pulled through the nails;
- nails pulled out of the ledger;
- ledgers split in cross–grain bending (Fig. 6.3).

Once the panel–to–roof connection failed, the roof framing system was susceptible to failure of the glulam–to–pilaster or purlin–to–ledger connections. Loss of these connections allowed the framing members to slip off their seats, leading to collapse of the roof. The out–of–plane resistance of the tilt–up panels is essentially zero once the adjacent roof element has fallen or the panel–to–roof connection has failed. The wall panel is then also susceptible to collapse.

Evaluation of the roof and wall collapses that occurred during the 1971 San Fernando earthquake indicates that most roof collapses originated in areas where the purlins framed into the wall panels (Fig. 6.4). High in–plane shear forces develop along the shorter side of the diaphragm and therefore the plywood–to–ledger connections along the end walls are more susceptible to damage than connections along the longitudinal walls. Also, beam seats provide more stability and redundancy to connections between glulam beams and concrete pilasters than the hangers used to form the connections between purlins and ledgers. After the plywood–to–ledger connections are lost, it is reasonable to assume that the next failure mechanism will occur at the connection of purlins to other framing elements.

Significant damage also occurred in buildings that did not collapse. Cracking and spalling of the pilasters or corbels was observed in three of the eight tilt–up buildings considered [41,55]. Cracking and permanent out–of–plane deformations were also observed in the wall panels. Damage to wall panels was attributed to excessive flexural deformation due to large in–plane roof deformations [41]. Damage to corbels and pilasters spalling was also attributed to displacement of the roof diaphragm.

As a result of the poor performance of the plywood–to–ledger connections during the 1971 San Fernando earthquake (Fig. 3.20), provisions were added to Section 2312(j) of the Uniform Building Code to prohibit the use of these connections in regions of high seismic risk [75]. Positive, direct connections between the roof diaphragms and the supporting walls are currently required in Section 2310 of the UBC [77].

6.3 The 1987 Whittier Narrows Earthquake

The 1987 Whittier Narrows earthquake provided the first major test of the tilt–up design requirements adopted following the San Fernando earthquake. The number of roof and wall panel collapses during the Whittier Narrows earthquake was greatly reduced compared with those during the 1971 San Fernando earthquake, and all occurred in structures built before 1971. However, the magnitude of the 1987 earthquake (M_L=5.9) was considered moderate, as compared with the 1971 earthquake (M_L=6.4). Therefore, the possibility that greater structural damage will occur during a stronger earthquake can not be dismissed for tilt–up buildings designed using the post–1978 UBC provisions.

The most severe damage in more modern tilt–up structures during the 1987 earthquake occurred in buildings that had wall panels with large openings. Observations of panels bowing out and cracking near the upper corners of openings were common in buildings constructed after 1983. This type of damage has been attributed to two sources [35]:

- insufficient panel reinforcement, or incorrect placement of reinforcement within the panel;
- openings had been cut into existing panels without providing additional reinforcement.

Adham et al. [10] suggest that panels with large openings should be proportioned to resist flexural action as if the panel were a frame: the vertical piers should be designed to resist their own inertial load plus that of the portion of the wall above the opening. Design of these piers should conform to provisions in Section 2625(f)9B of the UBC entitled "Wall Piers" [77].

When modifications are made to an existing building, many owners overlook the need to replace the strength and stability lost when an opening is cut in a tilt–up panel [10,35]. Steel columns or "kickers" are usually recommended to increase the lateral–load resistance of a panel with large openings (Fig. 6.5).

The the response of tilt–up buildings during the 1987 earthquake also highlighted the importance of tying the structure together and providing adequate collector elements to carry the force away from reentrant corners [35]. A number of failures of plywood in roof diaphragms could have been prevented if ties had been provided to ensure that the purlins did not separate from the glulam beams (Fig. 3.26). Distress of roof elements was reported near reentrant corners and skewed joints where framing members were often not able to transmit chord forces into the diaphragm (Fig. 6.6).

Cases of roof distress and plywood failure directly above vertical elements such as stair wells and interior columns or walls were also reported. In many cases, collector elements were not provided to transmit diaphragm forces into the vertical members.

The Whittier Narrows earthquake also provided information on the seismic performance of a number of common construction practices that were developed during the 1970's and 80's. In contrast to buildings constructed before 1971 when cast–in–place pilasters provided continuous connection between adjacent wall panels, the chord reinforcement at the elevation of the diaphragm is the often only panel–to–panel connection in modern tilt–up construction. Additional panel–to–panel connections are provided only in the corners of the building. Changes in the connection design were adopted to improve the durability of tilt–up construction under temperature and shrinkage induced loads. Two tilt–up buildings with minimal panel–to–panel connections were studied following the Whittier Narrows earthquake [10]. Little or no structural damage was observed. However, the individual panels were considered to be more susceptible to damage due to out–of–plane bending than comparable structures with pilasters. The reduction in the number of panel–to–panel connections is also believed to lead to panel uplift [9] .

The structural implications of using steel ledgers and metal screws for the panel–to–roof connections were investigated by studying the behavior of the Downey and Whittier buildings (Fig. 4.26) [10]. Typical panel–to–roof connection details are shown in Fig. 6.7 [9]. The metal screws failed along the transverse walls in the Downey building. Structural damage was expected to be considerably greater if the building had been subjected to the design–level earthquake [9]. Although replacing wooden ledgers with steel ledgers eliminates the cross–grain bending failure mechanism in the panel–to–roof connections shown in Fig. 6.3, it is not sufficient to guarantee acceptable connection performance.

6.4 The 1989 Loma Prieta Earthquake

The satisfactory performance of most engineered buildings during the 1989 Loma Prieta earthquake has been attributed to the relatively short duration of the ground motion [69].

Although there were isolated cases of major damage to tilt–up concrete industrial buildings, collapses were not as widespread as during the 1971 San Fernando earthquake. Several cases in which the contents of the building influenced the structural performance were identified. A tomato–storage warehouse in Hollister lost part of a wall when stacks of cans inside the building fell against the wall panels and broke the connection

between the wall panels and pilasters [69]. In an industrial park west of Watsonville, another tilt-up structure sustained moderate structural damage to several pilasters and a wall panel separated from the roof diaphragm when a free-standing steel-frame mezzanine struck the exterior walls [69].

6.5 Summary

The observed performance of tilt-up buildings during the 1964, 1971, 1987, and 1989 earthquakes indicates that this form of construction is susceptible to structural damage (Table 6.1). Damage in buildings constructed before the 1971 San Fernando earthquake may usually be attributed to:

- wood ledger members failing in cross-grain bending;
- nails pulling through the edges of the plywood at the ledger or at interior panel edges;
- edge nails pulling out of wood ledgers or interior framing members;
- brittle fracture of welded connections.

The damage statistics presented in Table 6.1 indicate that the seismic performance of tilt-up buildings constructed after the 1971 San Fernando earthquake improved significantly. However, the following susceptibilities were identified:

- cracking and permanent out-of-plane deformations in panels with large openings;
- excessive displacement or flexibility of the diaphragms, particularly for those with very large spans;
- improper connection or anchorage details between adjacent wall panels and between the wall panels and the foundation.

7. CONCLUSIONS

Tilt-up construction is a proven cost-effective method of erecting low-rise buildings. However, the need to develop methods to mitigate the seismic hazards continues to grow with the increasing use of tilt-up for commercial and industrial buildings that contain a large number of workers and expensive equipment. Past seismic performance indicates that initial savings during construction can be offset by the cost of repairing structural damage and of downtime following an earthquake.

Tilt-up buildings constructed before 1973 are susceptible to failure of the connections between the wall panels and the roof diaphragm which often leads to the collapse of the roof and wall panels. The 1971 San Fernando earthquake highlighted the risk of vulnerable connections, and building code provisions were soon modified [75] to avoid many problems, such as cross-grain bending in wood ledger beams. However, design procedures developed for traditional warehouse construction may not be appropriate for buildings with geometrically complex floor plans or a large number of openings in the panels. Damage to wall panels with openings and roof connector elements during the 1987 Whittier earthquake indicates that modern tilt-up buildings are also susceptible to seismic damage.

A review of current design procedures and detailed analytical models for tilt-up construction indicates that buildings are often treated as a group of individual components, rather than a complete structural system. The diaphragm and wall panels are considered independently and connections are typically not modelled in the analyses. Although the seismic response is closely tied to connector performance, analytical models are not currently available to evaluate the influence of connection details on the structural response.

The measured response of three tilt-up buildings in California was used to identify trends in the seismic behavior. The buildings represented different eras in tilt-up construction: the structures in Hollister and Redlands were one-story warehouses with plywood roof diaphragms and cast-in-place pilasters, while the structure in Milpitas was two-stories tall, included a metal-deck floor diaphragm and a wood roof, and had window openings in every panel. However, the general nature of response was similar in all three buildings:

- Transverse accelerations measured at the center of the roof were approximately three times larger than the corresponding ground accelerations.
- The amplitudes of the transverse accelerations and displacements at the center of the roof were larger than the amplitudes of the response measured at mid-height of the center longitudinal wall panel.
- The in-plane accelerations measured at the top of the transverse walls were essentially the same as those measured at the base of the walls.

In addition, data from the Redlands warehouse demonstrated that non-bearing partition walls and openings in wall panels may influence the response of tilt-up systems.

These observations are not consistent with the typical design assumptions. For example, the measured response indicated that wall panels do not behave as columns pinned at both ends. The roof of the Hollister warehouse sustained transverse displacements larger than 4 in. (1% of the building height) relative to the base

during the 1989 Loma Prieta earthquake. The middle of the panel experienced a maximum transverse displacement of approximately 2.5 in. during the same event.

The differences between the expected and measured response indicate that the seismic response of tilt–up construction is not completely understood. Additional work is required to develop analytical models that are sensitive to the nature of the critical connections in the building and can be used to mitigate seismic hazards in new and existing construction. With an improved understanding of system behavior, tilt–up construction can be made as safe as it is economical.

REFERENCES

1. ABK, A Joint Venture. "Methodology for Mitigation of Seismic Hazards in Existing Unreinforced Masonry Buildings:Diaphragm Testing." Agbabian/Barnes/Kariotis. *ABK–TR–03*. (R.D. Ewing, A.W. Johnson, and J.C. Kariotis, Principal Investigators). El Segundo, CA. December, 1981.

2. ABK, A Joint Venture. "Methodology for Mitigation of Seismic Hazards in Existing Unreinforced Masonry Buildings: Interpretation of Diaphragm Testing." Agbabian/Barnes/Kariotis. *ABK–TR–05*. (R.D. Ewing, A.W. Johnson, and J.C. Kariotis, Principal Investigators). El Segundo, CA. March 1982 (unpublished).

3. ACI Committee 551. "Tilt–Up Concrete Structures." *ACI 551R–92*. American Concrete Institute. Detroit, MI. 1992.

4. Adham, S.A. "Guidelines for Mitigation of Seismic Hazards in Tilt–Up Wall Structures – Phase 1." Agbabian Associates. Contract No. PFR–8009736. El Segundo, CA. February 1981.

5. Adham, S.A. "The Slender Wall Test Program: Conclusions and Recommendations." *Proceedings*. Structural Engineers Association of California. Sacramento, CA. 1982. pp. 423–447.

6. Adham, S.A. "Response of Slender Precast Concrete Walls to Out–of–Plane Loading." *Proceedings*. Seminar on Precast Concrete Construction in Seismic Zones. Japan Society for the Promotion of Science. Tokyo, Japan. 1986. pp. 311–324.

7. Adham, S.A. "Experimental Data Based Models for Seismic Tilt–Up Wall Design." Agbabian Associates. Vol. I: Final Report. *Report No. R–8515–6165*. El Segundo, CA. April 1987.

8. Adham, S.A. and Agbabian, M.S. "Seismic Design Guidelines for Tilt–Up–Wall Buildings Based on Experimental and Analytical Models." *Proceedings*. Third U.S. National Conference on Earthquake Engineering. Earthquake Engineering Research Institute. Charleston, SC. August 1986. Vol. 3, pp. 1767–1777.

9. Adham, S.A.; Anderson R.W.; Avanessian V.; Kariotis J.C.; and El Mostafa, A. "Evaluation of Tilt–Up–Wall Structural Systems Affected by the Whittier Narrows Earthquake." Agbabian Associates. *Report No. R–8828–6283*. El Segundo, CA. October 1989.

10. Adham, S.A.; Anderson, R.W.; and Kariotis, J.C. "Survey of Tilt–Up–Wall Structural Systems Affected by the Whittier Narrows Earthquake of October 1, 1987." Agbabian Associates. *Report No. R–8820–6296*. Pasedena, CA. September 1990.

11. Adham, S.A. and Ewing, R.D. "Interaction Between Unreinforced Masonry Structures and their Roof Diaphragms during Earthquakes." *Proceedings*. North American Masonry Conference. The Masonry Society. University of Colorado. Boulder, CO. August 1978. Paper No. 57.

12. Agbabian, M.S., and Ewing, R.D. "Anchorage and Diaphragm Systems for Tilt–Up Wall Buildings." *Proceedings*. Third Seminar on Repair and Retrofit of Structures. Ann Arbor, MI. May 1982. pp. 1–28.

13. Aiken, R. "Monolithic Concrete Wall Buildings – Methods, Construction, and Cost." *Concrete International: Design and Construction*. American Concrete Institute. April 1980. Vol. 2, No.4, pp. 24–30.

14. Amrhein, James E. *Reinforced Masonry Engineering Handbook: Clay and Concrete Masonry*. 4th Edition. Masonry Institute of America. Los Angeles, CA. 1983.

15. Arnold, C. "Seismic Performance of Low Rise Commercial Buildings." *Proceedings*. Seismic Performance of Low–Rise Buildings: State–of–the–Art Research Needs. American Society of Civil Engineers. New York, NY. May 1980. pp. 132–145.

16. Athey, J.W., ed. *Test Report on Slender Walls.* American Concrete Institute–SEASC Task Committee on Slender Walls. Los Angeles, CA. September, 1982.

17. Blume, J.A. "The Earthquake Resistance of California School Buildings – Additional Analyses and Design Implications." State of California, Department of Public Works. Sacramento, CA. 1962.

18. Blume, J.A.; Sharpe, R.L.; and Elsesser, E.A. "A Structural–Dynamic Investigation of Fifteen School Buildings Subjected to Simulated Earthquake Motion." State of California, Department of Public Works. Sacramento, CA. 1961.

19. Brooks, H. *The Tilt–Up Design & Construction Manual, Second Edition.* HBA Publications. Newport Beach, CA. 1990.

20. Brown, D.H.; Adams, N.R.; and Hiner, D.L. "Holding Power of Roofing Nails in $^3/_8$" and ½" Plywood." *Laboratory Report Number 87.* Douglas Fir Plywood Association. Tacoma, WA. February 1961.

21. Clough, D.P. "A Seismic Design Methodology for Medium–Rise Precast Concrete Buildings." *Proceedings.* U.S.–Japan Seminar on Precast Concrete Construction in Seismic Zones. Tokyo, Japan. October 1986. Vol. 1, pp. 101–126.

22. *Connectors for Wood Construction: Product and Instruction Manual.* Simpson Strong–Tie Company, Inc. Catalog C–91H–1. San Leandro, CA. January 1991.

23. Countryman, D. "Lateral Tests on Plywood Sheathed Diaphragms". Douglas Fir Plywood Association. *Report No. 55.* Tacoma, WA. March 1952.

24. Courtois, P.D. "Architectural Esthetics of Tilt–Up Panels." *Concrete International: Design and Construction.* American Concrete Institute. June 1986. Vol. 8, No. 6, pp. 16–20.

25. Diekmann, E.F. "Design Details for the Transfer of Forces in Wood Diaphragms to Vertical Elements." *Proceedings.* Workshop on Design of Horizontal Wood Diaphragms. Applied Technology Council. Berkeley, CA. 1980. pp. 199–252.

26. Dolan, J.D. "The Dynamic Response of Timber Shear Walls." Ph.D. Thesis, submitted to the Graduate College, University of British Columbia. Vancouver, Canada. October 1989.

27. Ewing, R.D. "Seismic Performance of Low–Rise Concrete and Masonry Buildings." *Proceedings.* Seismic Performance of Low–Rise Buildings: State–of–the–Art Research Needs. American Society of Civil Engineers. New York, NY. May 1980. pp. 66–71.

28. Ewing, R.D. and Adham, S.A. "Guidelines for Mitigation of Seismic Hazards in Tilt–Up Wall Structures – Phase 2." Agbabian Associates. *Report No. R–8216–5771.* El Segundo, CA. January 1985.

29. Ewing, R.D.; Kariotis, J.C.; and El–Mustapha, A.M. "LPM/I: A Computer Program for the Nonlinear, Dynamic Analysis of Lumped Parameter Models." *TCCMAR Report 2.3.1.* Kariotis and Associates. South Pasadena, CA. July 1988.

30. Foley, R.P. "Tilt–Up Construction and the Designer–Contractor Team." *Concrete International: Design and Construction.* American Concrete Institute. June 1986. Vol. 8, No. 6, pp. 51–53.

31. Forbes, M.A. "Implementation and Performance of Structural Details – Tilt–Up Concrete." Structural Engineers Association of Northern California. San Francisco, CA. 1991.

32. George, W.; Knowles, P.; Allender, J.K.; Sizemore, J.F.; and Carson, D.E. "Structures on Military Installations." *The Great Alaska Earthquake of 1964: Engineering.* National Academy of Sciences, Washington, D.C., 1973. pp. 873–957.

33. *Glulam Panelized Wood Roof Systems*. The American Institute of Timber Construction. Englewood, CO. 1986.

34. *Guidelines for the Design of Horizontal Wood Diaphragms*. Prepared for the Applied Technology Council by H.J. Brunnier Associates. Berkeley, CA. September 1981.

35. Hamburger, R.O.; McCormick, D.L.; and Hom, S. "The Whittier Narrows Earthquake of October 1, 1987 – Performance of Tilt–Up Buildings." *Earthquake Spectra*. Earthquake Engineering Research Institute. May 1988. Vol. 4, No. 2, pp. 219–254.

36. Hart, G.C. and Kariotis, J.C., ed. "U.S.–Japan Coordinated Research Program." *Proceedings*. Fourth North American Masonry Conference. University of California, Los Angeles, CA. Vol. 2, August 1987. pp. 38–1 to 47–17.

37. Huang, M.; Shakal, A.; Cao, T.; Fung, P.; Sherburne, R.; Sydnor, R.; Malhotra, P.; Cramer, C.; Su, F.; Darragh, R.; and Wampole, J. "CSMIP Strong–Motion Records from the Big Bear, California Earthquake of 28 June 1992." *Report No. OSMS 92–10*. California Strong Motion Instrumentation Program, California Department of Conservation, Division of Mines and Geology, Office of Strong Motion Studies, August 1992.

38. Huang, M.J.; Shakal, A.F.; Parke, D.L.; Sherburne, R.W.; and Nutt, R.V. "Processed Data from the Strong–Motion Records of the Morgan Hill Earthquake of 24 April 1984 — Part II. Structural–Response Records." *Report No. OSMS 85–05*. California Strong Motion Instrumentation Program, California Department of Conservation, Division of Mines and Geology, Office of Strong Motion Studies, December 1985.

39. Itani, R.Y. and Falk, R.H. "Damage and Collapse Behavior of Low–Rise Wood–Framed Buildings: Diaphragms." Final Report to the National Science Foundation. Washington State University. Department of Civil Engineering. Pullman, WA. 1986.

40. Janke, R. Private Communications. Engineers Northwest, Seattle, WA. April 1991.

41. Jennings, P.C. "Engineering Features of the San Fernando Earthquake of February 9, 1971." California Institute of Technology. Division of Earthquake Engineering and Applied Science. *EERL 71–02*. Pasadena, CA. June 1971. pp. 230–258 and 297–298.

42. Jephcott, D.K. and Dewdney, H.S. "Analysis Methods for Horizontal Wood Diaphragms." *Proceedings*. Workshop on Design of Horizontal Wood Diaphragms. Applied Technology Council. Berkeley, CA. 1980. pp. 173–198.

43. Johnson, J.W. "Lateral Test on a 12– by 60–Foot Plywood–Sheathed Roof Diaphragm." Oregon Forest Products Laboratory. *Report No. T–11*. School of Forestry. Oregon St. College. Corvallis, OR. January 1955.

44. Johnson, J.W. "Lateral Test on a 20– by 60–Foot Roof Diaphragm With Stapled Plywood Sheathing." Oregon Forest Products Laboratory. *Report No. T–13*. School of Forestry. Oregon St. College. Corvallis, OR. December 1955.

45. Johnson, J.W. "Lateral Test of a 20– by 60–Foot Roof Section Sheathed with Plywood Overlaid on Decking." Forest Research Laboratory. *Report T–29, Paper 794*. School of Forestry. Oregon State University. Corvallis, OR. November 1971.

46. Kelly, D.L. "Rigging the Tilt–Up." *Concrete International: Design and Construction*. American Concrete Institute. June 1986. Vol. 8, No. 6, pp. 36–40.

47. Luttrell, L.D. *Diaphragm Design Manual, DDM01*. Steel Deck Institute. St. Louis, MO. 1981.

48. Luttrell, L.D. *Diaphragm Design Manual, Second Edition.* Steel Deck Institute. Canton, OH. 1991.

49. Luttrell, L.D. and Huang, H.T. "Steel Deck Diaphragm Studies." *Diaphragm Design Manual, DDM01.* Steel Deck Institute. St. Louis, MO. 1981.

50. Malhotra, S.K. "State–of–the–Art Report:Analysis and Design of Wood Shear Walls and Diaphragms." *Proceedings.* International Conference on Engineering for Protection from Natural Disasters. Asian Institute of Technology. Bangkok, Thailand. January 1980. pp. 287–298.

51. McBean, R.P. "Seismic Analysis of Rigid Diaphragms and Shear Walls." *Seismic Design of Commercial and Industrial Buildings*, University of Missouri, Columbia, MO, 1987.

52. McLean, R.S. "Testing of Slender Walls." *Proceedings.* Structural Engineers Association of California. Sacramento, CA. 1982. pp. 409–422.

53. Mehrain, M. and Graf, W.P. "Dynamic Analysis of Tilt–Up Buildings." *Proceedings.* Fourth U.S. National Conference on Earthquake Engineering, Earthquake Engineering Research Institute. Palm Springs, CA. May 1990. Vol. 2, pp. 299–307.

54. Mehrain, M. and Silver, D. "Concrete Wall Anchorage Forces in Industrial Buildings with Flexible Roof Diaphragms." *Proceedings.* Ninth World Conference on Earthquake Earthquake. Tokyo–Kyoto, Japan. August 1988. Vol. 5, pp. 527–531.

55. NOAA/Earthquake Engineering Research Institute Earthquake Investigation Committee, Subcommittee on Buildings. "Low–Rise Industrial and Commercial Buildings." *San Fernando, California, Earthquake of February 9, 1971.* U.S. Department of Commerce, Washington, D.C., 1973. Vol. 1, Part A, pp. 41–128.

56. Peterson, J. "Bibliography of Lumber and Wood Panel Diaphragms." *Journal of Structural Engineering.* ASCE. Vol. 109, No. 12, December 1983, pp. 2838–2852.

57. *Plywood Diaphragm Construction.* American Plywood Association. Tacoma, WA. 1978. 13 p.

58. Polensek, A. "Damping Capacity of Nailed Wood–Joist Floors." *Wood Science.* Vol. 8, No. 2, October 1975, pp. 141–151.

59. "Processed Strong–Motion Data from the Milpitas 2–Story Industrial Building for the Alum Rock Earthquake of 12 June 1988." *Report No. OSMS 91–13.* California Strong Motion Instrumentation Program, California Department of Conservation, Division of Mines and Geology, Office of Strong Motion Studies. 1991.

60. "Processed Strong–Motion Data from the Loma Prieta Earthquake of 17 October 1989 — Building Records." *Report No. OSMS 91–07.* California Strong Motion Instrumentation Program, California Department of Conservation, Division of Mines and Geology, Office of Strong Motion Studies. 1991

61. "Processed Strong–Motion Data from the Palm Springs Earthquake of 8 July 1986 — Building Records." *Report No. OSMS 91–16.* California Strong Motion Instrumentation Program, California Department of Conservation, Division of Mines and Geology, Office of Strong Motion Studies. 1991

62. Rea, D.; Boukamp, J.G.; and Clough, R.W. "Dynamic Properties of McKinley School Buildings". University of California. *EERC 68–4.* Berkeley, CA. November 1968.

63. Robb, J.O. "Seismic Performance of Low–Rise Buildings Experience with Los Angeles Building Code." *Proceedings.* Seismic Performance of Low–Rise Buildings: State–of–the–Art Research Needs. American Society of Civil Engineers. New York, NY. May 1980. pp. 42–52.

64. *Roof Decks.* Verco Manufacturing Co. Catalog V–19D. Phoenix, AZ.

65. "Seismic Design for Buildings." U.S. Army TM 5–809–10. Departments of the Army, the Navy and the Air Force. April 1973.

66. Shakal, A.; Huang, M.; Cao, T.; Sherburne, R.; Sydnor, R.; Fung, P.; Malhotra, P.; Cramer, C.; Su, F.; Darragh, R.; and Wampole, J. "CSMIP Strong–Motion Records from the Landers, California Earthquake of 28 June 1992." *Report No. OSMS 92–09*. California Strong Motion Instrumentation Program, California Department of Conservation, Division of Mines and Geology, Office of Strong Motion Studies, August 1992.

67. Shakal, A.; Huang, M.; Reichle, M.; Ventura, C.; Cao, T.; Sherburne, R.; Savage, M.; Darragh, R.; and Peterson, C. "CSMIP Strong–Motion Records from the Santa Cruz Mountains (Loma Prieta), California Earthquake of 17 October 1989." *Report No. OSMS 89–06*. California Strong Motion Instrumentation Program, California Department of Conservation, Division of Mines and Geology, Office of Strong Motion Studies, November 1989.

68. Shakal, A.F. and Ragsdale, J.T. "Acceleration, Velocity and Displacement Noise Analysis for the CSMIP Accelerogram Digitization System." *Proceedings*, Eighth World Conference on Earthquake Engineering, Earthquake Engineering Research Institute, Vol. II, San Francisco, 1984, pp. 111–118.

69. Shepherd, Robin, ed. "Buildings, Loma Prieta Earthquake Reconnaissance Report." *Earthquake Spectra*. Earthquake Engineering Research Institute. May 1990. Vol. 6 (supplement), pp. 127–149.

70. Spears, R.E. "Tilt–Up Construction, Design Considerations – An Overview." *Concrete International: Design and Construction*. American Concrete Institute. April 1980. Vol. 2, No. 4, pp. 33–38.

71. Stern, E.G. "Performance of Mechanical Fasteners in Wood Diaphragms." *Proceedings*. Workshop on Design of Horizontal Wood Diaphragms. Applied Technology Council. Berkeley, CA. 1980. pp. 109–142.

72. Stillinger, J.R., and Countryman, D. "Lateral Tests on Full–Scale Plywood–Sheathed Roof Diaphragms." Oregon Forest Products Laboratory. *Report No. T–5*. School of Forestry. Oregon St. College. Corvallis, OR. October 1953.

73. Tarlton, D.L. "Diaphragm Action." *Design in Cold Formed Steel*. University of Waterloo – Solid Mechanics Division. University of Waterloo Press. Waterloo, Ontario. 1974. pp. 161–182.

74. Tissell, J.R. and Elliott, J.R. "Plywood Diaphragms." American Plywood Association. *Research Report 138*. Technical Services Division. Tacoma, WA. 1990 (revised).

75. *Uniform Building Code*. International Conference of Building Officials. Whittier, CA. 1976.

76. *Uniform Building Code*. International Conference of Building Officials. Whittier, CA. 1988.

77. *Uniform Building Code*. International Conference of Building Officials. Whittier, CA. 1990.

78. Varon, Joseph. "Some Practical Tips in the Architectural Design of Tilt–Up." *Concrete International: Design and Construction*. American Concrete Institute. June 1986. Vol. 8, No. 6, pp. 21–23.

79. Waddell, Joseph J. "Precast Concrete: Handling and Erection." American Concrete Institute. Monograph No. 8. 1974.

80. Weiler, G. "Connections for Tilt–Up Construction." *Concrete International: Design and Construction*. American Concrete Institute. June 1986. Vol. 8, No. 6, pp. 24–28.

81. White, Robert S. (chair). "Recommended Tilt–Up Wall Design." Structural Engineers Association of Southern California. Los Angeles, CA. June 1979.

82. Yasumura, M. and Sugiyama, H. "Rigidity and Strength of Plywood–Sheathed Wall Panels under Reversed Cyclic Loading." *Transactions.* Architectural Institute of Japan. No. 329, July 1983, pp. 64–73.

83. Young, D.H. and Medearis, K. "An Investigation of the Structural Damping Characteristics of Composite Wood Structures Subjected to Cyclic Loading." Department of Civil Engineering, Stanford University. Stanford, CA. April 1962.

84. Zacher, E.G. and Gray, R.G. "Dynamic Tests of Wood Framed Shear Panels." *Proceedings.* 1985 Convention. Structural Engineers Association of California. San Diego, CA. October 1985, pp. 41–61.

85. Zacher, E.G. and Gray, R.G. "Lessons Learned from Dynamic Tests of Shear Panels." *Structural Design, Analysis, and Testing. Proceedings.* Structures Congress 1989. American Society of Civil Engineers. San Francisco, CA. May 1989, pp. 132–142.

TABLE 3.1 ALLOWABLE SHEAR IN LB/FT FOR HORIZONTAL PLYWOOD DIAPHRAGMS WITH FRAMING OF DOUGLAS FIR–LARCH OR SOUTHERN PINE[1] [77]

Plywood Grade	Common Nail Size	Minimum Nominal Penetration in Framing (in.)	Minimum Nominal Plywood thickness (in.)	Minimum Nominal Width of Framing Member (in.)	Blocked Diaphragms				Unblocked Diaphragms	
					Nail spacing at diaphragm boundaries (all cases), at continuos panel edges parallel to load (Cases 3 and 4) and at all panel edges (Cases 5 and 6)				Nails spaced at 6" max. at supported end	
					6	4	2½[2]	2[2]	Load perpendicular to unblocked edges and continuous panel joints (Case 1)	Other configurations (Cases 2, 3, 4, 5 and 6)
					Nail spacing at other plywood panel edges					
					6	6	4	3		
STRUCTURAL I	6d	1 ¼	5/16	2	185	250	375	420	165	125
				3	210	280	420	475	185	140
	8d	1 ½	3/8	2	270	360	530	600	240	180
				3	300	400	600	675	265	200
	10d	1 5/8	15/32	2	320	425	640	730	285	215
				3	360	480	720	820	320	240
C–D, C–C, STRUCTURAL II and other grades covered in U.B.C. Standard No. 25–9	6d	1 ¼	5/16	2	170	225	335	380	150	110
				3	190	250	380	430	170	125
			3/8	2	185	250	375	420	165	125
				3	210	280	420	475	185	140
	8d	1 ½	3/8	2	240	320	480	545	215	160
				3	270	360	540	610	240	180
			15/32	2	270	360	530	600	240	180
				3	300	400	600	675	265	200
	10d	1 5/8	15/32	2	290	385	575	655	255	190
				3	325	430	650	735	290	215
			19/32	2	320	425	640	730	285	215
				3	360	480	720	820	320	240

1 These values are for short–term loads due to wind or earthquake and must be reduced 25% for normal loading. Space nails 12 in. on center along intermediate framing members.
Allowable shear values for nails in framing members of other species set forth in Table No. 25–17–J of the U.B.C. Standards shall be calculated for all grades by multiplying the values for nails in Structural I by the following factors: Group III, 0.82 and Group IV, 0.65.

2 Framing at adjoining panel edges shall be 3–in. nominal or wider and nails shall be staggered where nails are spaced 2 in. or 2½ in. on center.

3 Framing at adjoining panel edges shall be 3–in. nominal or wider and nails shall be staggered where 10d nails having penetration into framing of more than 1 5/8 in. are spaced 3 in. or less on center.

TABLE 3.2 DIAPHRAGM SHEAR STIFFNESS [3]

Category	Range of Shear Stiffness (k/in.)	Type of Diaphragm
Very Flexible	< 6.7	straight and diagonally sheathed wood diaphragms
Flexible	6.7 – 15	special diagonally sheathed wood diaphragms, plywood sheathing, lightly–fastened light–gauge steel decks
Semi–Flexible	15 – 100	plywood sheathing, moderately–fastened medium–gauge steel decks
Semi–Rigid	100 – 1000	heavily–fastened heavy–gauge steel decks, composite diaphragms
Rigid	> 1000	cast–in–place concrete decks

TABLE 3.3 FASTENER SLIP EQUATIONS [74]

Fastener	Minimum Penetration (in.)	For Maximum Loads up to (lb)	Approximate Slip, e_n (in.) [a,b]	
			Green/Dry	Dry/Dry
6d common nail	$1\ ^1/_4$	180	$(V_n/434)^{2.314}$	$(V_n/456)^{3.144}$
8d common nail	$1\ ^7/_{16}$	220	$(V_n/857)^{1.869}$	$(V_n/616)^{3.018}$
10d common nail	$1\ ^5/_8$	260	$(V_n/977)^{1.894}$	$(V_n/769)^{3.276}$
14–ga staple	1 to 2	140	$(V_n/902)^{1.464}$	$(V_n/596)^{1.999}$
14–ga staple	2	170	$(V_n/674)^{1.873}$	$(V_n/461)^{2.776}$

[a] Fabricated green/tested dry (seasoned); fabricated dry/tested dry. V_n = fastener load.

[b] Values based on Structural I plywood fastened to Group II lumber. Increase slip by 20% when plywood is not Structural I.

TABLE 3.4 STRENGTH OF METAL–DECK DIAPHRAGMS [48]

Mode of Failure	Nominal Strength (kip/ft)	Allowable Shear for Design (kip/ft)
Failure of Connections		
Edge Connections	$S_u = \left(2a_1 + n_p\, a_2 + n_e\right)\frac{Q_f}{L}$	$S \le \frac{S_u}{2.75}$ for welded connections
Interior Panel	$S_u = (2A\ (\lambda - 1) + B)\frac{Q_f}{L}$	
Corner Fasteners	$S_u = \sqrt{\frac{(N^2B^2)}{(L^2N^2 + B^2)}}\ Q_f$	$S \le \frac{S_u}{2.35}$ for mechanical connections
Stability	$S_c = \left(\frac{3250}{L_v^2}\right)\left(\frac{I^3 t^3 d}{s}\right)^{0.25}$	$S \le \frac{S_c}{2.0}$

Notation:

- S_u = nominal shear strength of diaphragm, kip/ft
- S_c = critical shear for stability of diaphragm, kip/ft
- S = allowable shear strength for design, kip/ft
- L = panel length, ft
- L_v = purlin spacing, ft
- d = corrugation pitch, in.
- w = width of the deck panel, in.
- t = thickness of the metal deck, in.
- D = panel depth, in.
- Q_f = strength of a structural fastener, kip (defined in Table 3.5)
- Q_s = strength of a sidelap fastener, kip (defined in Table 3.5)
- a_1 = $\Sigma\, x_e\, /w$ = end distribution factor
- a_2 = $\Sigma\, x_p\, /w$ = purlin distribution factor
- a_s = ratio of sidelap fastener strength to structural fastener strength, Q_s/Q_f
- x_e = distance from the panel centerline to a fastener at the end support, in.
- x_p = distance from the panel centerline to a fastener at purlin support, in.
- n_e = number of intermediate sheet–to–structure connections per panel length and between purlins at the diaphragm edge
- n_p = number of purlins excluding those at ends or endlaps
- n_s = number of stitch connections within length L
- A = 1 for single–edge fasteners
  2 for double–edge fasteners
- N = number of fasteners per foot along the ends
- I = moment of inertia of the sheet, $\text{in.}^4/\text{ft}$
- s = developed flute width ($2(e+w) + f$ in Fig. 3.7), in.

$$B = n_s\, a_s + \left(2n_p\, \Sigma\, x_p^2 + 4\, \Sigma\, x_e^2\right)$$

$$\lambda = 1 - \frac{DL_v}{240\sqrt{t}}$$

TABLE 3.5 STRENGTH AND FLEXIBILITY OF CONNECTIONS IN METAL DECK DIAPHRAGMS [48]

(a) Structural Connections

Type of Connector	Strength Q_f (kip)	Flexibility S_f (in./kip)	Notes
Puddle Welds without washers	$2.2\ t\ F_u\ (d - t)$	$\frac{0.00115}{\sqrt{t}}$	(1)
with washers	$99\ t\ (\ 1.33\ d_o + 0.3\ F_{xx}\ t\ )$		(2)
Screwed Connections	$1.25\ F_y\ t\ (1 - 0.005\ F_y)$	$\frac{0.0013}{\sqrt{t}}$	(3)
Power–Driven Pins Ramset 26SD	$62.5\ t\ (1 - 5t)$	$\frac{0.0025}{\sqrt{t}}$	(4)
Hilti ENP2–21–L15 Hilti ENP3–21–L15	$61.1\ t\ (1 - 4t)$	$\frac{0.00125}{\sqrt{t}}$	
Hilti ENKK	$52.0\ t\ (1 - 3t)$	$\frac{0.00156}{\sqrt{t}}$	

(b) Sidelap Connections

Type of Connector	Strength Q_s (kip)	Flexibility S_s (in./kip)	Notes
Puddle Welds without washers	$1.65\ t\ F_u\ (d - t)$	$\frac{0.00125}{\sqrt{t}}$	(1)
with washers	$74.25\ t\ (\ 1.33\ d_o + 0.3\ F_{xx}\ t\ )$		(2)
Screwed Connections	$115\ d\ t$	$\frac{0.0030}{\sqrt{t}}$	(5)
Power–Driven Pins	$240\ t^2$	$\frac{0.030}{\sqrt{t}}$	(6)

Notation:

t = thickness of metal deck, in.
d = average visible diameter of weld, in. or major diameter of screw, in.
F_u = specified minimum strength of metal deck, ksi
d_o = diameter of hole in washer, in.
F_{xx} = electrode strength, ksi
F_y = yield stress of metal deck, ksi.

Notes:

(1) Applicable for deck thicknesses between 0.0285 and 0.0635 in.
(2) Washers are recommended for deck thicknesses less than 0.028 in.
(3) Equations developed for No. 12 and No. 14 screws.
(4) Applicable for deck thicknesses between 0.024 and 0.60 in.
(5) Strength is independent of screw because deck typically fails before screws yield.
(6) Strength and flexibility do not depend on the type of pin.

TABLE 3.6 STRENGTH OF COMPOSITE DIAPHRAGMS [48]

Type of Concrete	Nominal Strength (kip/ft)	Allowable Shear for Design (kip/ft)
Structural	$S_u = \frac{BQ_f}{L} + \frac{\omega^{\frac{3}{2}}\sqrt{f_c'}}{19500}$	$S \le \frac{S_u}{3.25}$
Type I – insulating	$S_u = \frac{BQ_f}{L} + 0.040\sqrt{f_c'}$	
Type II – insulating	$S_u = \frac{BQ_f}{L} + 0.064\sqrt{f_c'}$	

Notation:

S_u = nominal shear strength of diaphragm, kip/ft
S = allowable shear strength for design, kip/ft
L = panel length, ft
w = width of the deck panel, in.
Q_f = strength of a structural fastener, kip (defined in Table 3.4)
Q_s = strength of a sidelap fastener, kip (defined in Table 3.4)
α_s = ratio of sidelap fastener strength to structural fastener strength, Q_s/Q_f
x_e = distance from the panel centerline to a fastener at the end support, in.
x_p = distance from the panel centerline to a fastener at purlin support, in.
n_e = number of intermediate sheet–to–structure connections per panel length and between purlins at the diaphragm edge
n_p = number of purlins excluding those at ends or endlaps
n_s = number of stitch connections within length L
ω = unit weight of concrete, lb/ft^3
f_c' = specified compressive strength of the concrete, psi.
$B = n_s \alpha_s + (2n_p \Sigma x_p^2 + 4 \Sigma x_e^2)$

TABLE 3.7 MAXIMUM DIAPHRAGM DIMENSION RATIOS [77]

Material	Horizontal Diaphragms	Vertical Diaphragms
	Maximum Span–Width Ratios	Maximum Height–Width Ratios
1. Diagonal sheathing, conventional	3:1	2:1
2. Diagonal sheathing, special	4:1	3½:1
3. Plywood and particleboard, nailed all edges	4:1	3½:1
4. Plywood and particle board, blocking omitted at intermediate joints	4:1	2:1

TABLE 4.1 SUMMARY OF EXPERIMENTAL TESTS OF DIAPHRAGMS SUBJECTED TO LOAD REVERSALS

Reference	Number of Diaphragms Tested	Diaphragm Material	Diaphragm Size	Type of Loading	Experimental Variables
Young and Medearis (1962) [83]	8	plywood	8′ x 8′	Static load reversals	Plywood thickness Nail size and spacing Influence of low–amplitude cycles
ABK (1981) [1]	5 6 3	plywood 1″x6″ sheathing metal deck	20′ x 60′	Load reversals (28 mm/sec) Forced vibration (earthquake motion)	Plywood thickness Roofing material and overlays Blocking and chords
Zacher and Gray (1985) [84,85]	9 4	plywood gypsum board	8′ x 8′	Dynamic (2 Hz) 3 cycles per displacement level	Type of fasteners Influence of over–driving fastener Size of nail
Itani and Falk (1986) [39]	5 5	plywood gypsum board	8′ x 24′, 16′ x 16′, or 16′ x 28′	Forced vibration (earthquake motion and sine sweep) Free vibration Static load reversals	Influence of openings Sheathing orientation
Dolan (1989) [26]	19 16	plywood waferboard	8′ x 8′	Static load reversals Sinusoidal loading Shaking table (earthquake motion)	Sheathing orientation Nail spacing Vertical load

TABLE 4.2 SUMMARY OF ABK DIAPHRAGM TESTS [1]

Diaphragm ID	Description	Number of Static Tests	Number of Dynamic Tests	Average Initial Stiffness* (k/in.)
B	½″ plywood, unblocked, chorded	4	6	9.1
C	½″ plywood, unblocked, unchorded, built–up roofing	4	6	6.2
D	½″ plywood, unblocked, chorded, built–up roofing, retrofit nailing	4	7	12.0
E	1″ x 6″ straight sheathing, unchorded, built–up roofing	4	6	6.6
E_1	1″ x 6″ straight sheathing, unchorded, built–up roofing, retrofit nailing	—	4	—
H	1″ x 6″ straight sheathing, 5/16″ plywood overlay, chorded	4	7	14.7
I	1″ x 6″ diagonal sheathing, unchorded, built–up roofing	3	6	18.1
I_1	1″ x 6″ diagonal sheathing, unchorded, built–up roofing, retrofit nailing	—	4	—
K	1″ x 6″ diagonal sheathing, 1″ x 6″ straight sheathing overlay, chorded,	5	7	45.5
N	½″ plywood, blocked, chorded	4	10	20.4
P	¾″ plywood, ¾″ plywood overlay, blocked, chorded,	4	6	52.9
Q	20–ga steel decking, unfilled, unchorded, button–punched seams 18″ O.C.	4	8	16.6
R	20–ga steel decking, unfilled, chorded, button–punched seams 16″ O.C.	4	6	27.9
S	20–ga steel decking, 2½″ concrete fill, chorded, button–punched seams 18″ O.C.	4	7	—

* Measured stiffness during low–amplitude, quasi–static tests.

TABLE 4.3 SUMMARY OF DYNAMIC TESTS OF TILT–UP WALL PANELS [6, 8, 7]

Test No.	Motion Seq. No.	Earthquake*	Effective Peak Acceleration (g)	Diaphragm Stiffness	Panel No.	Reinforcement
1	1	El Centro	0.2	Flexible		
2	2	El Centro	0.2	Rigid		
3	3	Castaic	0.2	Flexible		
4	4	Castaic	0.2	Rigid		
5	5	El Centro	0.4	Flexible		
6	6	El Centro	0.4	Rigid	2	5–#4
7	7	Castaic	0.4	Flexible		
8	8	Castaic	0.4	Rigid		
9	1	El Centro	0.2	Flexible		
10	1	El Centro	0.2	Flexible		
11	2	El Centro	0.2	Rigid		
12	3	Castaic	0.2	Flexible		
13	4	Castaic	0.2	Rigid		
14	5	El Centro	0.4	Flexible		
15	6	El Centro	0.4	Rigid		
16	7	Castaic	0.4	Flexible	3	5–#3
17	8	Castaic	0.4	Rigid		
18	6	El Centro	0.4	Rigid		
19	1	El Centro	0.2	Flexible		
20	2	El Centro	0.2	Rigid		
21	3	Castaic	0.2	Flexible		
22	4	Castaic	0.2	Rigid		
23	5	El Centro	0.4	Flexible		
24	6	El Centro	0.4	Rigid	4	5–#4
25	7	Castaic	0.4	Flexible		
26	8	Castaic	0.4	Rigid		
27	6	El Centro	0.4	Rigid		
28	6	El Centro	0.4	Rigid		
29	6	El Centro	0.4	Rigid		
30**	2	El Centro	0.2	Flexible	4**	5–#4
31**	6	El Centro	0.4	Flexible		

* El Centro – NS component from 1940 El Centro earthquake
Castaic – N69W component from 1971 San Fernando earthquake.

** Panel #4 was repaired with epoxy after Test 29. Tests 30 and 31 were conducted on the repaired panel.

TABLE 5.1 CHARACTERISTICS OF INSTRUMENTED TILT–UP BUILDINGS

Building	Year Designed	Plan Dimensions (ft)	Typical Panel Dimensions*	Connections Between Panels	Type of Diaphragm	Earthquake Records
Hollister Warehouse	1979	300 x 100	18 ft (W) 30 ft (H) 6 in. (T)	Pilasters	Plywood Roof	1984 Morgan Hill 1986 Hollister 1989 Loma Prieta
Redlands Warehouse	1971	242 x 90	22 ft (W) 27 ft (H) 7 in. (T)	Pilasters	Plywood Roof	1986 Palm Springs 1992 Landers*** 1992 Big Bear***
Milpitas Industrial Building (two–story)	1984	168 x 120	24 ft (W) 38 ft (H) 8 in. (T)**	Chord reinforcement welded at roof and 2nd floor levels.	Plywood Roof Metal Deck (2nd Floor)	1988 Alum Rock 1989 Loma Prieta

* W – width of panel, H – height of panel, T – panel thickness

** The thickness of most panels is increased to 16 in. along the vertical edges.

*** Digitized data are not yet available from CSMIP.

TABLE 5.2 SUMMARY OF STRONG-MOTION INSTRUMENTS IN THE HOLLISTER WAREHOUSE

Channel Number	Location	Elevation	Direction	Maximum Acceleration Response (g)			Predominant Frequency (Hz)		
				1984 Morgan Hill	1986 Hollister	1989 Loma Prieta	1984 Morgan Hill	1986 Hollister	1989 Loma Prieta
1	Center North Wall	Ground	Vertical	0.306	0.308	0.177	4.54	3.56	0.29
2	1/4 Point South Wall	Roof	EW	0.066	0.139	0.268	0.66	0.83	0.59
3	Center North Wall	Roof	EW	0.088	0.139	0.257	0.66	0.81	0.59
4	Center	Roof	EW	0.251	0.296	0.818	1.64	1.71	1.10
5	Center West Wall	Roof	EW	0.227	0.281	0.718	1.64	1.71	1.10
6	Center West Wall	Midpanel	EW	0.208	0.347	0.553	1.64	1.71	1.10
7	Center West Wall	Ground	EW	0.058	0.112	0.252	0.66	0.83	0.59
8	Center North Wall	Ground	EW	0.079	0.117	0.254	0.66	0.81	0.59
9	1/4 Point South Wall	Ground	EW	0.062	0.110	0.237	0.66	0.83	0.59
10	Center West Wall	Roof	NS	0.065	0.147	0.388	0.76	1.22	1.94
11	Center	Roof	NS	0.115	0.248	0.445	6.84	6.40	1.90
12	Center East Wall	Roof	NS	0.069	0.126	0.349	0.81	1.22	1.90
13	Center North Wall	Ground	NS	0.065	0.140	0.361	0.81	1.22	1.90

TABLE 5.3 SUMMARY OF RELATIVE DISPLACEMENT DATA FROM THE HOLLISTER WAREHOUSE

Channel Number	Location	Elevation	Direction	Ref. Channel*	Maximum Relative Displacement (in.)					
					1984 Morgan Hill		1986 Hollister		1989 Loma Prieta	
					Unfiltered	Filtered	Unfiltered	Filtered	Unfiltered	Filtered
2	1/4 Point South Wall	Roof	EW	9	0.25	0.06	0.12	0.05	0.60	0.36
3	Center North Wall	Roof	EW	8	0.16	0.05	0.16	0.05	0.38	0.30
4	Center	Roof	EW	7	0.69	0.72	0.73	0.61	4.89	4.30
5	Center West Wall	Roof	EW	7	0.74	0.67	0.66	0.59	4.86	4.20
6	Center West Wall	Midpanel	EW	7	0.44	0.37	0.46	0.41	2.71	2.60
10	Center West Wall	Roof	NS	13	0.20	0.08	0.13	0.06	0.57	0.24
11	Center	Roof	NS	13	0.19	0.06	0.15	0.09	0.58	0.43
12	Center East Wall	Roof	NS	13	0.17	0.07	0.13	0.08	0.36	0.24

* Location of Reference Channels:
Channel 7: Ground, Center West Wall
Channel 8: Ground, Center North Wall
Channel 9: Ground, 1/4 Point South Wall
Channel 13: Ground, Center North Wall

TABLE 5.4 SUMMARY OF THE STRONG-MOTION INSTRUMENTS IN THE REDLANDS WAREHOUSE

Channel Number	Location	Elevation	Direction	Maximum Acceleration Response (g)			Predominant Frequency (Hz)		
				1986 Palm Springs	1992 Landers	1992 Big Bear	1986 Palm Springs	1992 Landers	1992 Big Bear
1	Center West Wall	Ground	Vertical	0.027	0.04	0.06	5.62	–	–
2	Center West Wall	Midpanel	EW	0.094	0.24	0.43	2.56	–	–
3	Center West Wall	Roof	EW	0.129	0.41	0.75	2.56	–	–
4	Center	Roof	EW	0.121	0.34	0.69	2.56	–	–
5	1/4 Point West Wall	Roof	EW	0.242	0.50	0.60	2.56	–	–
6	Center South Wall	Roof	EW	0.039	0.13	0.16	2.05	–	–
7	Center North Wall	Roof	EW	0.050	0.12	0.18	2.05	–	–
8	Center East Wall	Roof	NS	0.044	0.12	0.14	2.61	–	–
9	Center South Wall	Roof	NS	0.113	0.48	0.44	3.15	–	–
10	Center West Wall	Roof	NS	0.041	0.12	0.13	3.15	–	–
11	Center West Wall	Ground	NS	0.041	0.12	0.13	2.71	–	–
12	Center West Wall	Ground	EW	0.046	0.10	0.17	2.05	–	–

TABLE 5.5 SUMMARY OF RELATIVE DISPLACEMENT DATA FROM THE REDLANDS WAREHOUSE

Channel Number	Location	Elevation	Direction	Ref. Channel*	Maximum Relative Displacement (in.) 1986 Palm Springs	
					Unfiltered	Filtered
2	Center West Wall	Midpanel	EW	12	0.12	0.10
3	Center West Wall	Roof	EW	12	0.20	0.19
4	Center	Roof	EW	12	0.21	0.19
5	1/4 Point West Wall	Roof	EW	12	0.34	0.36
6	Center South Wall	Roof	EW	12	0.06	0.02
7	Center North Wall	Roof	EW	12	0.05	0.01
8	Center East Wall	Roof	NS	11	0.02	0.01
9	Center South Wall	Roof	NS	11	0.07	0.07
10	Center West Wall	Roof	NS	11	0.02	0.01

* Location of Reference Channels:
Channel 11: Ground, Center West Wall
Channel 12: Ground, Center West Wall

TABLE 5.6 SUMMARY OF THE STRONG-MOTION INSTRUMENTS IN THE MILPITAS INDUSTRIAL BUILDING

Channel Number	Location	Elevation	Direction	Maximum Acceleration Response (g)		Predominant Frequency (Hz)	
				1988 Alum Rock	1989 Loma Prieta	1988 Alum Rock	1989 Loma Prieta
1	North End of East Wall	Ground	Vertical	0.034	0.081	1.64	0.44
2	South End of East Wall	Ground	Vertical	0.035	0.081	1.64	0.44
3	Center of East Wall	Roof	NS	0.076	0.114	3.49	0.18
4	Center of North Wall	Roof	NS	0.174	0.329	4.83	3.69
5	Center of West Wall	Roof	NS	0.077	0.140	3.49	0.18
6	Center of East Wall	2nd Floor	NS	0.072	0.108	3.49	0.18
7	Center of North Wall	2nd Floor	NS	0.094	0.165	3.49	0.18
8	Center of West Wall	2nd Floor	NS	0.074	0.125	1.39	0.18
9	Center of East Wall	Ground	NS	0.067	0.092	1.29	0.18
10	Center of West Wall	Ground	NS	0.063	0.101	1.29	0.18
11	Center of East Wall	Roof	EW	0.465	0.585	5.44	4.52
12	Center of East Wall	2nd Floor	EW	0.127	0.255	5.18	4.52
13	Center of East Wall	Ground	EW	0.077	0.139	1.68	0.43

TABLE 5.7 SUMMARY OF RELATIVE DISPLACEMENT DATA FROM THE MILPITAS INDUSTRIAL BUILDING

Channel Number	Location	Elevation	Direction	Ref. Channel*	Maximum Relative Displacement (in.)			
					1988 Alum Rock		1989 Loma Prieta	
					Unfiltered	Filtered	Unfiltered	Filtered
3	Center East Wall	Roof	EW	9	0.02	0.01	0.37	0.03
4	Center North Wall	Roof	EW	9	0.09	0.07	0.38	0.18
5	Center West Wall	Roof	EW	10	0.02	0.01	0.29	0.04
6	Center East Wall	2nd Floor	EW	9	0.02	0.01	0.34	0.02
7	Center North Wall	2nd Floor	EW	9	0.06	0.03	0.41	0.08
8	Center West Wall	2nd Floor	EW	10	0.03	0.01	0.45	0.04
11	Center East Wall	Roof	NS	13	0.21	0.16	0.99	0.26
12	Center East Wall	Roof	NS	13	0.06	0.04	0.27	0.07

* Location of Reference Channels:
Channel 9: Ground, Center East Wall
Channel 10: Ground, Center West Wall
Channel 13: Ground, Center East Wall

TABLE 6.1 SUMMARY OF OBSERVED DAMAGE IN TILT-UP BUILDINGS FOLLOWING EARTHQUAKES IN THE U.S.

Observed Damage	Number of Observations of Damage					
	1964 Alaska	1971 San Fernando	1987 Whittier Narrows		1989 Loma Prieta	
			Buildings constructed before 1973	Buildings constructed after 1973	Buildings constructed before 1973	Buildings constructed after 1973
Damage to connection between plywood and interior purlin or plywood and ledger		4	5	1		
Damage to connection between roof framing member and wall panel	1	4	12		1	
Damage to panel to panel connection		2			1	1
Damage to panel to foundation connection				2		
Damage observed in wall panels without openings		4	6	6		2
Damage observed in wall panels with openings			1	15		
Damage to concrete wall panels or pilasters due to bearing		5	2	3	1	
Damage to roof collector elements				5		
Collapse of roof or wall panel	1	4	4		1	
No significant damage			13	19	1	
Total number of buildings surveyed	2	7	35	46	3	2

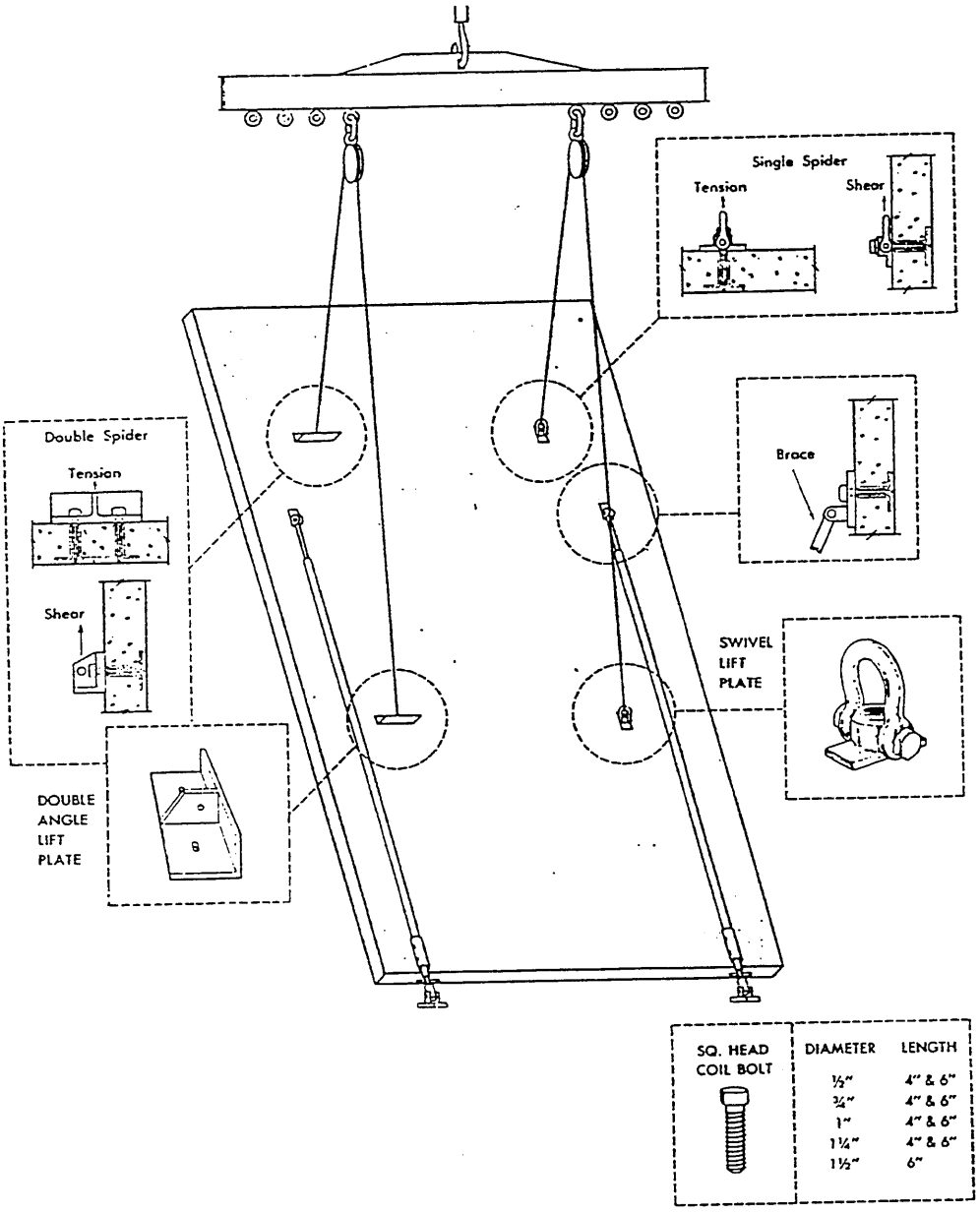

Fig. 2.1 Common arrangement of panel pick points [79].

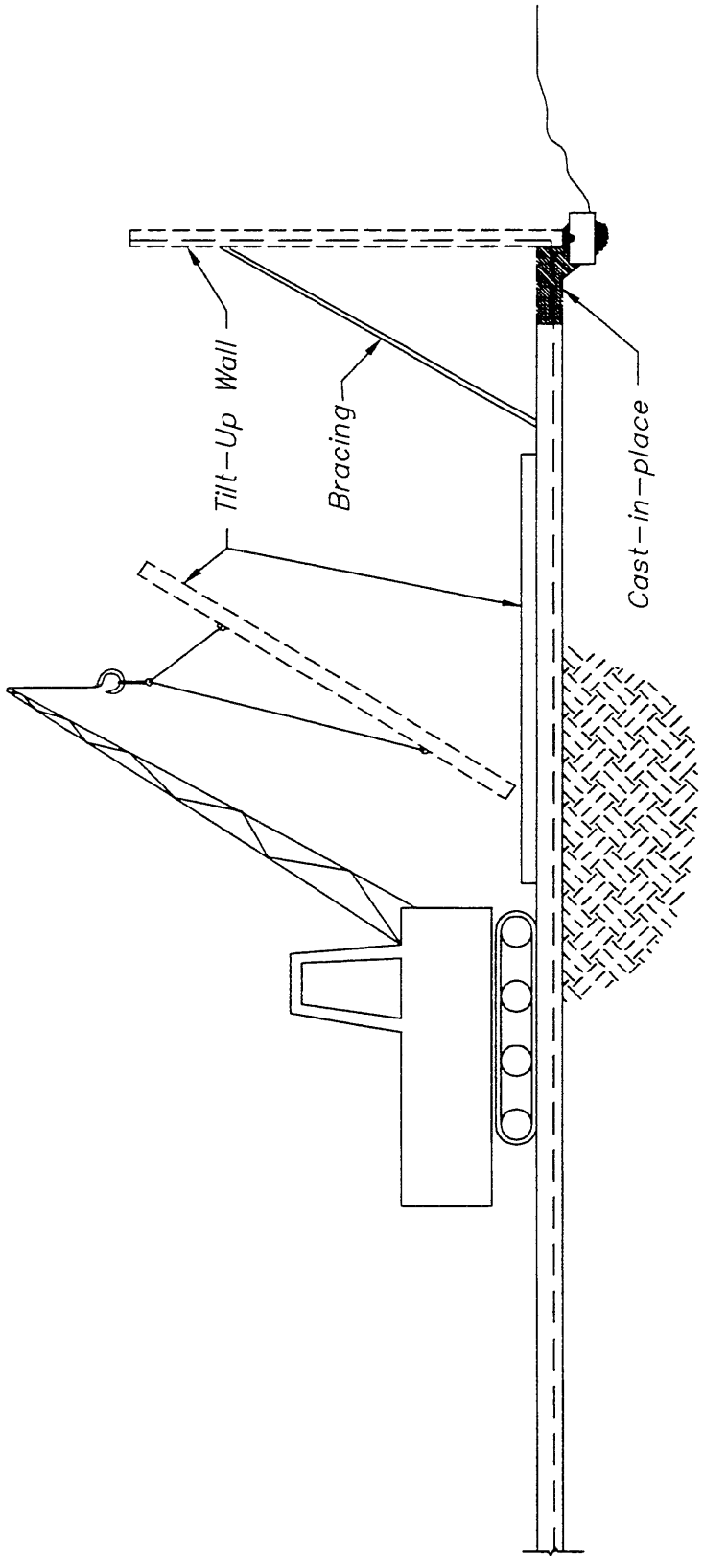

Fig. 2.2 Tilting procedure.

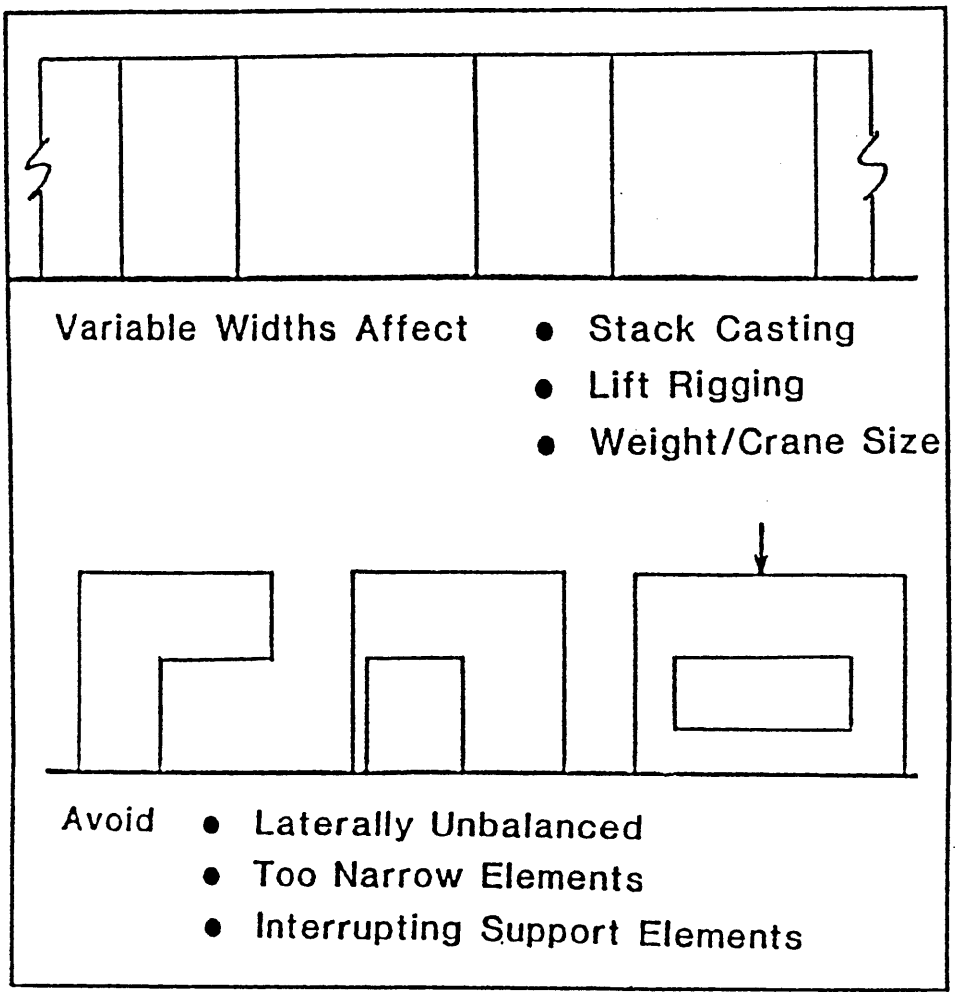

Fig. 2.3 Examples of improper placement of openings [78].

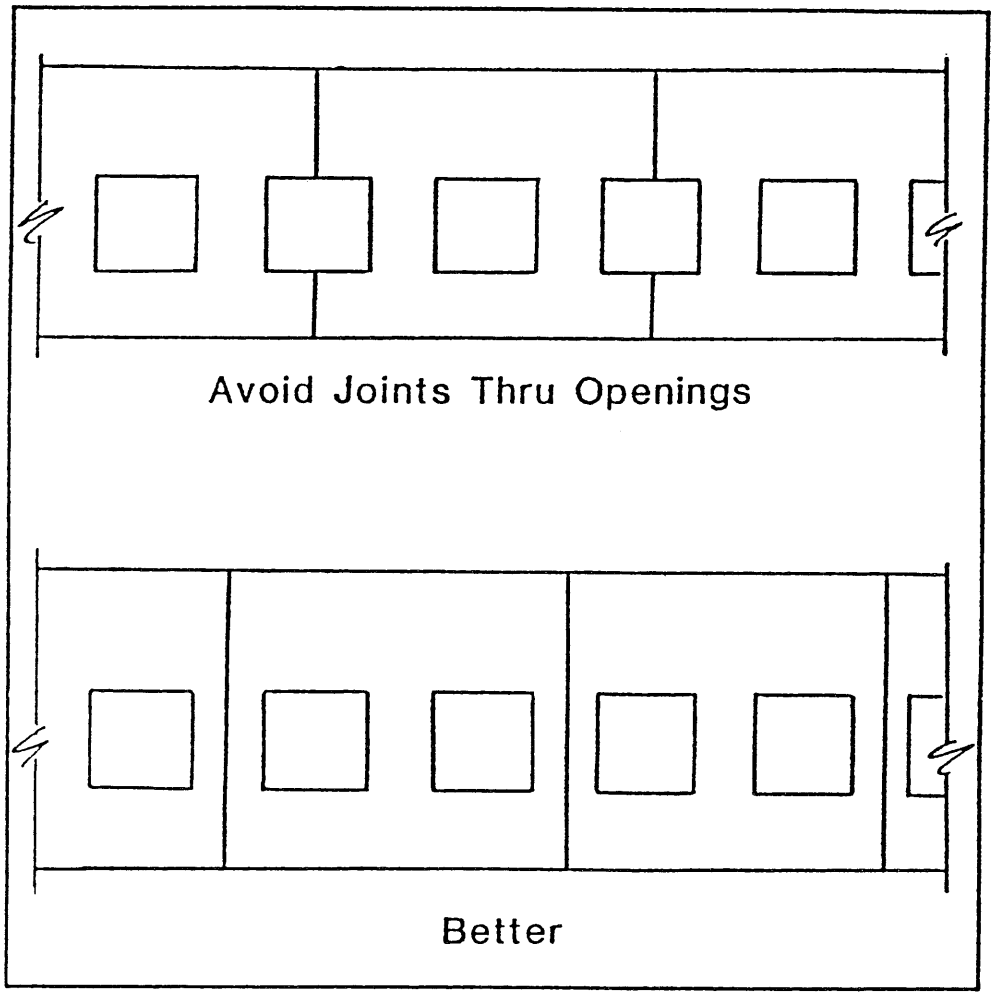

Fig. 2.4 Locations of openings within tilt–up panels [78].

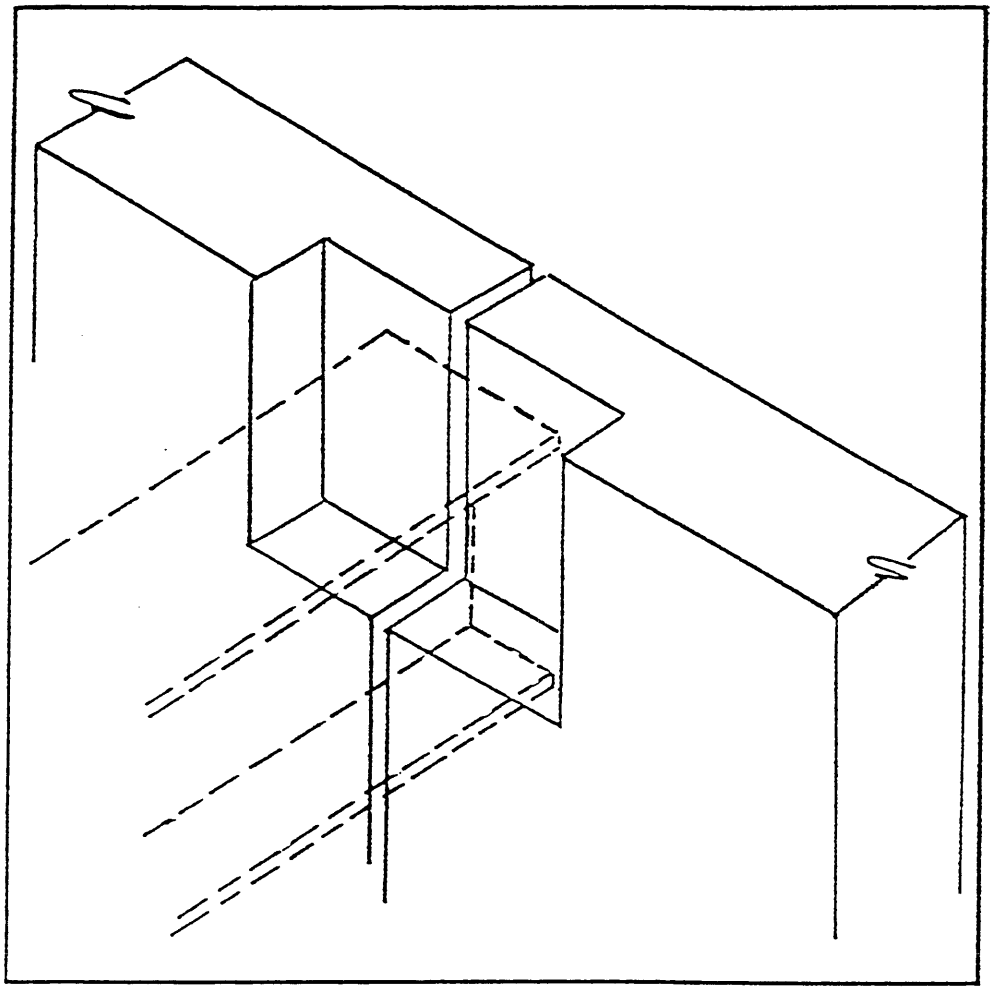

Fig. 2.5 Roof framing member connected to the tilt–up panels at the panel–to–panel joint [78].

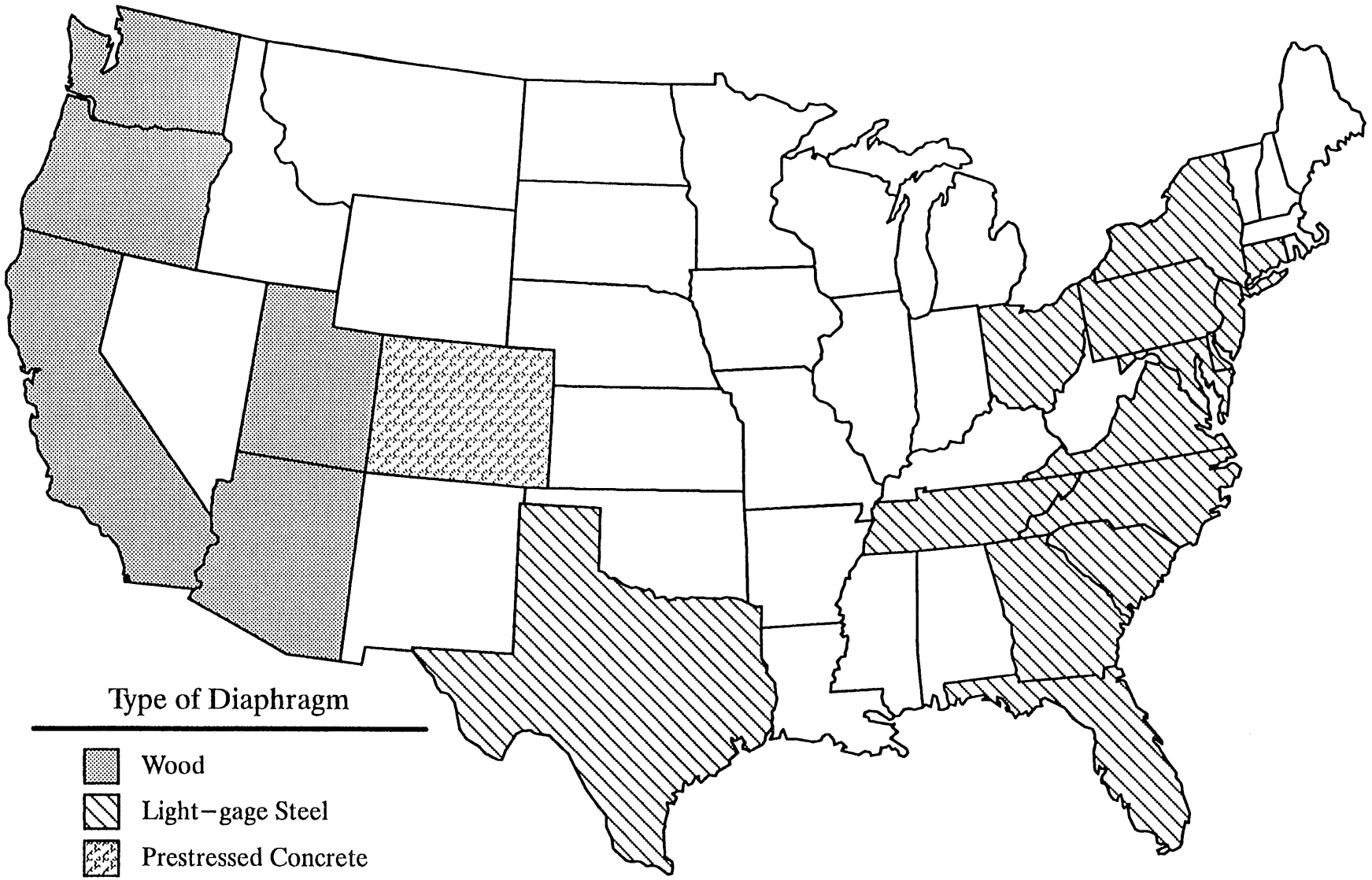

Fig. 2.6 Common types of diaphragms used in tilt–up construction throughout the U.S. [10].

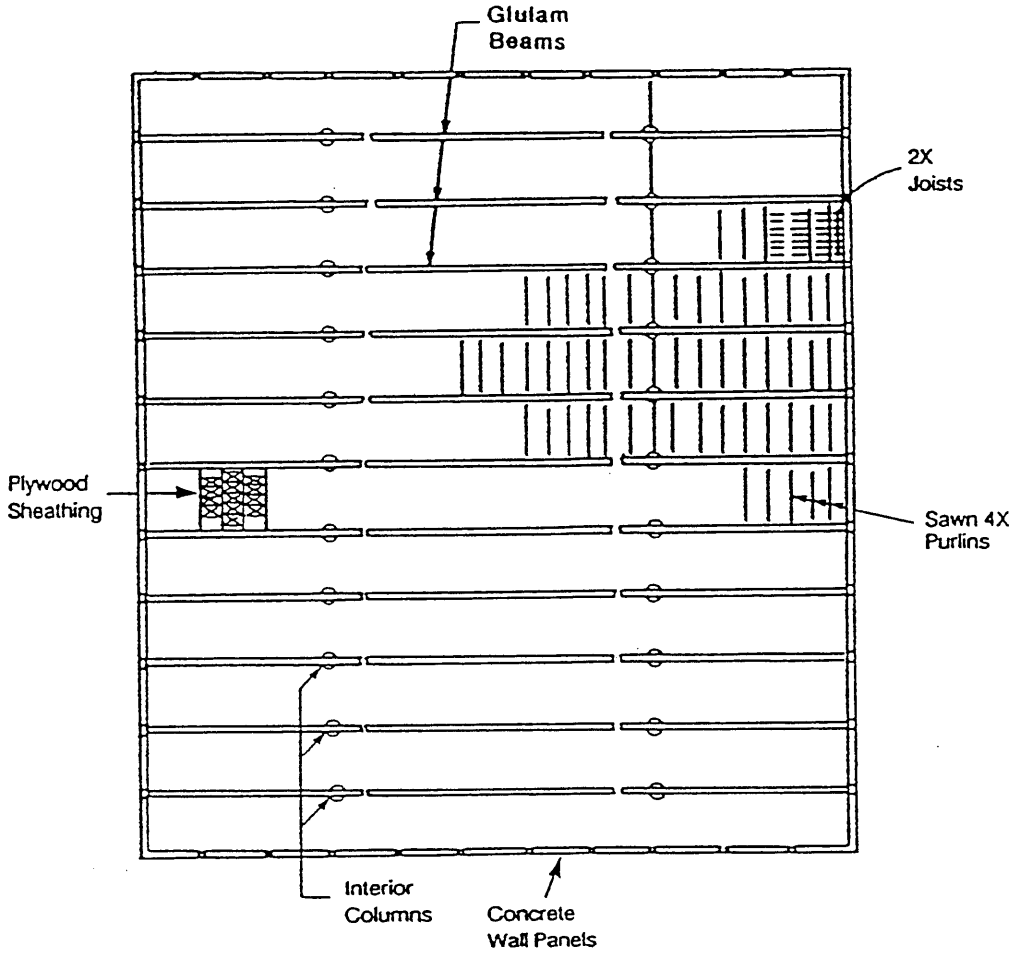

Fig. 2.7 Typical plywood diaphragm [35].

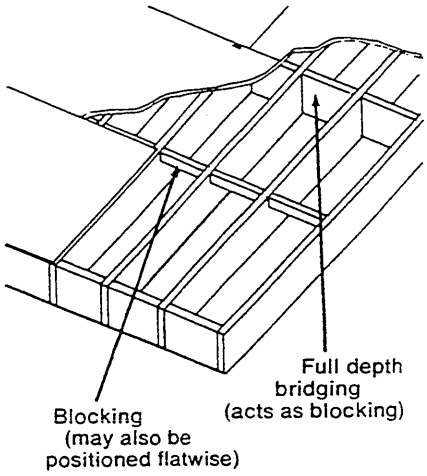

Fig. 2.8 Blocked section of a plywood roof diaphragm [57].

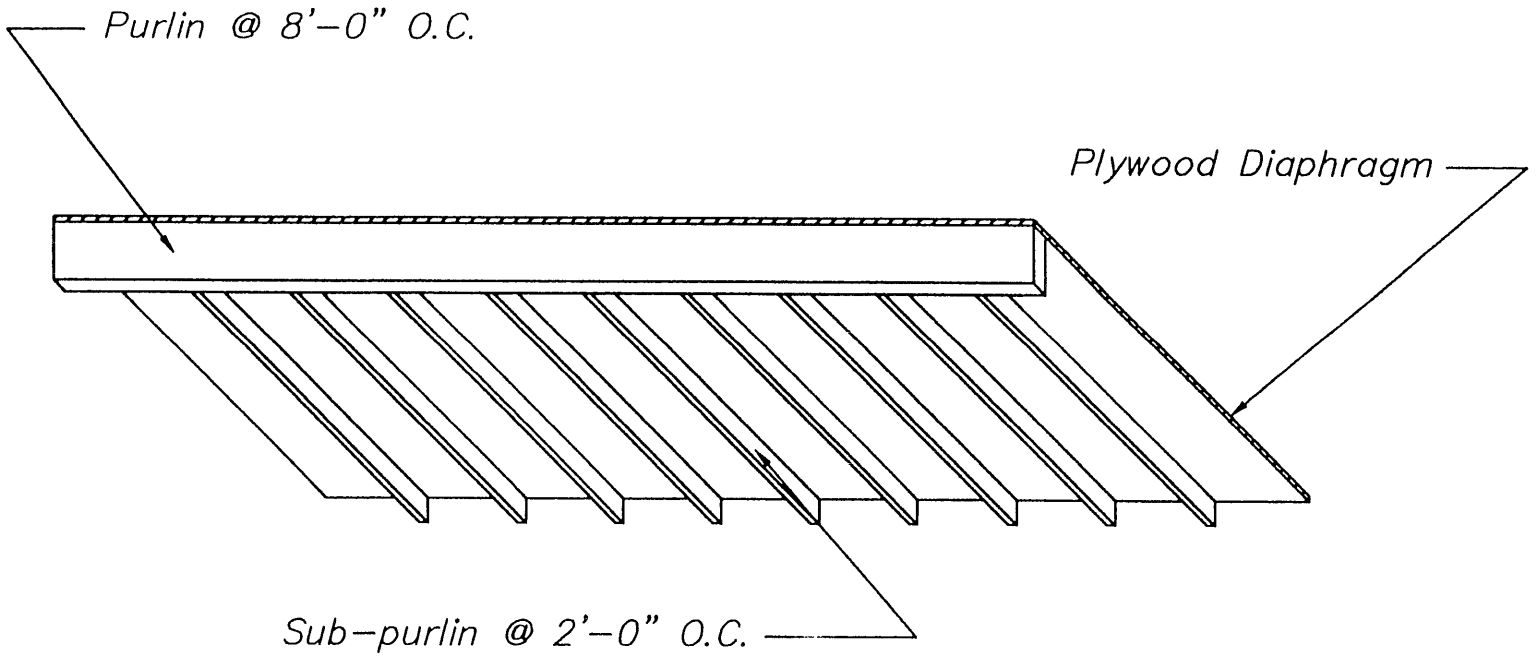

Fig. 2.9 Prefabricated section of a plywood roof diaphragm [33].

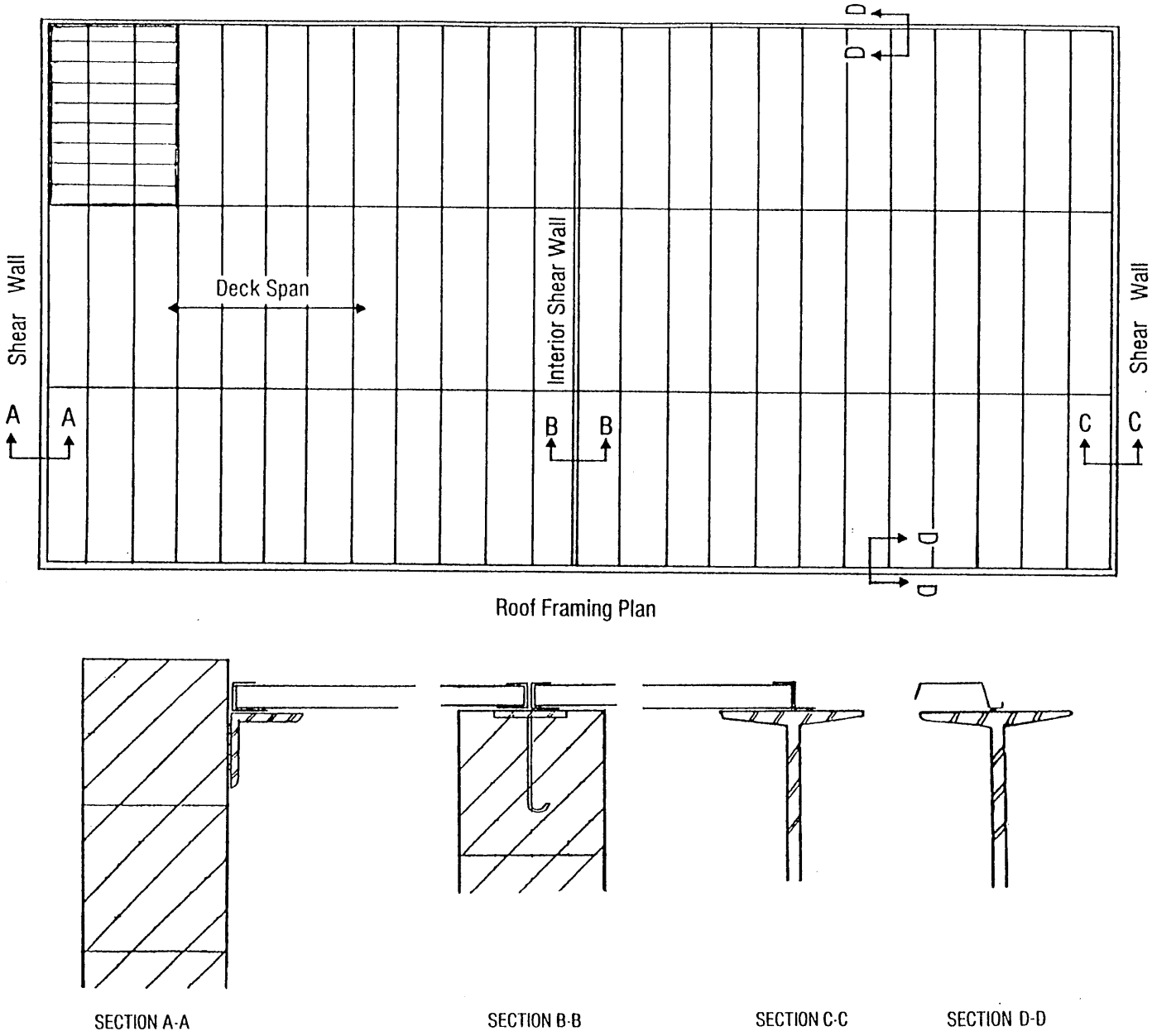

Fig. 2.10 Plan view of a steel diaphragm [64].

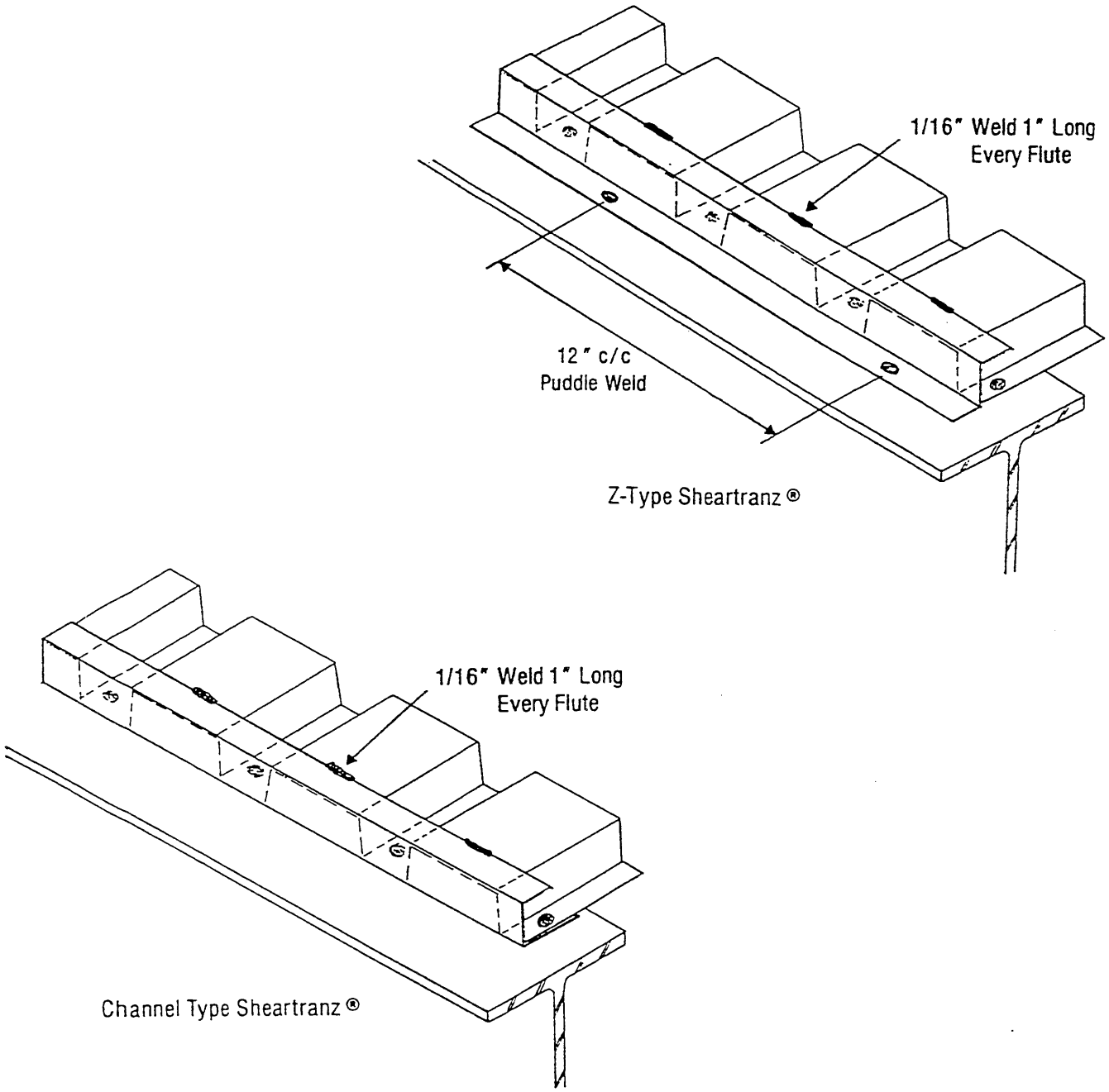

Fig. 2.11 Typical Z– and C– type shear transfer connections [64].

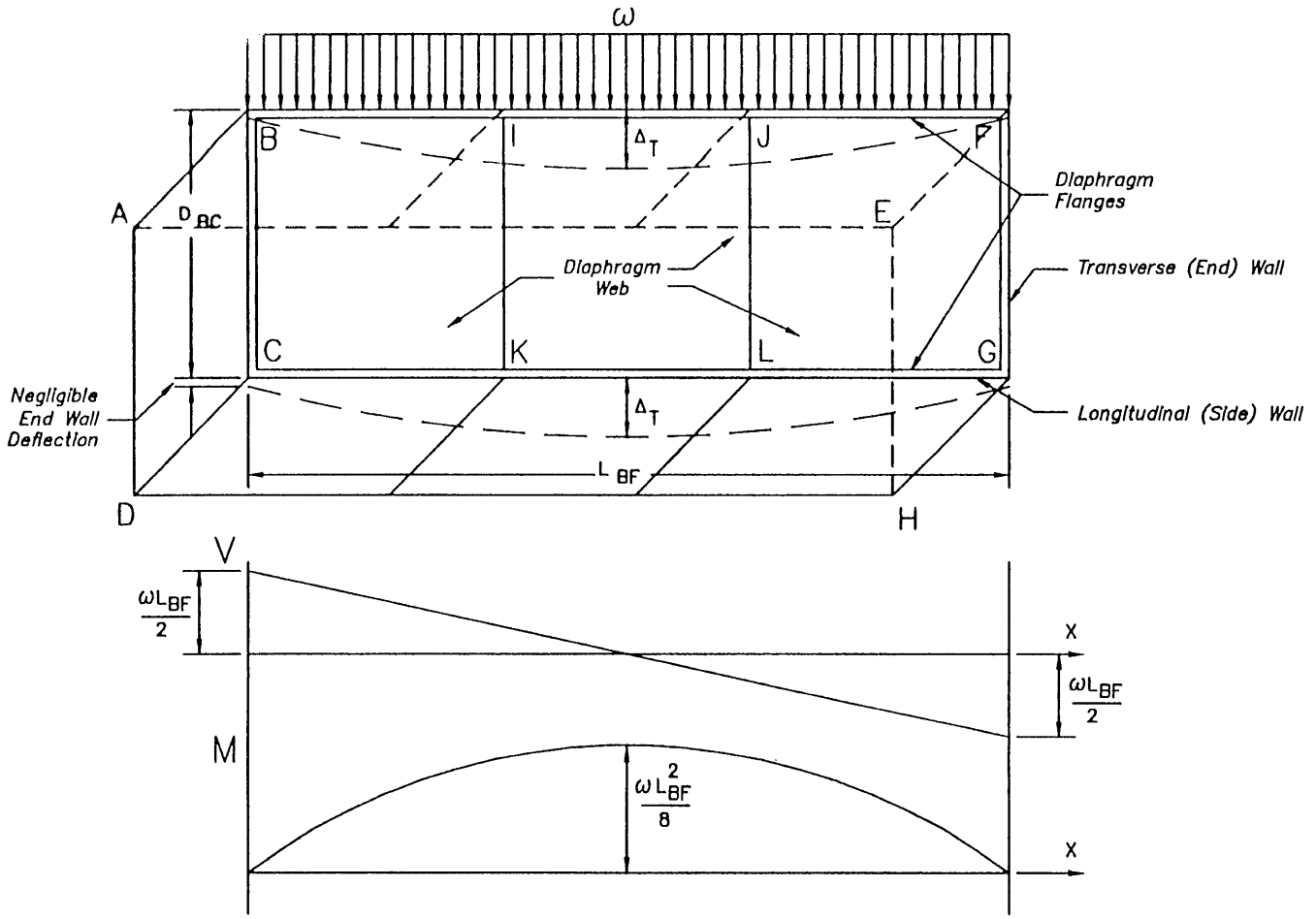

v_{max} = Maximum Shear/ft @ Transverse Walls = $\frac{\omega L_{BF}}{2D_{BC}}$

$T_{CG_{max}}$ or $C_{BF_{max}}$ = Maximum Tensile or Compressive Force in Flange = $\frac{\omega L_{BF}^2}{8D_{BC}}$

For derivation of Δ_T, see Sec. 3.2.1

Fig. 3.1 Idealized force distribution in diaphragm [33].

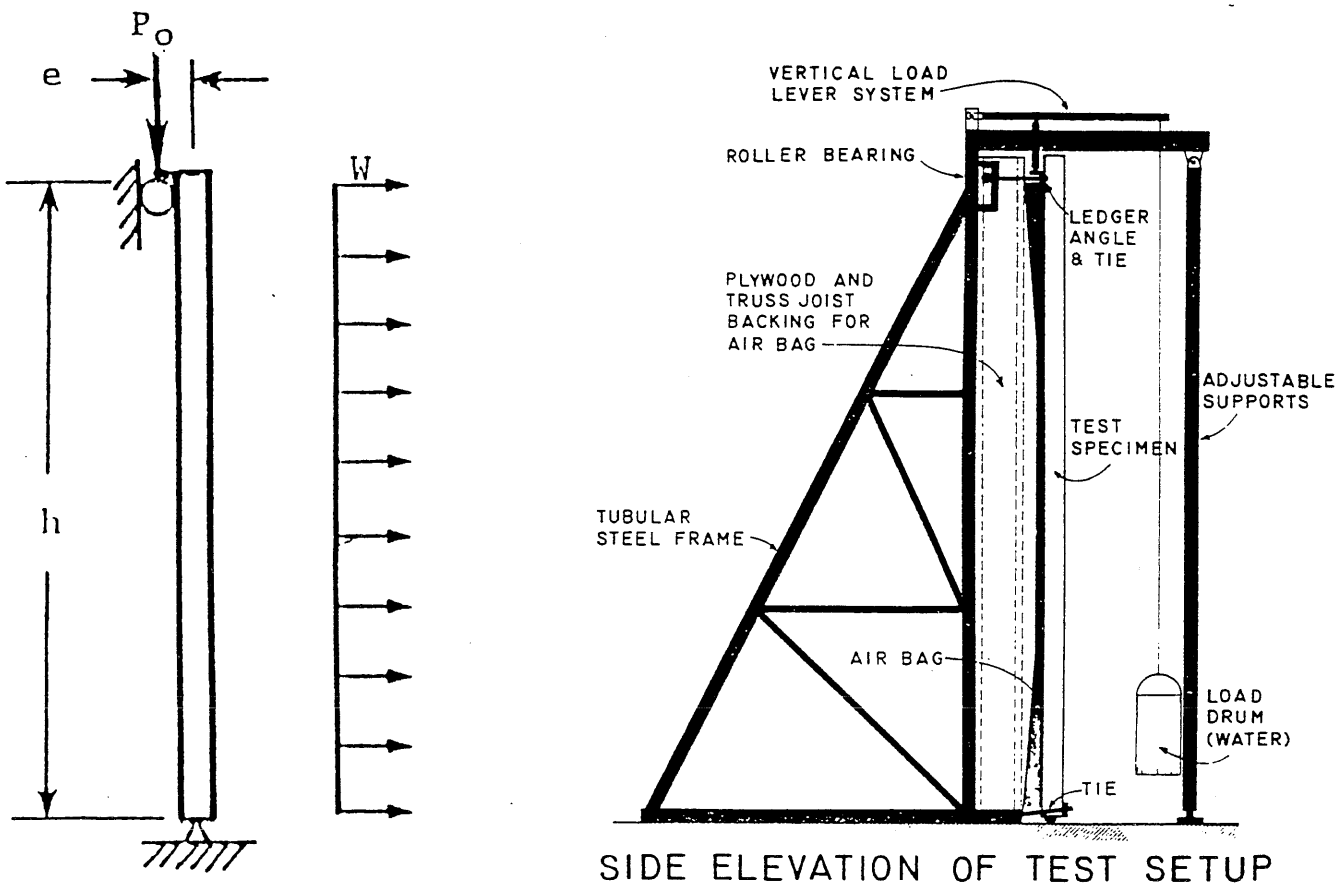

Fig. 3.2 Idealized model of a tilt–up wall panel [16].

Fig. 3.3 Test configuration for ACI–SEASC lateral load tests [16].

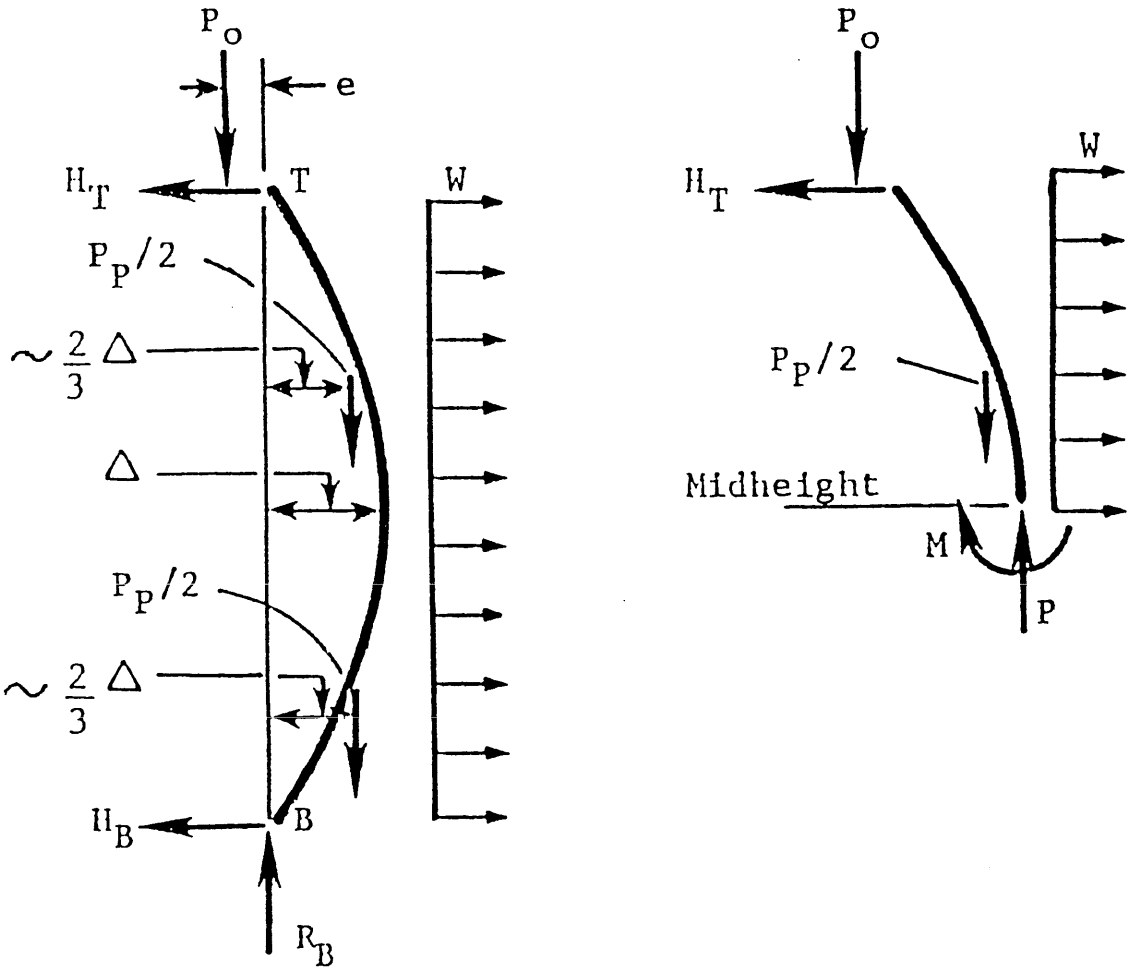

Fig. 3.4 Free body diagram of a tilt–up panel subjected to lateral loading [16].

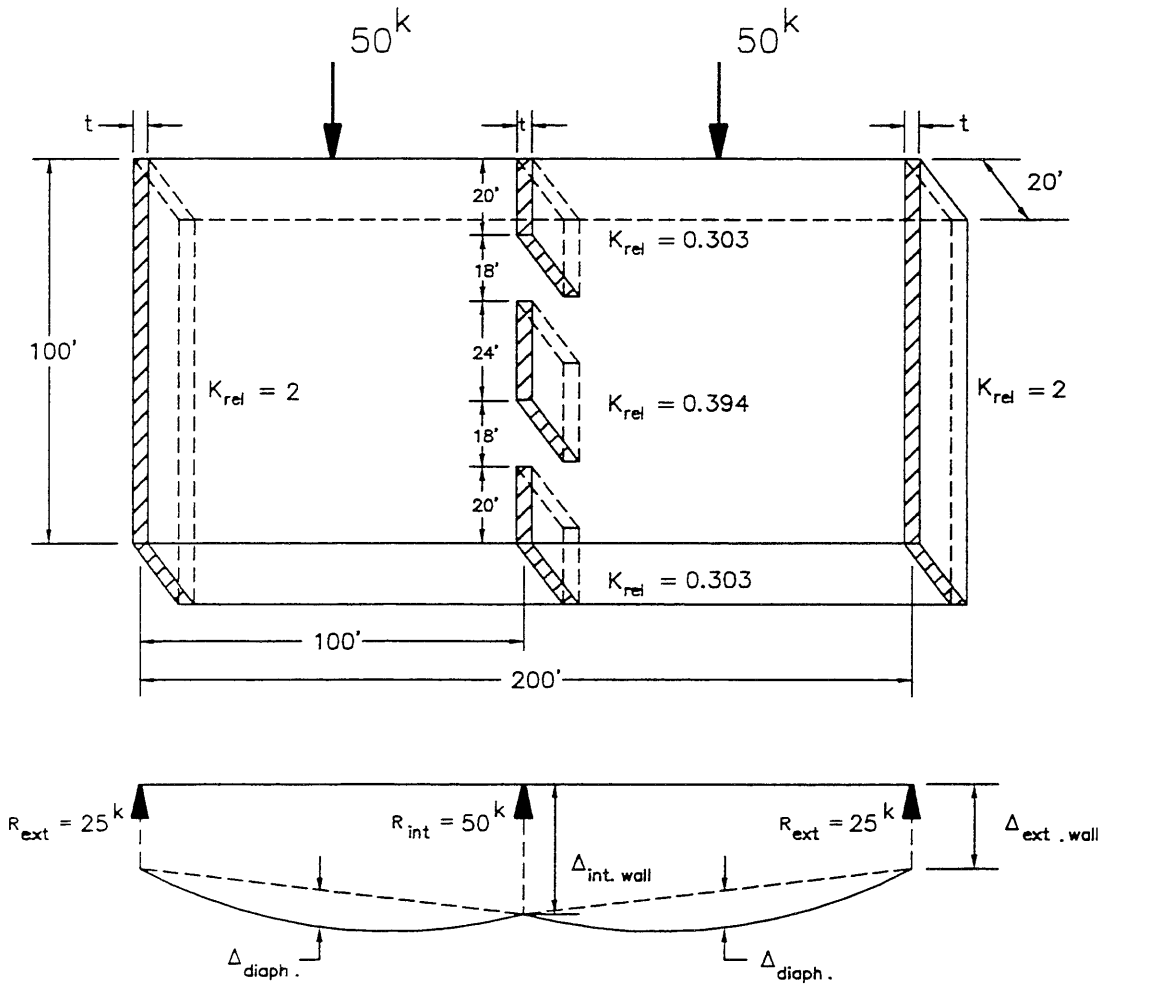

(a) Flexible Diaphragm

(b) Rigid Diaphragm

Fig. 3.5 Distribution of lateral forces to supporting walls in structures with flexible and rigid diaphragms [65].

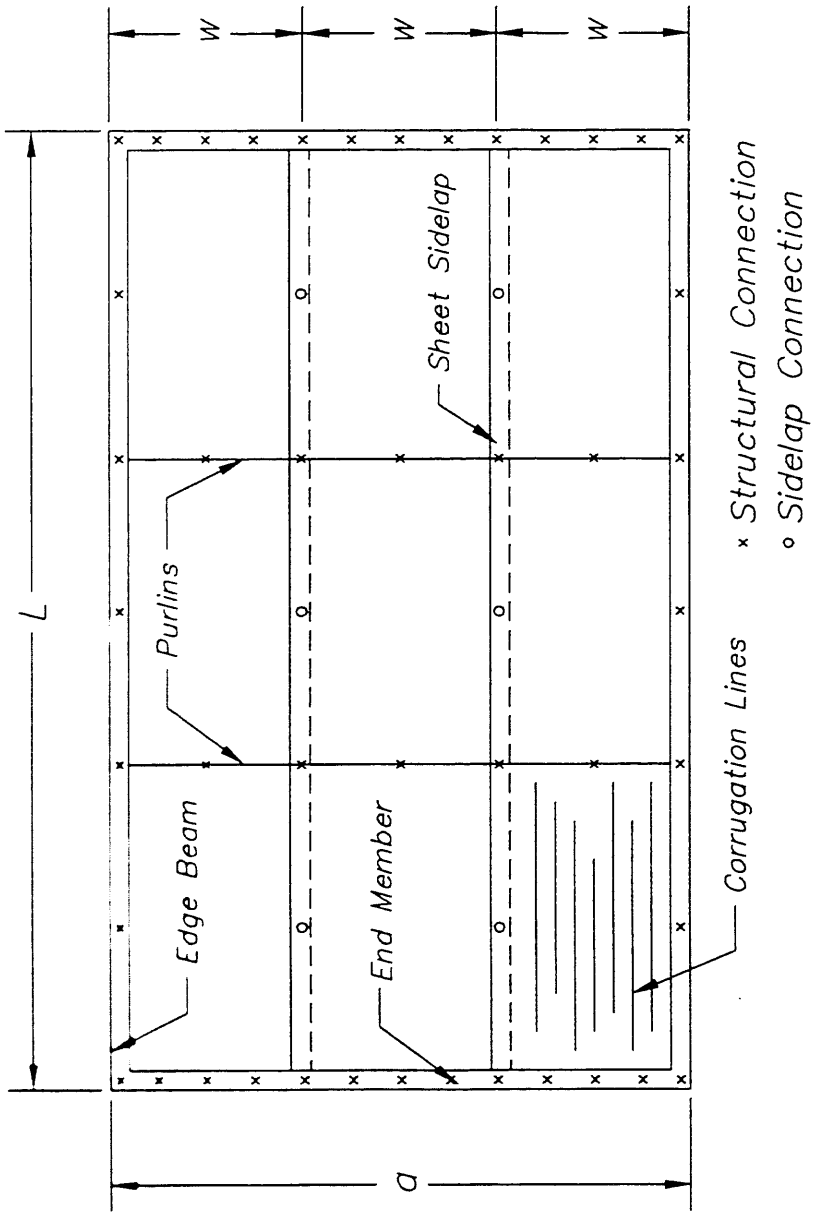

Fig. 3.6 Configuration of metal–deck diaphragm.

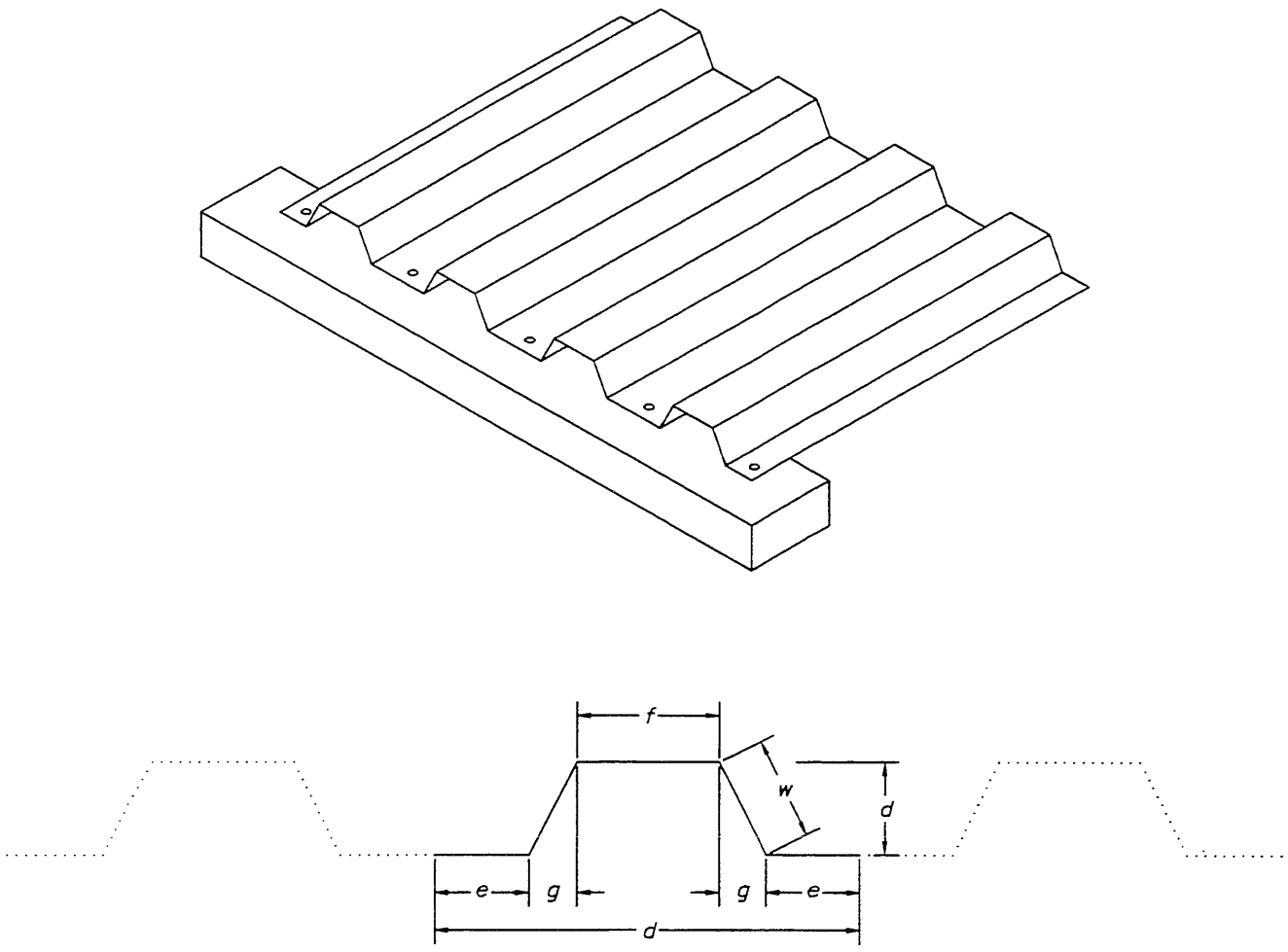

Fig. 3.7 Corrugations in metal decking [48].

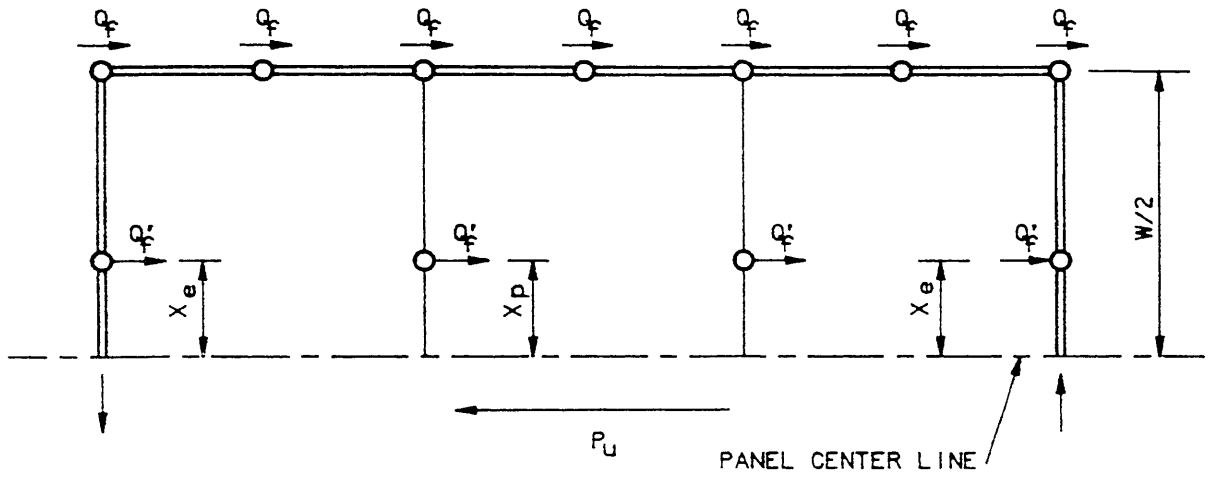

Fig. 3.8 Strength of metal–deck diaphragm limited by connections along edge of diaphragm [48].

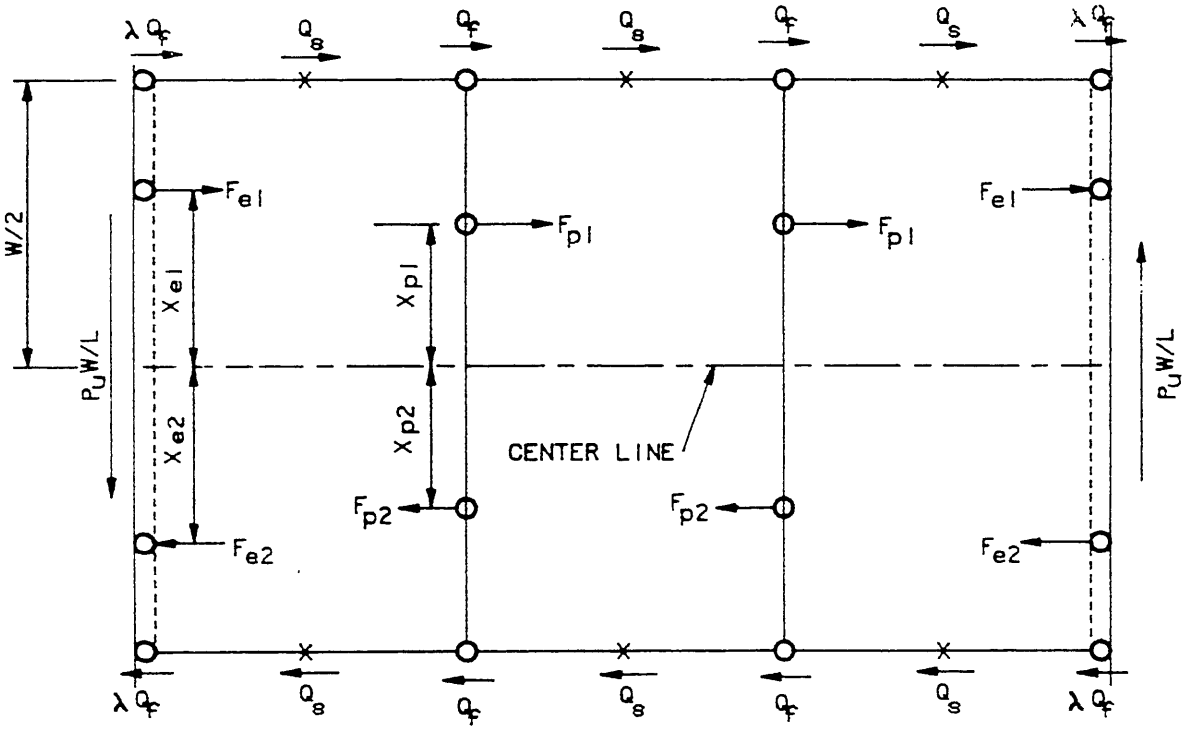

Fig. 3.9 Strength of metal–deck diaphragm limited by connections in an interior panel [48].

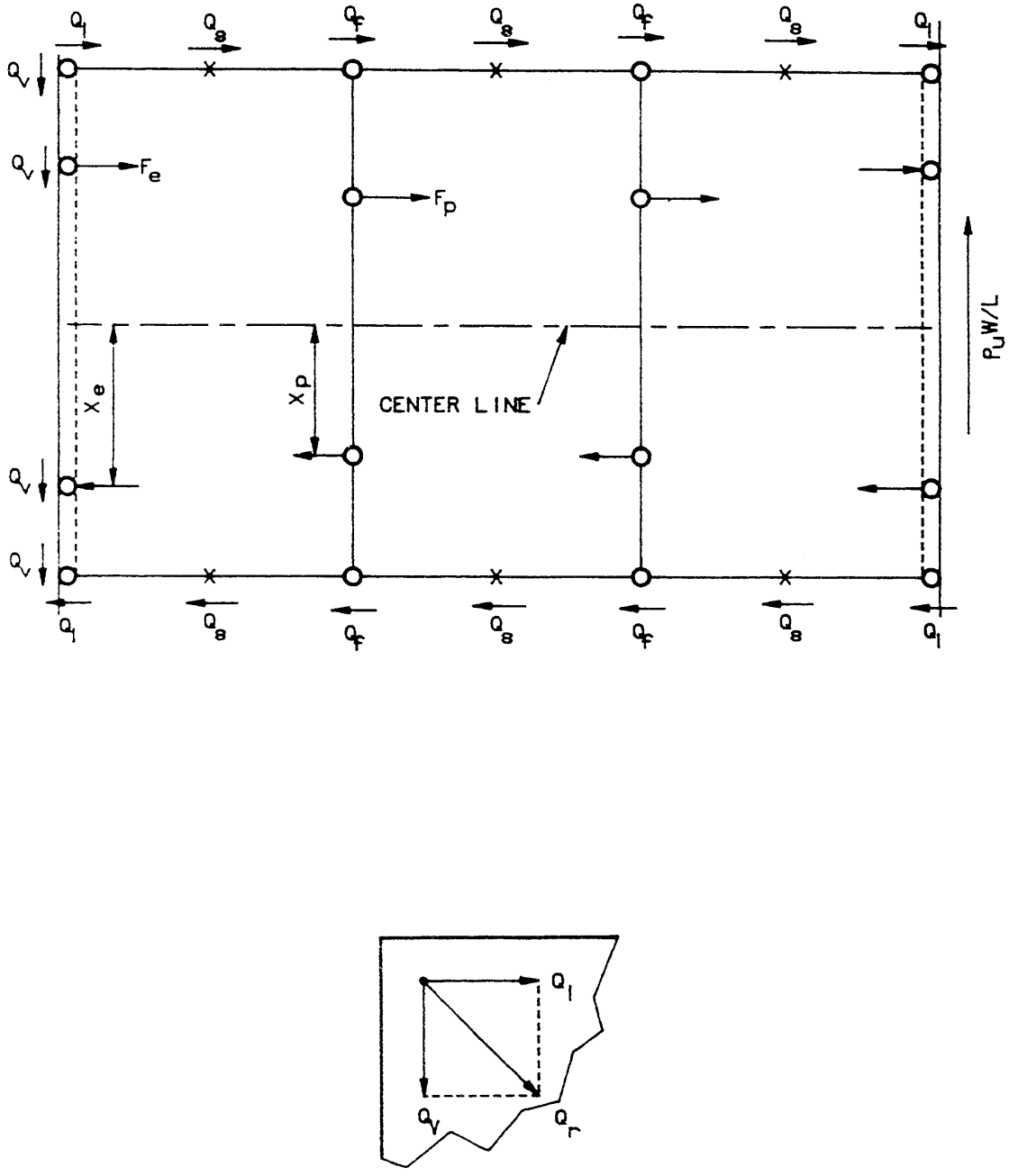

Fig. 3.10 Strength of metal–deck diaphragm limited by connections in corner [48].

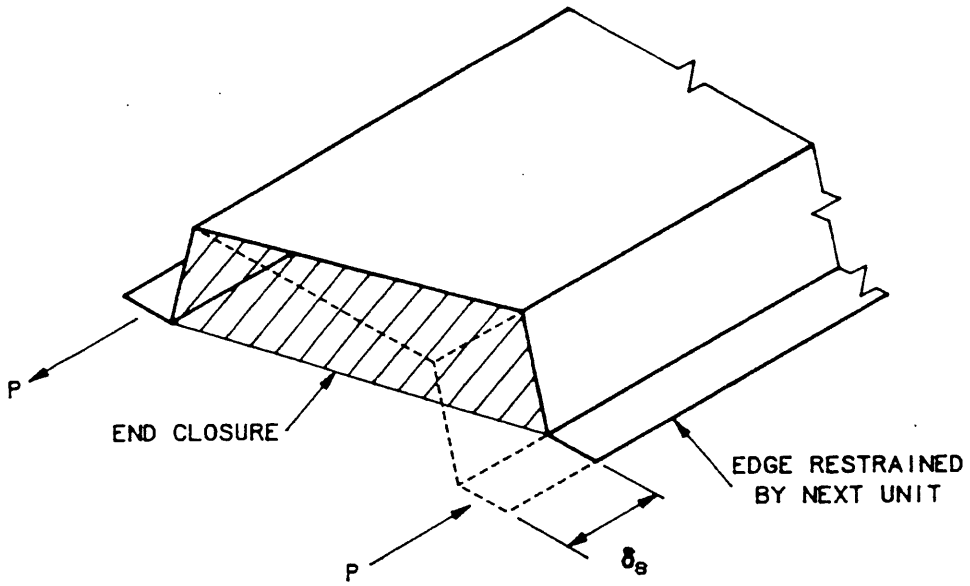

(a) UNIT RESTRAINED AGAINST END WARPING

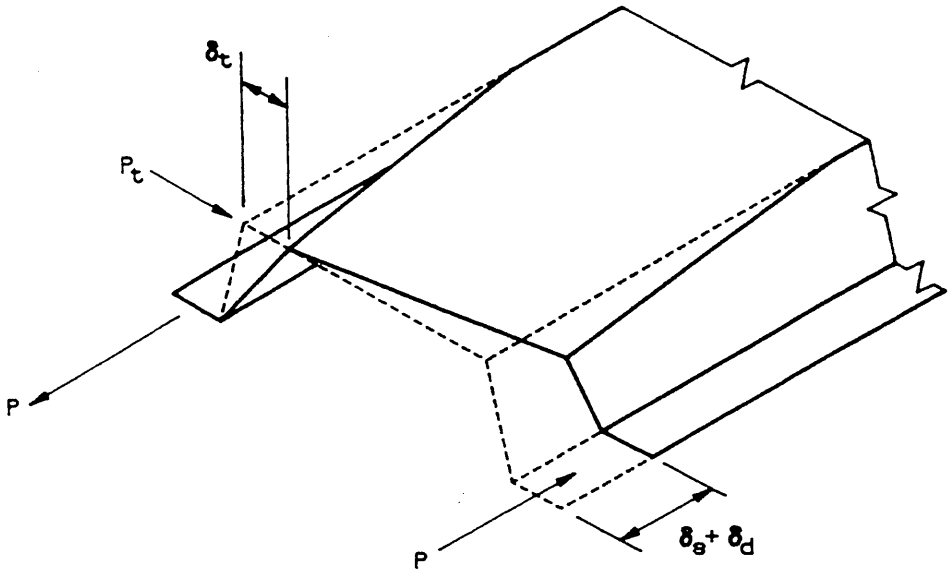

(b) OPEN-ENDED UNIT

Fig. 3.11 Deformation of metal deck [48].

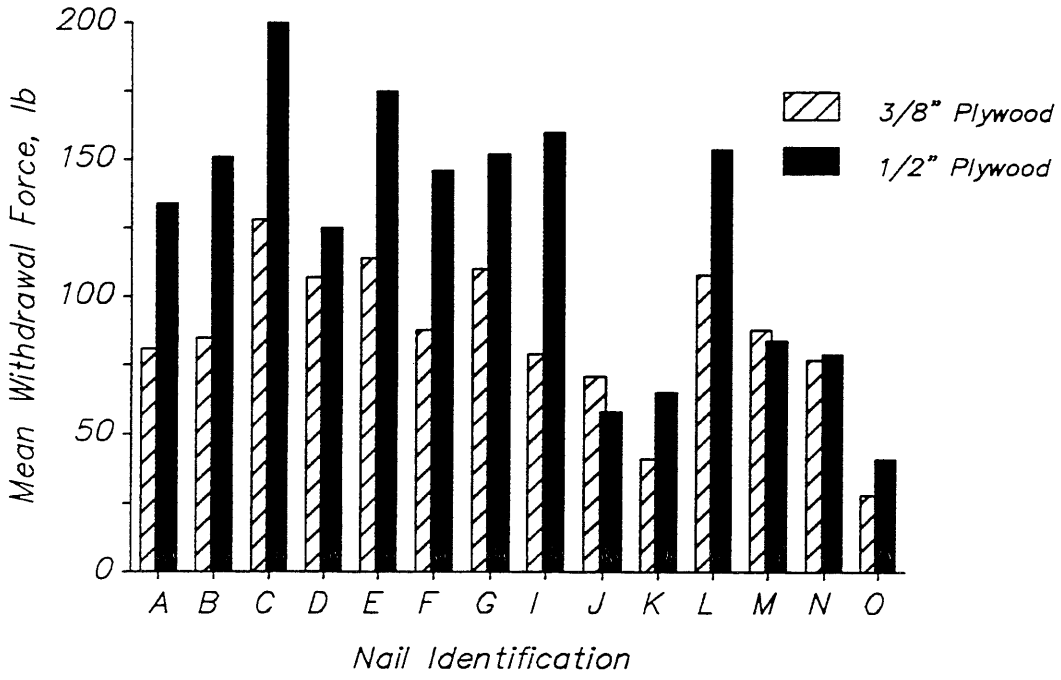

Nail Id	Type	Length in.	Diameter in.	
A	Annular Ring Shank	3/4	0.130	24 rings/in., bright steel
B	Annular Ring Shank	1	0.105	22 rings/in. bright steel
C	Screw Shank	1	0.150	aluminum
D	Annular Ring Shank	7/8	0.100	22 rings/in., bright steel
E	Annular Ring Shank	1	0.140	24 rings/in. bright steel
F	Screw Shank	1	0.120	24 threads/in., aluminum
G	Screw Shank	7/8	0.102	32 rings/in., aluminum
I	Annular Ring Shank	1	0.120	20 rings/in., bright steel
J	Staple	1 1/8	16 ga	bright steel
K	File Shank	1	0.130	bright steel
L	Annular Ring Shank	1 1/8	0.115	24 rings/in., aluminum
M	Steep Spiral Screw Shank	1	0.140	bright steel
N	Barbed	3/4	0.145	galvanized
O	6d Common	2	0.113	bright steel

Fig. 3.12 Pull–out strength of various roofing nails [20].

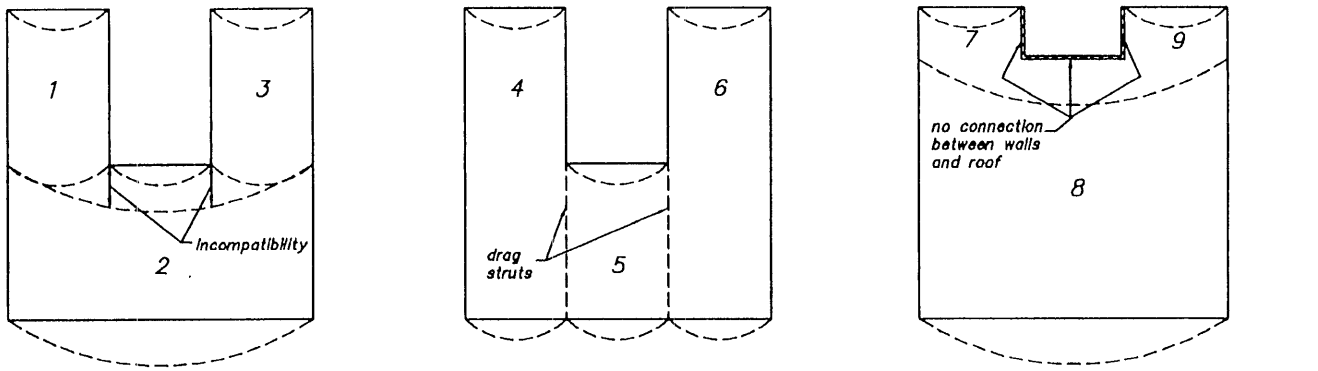

(a) Displacements in diaphragms 1 and 3 are not compatible with displacements in diaphragm 2.

(b) With the addition of drag struts, displacements in diaphragms 4, 5, and 6 are now compatible.

(c) Offset walls should not be connected to the roof if high shears are expected at the re-entrant corners.

Fig. 3.13 Displacement discontinuities in non-rectangular diaphragms [14].

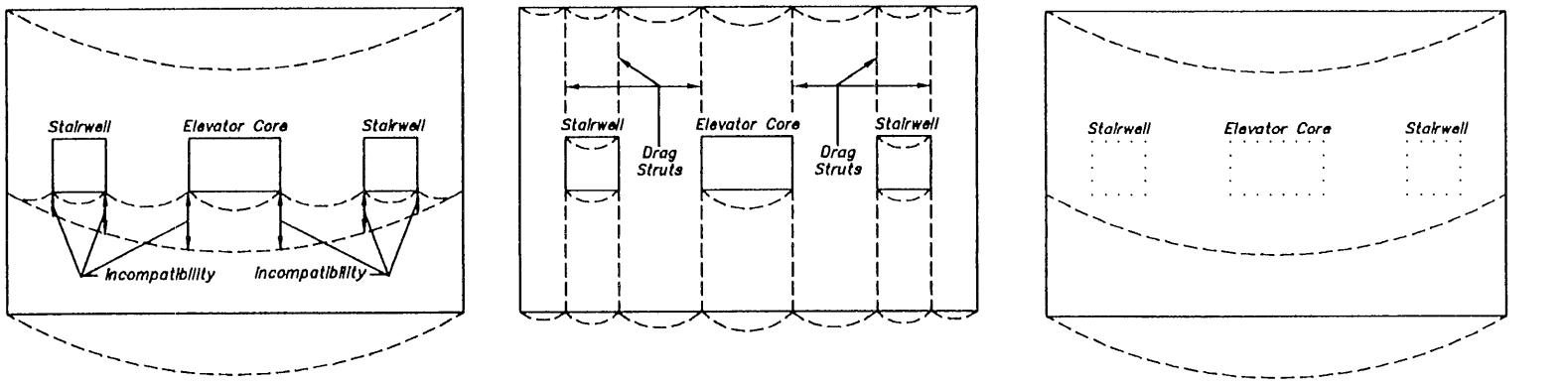

(a) Displacements in diaphragm are not compatible with displacements in stairwells and elevator core.

(b) With the addition of drag struts, displacements are now compatible throughout the diaphragm.

(c) Without panel–to–roof connections at the stairwells and elevator cors, the roof diaphragm does not develop the displacement incompatibilities shown in (a) because the diaphragm is not restrained at these points.

Fig. 3.14 Displacement discontinuities in buildings with stairwells and elevator cores [14].

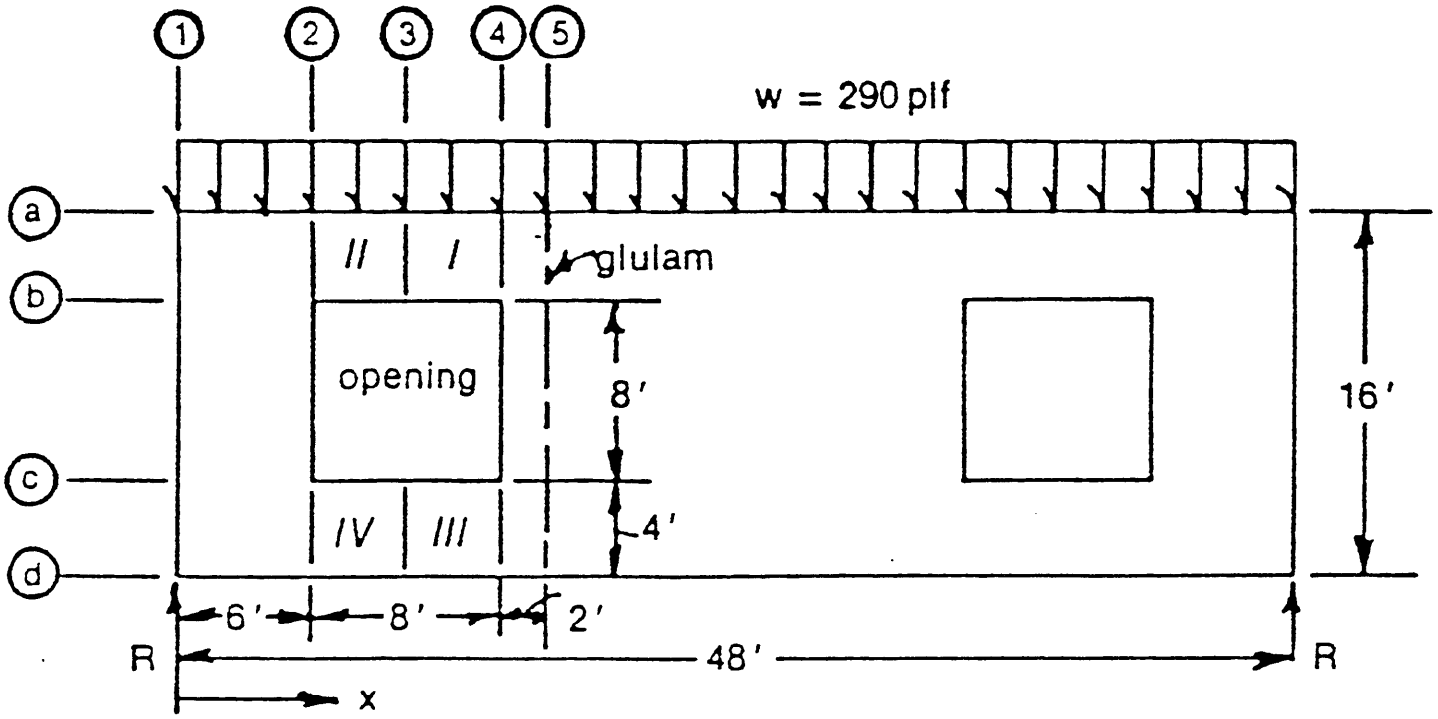

(a) Plan view

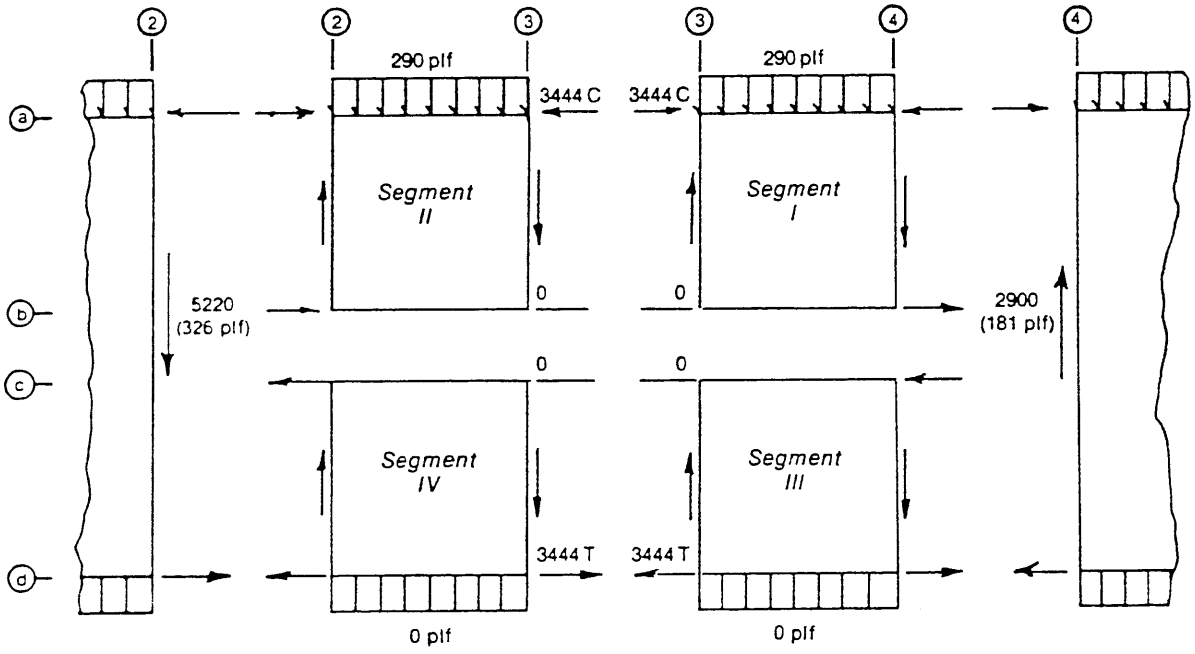

(b) Free–body diagram

Fig. 3.15 Analysis of diaphragm modelled as a Vierendeel truss [74].

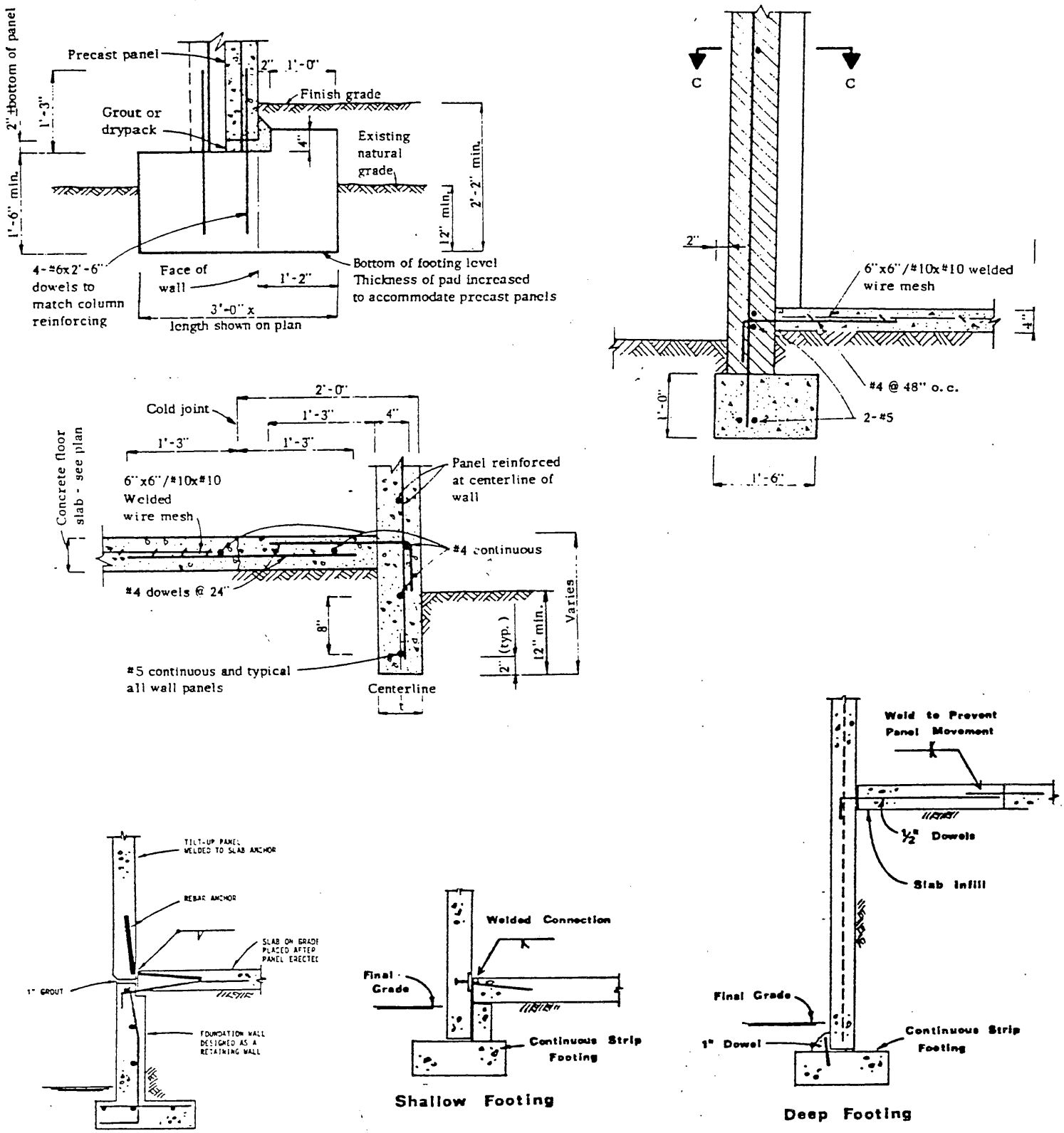

Fig. 3.16 Typical panel–to–foundation connections in buildings constructed before 1971 [55,80]

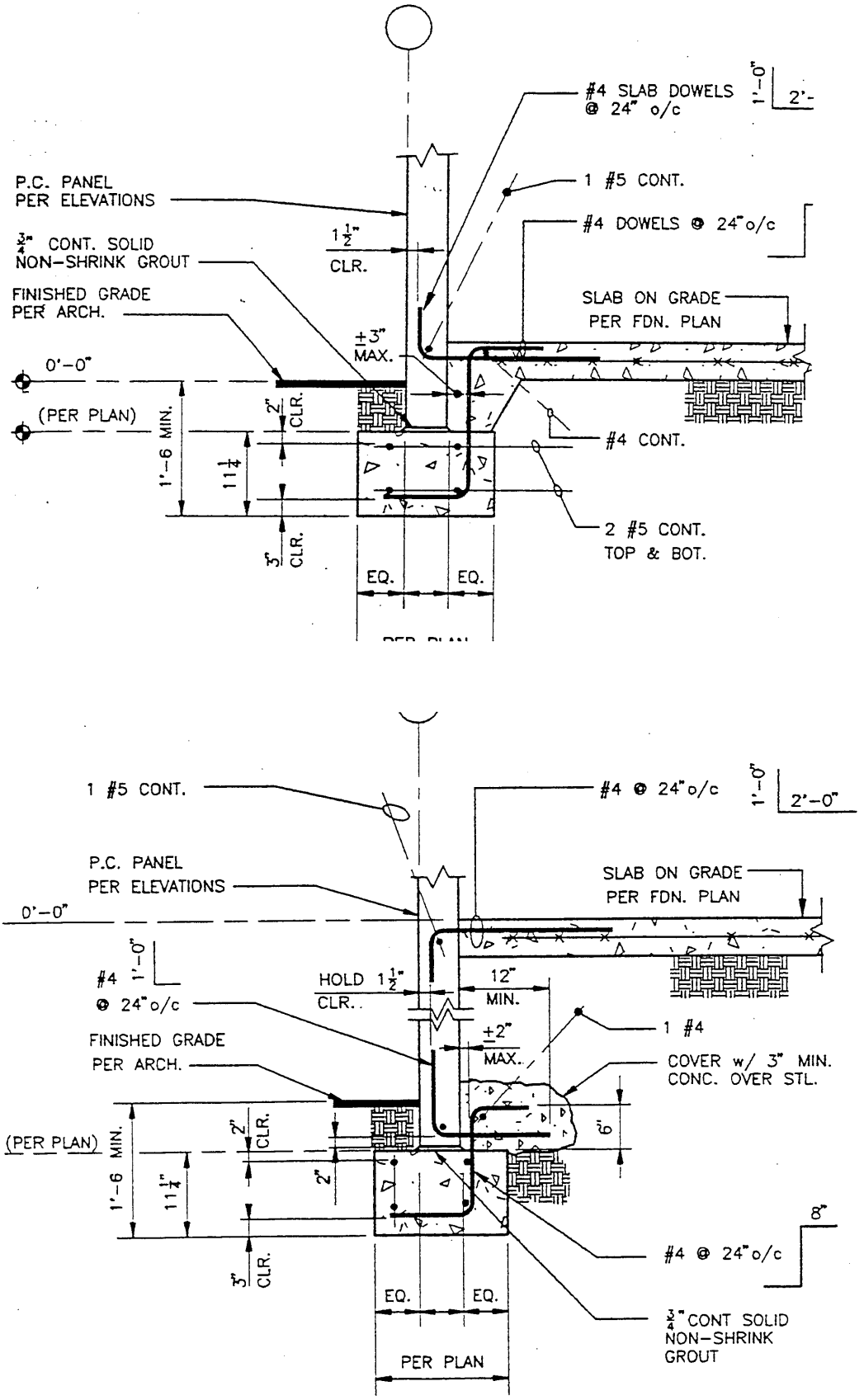

Fig. 3.17 Typical panel–to–foundation connections in buildings constructed after 1971 [40].

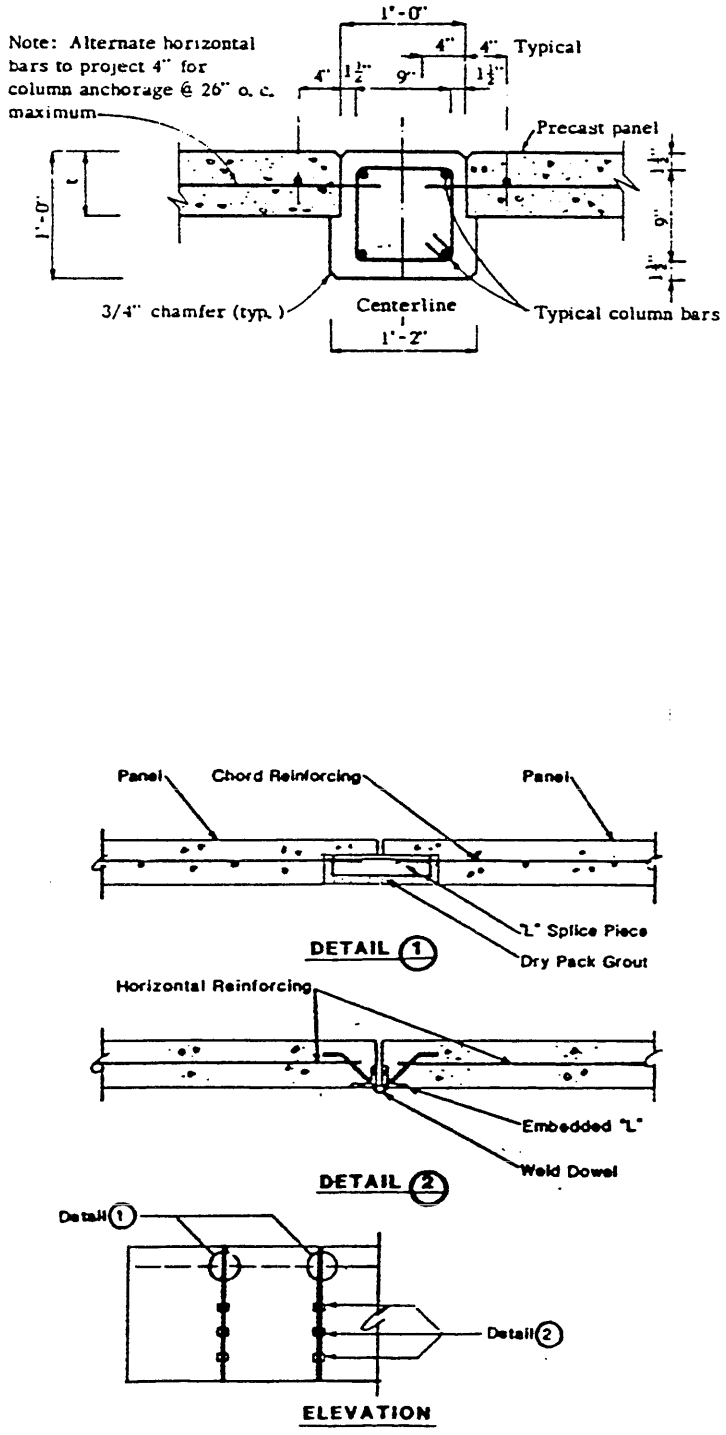

Fig. 3.18 Typical panel-to-panel connections in buildings constructed before 1971 [55,80]

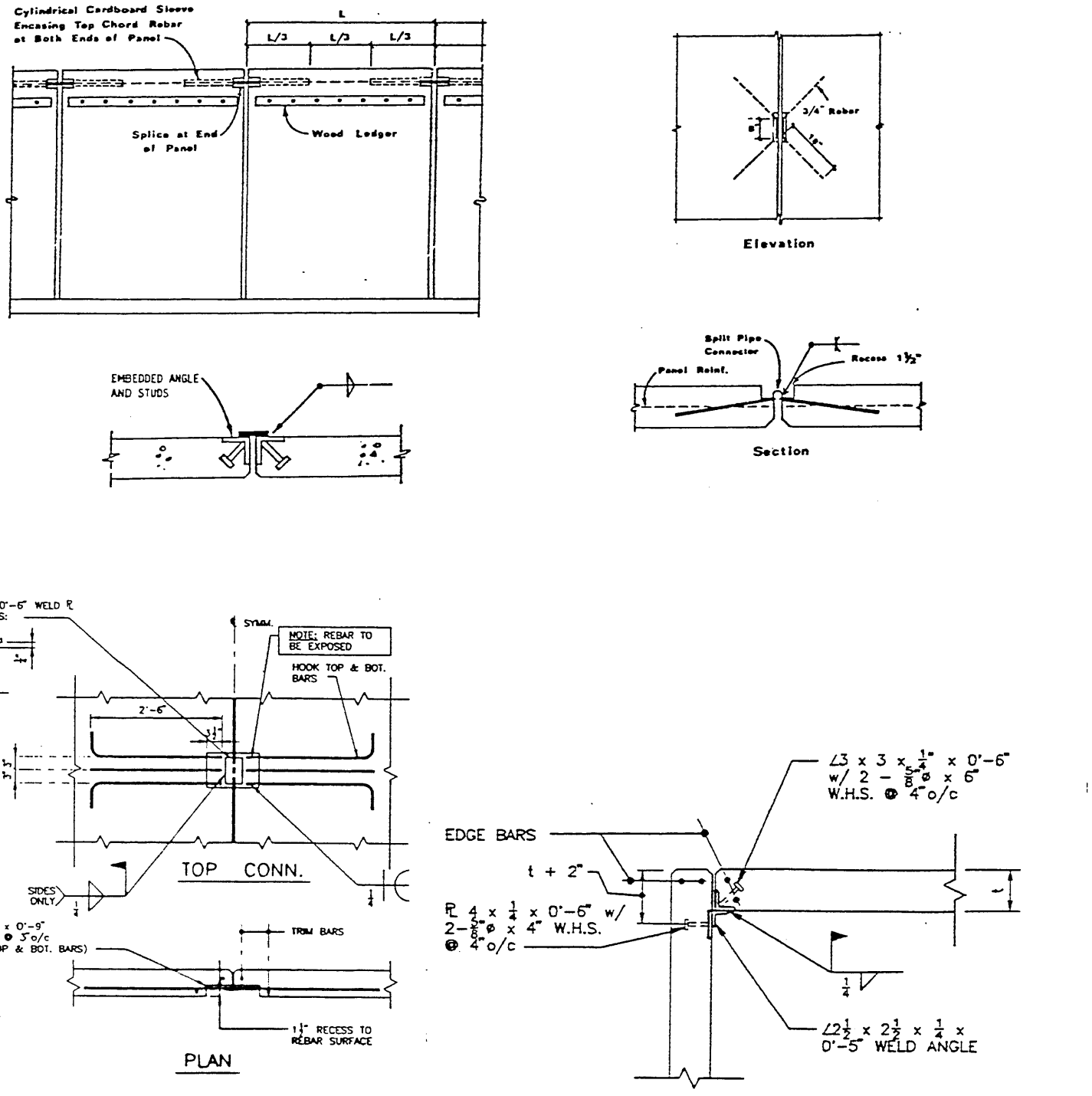

Fig. 3.19 Typical panel–to–panel connections in buildings constructed after 1971 [40,80].

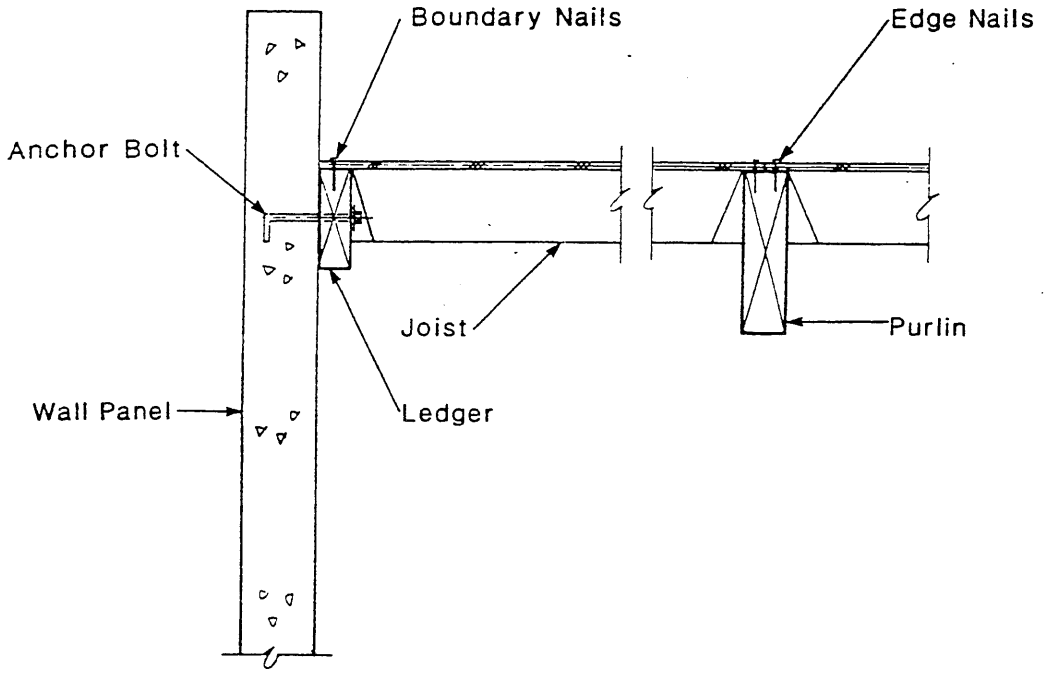

Fig. 3.20 Typical purlin to wood ledger connection in buildings constructed before 1971 [35].

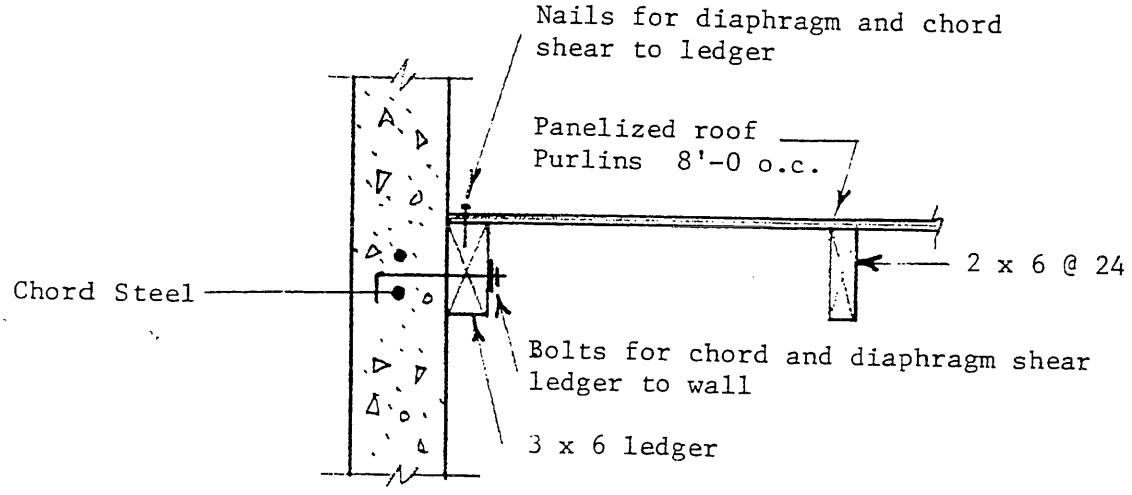

Fig. 3.21 Typical plywood to wood ledger connection in buildings constructed before 1971 [25].

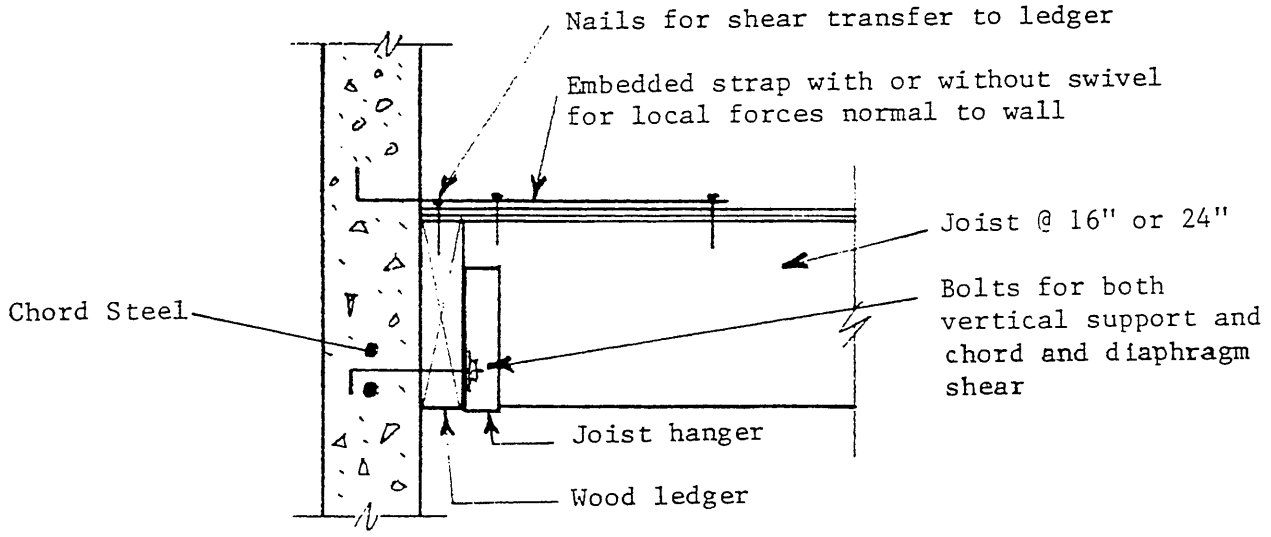

Advantages:

a. Few pieces with simple, standard hardware.
b. Easy to install with standard carpentry techniques.
c. Good, direct shear transfer to wall.
d. Accommodates ceiling on underside of joists.

Disadvantages:

a. Embedded straps have to cycle and align with joists and follow slope of ledger which requires setting joist locations at an early stage so joists and straps coincide. Swivel is of dubious merit if placement is significantly off as strap will run diagnonally across joists and nailing is partially lost.
b. May be adversely affected by shrinkage as strap is permanent in elevation into wall while roof and roofing settle around it. Strap also places bump in roof membrane subject to different thermal behavior than rest of roof.

Comment: This is a good current detail essentially developed after the San Ferando earthquake to provide a positive tie into diaphragm for local forces. There are some field problems setting the straps at the proper elevation and proper lateral location and some concerns over the effect of the straps on the roof membrane.

Fig. 3.22 Typical purlin to wood ledger connection in buildings constructed after 1971 [25].

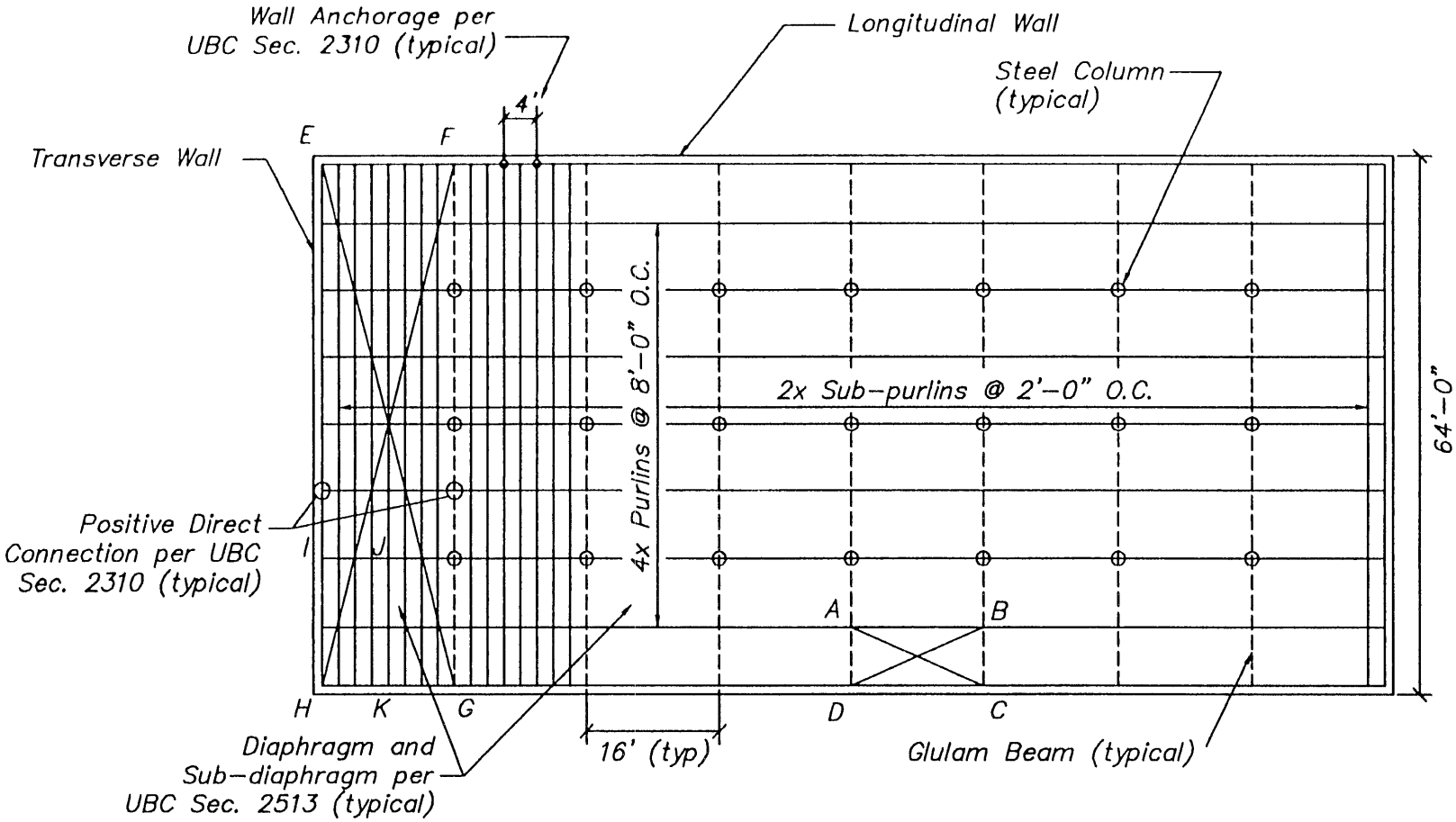

Fig. 3.23 Plan view of roof framing members showing subdiaphragm details.

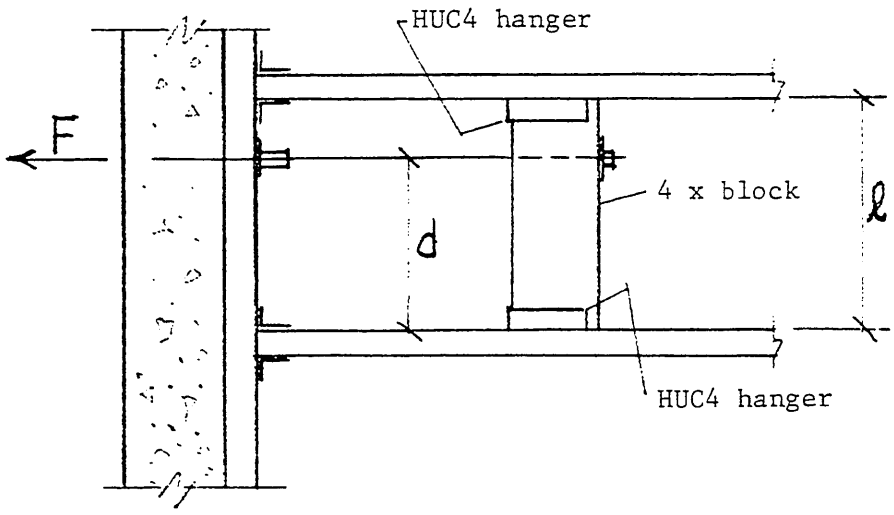

PLAN VIEW

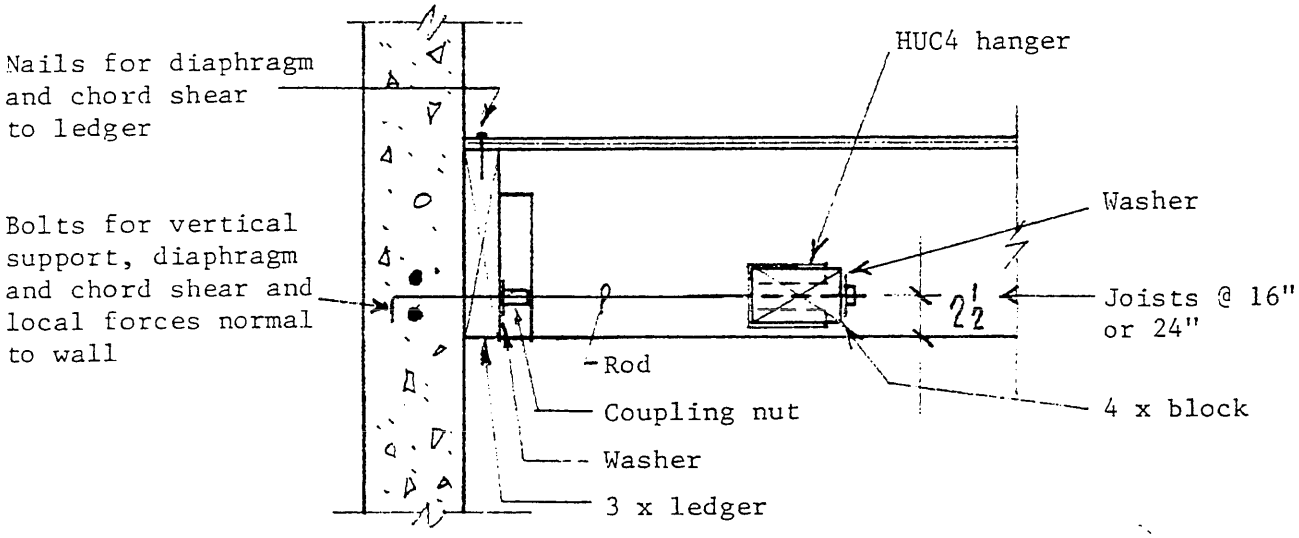

ELEVATION

Advantages:

a. Standard hardware.
b. Installs with normal carpentry tools and technique.
c. Independent of joist positioning provided wall bolts are not within 4-inches of joist centerline. Tight tolerances not required.
d. Good, direct shear transfer to wall,
e. Not adversely affected by wood shrinkage.

Fig. 3.24 Strengthening of existing panel–to–roof connections for walls with parapets [25].

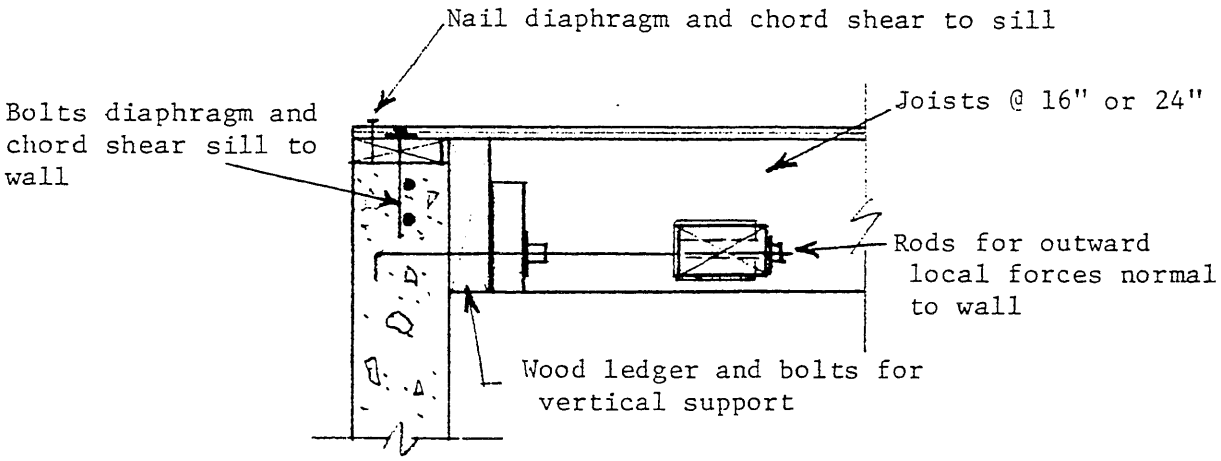

See Figure 9 for details of rod connection

Advantages:

a) Simple connection installed with standard carpentry techniques.
b) Can be installed on existing construction almost as easily as on new.

Disadvantages: Number of small parts resulting in an increased cost.

Fig. 3.25 Strengthening of existing panel–to–roof connections at top of wall [25].

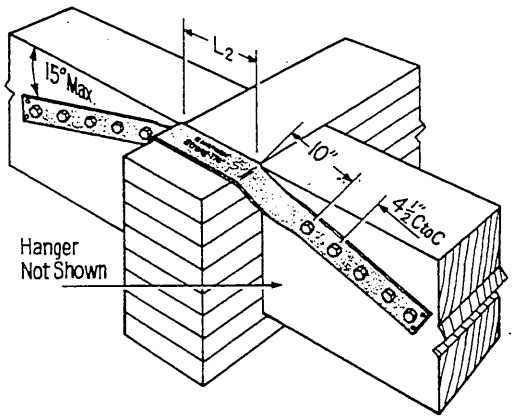

Fig. 3.26 Purlin–to–purlin connection across a glulam beam [22].

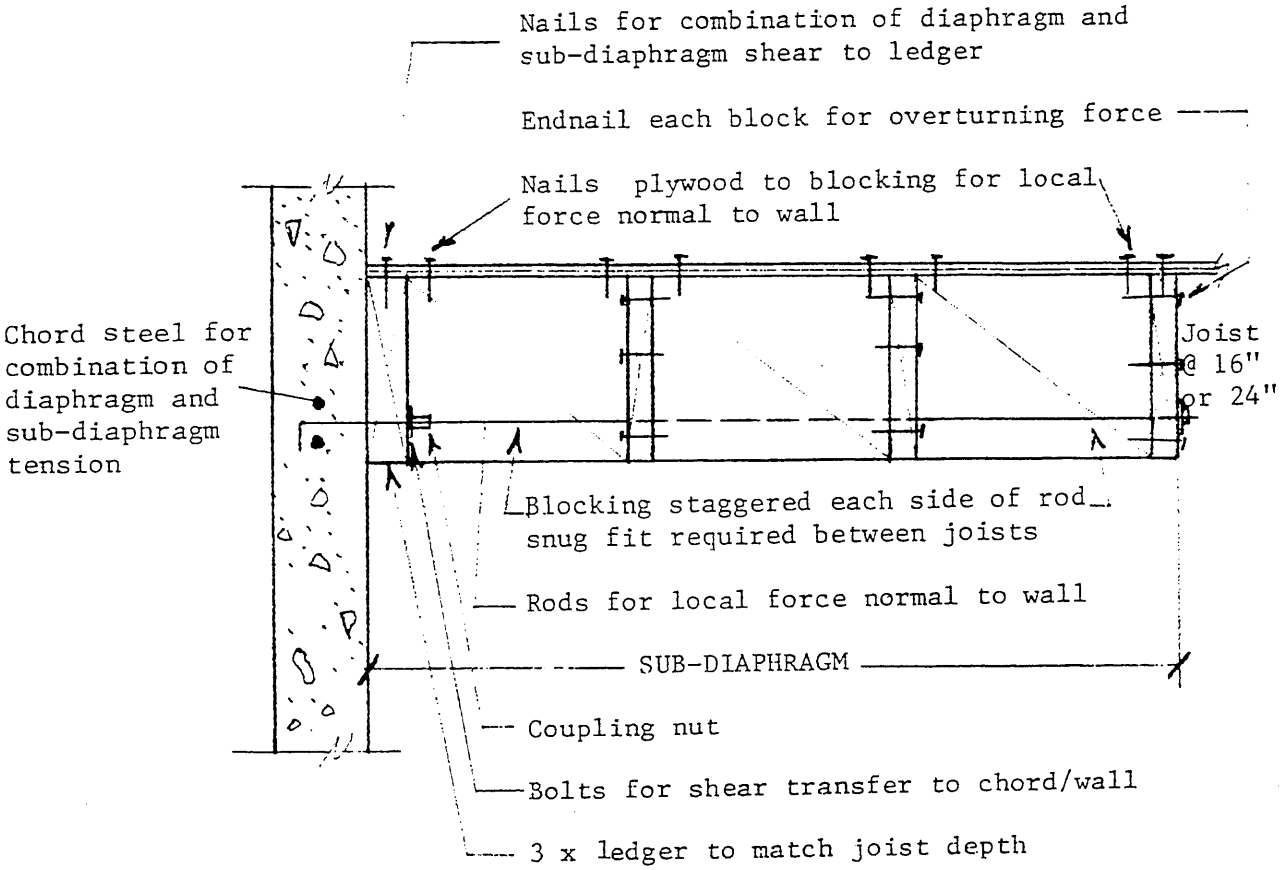

Advantages:

a. Relatively simple carpentry
b. Tolerances are relatively loose.
c. Not adversely affected by joist shrinkage.
d. Can be applied to existing as well as new construction.

Disadvantages:

a. Increased hardware, lumber and nailing relative to (13).
b. Snug fit on blocking hard to obtain unless rods are tightened before sheathing is in place.
c. Problem in blind nailing plywood into staggered blocks.

Fig. 3.27 Use of metal ties through purlins to create a subdiaphragm (walls with parapets) [25].

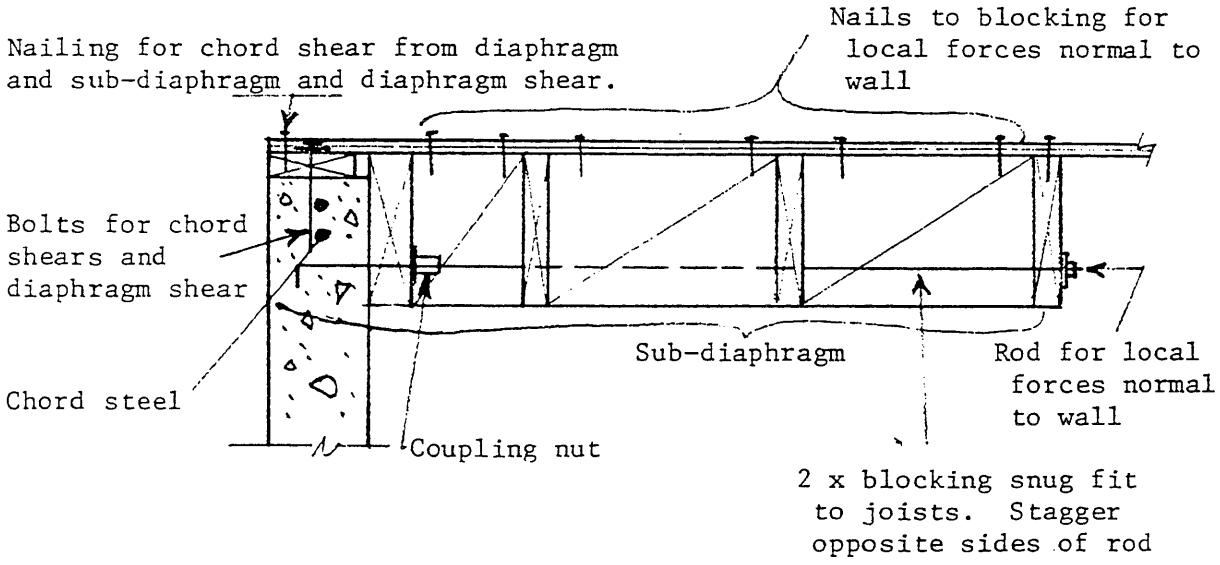

Fig. 3.28 Use of metal ties through purlins to create a subdiaphragm (top of wall) [25].

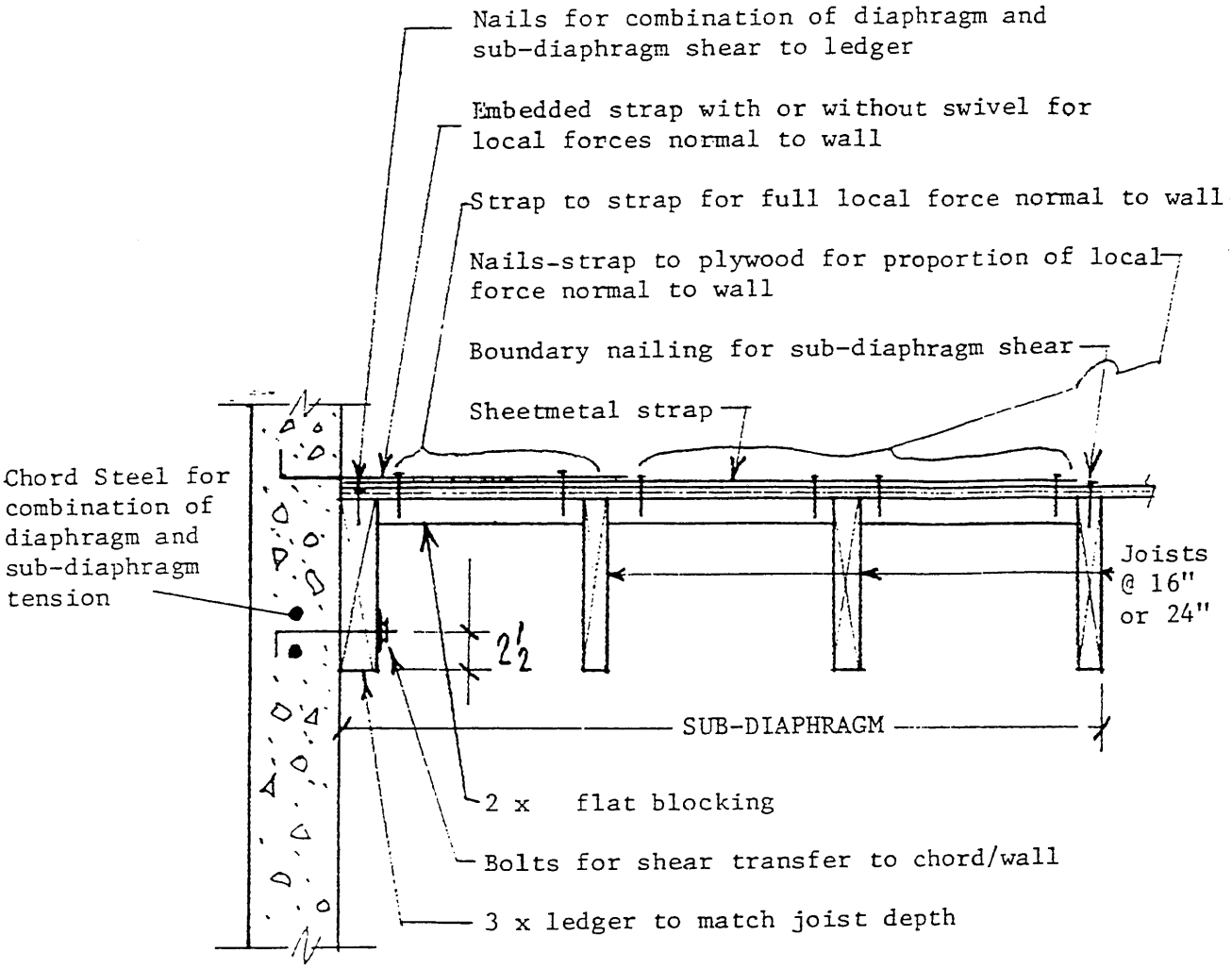

Advantages:

a. Relatively simple carpentry.
b. Work done from above.

Disadvantages:

a. Non-standard sheet metal strap.
b. Strap has to be set accurately to elevation following slope of roof.
c. May be adversely affected by shrinkage as strap is permanent in elevation into wall while roof and roofing settle around it. Strap also places bump in roof membrane subject to different thermal behavior than rest of roof.

Fig. 3.29 Use of metal strap attached to plywood and blocking to create a subdiaphragm [25].

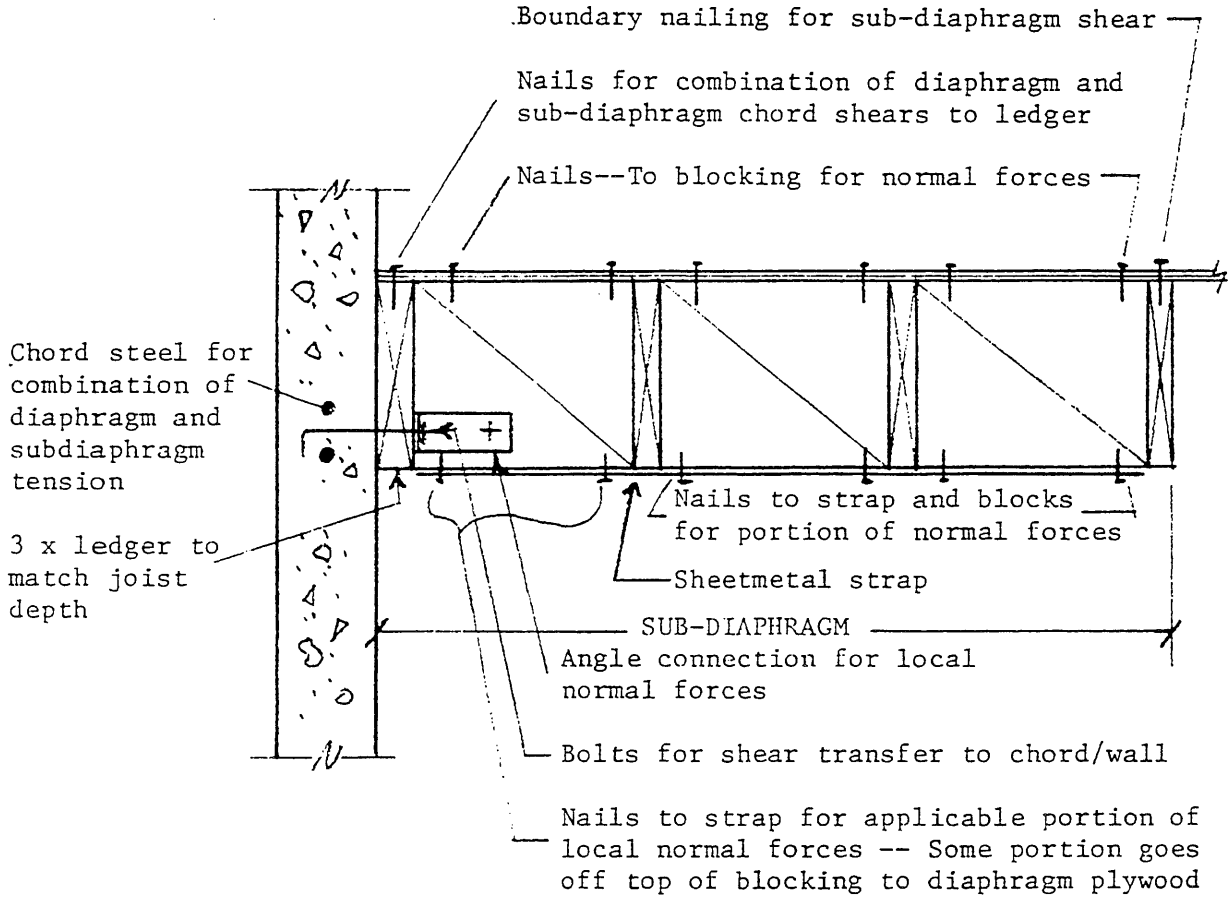

Advantages:

a. Relatively simple carpentry without close tolerances.
b. Adjusts to shrinkage.

Disadvantages:

a. Non-standard angle and strap.
b. Nailing to strap overhead - probably requires scaffolding.
c. Requires duplicate nailing to blocks.
d. Blocks must be end connected for overturning.

Fig. 3.30 Use of metal strap attached to blocking to create a subdiaphragm [25].

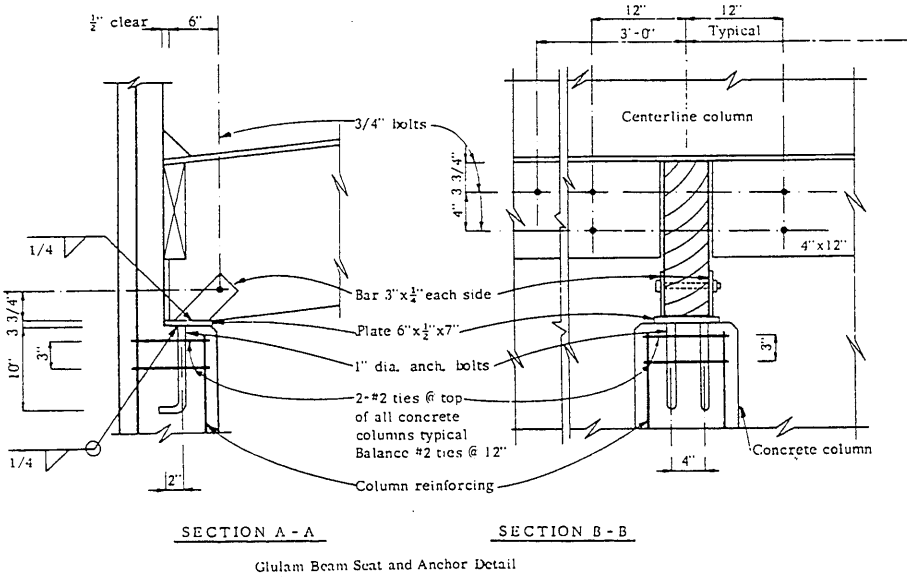

Glulam Beam Seat and Anchor Detail

Fig. 3.31 Detail of a direct glulam–to–panel connection [55].

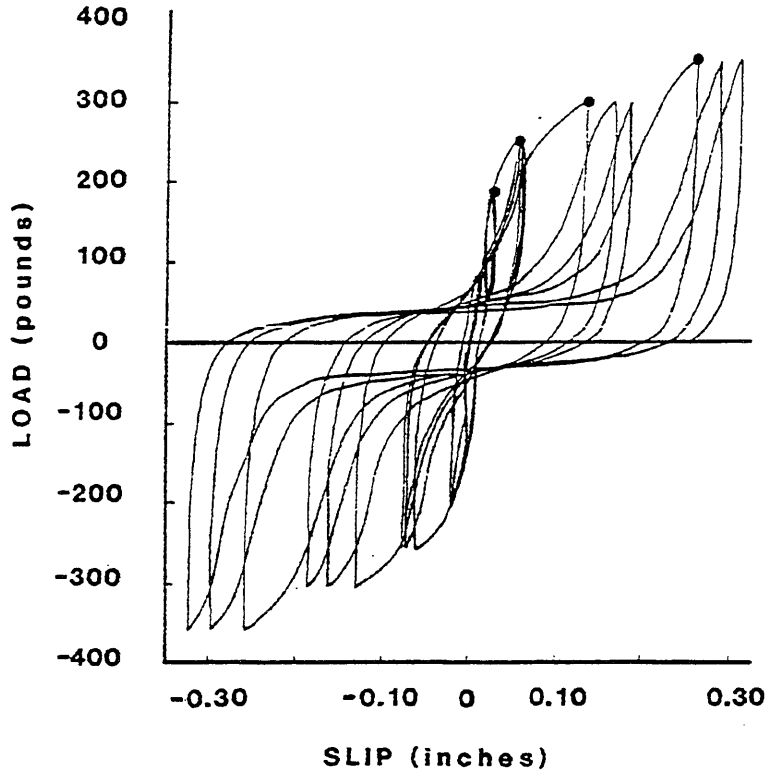

(a) Cycles to a given force level [39].

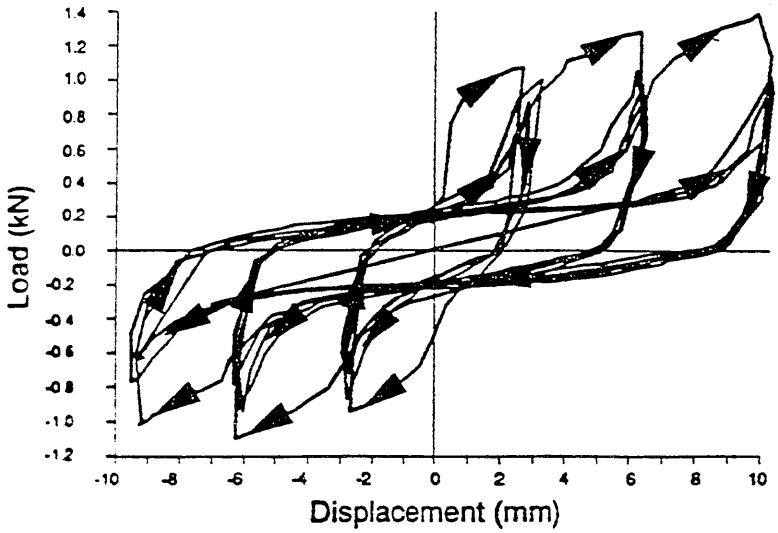

(b) Cycles to a given displacement level [26].

Fig. 4.1 Measured force–displacement response of nailed connections.

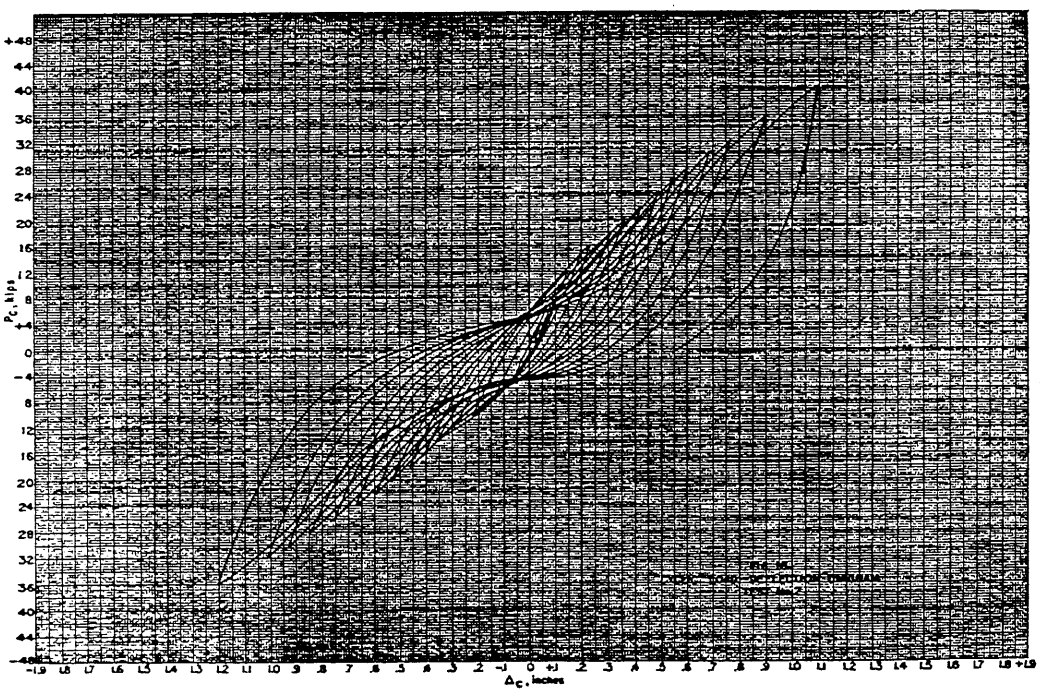

(a) Static load reversals [83].

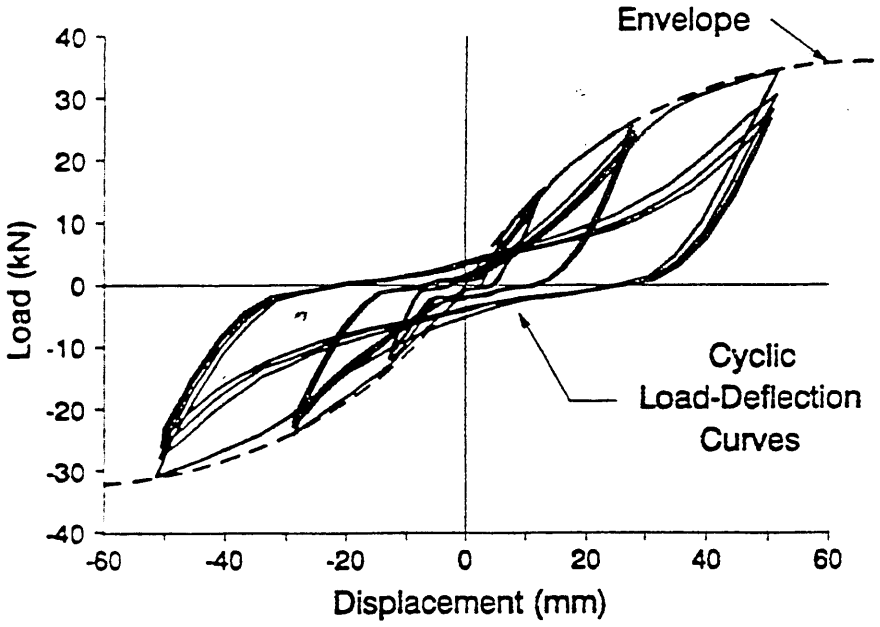

(b) Static load reversals [26].

Fig. 4.2 Measured force–displacement response of plywood wall panels and diaphragms.

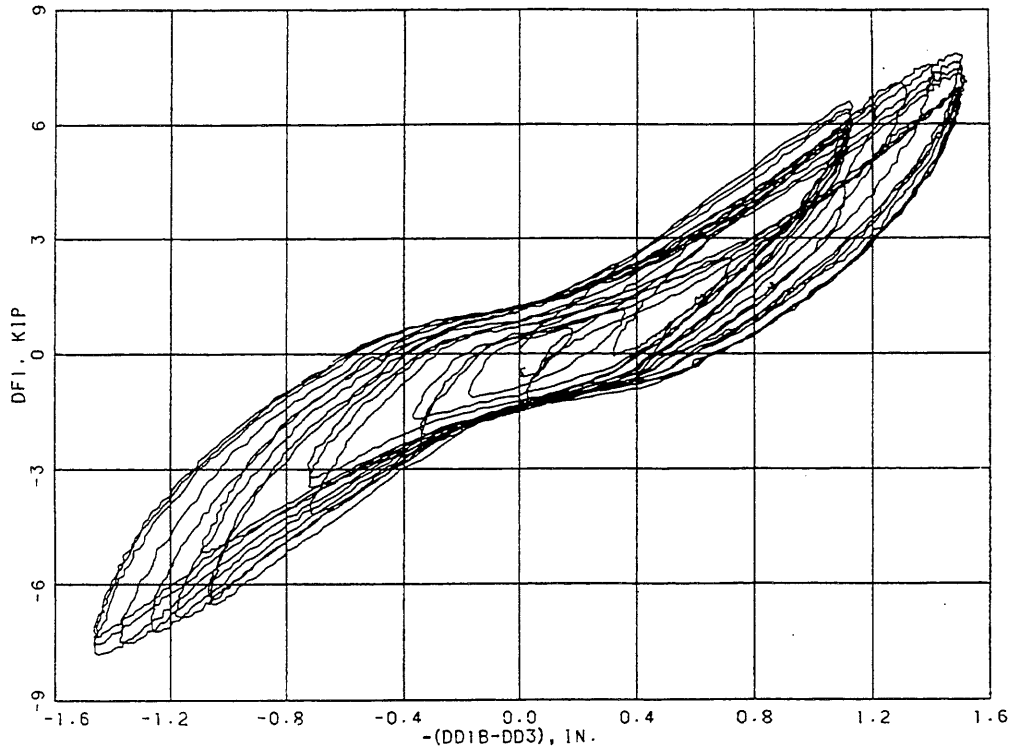

(c) Quasi–static load reversals [1].

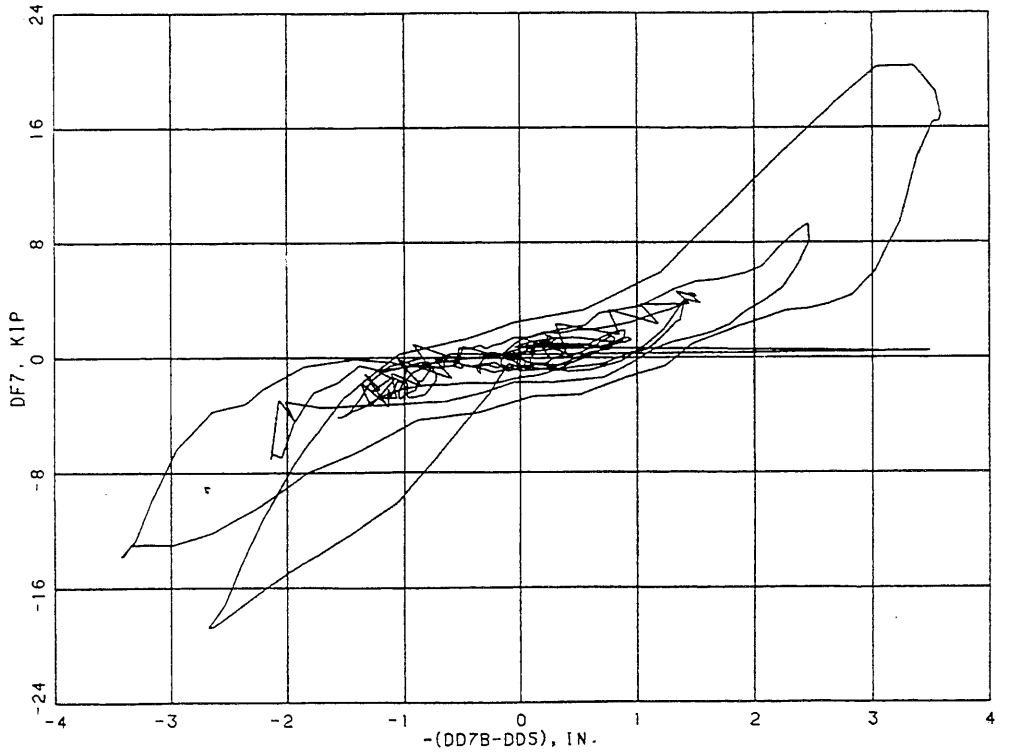

(d) Dynamic loading [1].

Fig. 4.2 (cont.) Measured force–displacement response of plywood wall panels and diaphragms.

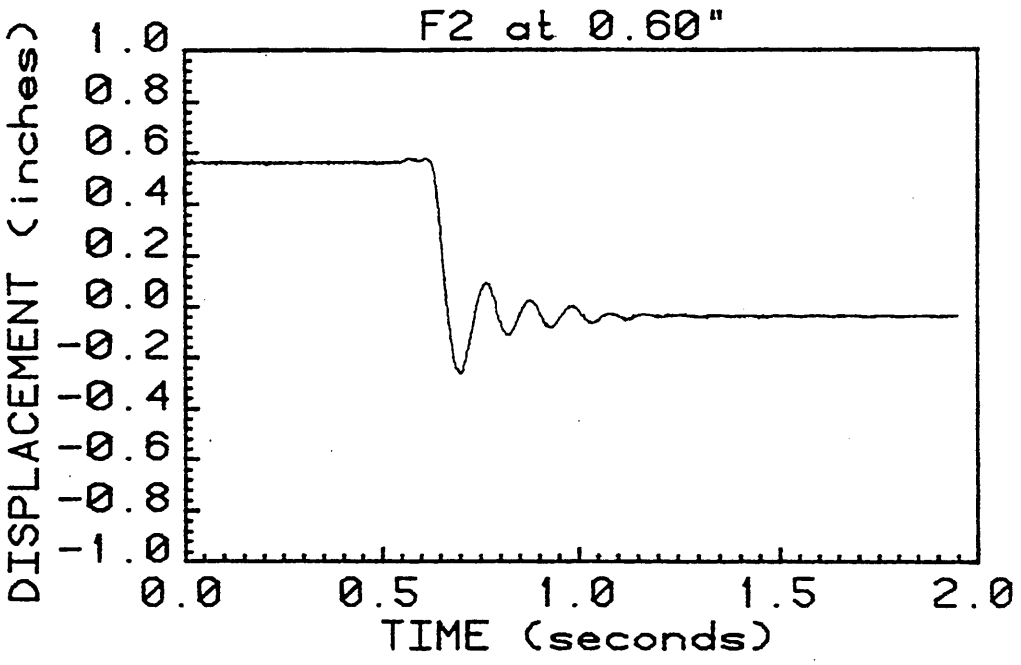

(a) Initial displacement of 0.6 in.

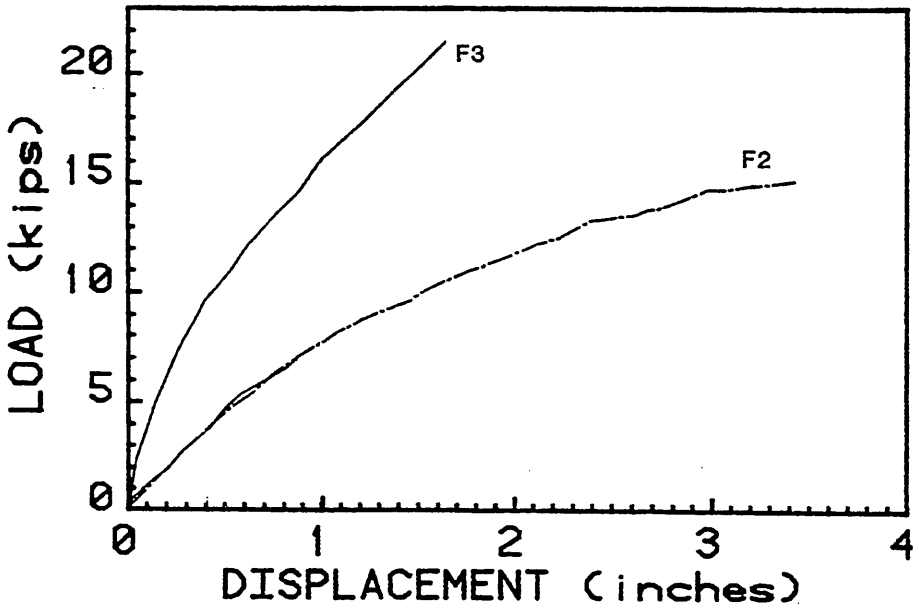

(b) Force–displacement curve for monotonic loading to failure.

Fig. 4.3 Measured free–vibration response of plywood diaphragm [39].

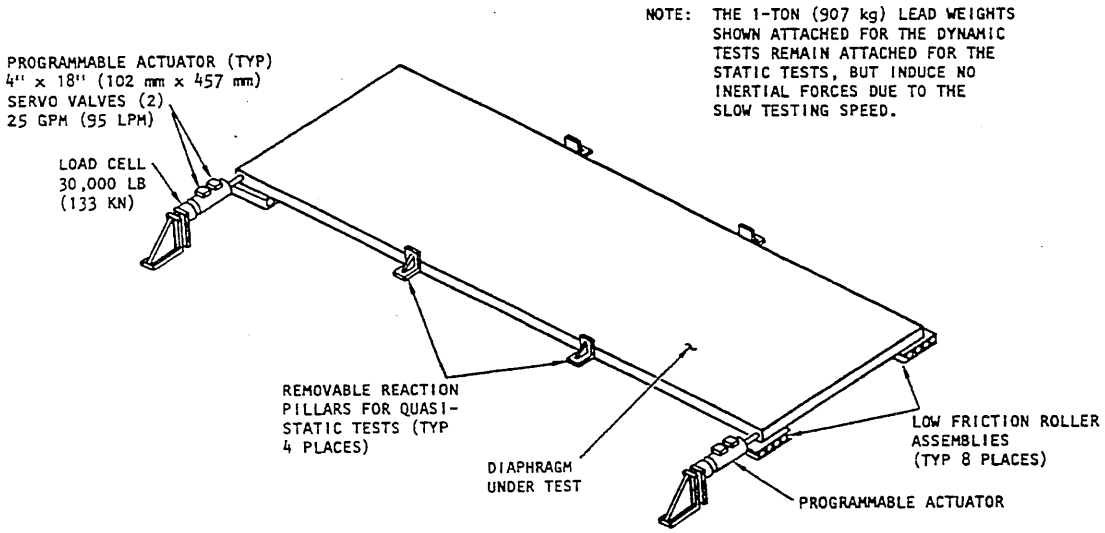

(a) Quasi–static tests.

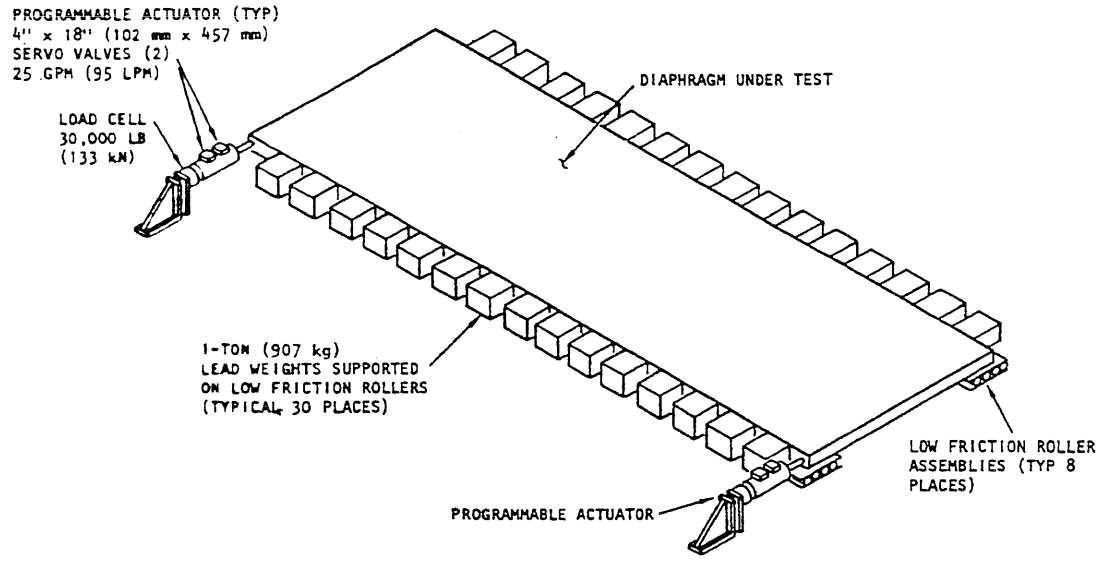

(b) Dynamic tests.

Fig. 4.4 Test configuration for ABK diaphragm tests [1].

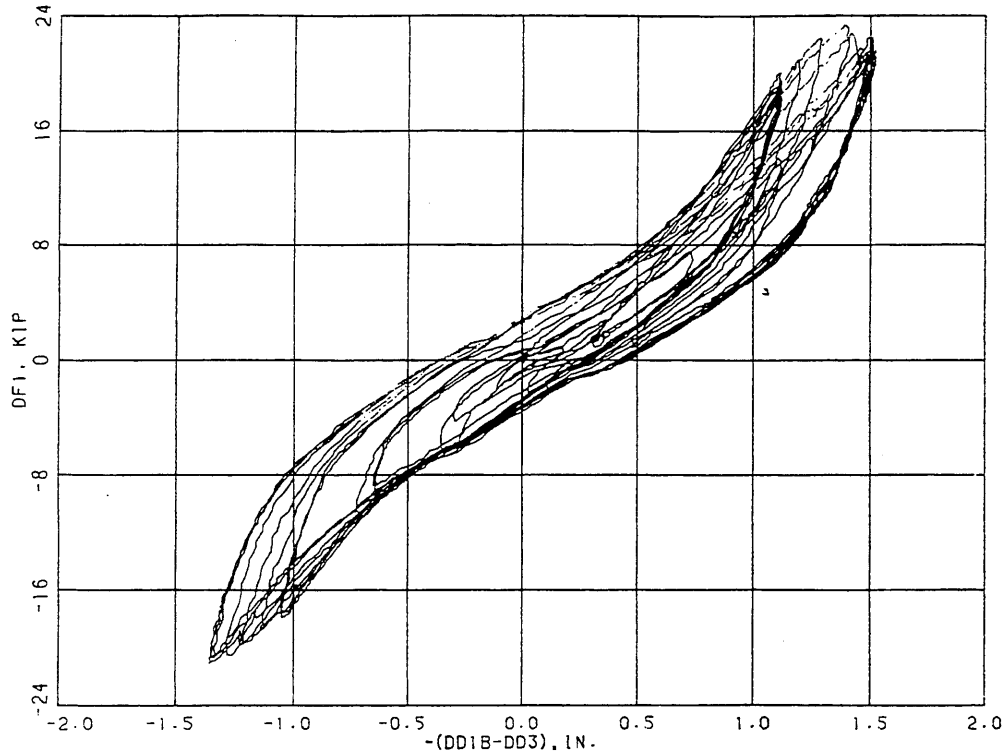

(a) Quasi–static load reversals.

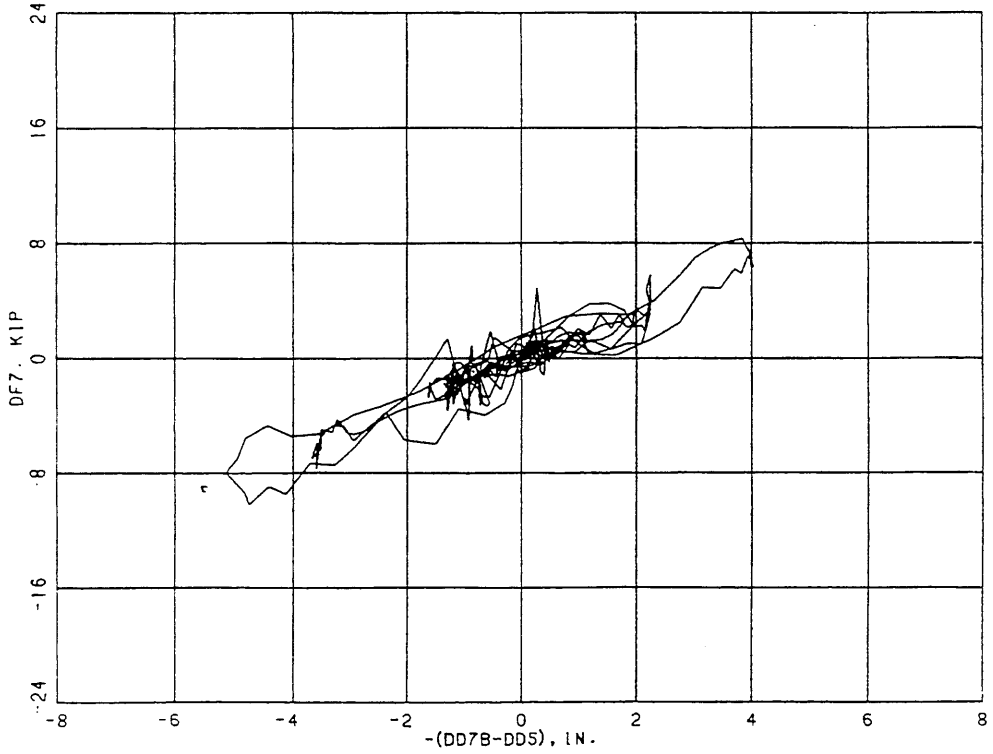

(b) Dynamic loading.

Fig. 4.5 Measured force–displacement response of metal–deck diaphragm [1].

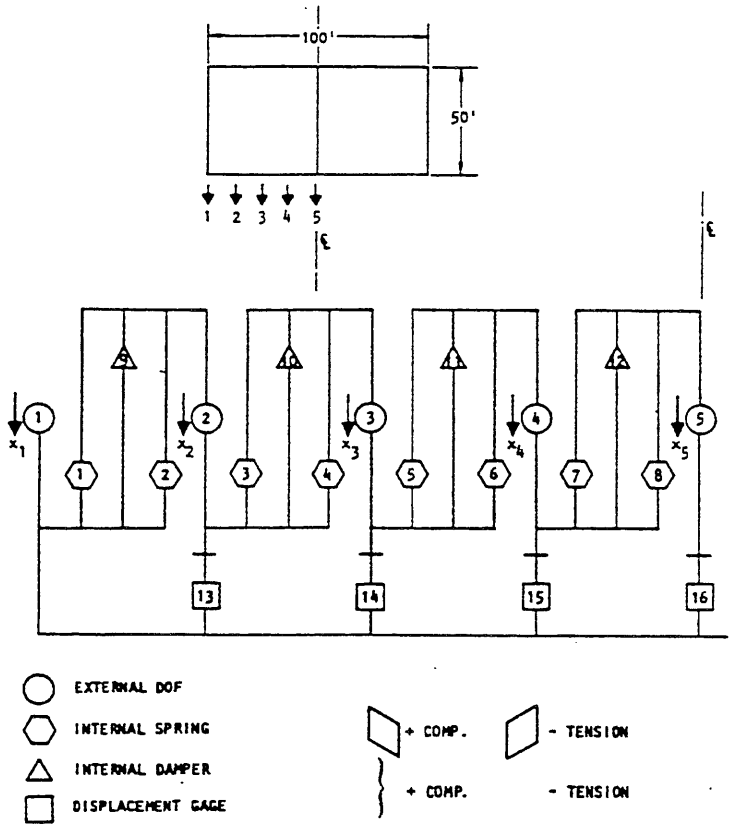

Fig. 4.6 Representation of plywood diaphragm as a series of nonlinear springs [11].

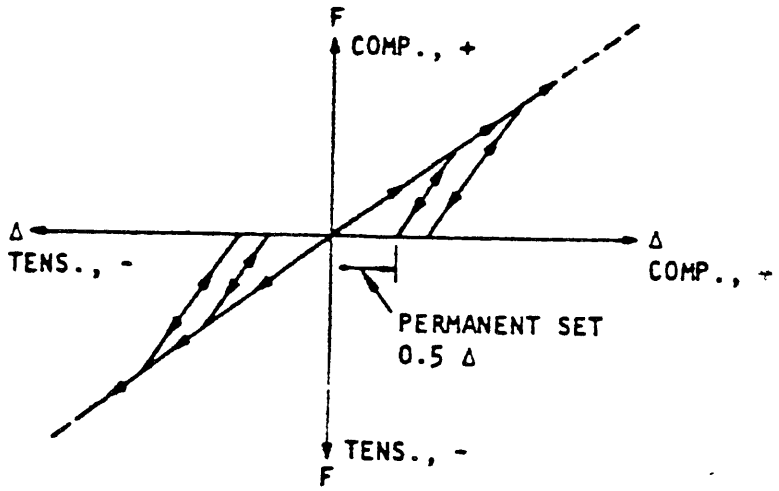

Fig. 4.7 Initial hysteresis rules for plywood diaphragms [11].

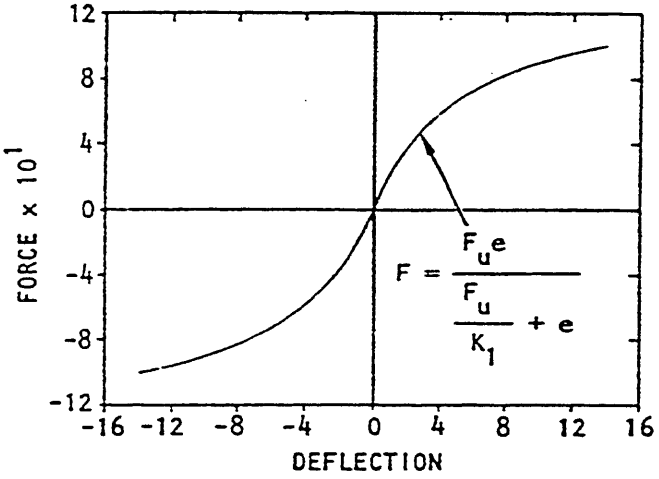

Force-deflection envelope of model

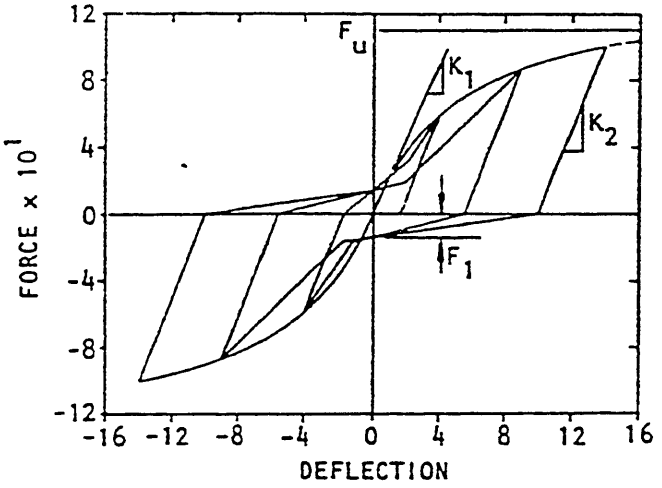

Typical cyclic load-deflection diagram for model

Fig. 4.8 Force–deflection envelope and hysteresis rules for plywood diaphragms developed after ABK tests [4].

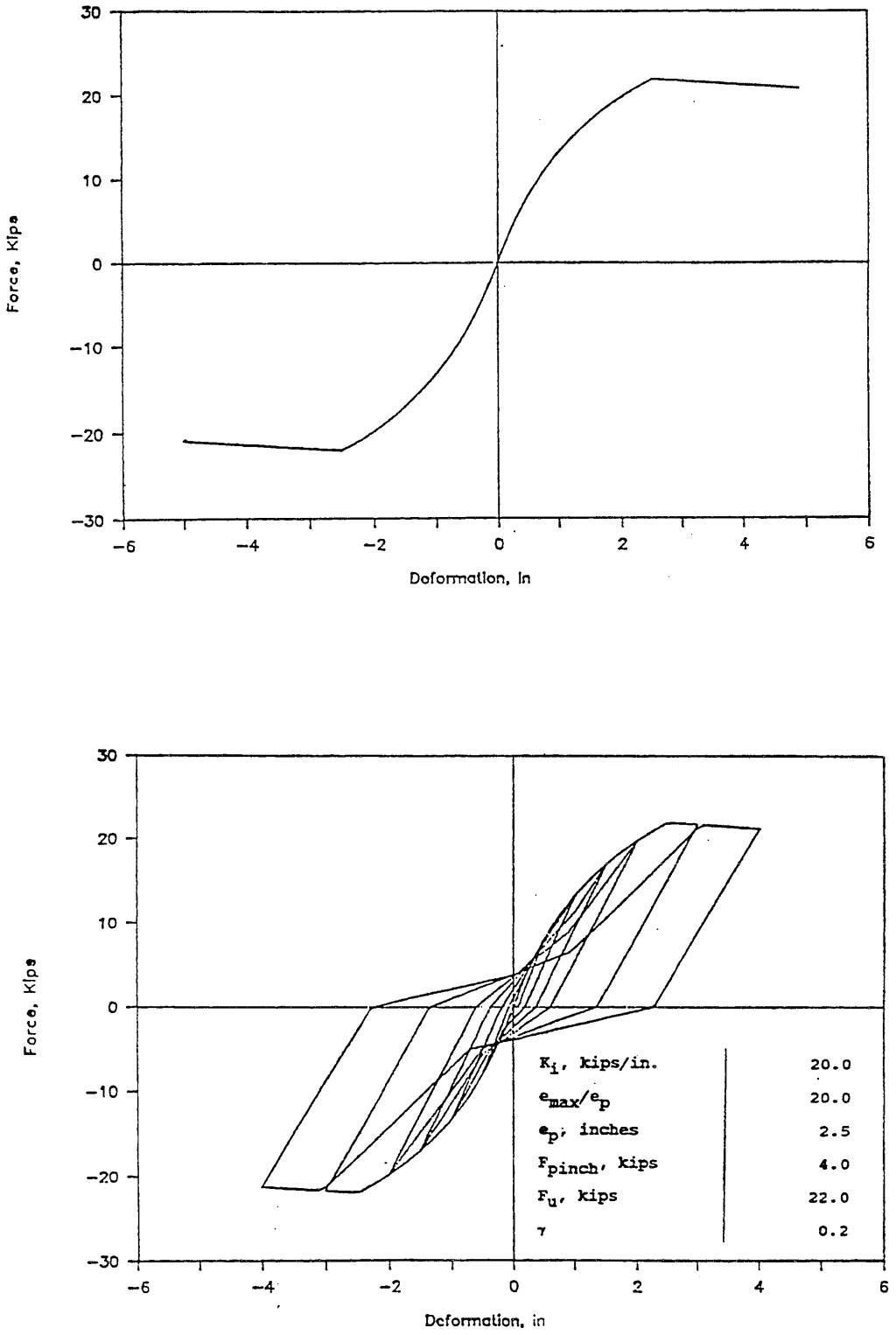

Fig. 4.9 Revised force–deflection envelope and hysteresis rules for plywood diaphragm [9].

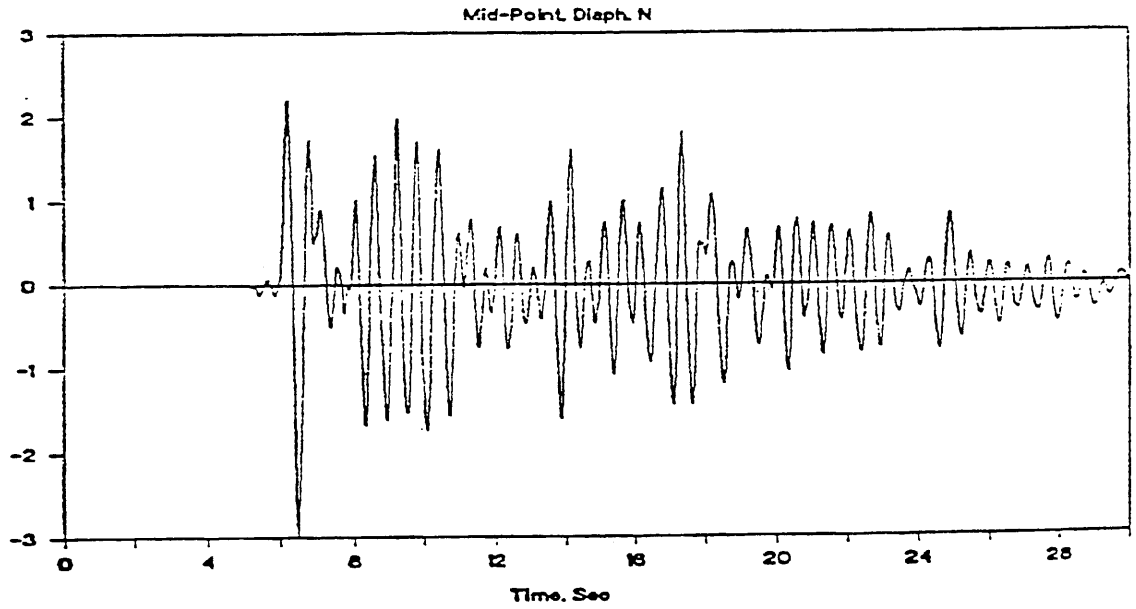

(a) Calculated response.

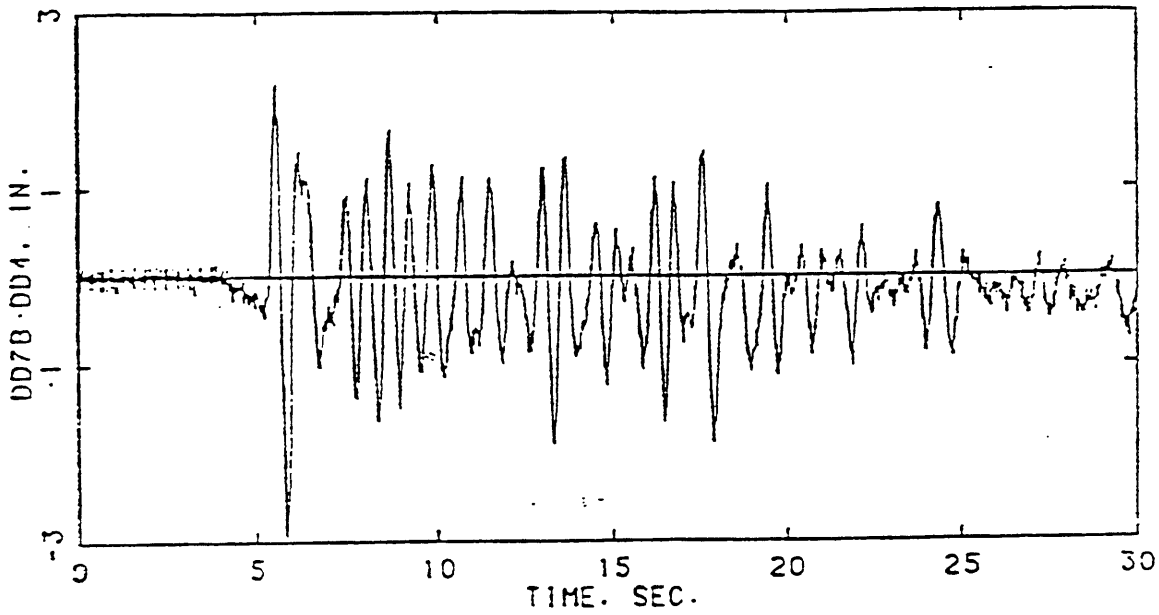

(b) Measured response.

Fig. 4.10 Comparison of measured and calculated displacement response of diaphragm N [9].

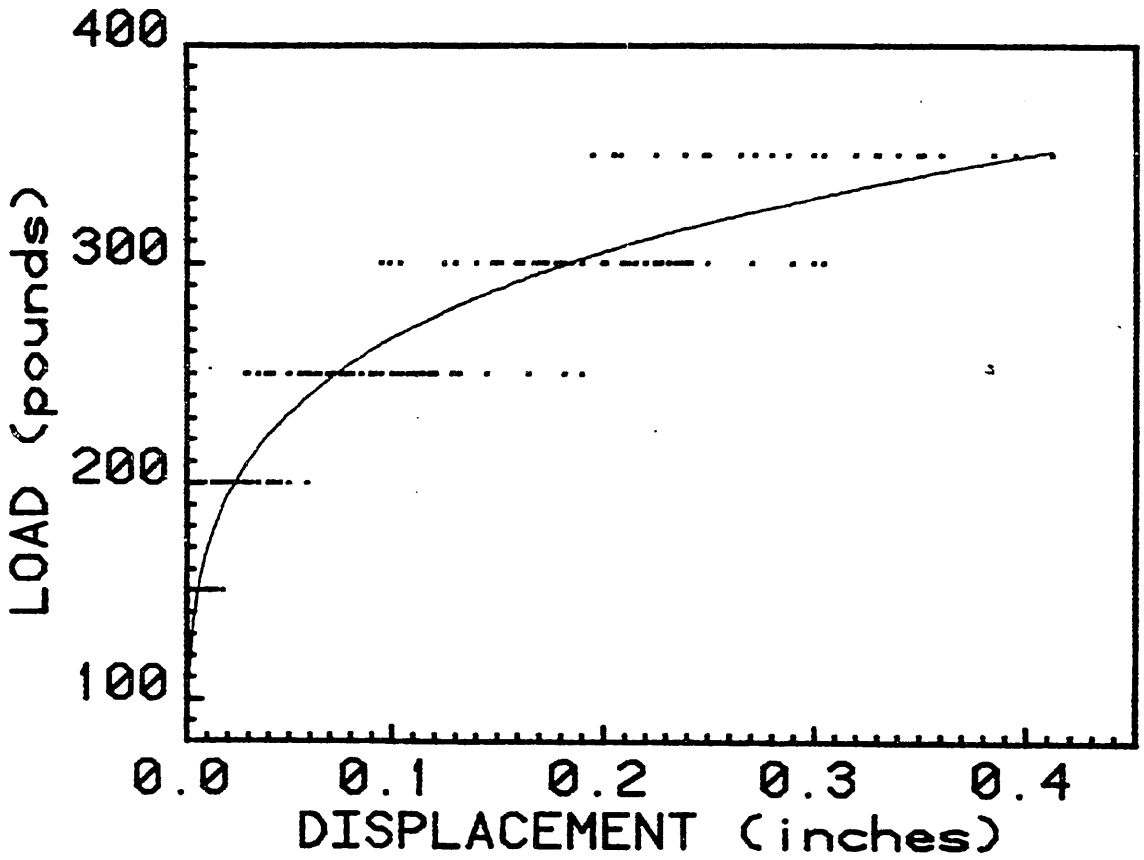

Fig. 4.11 Best–fit backbone curve through load–displacement data for nailed connections [39].

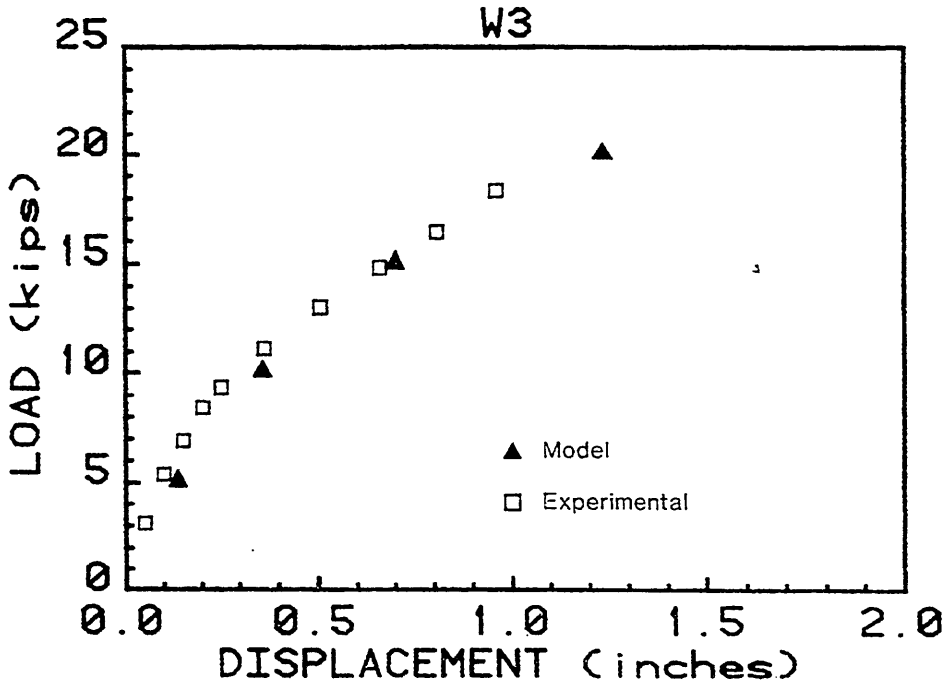

(a) Finite–element model developed by Itani and Falk [83].

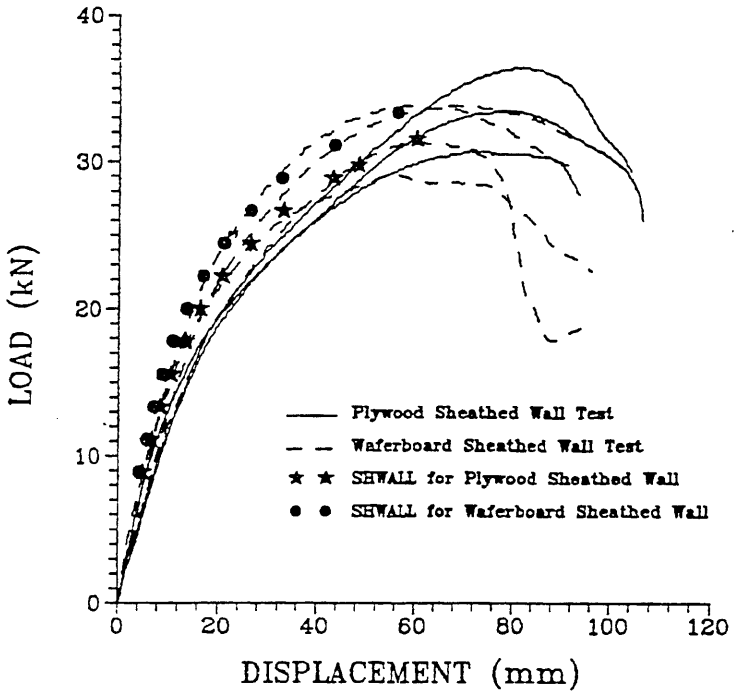

(b) Finite–element model developed by Dolan [26].

Fig. 4.12 Comparison of measured and calculated response of wall panels.

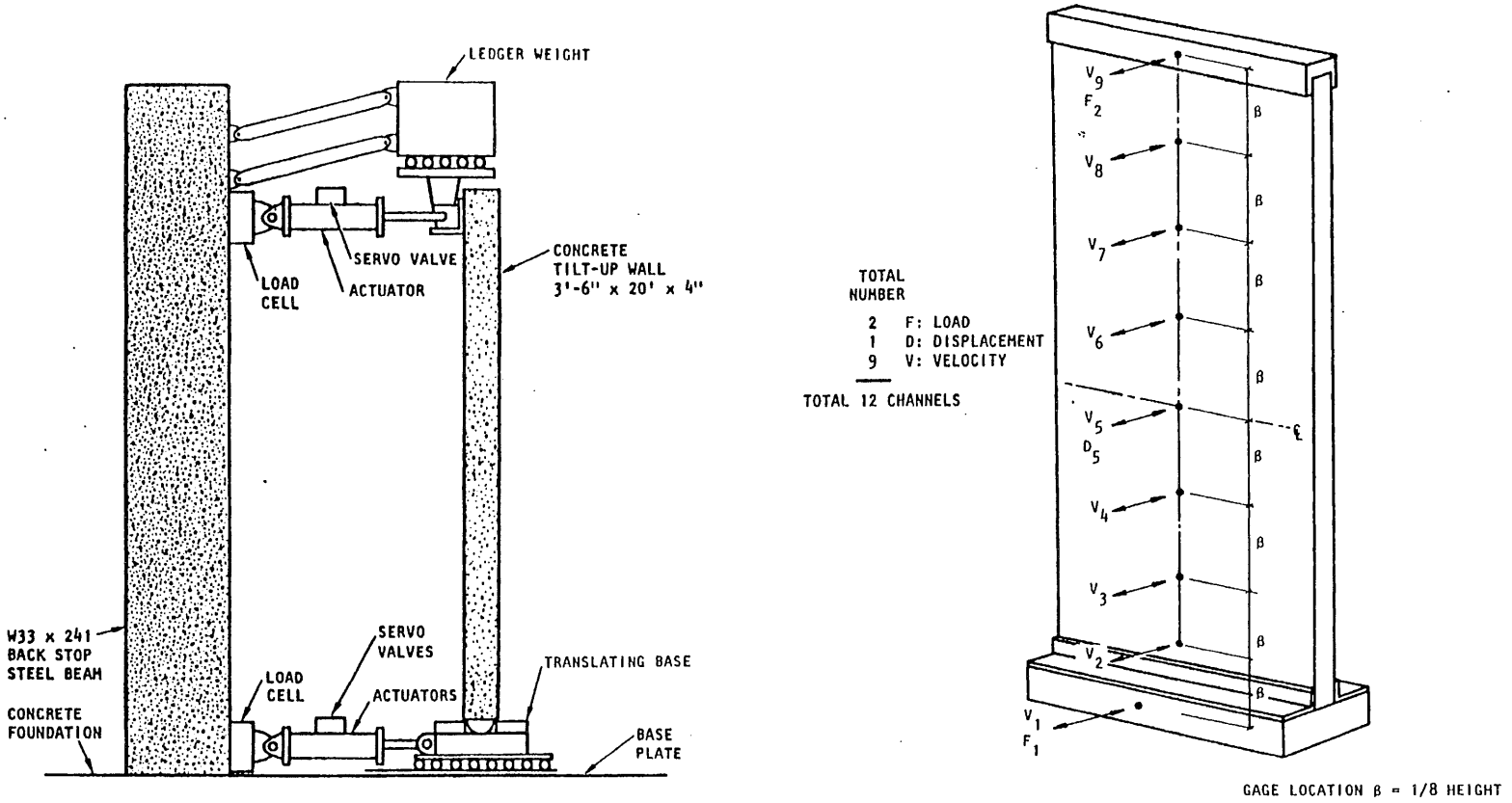

Fig. 4.13 Test configuration for dynamic testing of tilt–up wall panels [6,8,7].

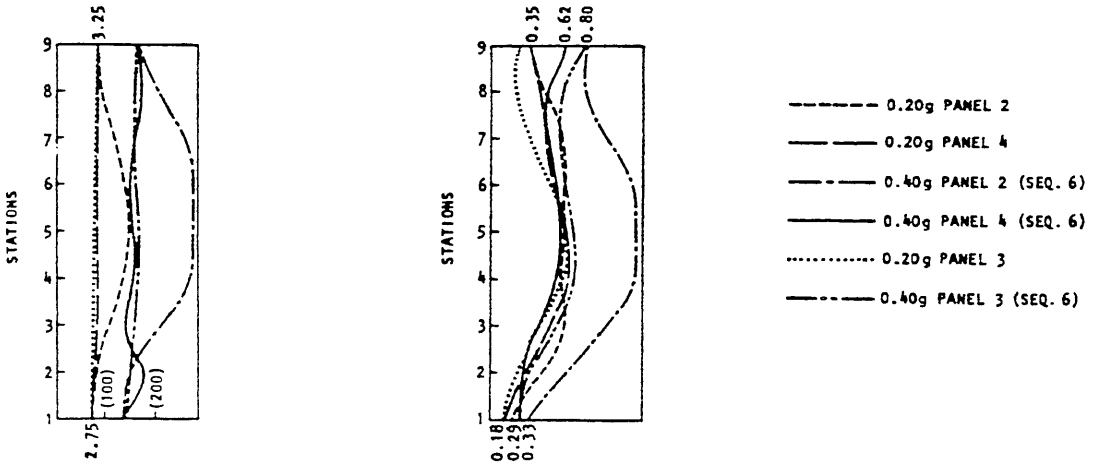

(a) Displacements, in.(mm) (b) Accelerations, g

Fig. 4.14 Comparison of maximum response of panels 2, 3, and 4 with a rigid roof diaphragm subjected to El Centro base motion [6,8,7].

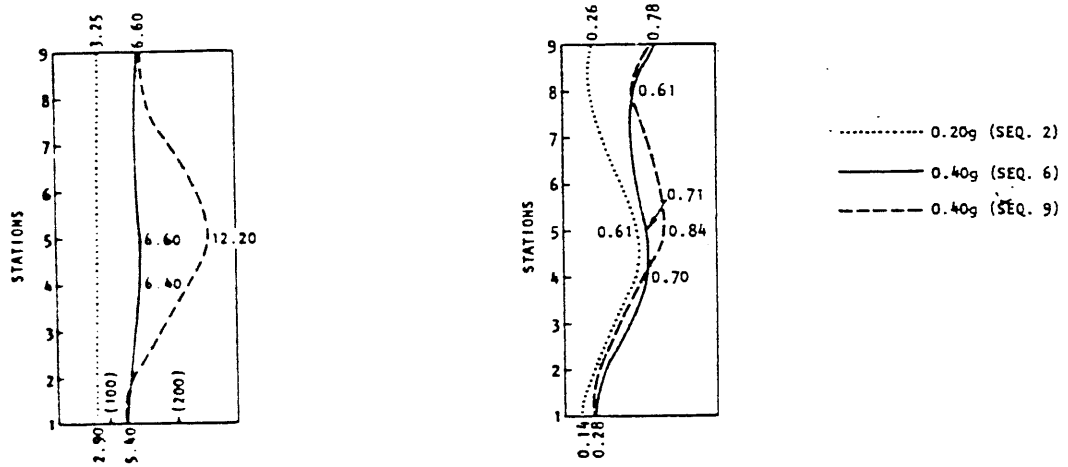

(a) Displacements, in. (mm) (b) Accelerations, g

Fig. 4.15 Displacement and acceleration distributions in panel 3 with a rigid roof diaphragm subjected to varying intensities of the El Centro base motion [6,8,7].

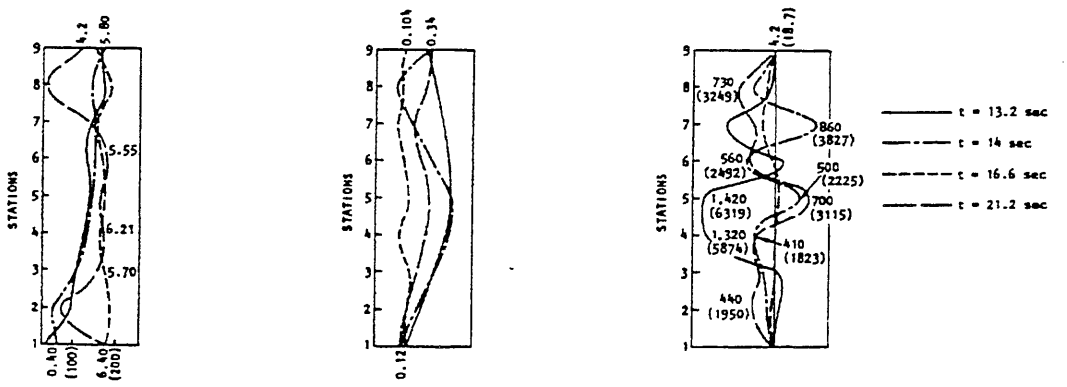

(a) Displacements, in. (mm) (b) Accelerations, g (c) Moments, in.-lb (N. m)

Fig. 4.16 Displacement, acceleration, and moment distributions in panel 4 with a rigid roof diaphragm subjected to varying intensities of the El Centro base motion [6, 8, 7].

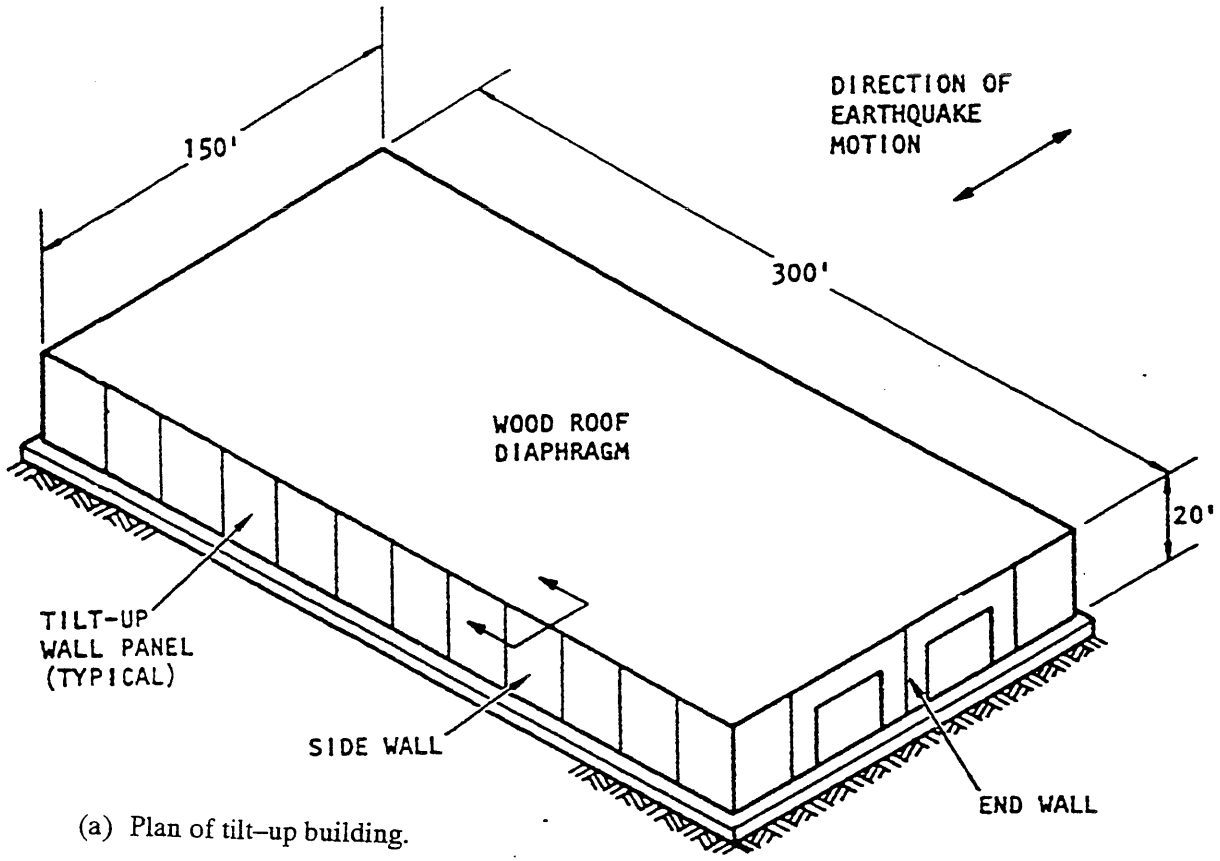

(a) Plan of tilt–up building.

Fig. 4.17 One–story tilt–up building used to develop analytical model [4].

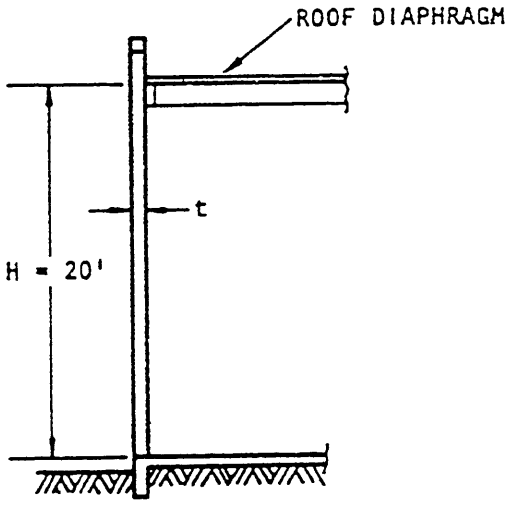

(b) Cross section.

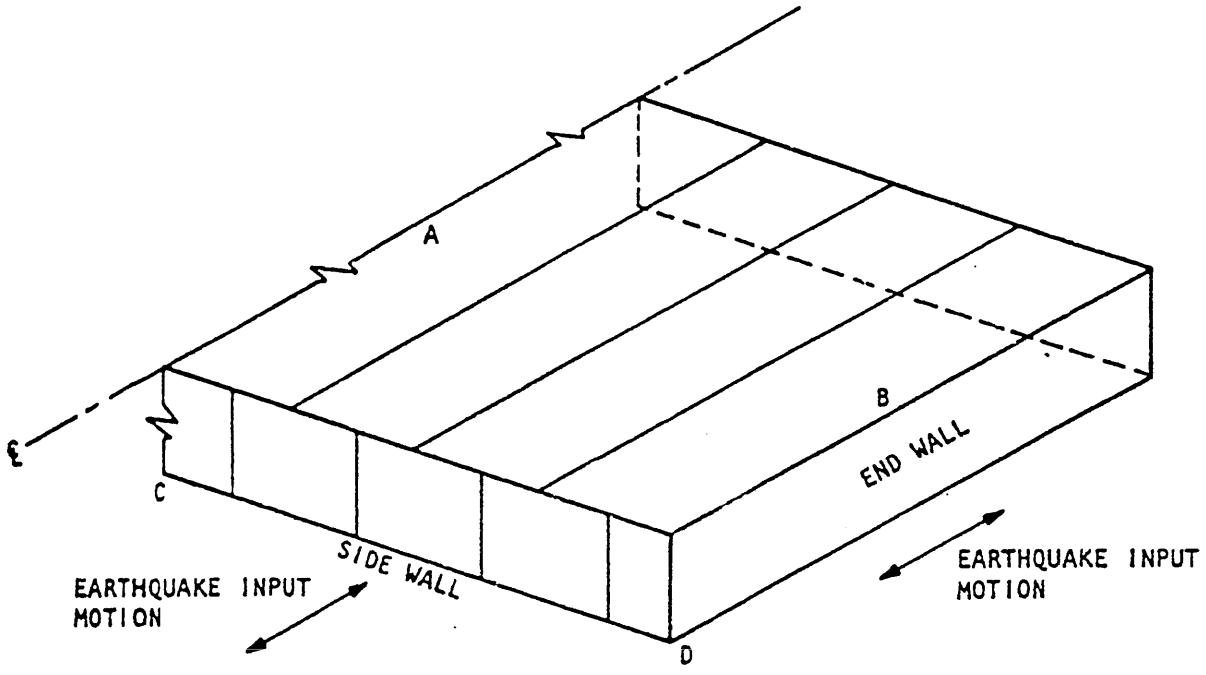

(c) Conceptual model of building.

Fig. 4.17 (cont.) One–story tilt–up building used to develop analytical model [4].

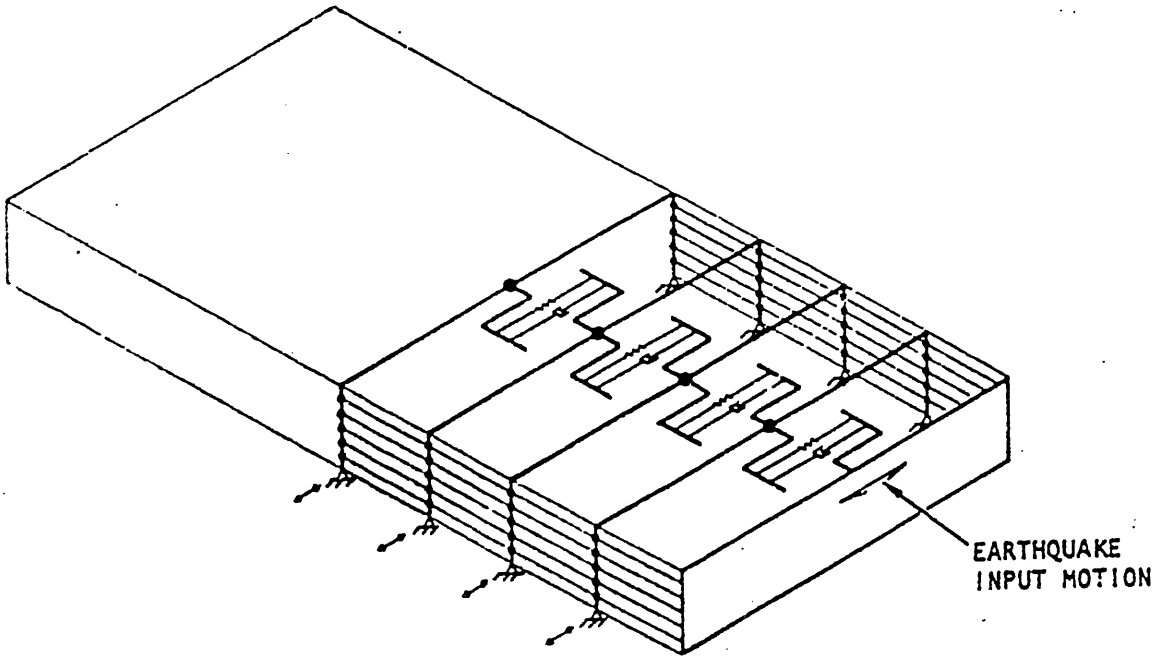

(d) Representation of building with linear beam elements and nonlinear diaphragm elements.

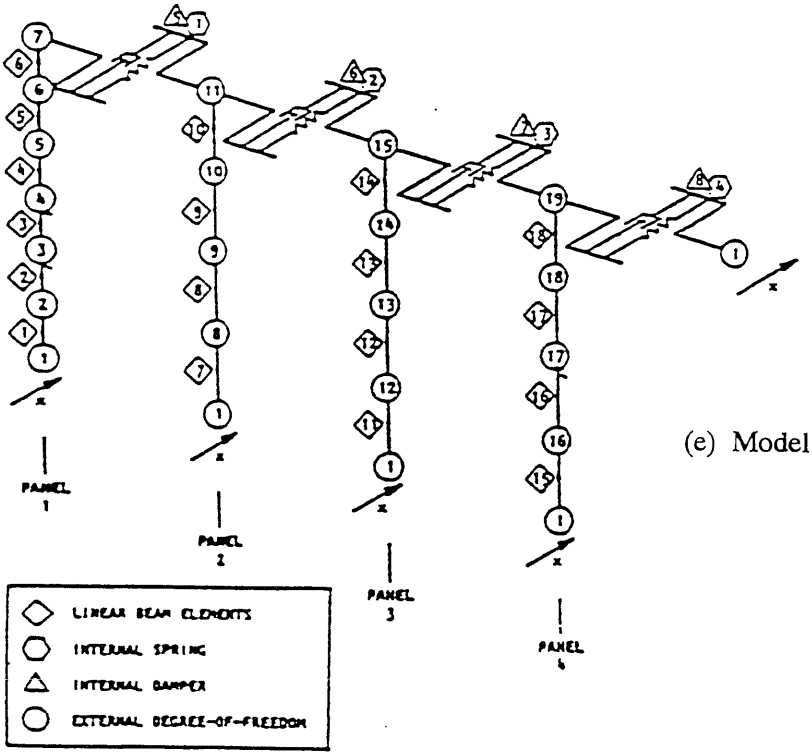

(e) Model of building used in analyses.

Fig. 4.17 (cont.) One–story tilt–up building used to develop analytical model [4].

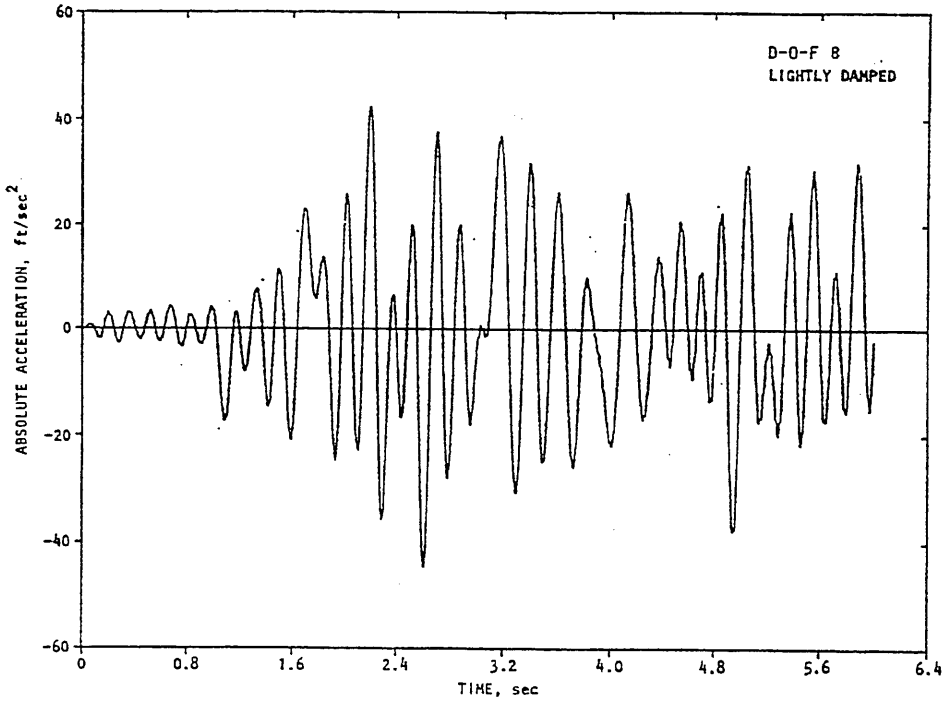

(a) Acceleration at mid–height of panel.

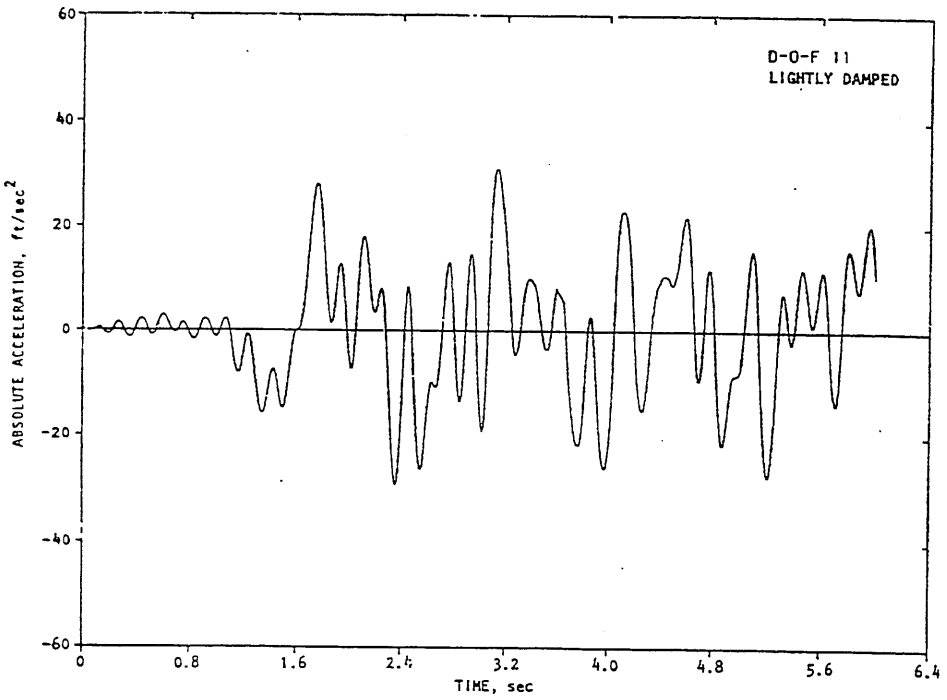

(b) Acceleration at top of panel.

Fig. 4.18 Calculated acceleration response of center longitudinal wall panel for lightly–damped model [4].

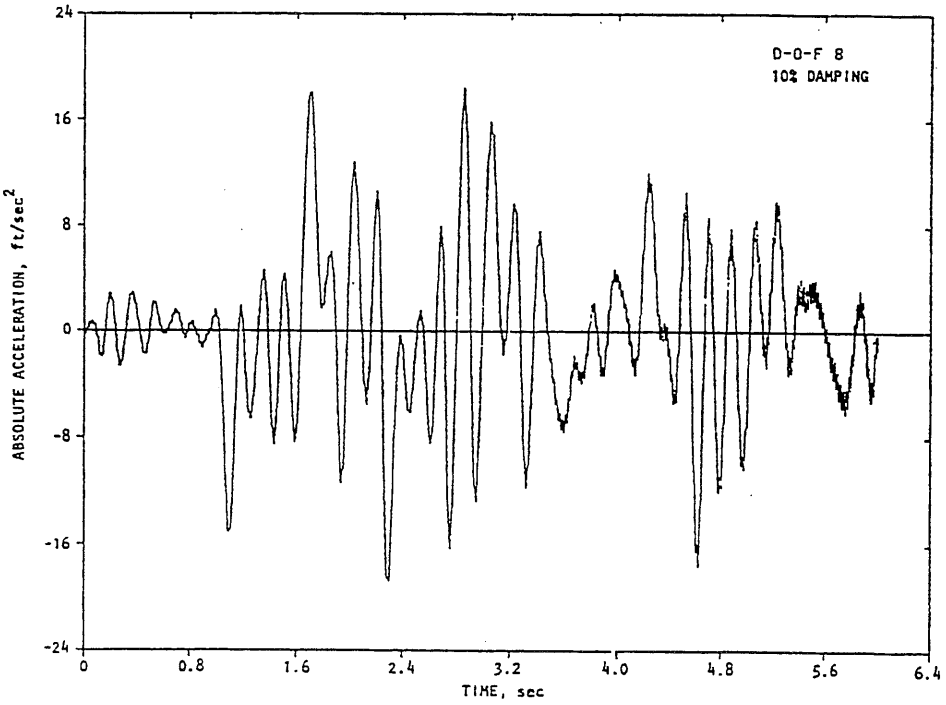

(a) Acceleration at mid–height of panel.

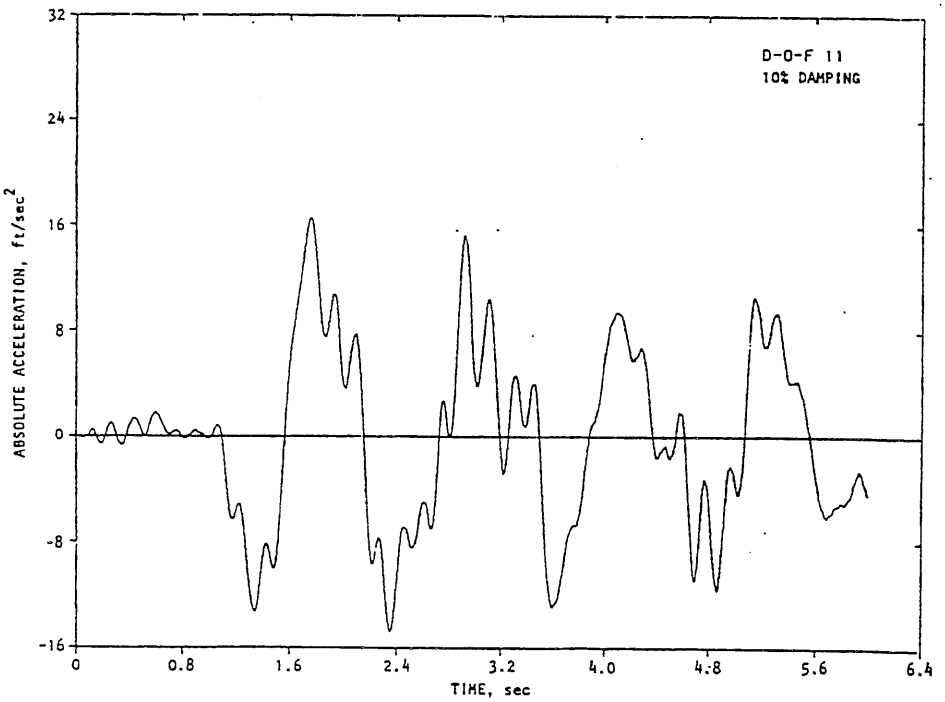

(b) Acceleration at top of panel.

Fig. 4.19 Calculated acceleration response of center longitudinal wall panel for moderately–damped model [4].

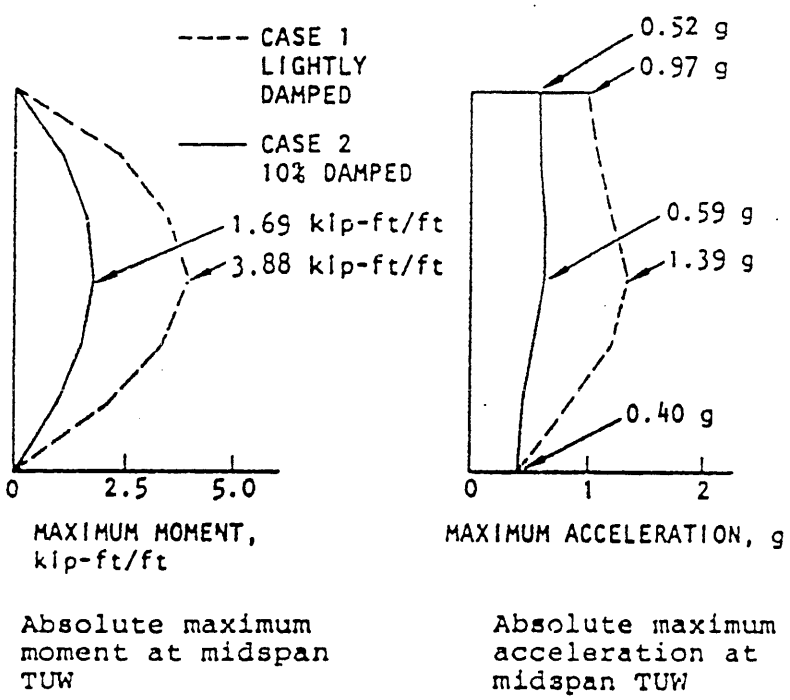

Fig. 4.20 Calculated distributions of acceleration and moment along the height of the center longitudinal wall panel [4].

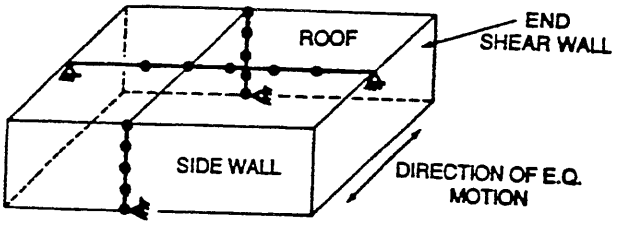

(a) Idealized tilt–up building.

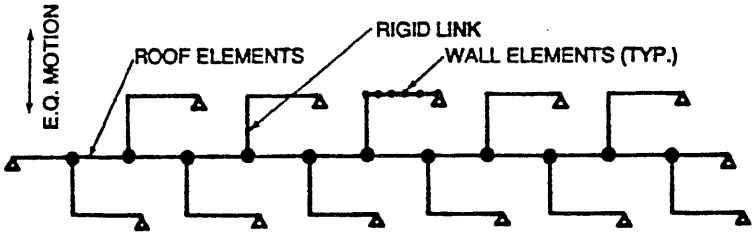

(b) Model used for linear analyses.

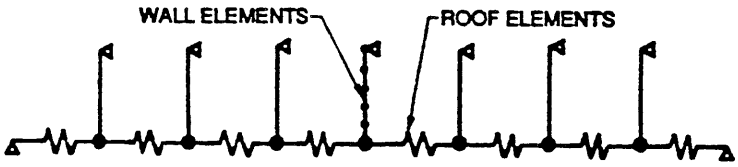

(c) Model used for nonlinear analyses.

Fig. 4.21 Analytical models of one–story tilt–up building [53,54].

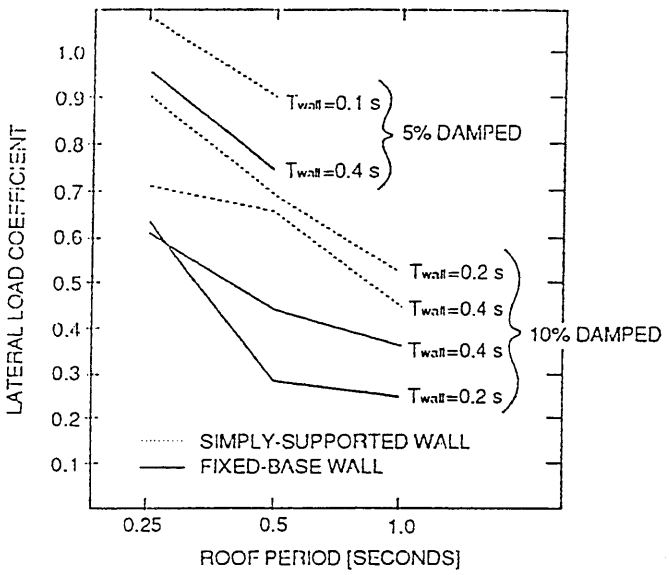

Fig. 4.22 Calculated roof–to–panel connection forces [53,54].

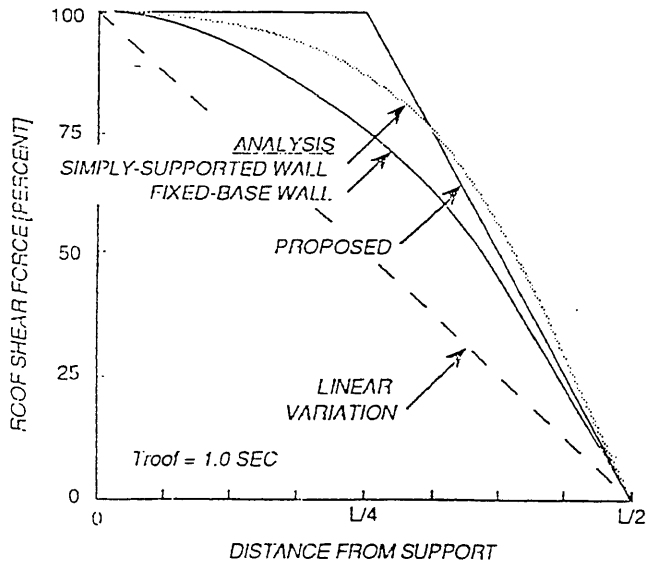

Fig. 4.23 Calculated distribution of shear forces in the diaphragm [53,54].

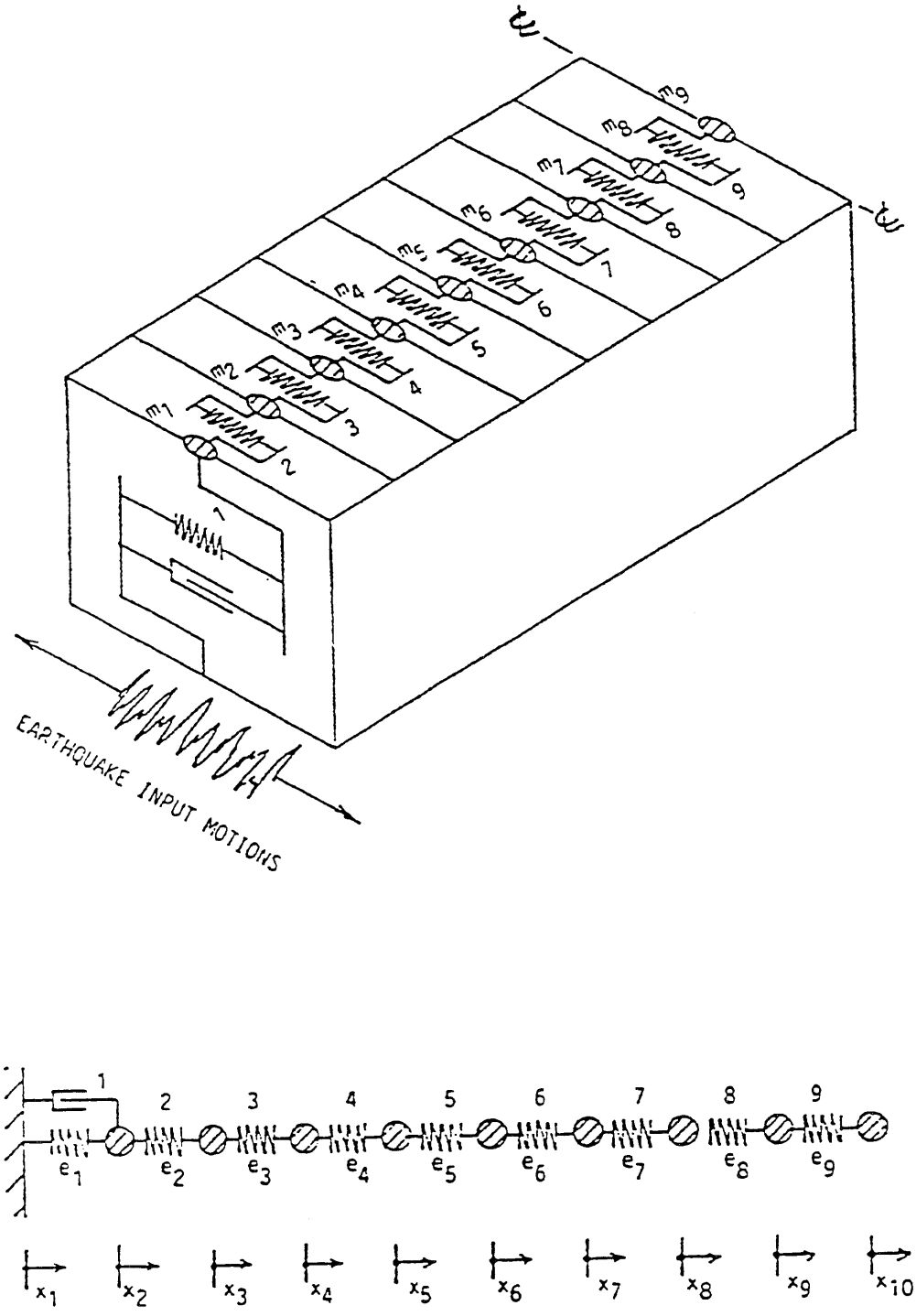

Fig. 4.24 Analytical model of Hollister warehouse for input motion in the transverse direction [9].

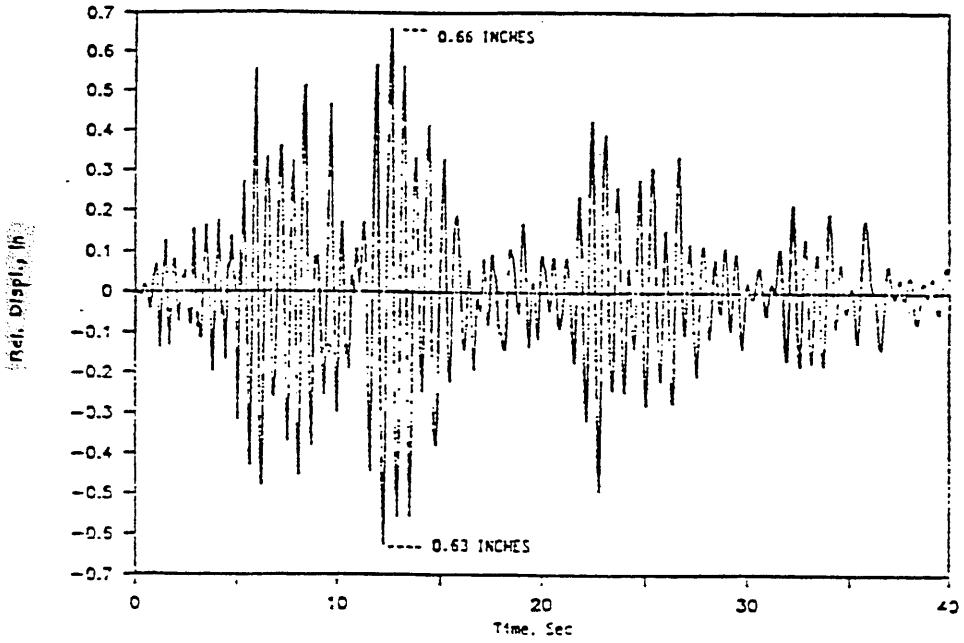

(a) Calculated response.

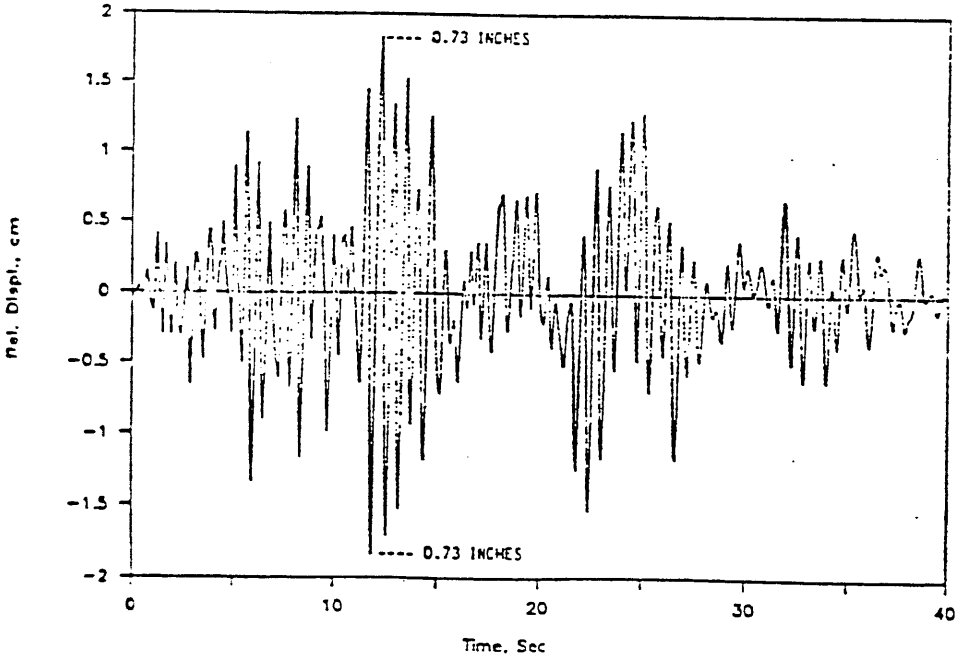

(b) Measured response.

Fig. 4.25 Relative displacements at the center of the diaphragm in the Hollister warehouse during the 1986 Morgan Hill earthquake [9].

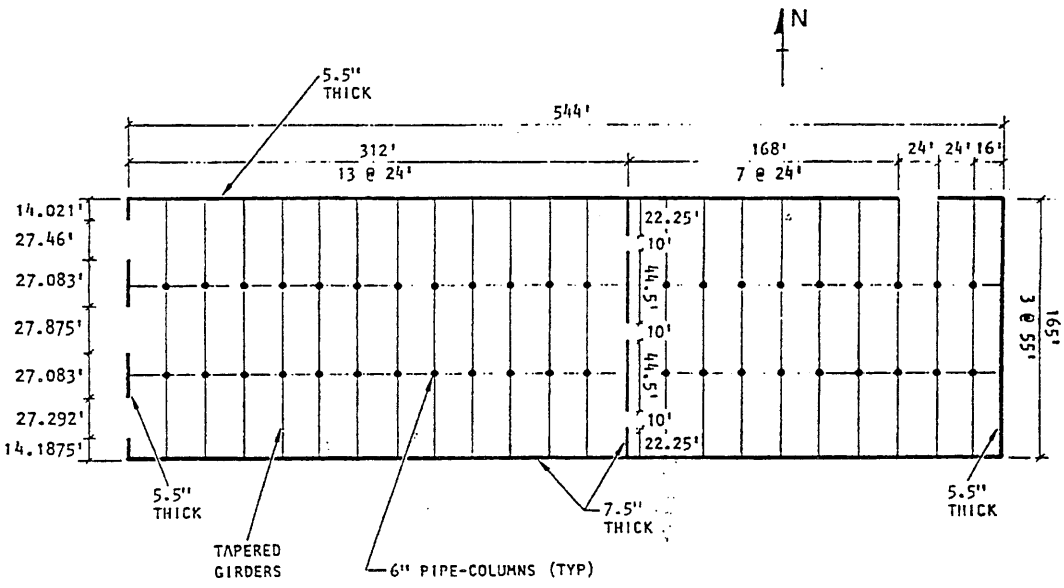

DOWNEY BUILDING

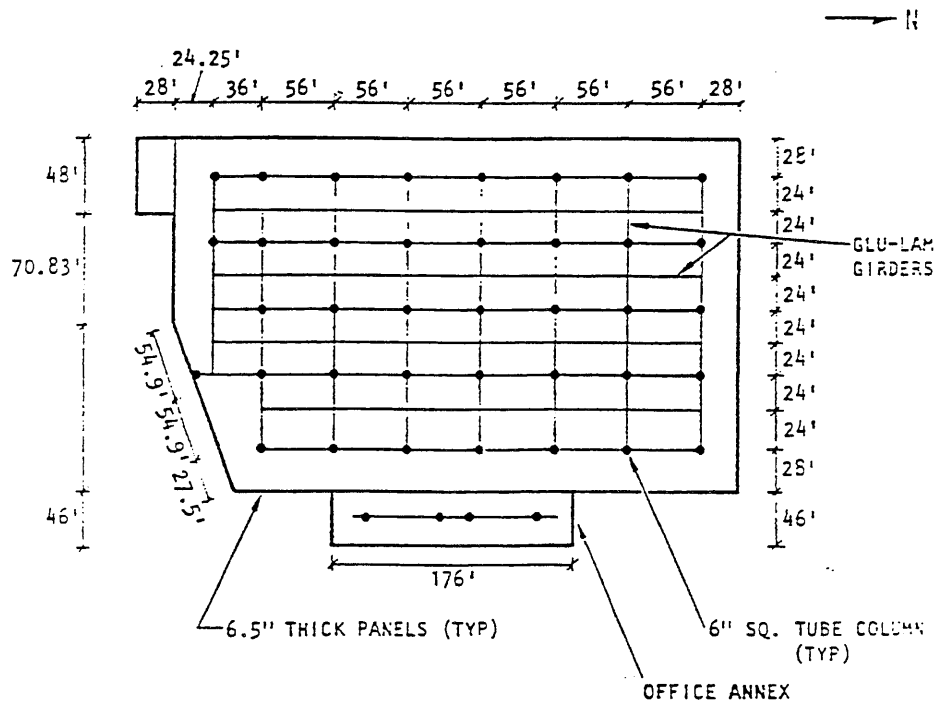

WHITTIER BUILDING

Fig. 4.26 Plan views of tilt–up buildings in Downey and Whittier [9].

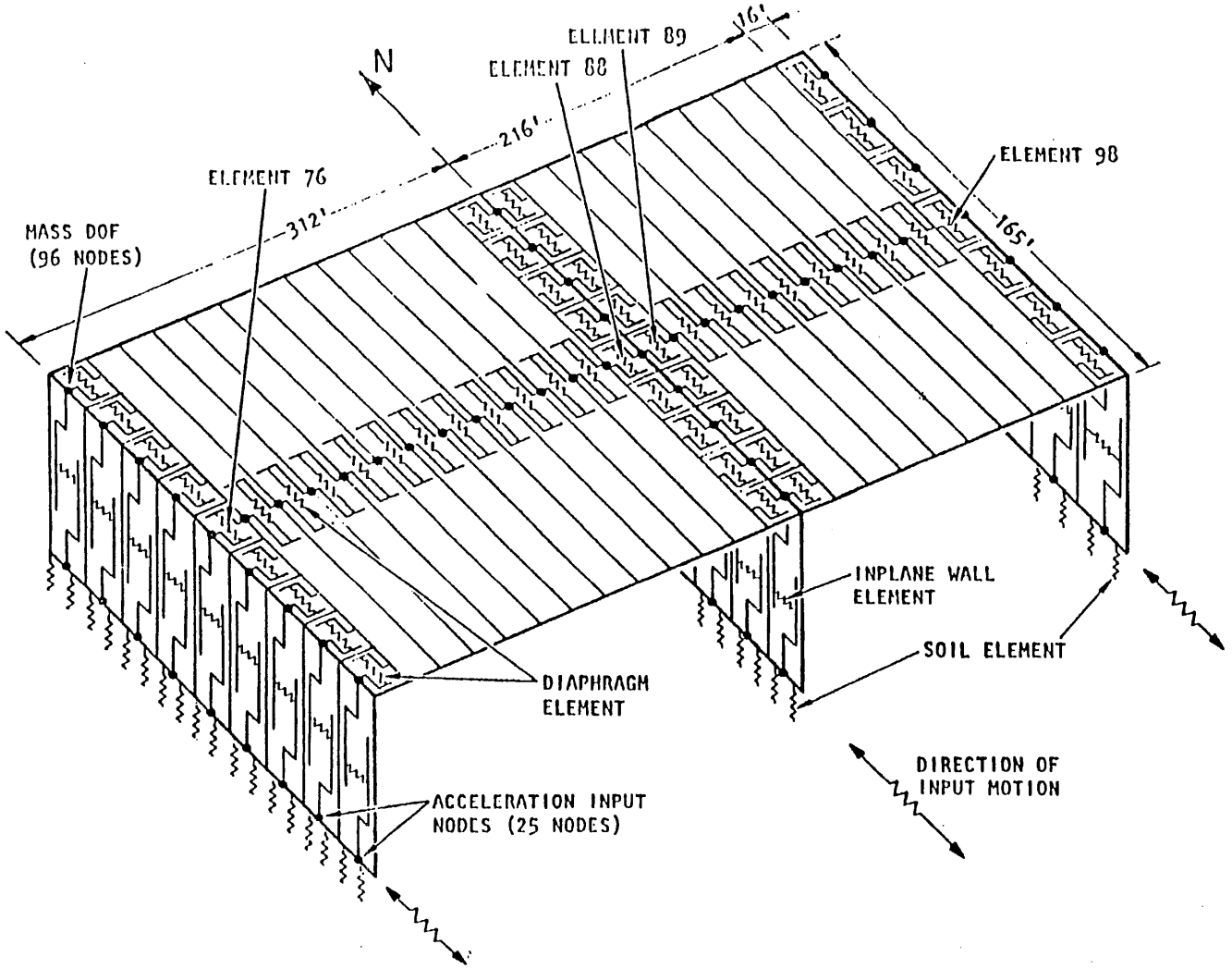

Fig. 4.27 Analytical model of Downey building for input motion in the transverse direction [9].

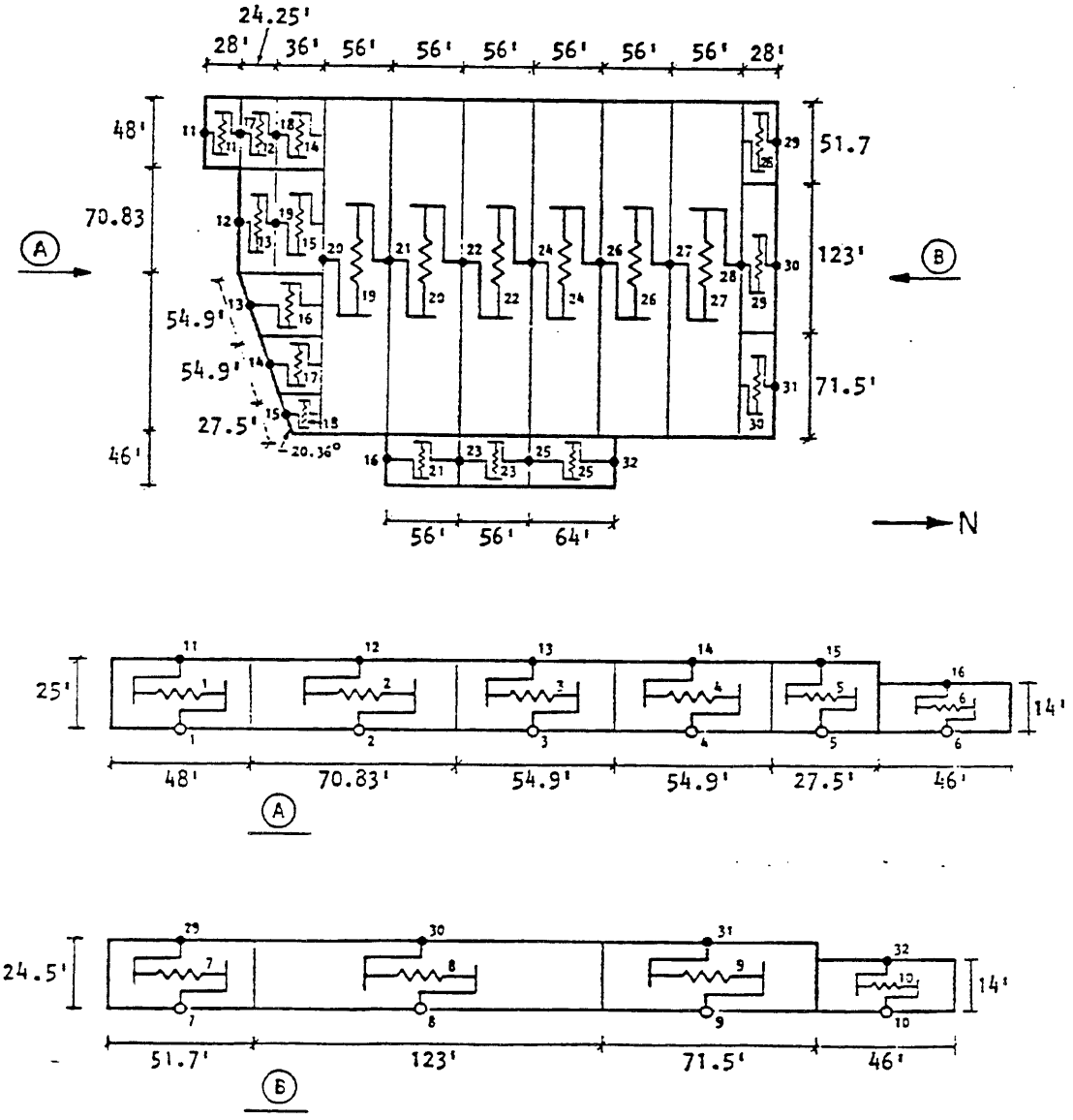

Fig. 4.28 Analytical model of Whittier building for input motion in the transverse direction [9].

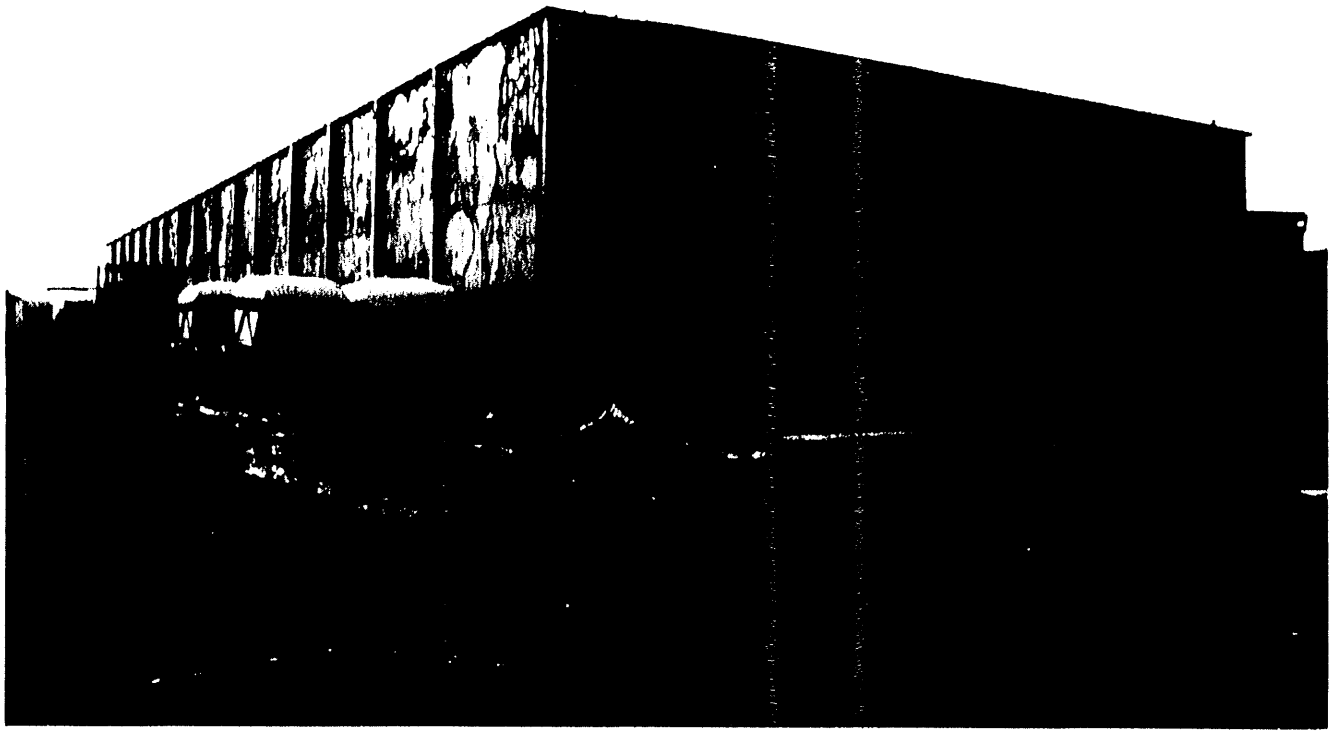

Fig. 5.1 Hollister warehouse.

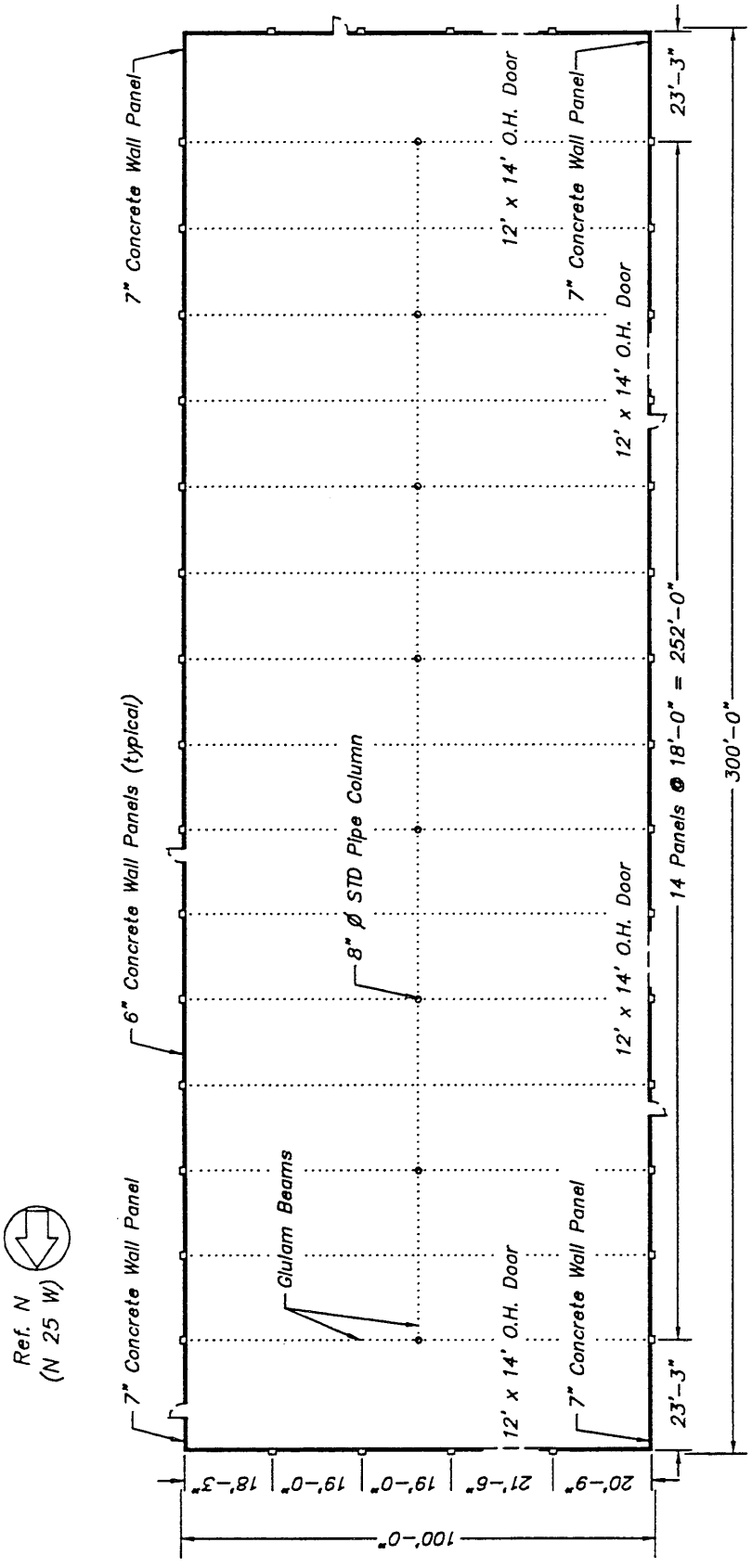

Fig. 5.2 Floor plan – Hollister warehouse.

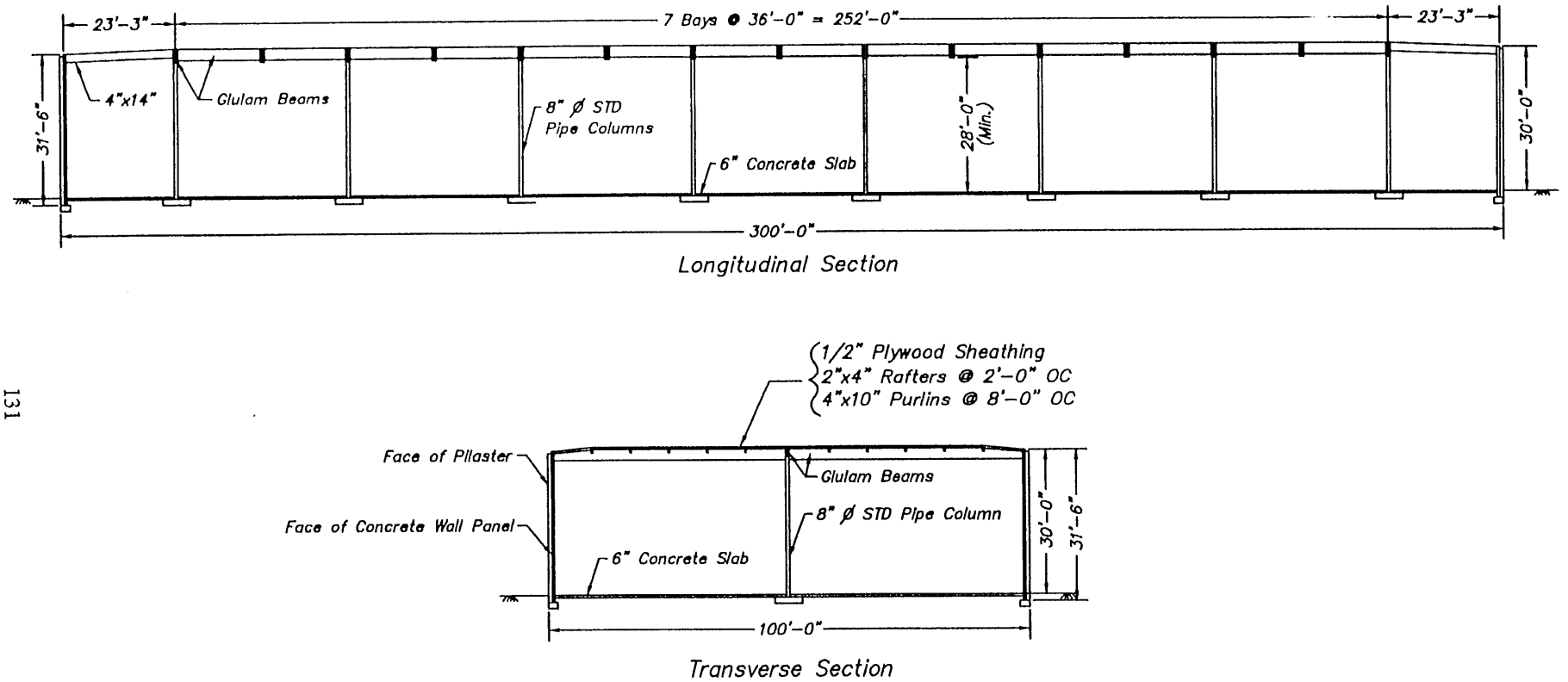

Fig. 5.3 Cross sections – Hollister warehouse.

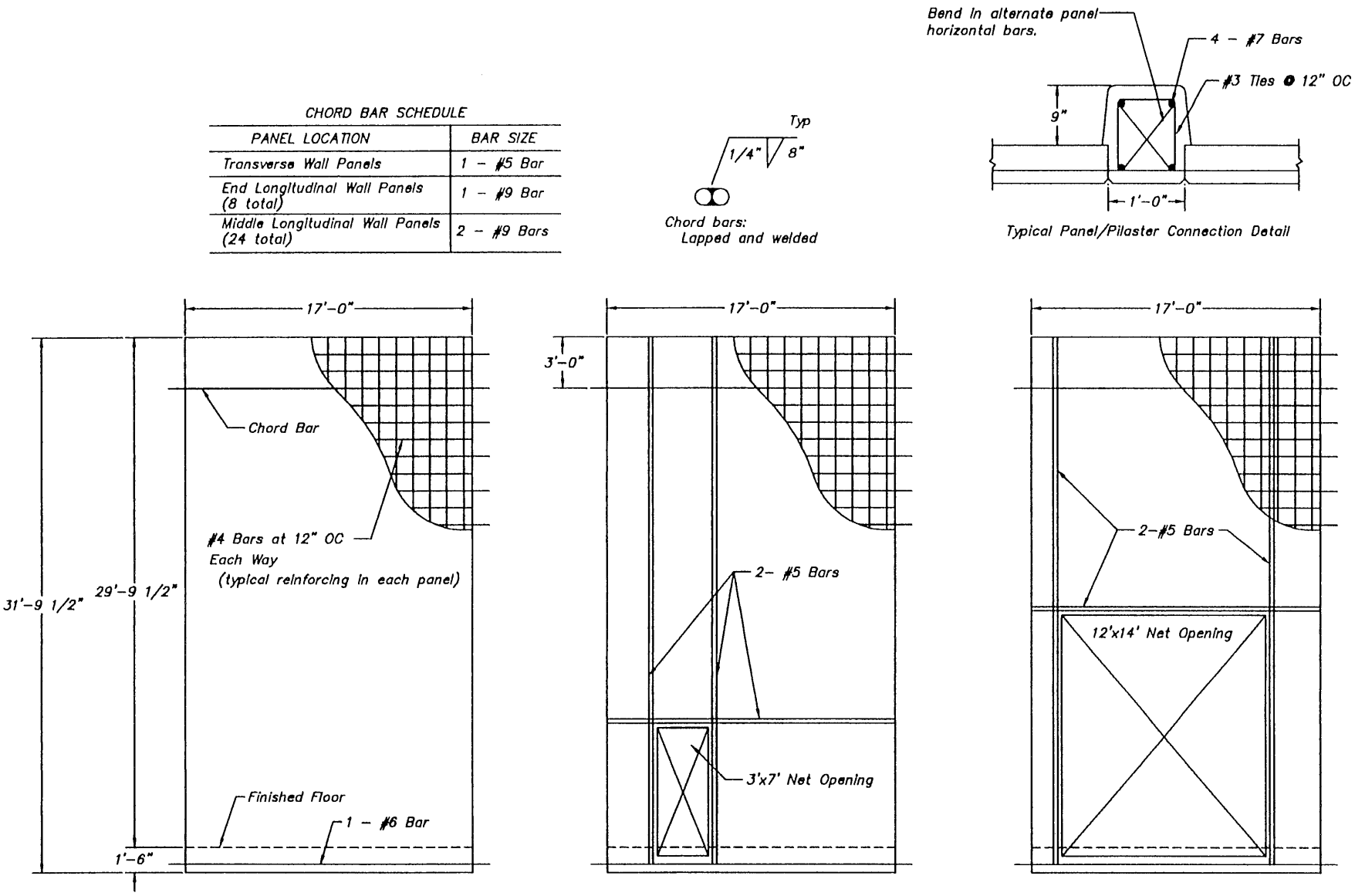

Fig. 5.4 Typical panel reinforcement details – Hollister warehouse.

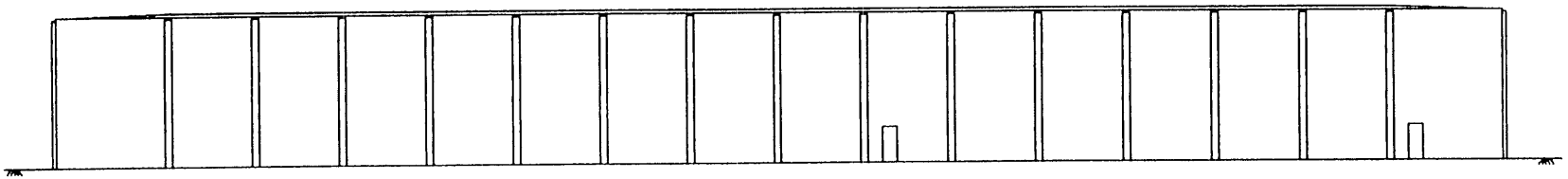

East Elevation

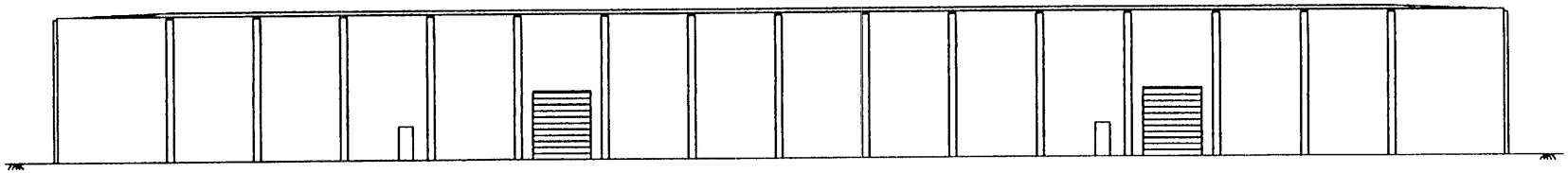

West Elevation

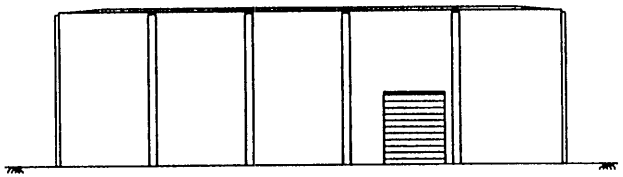

North Elevation

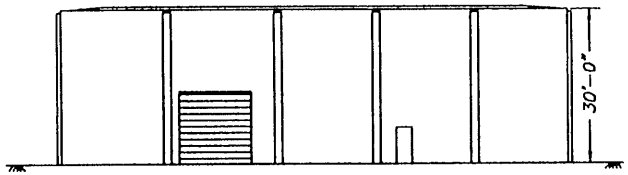

South Elevation

Fig. 5.5 Elevations – Hollister warehouse.

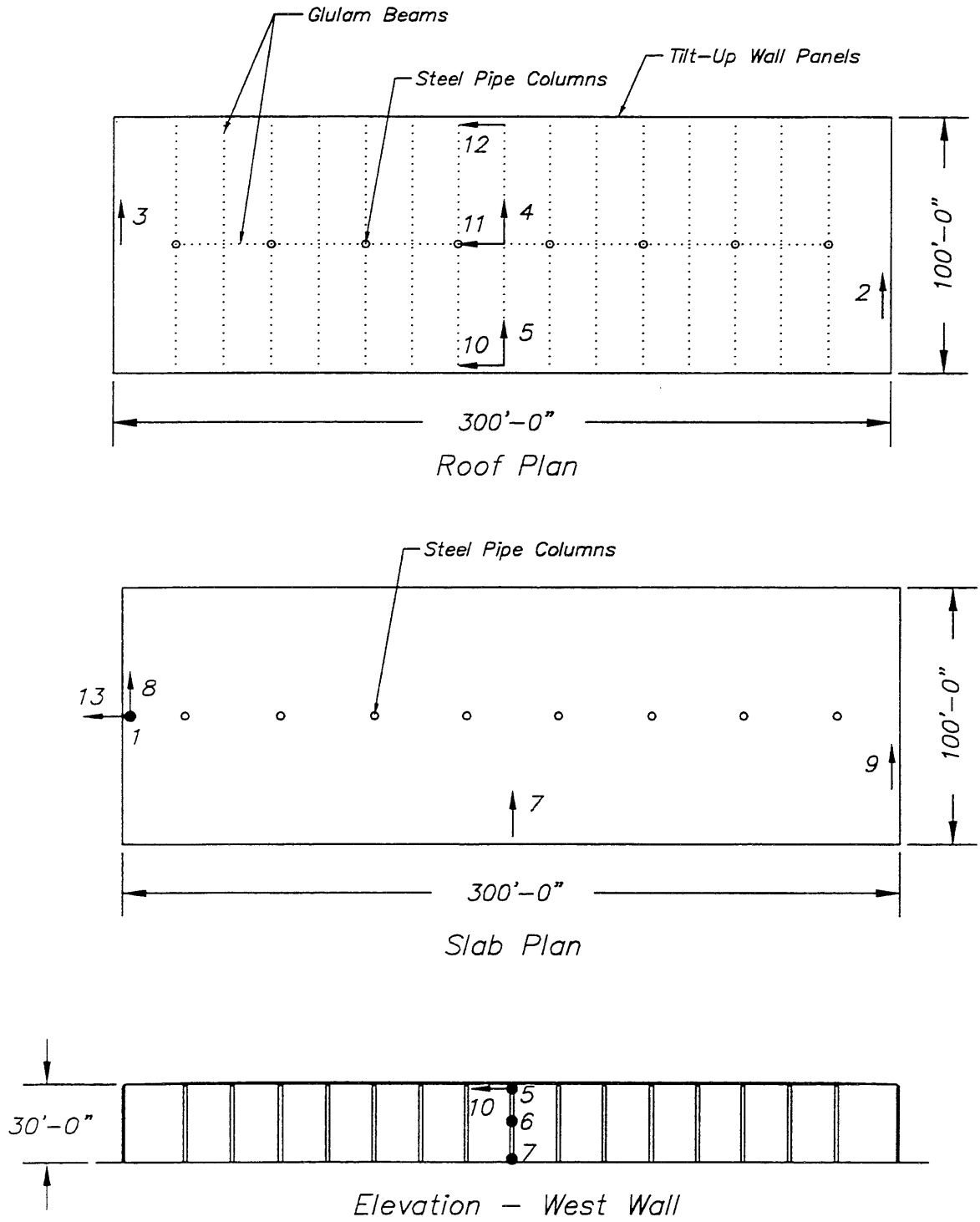

Fig. 5.6 Locations of strong–motion instruments – Hollister warehouse.

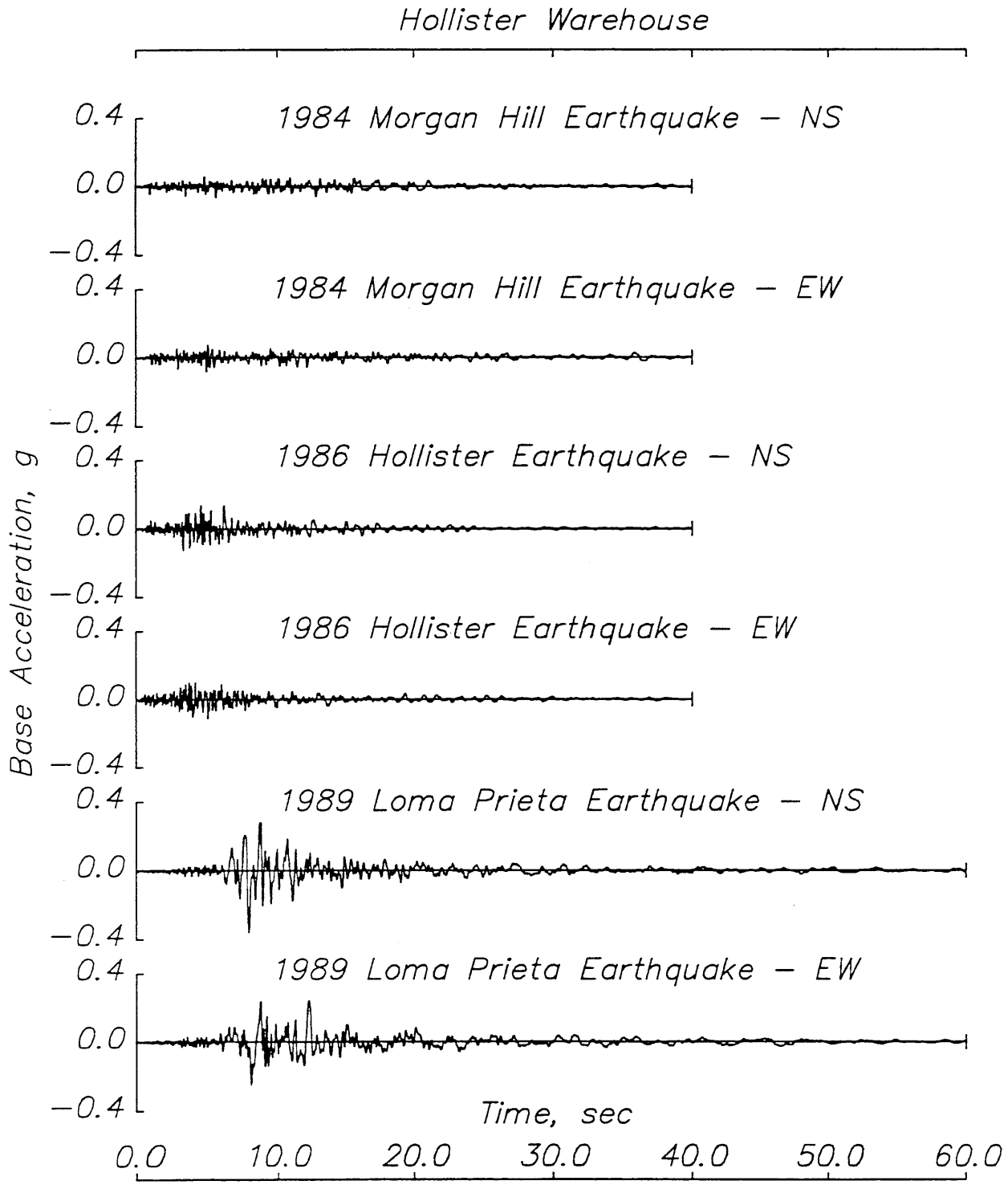

Fig. 5.7 Measured ground accelerations – Hollister warehouse.

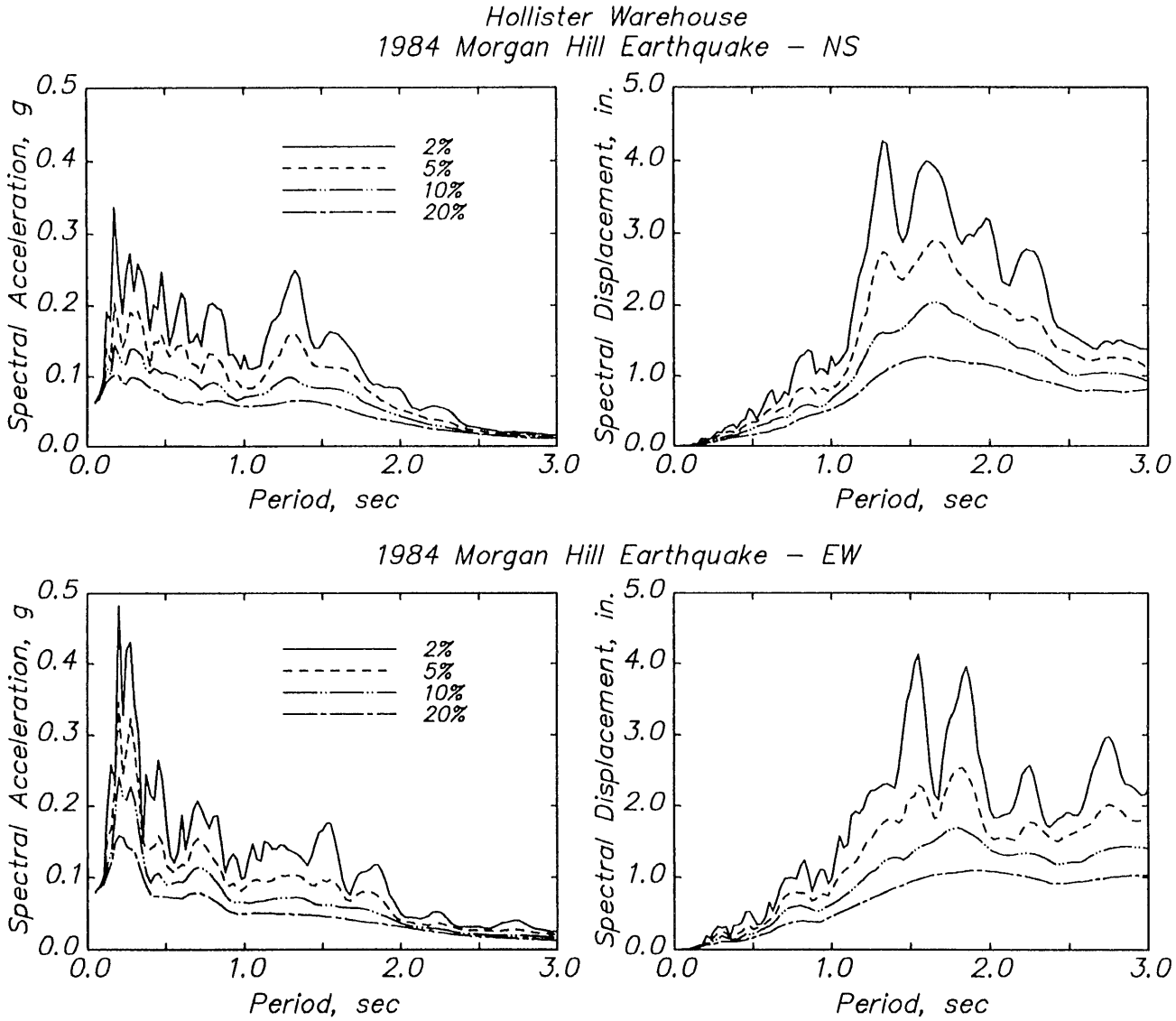

Fig. 5.8 Linear response spectra – Hollister warehouse.

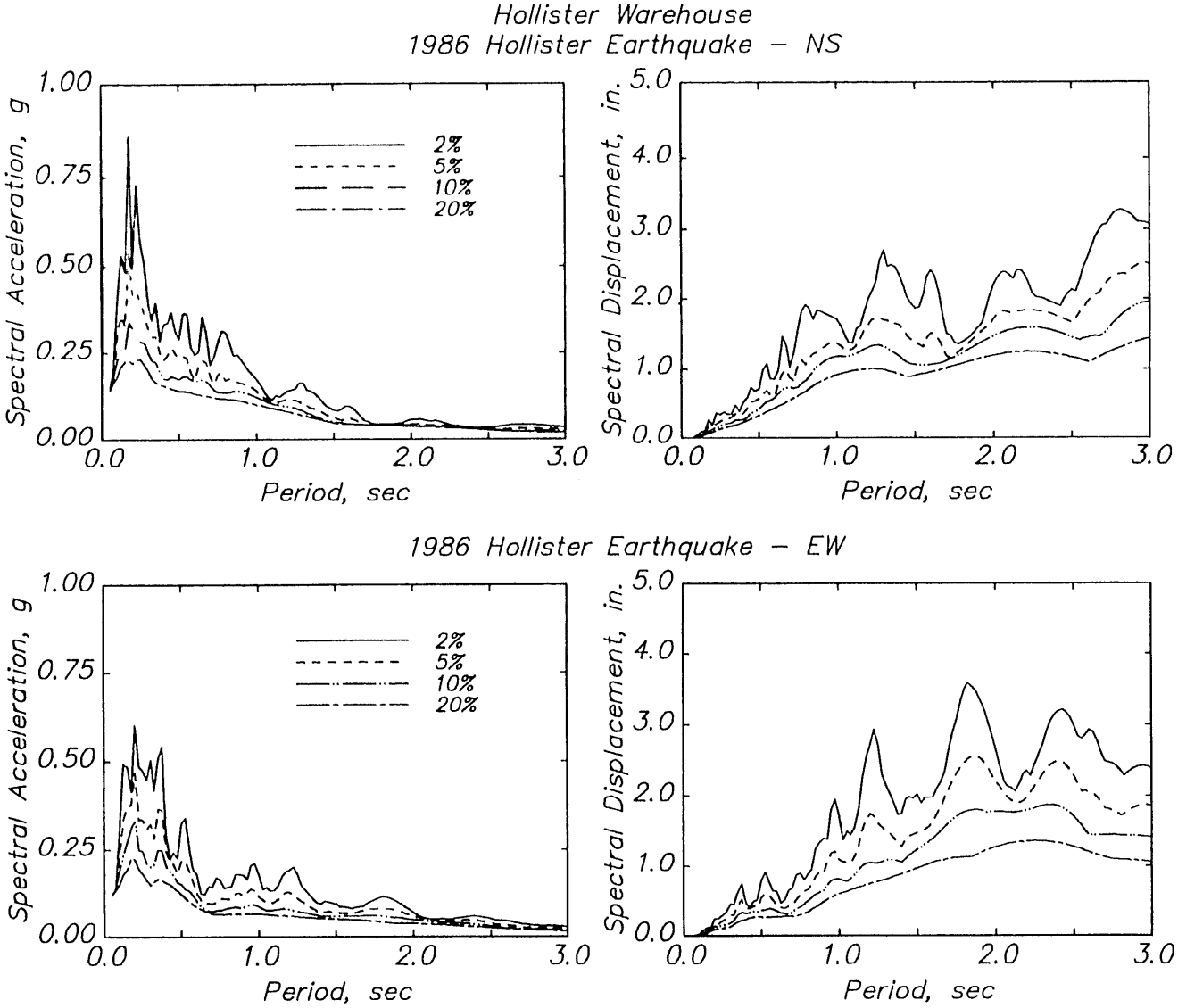

Fig. 5.8 (cont.) Linear response spectra – Hollister warehouse.

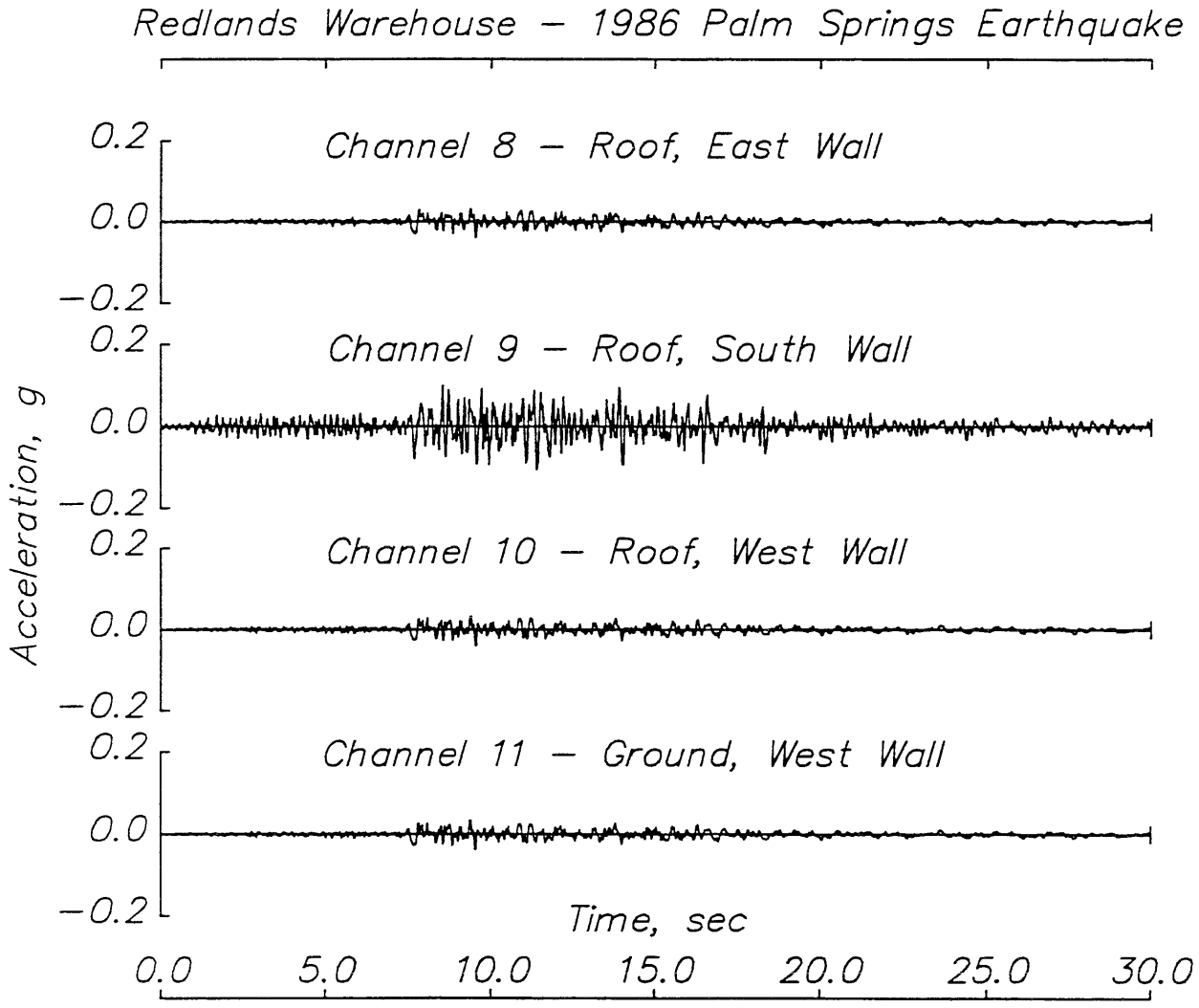

Fig. 5.26 Redlands warehouse – 1986 Palm Springs earthquake.
(b) Longitudinal acceleration response.

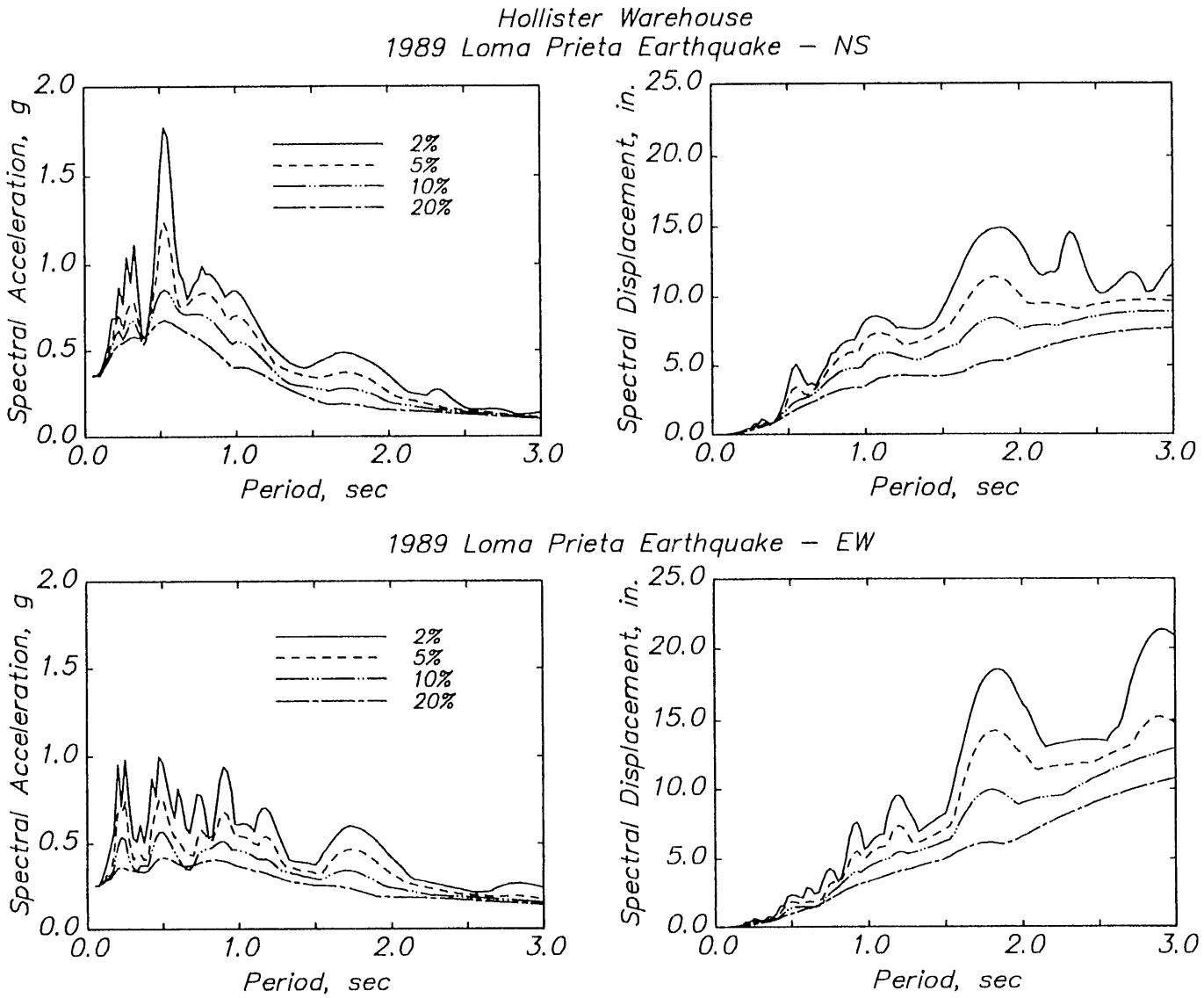

Fig. 5.8 (cont.) Linear response spectra – Hollister warehouse.

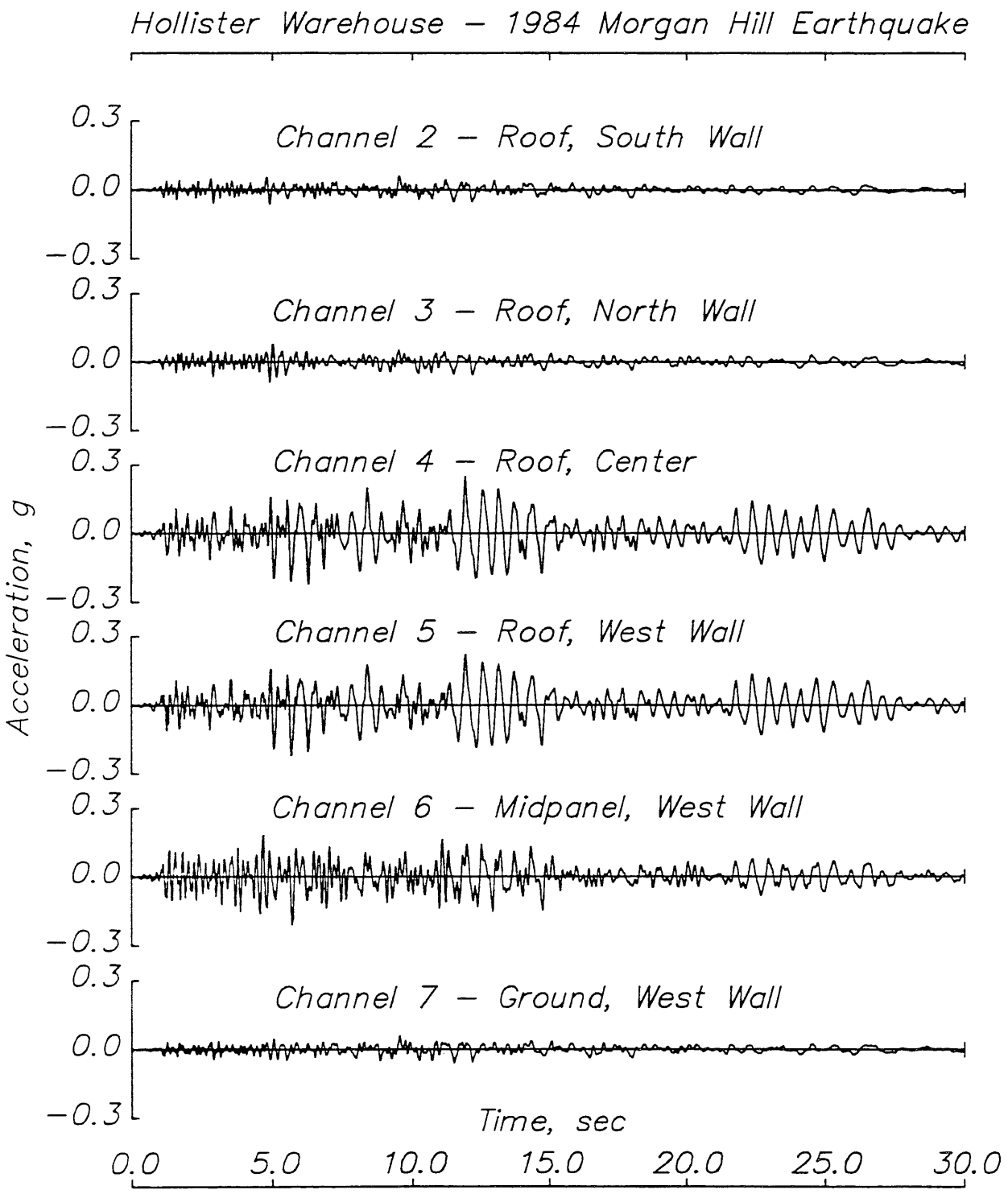

Fig. 5.9 Hollister warehouse – 1984 Morgan Hill earthquake.
(a) Transverse acceleration response.

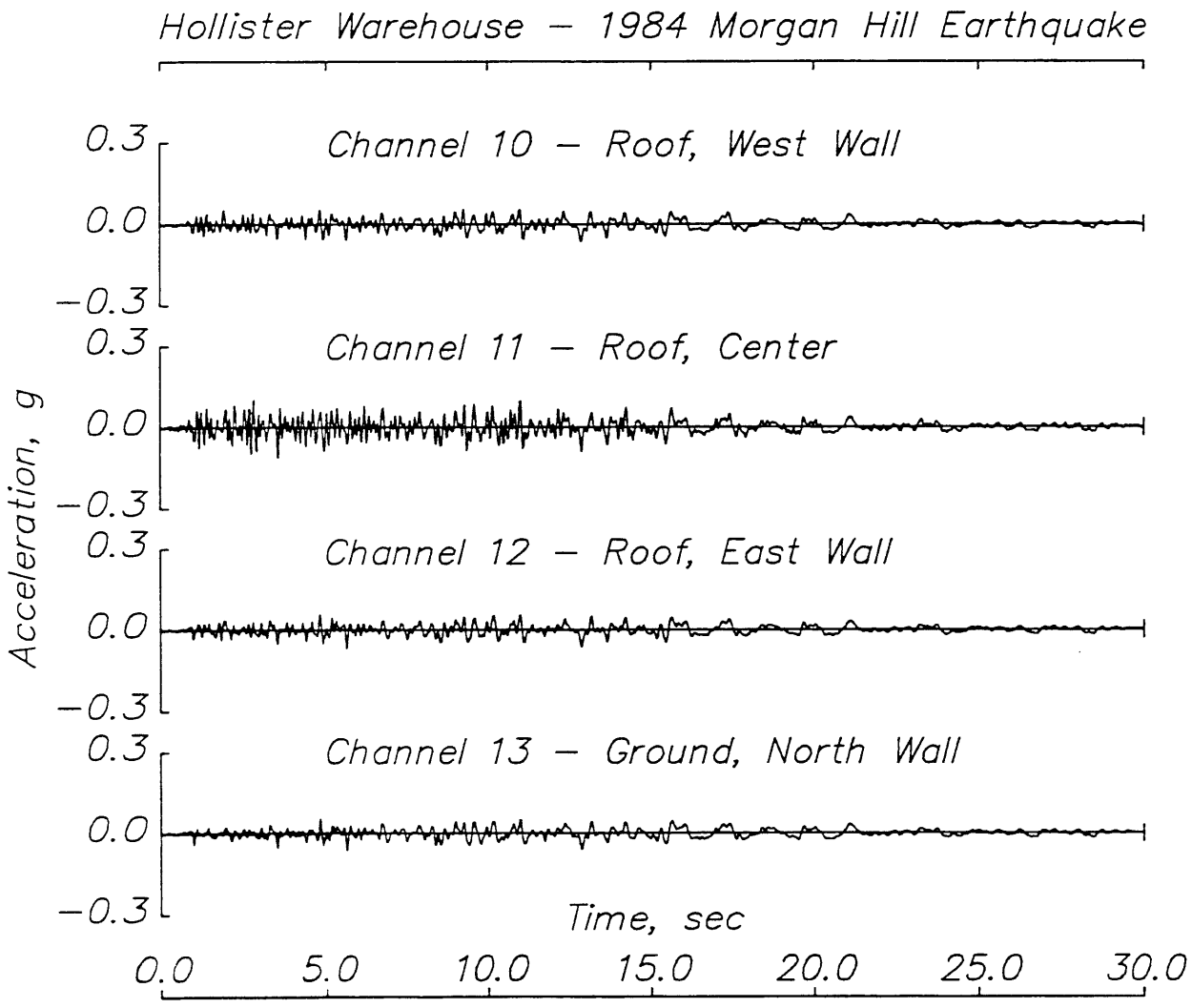

Fig.5.9 (cont.) Hollister warehouse – 1984 Morgan Hill earthquake.
(b) Longitudinal acceleration response.

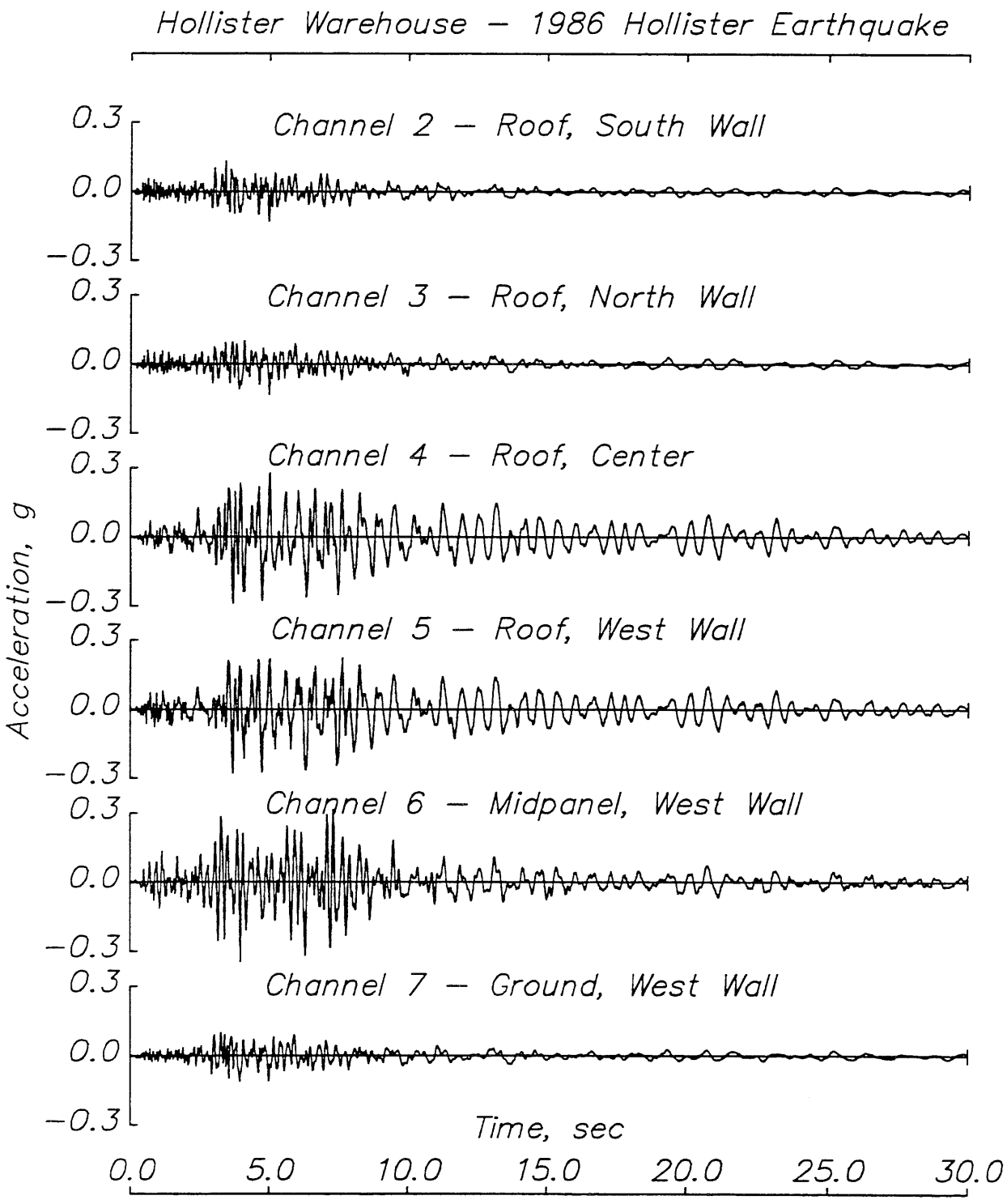

Fig. 5.10 Hollister warehouse – 1986 Hollister earthquake.
(a) Transverse acceleration response.

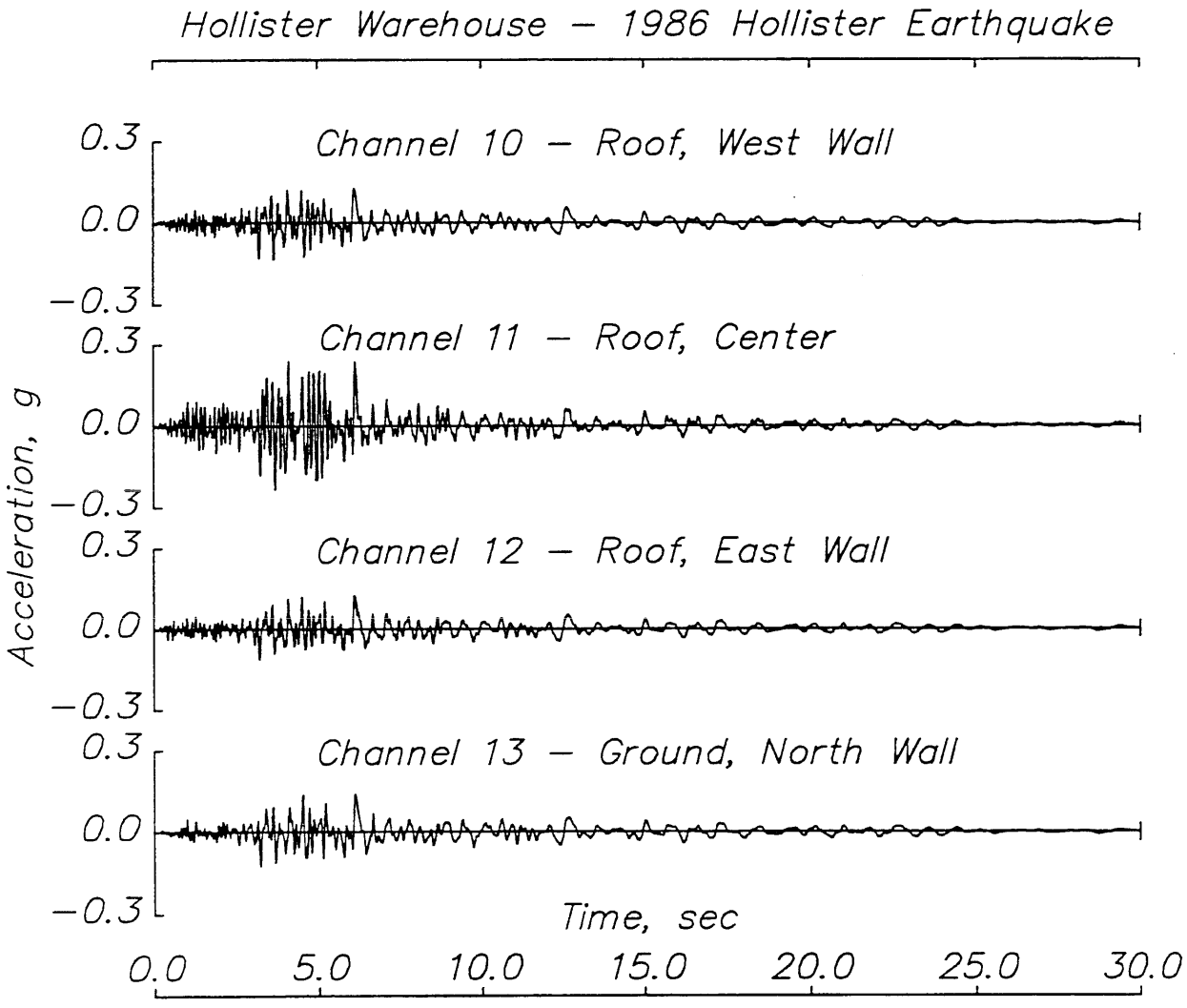

Fig. 5.10 (cont.) Hollister warehouse – 1986 Hollister earthquake.
(b) Longitudinal acceleration response.

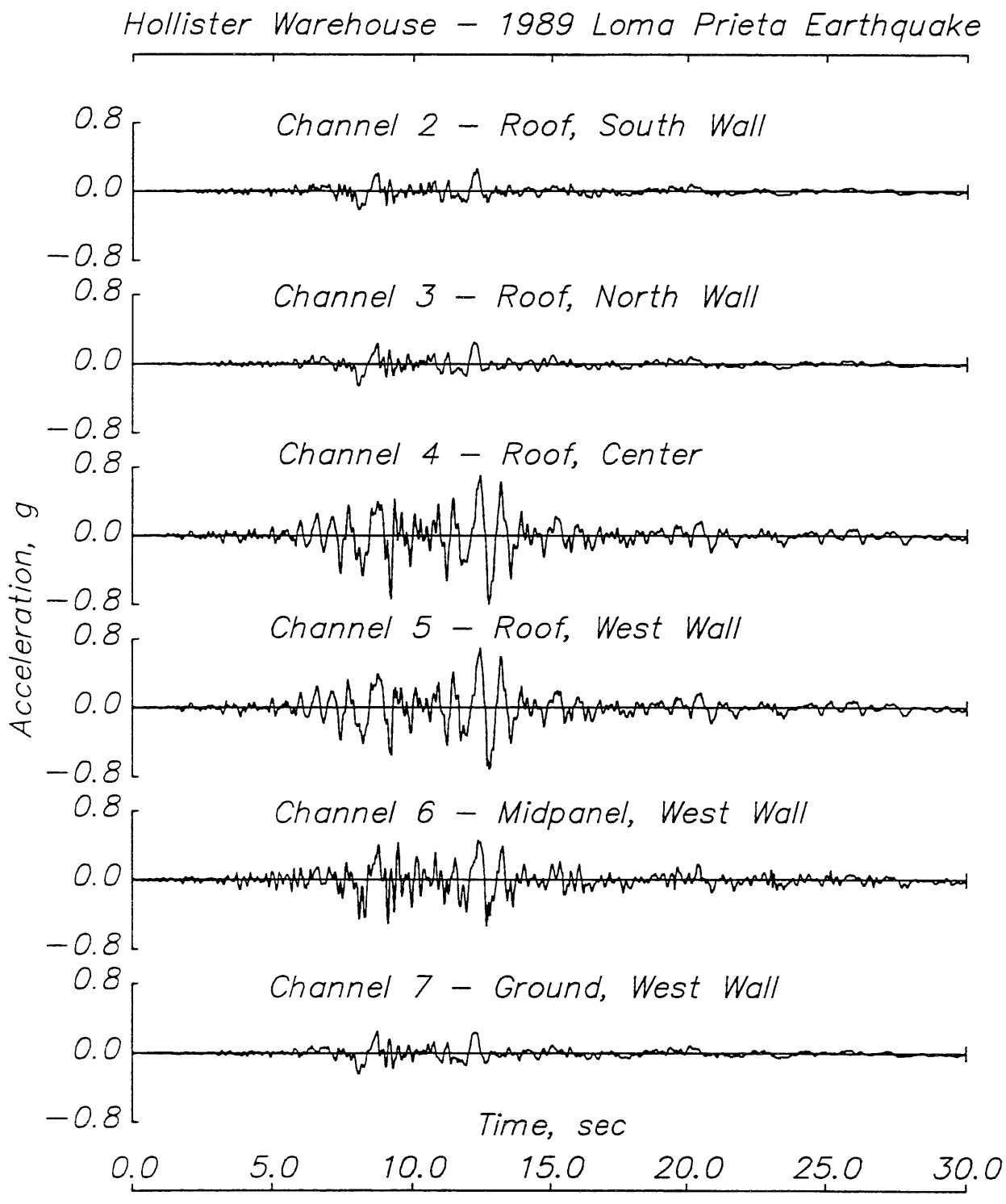

Fig. 5.11 Hollister warehouse – 1989 Loma Prieta earthquake.
(a) Transverse acceleration response.

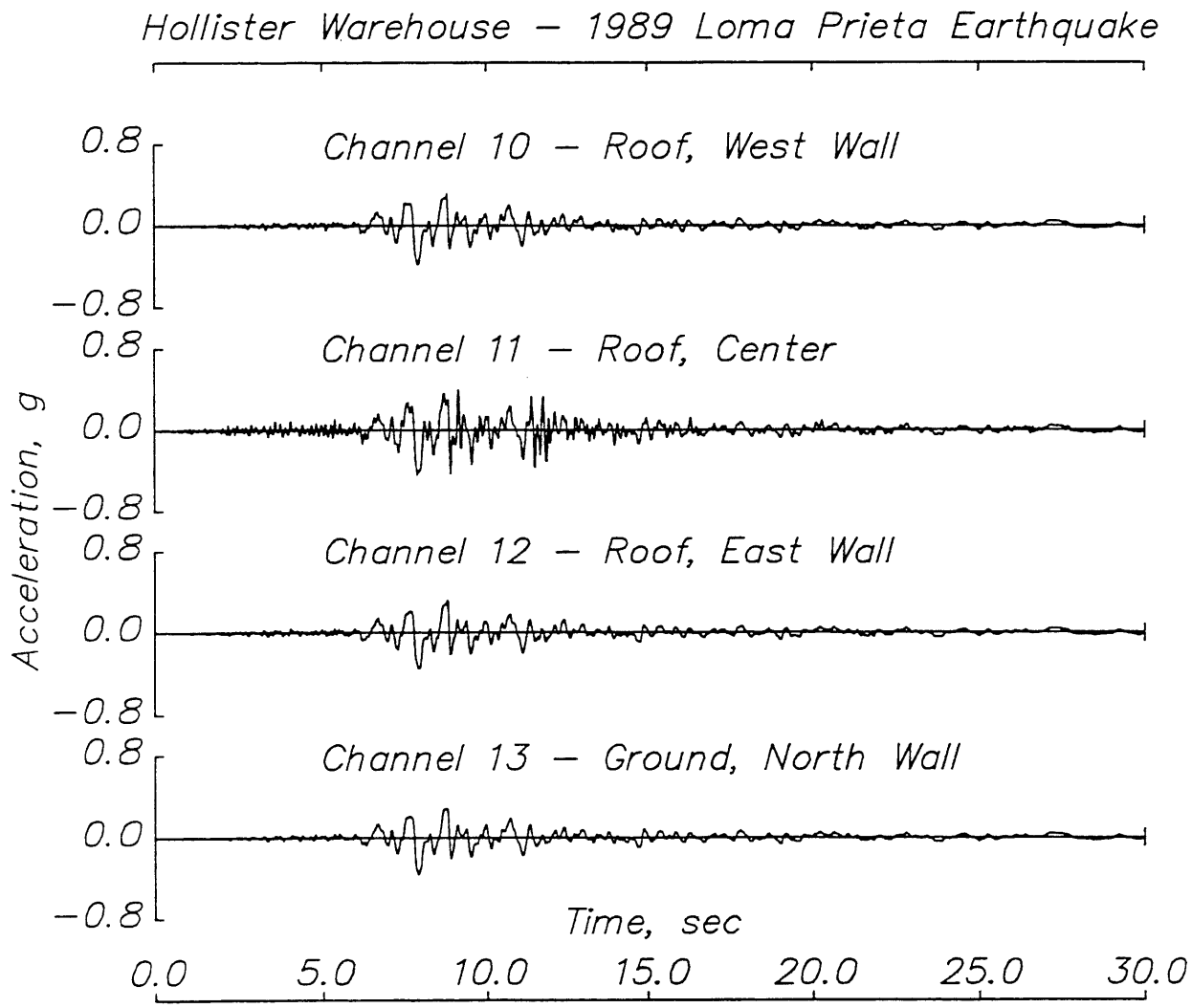

Fig. 5.11 (cont.) Hollister warehouse – 1989 Loma Prieta earthquake.
(b) Longitudinal acceleration response.

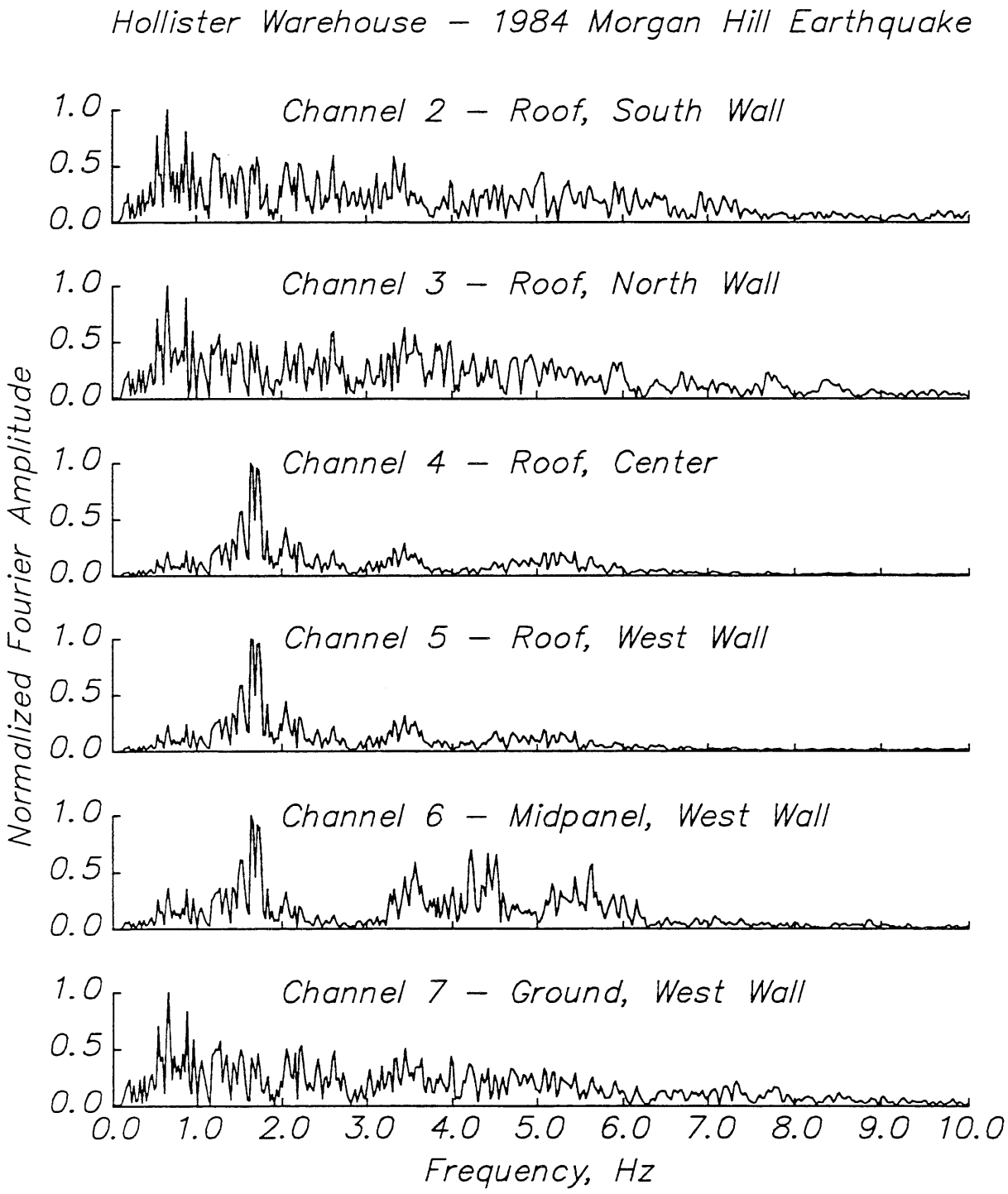

Fig. 5.12 Hollister warehouse – 1984 Morgan Hill earthquake.
(a) Normalized Fourier amplitude spectra of transverse acceleration response.

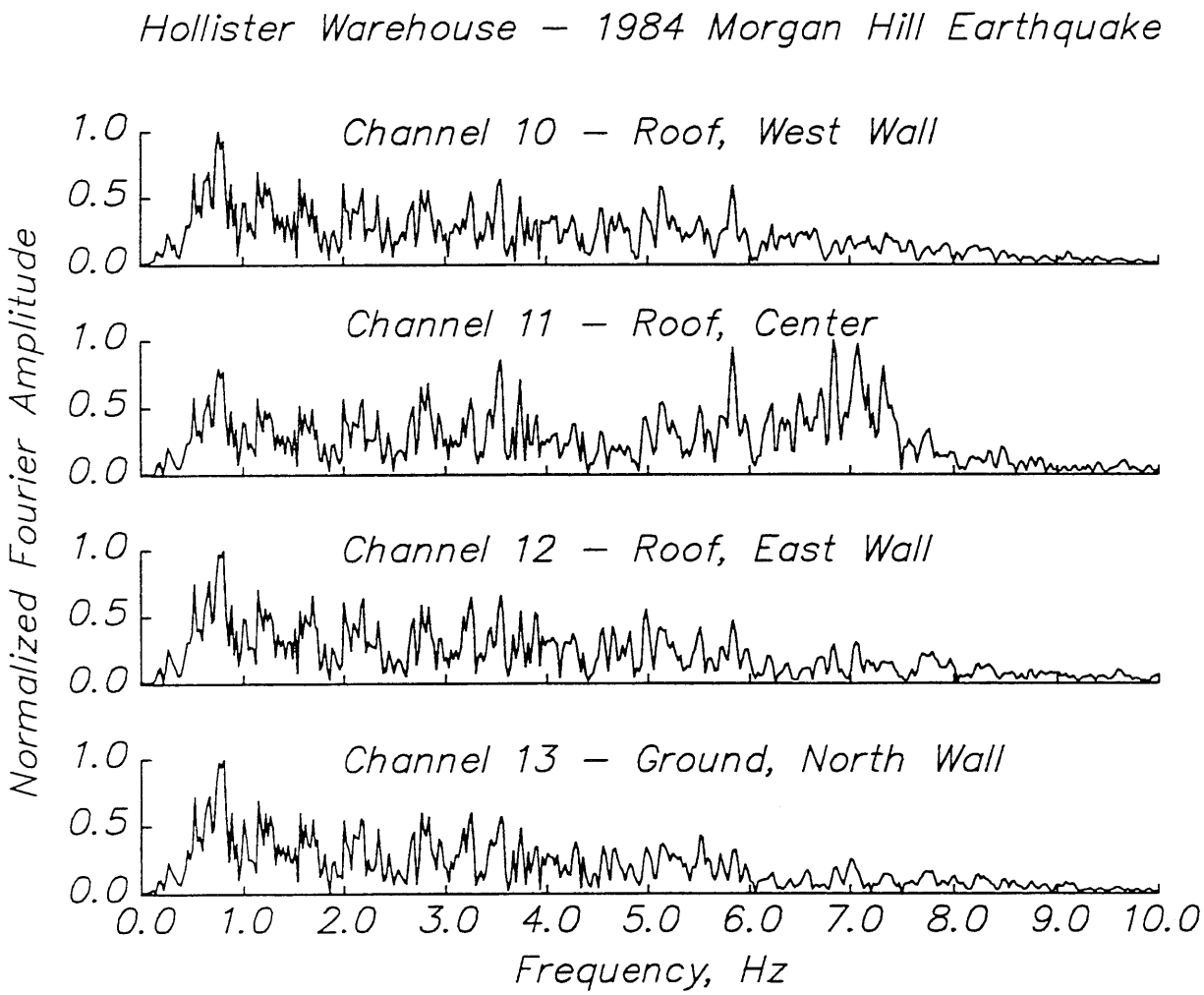

Fig. 5.12 (cont.) Hollister warehouse – 1984 Morgan Hill earthquake.
(b) Normalized Fourier amplitude spectra of longitudinal acceleration response.

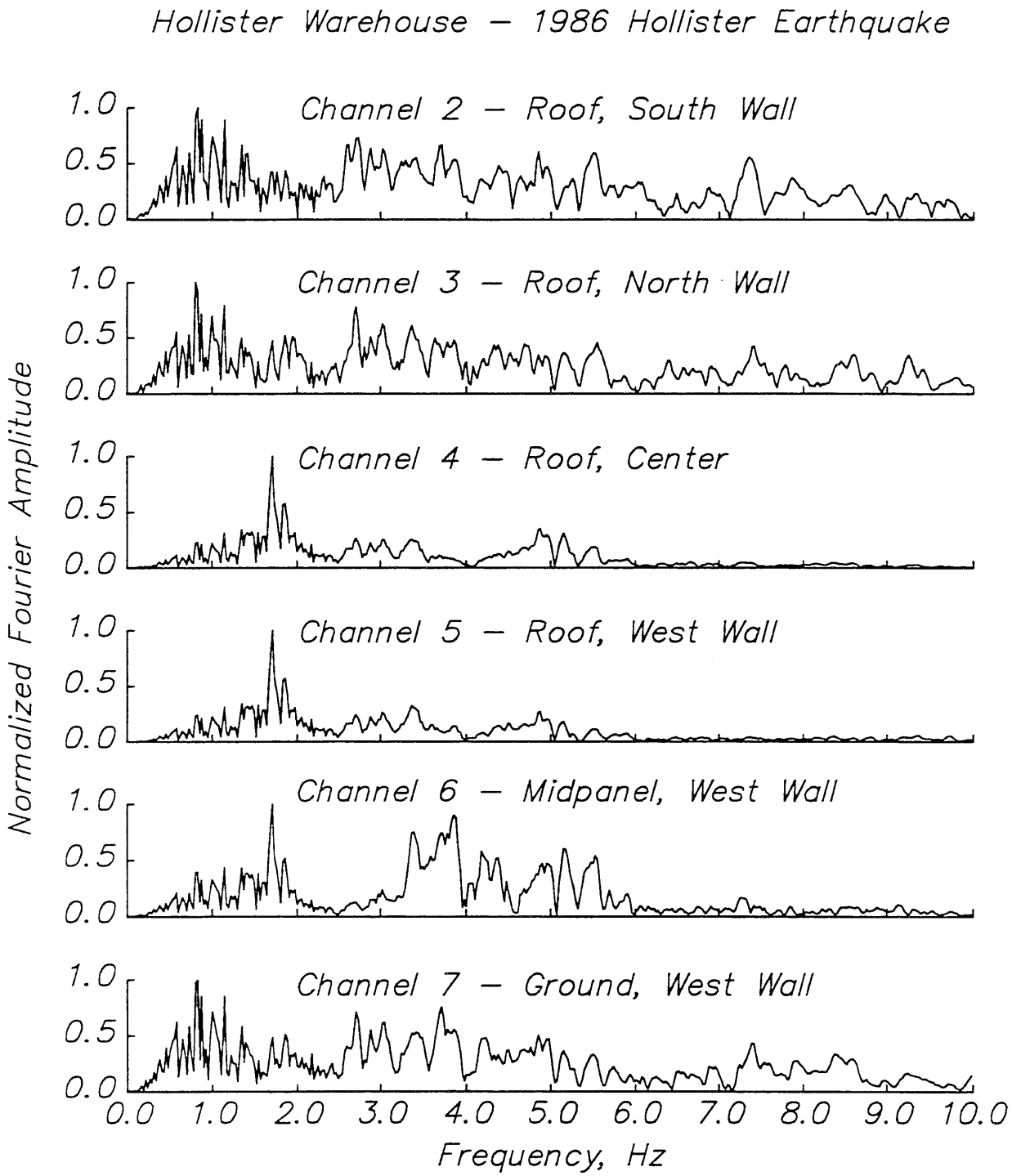

Fig. 5.13 Hollister warehouse – 1986 Hollister earthquake.
(a) Normalized Fourier amplitude spectra of transverse acceleration response.

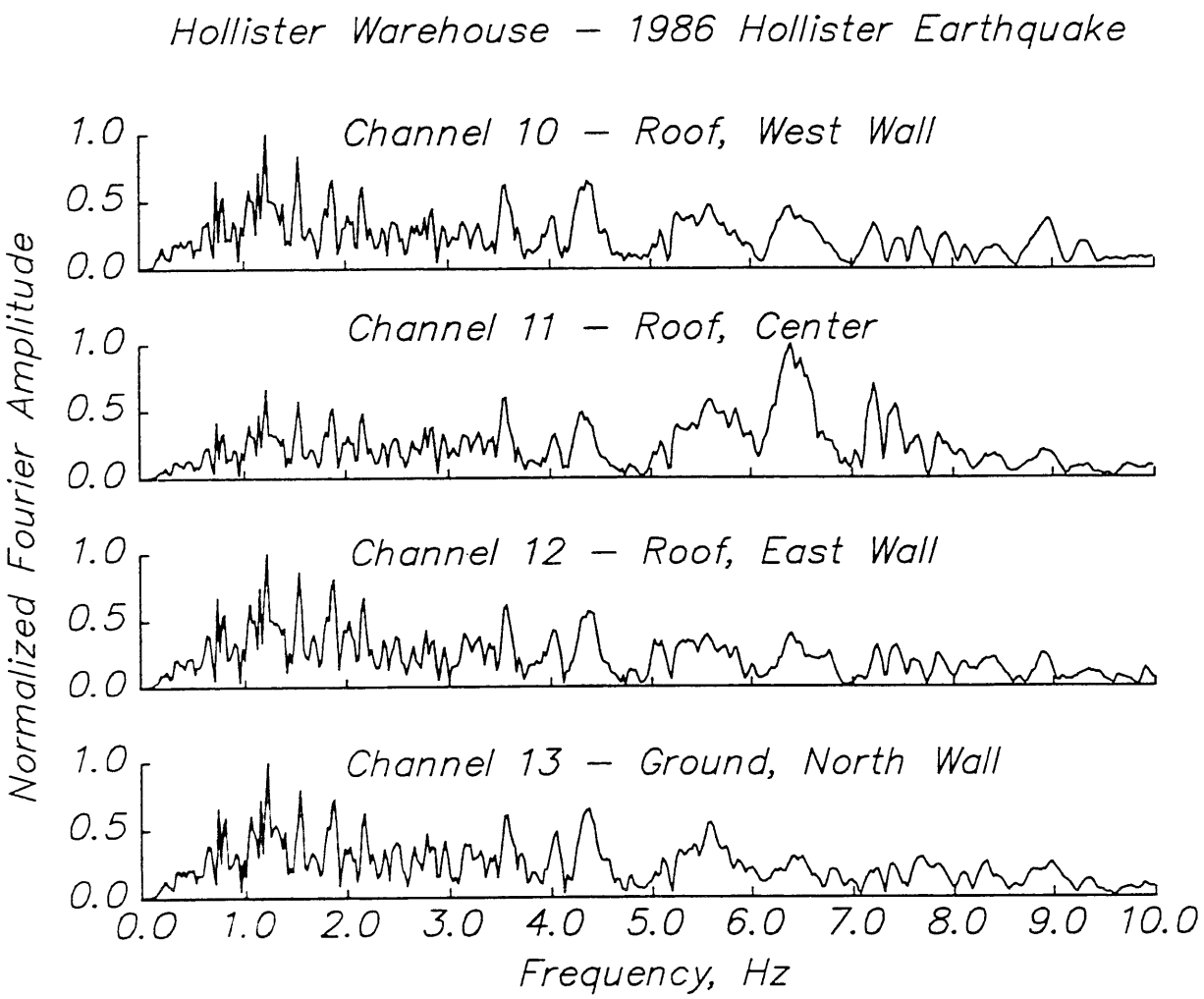

Fig. 5.13 (cont.) Hollister warehouse – 1986 Hollister earthquake.
(b) Normalized Fourier amplitude spectra of longitudinal acceleration response.

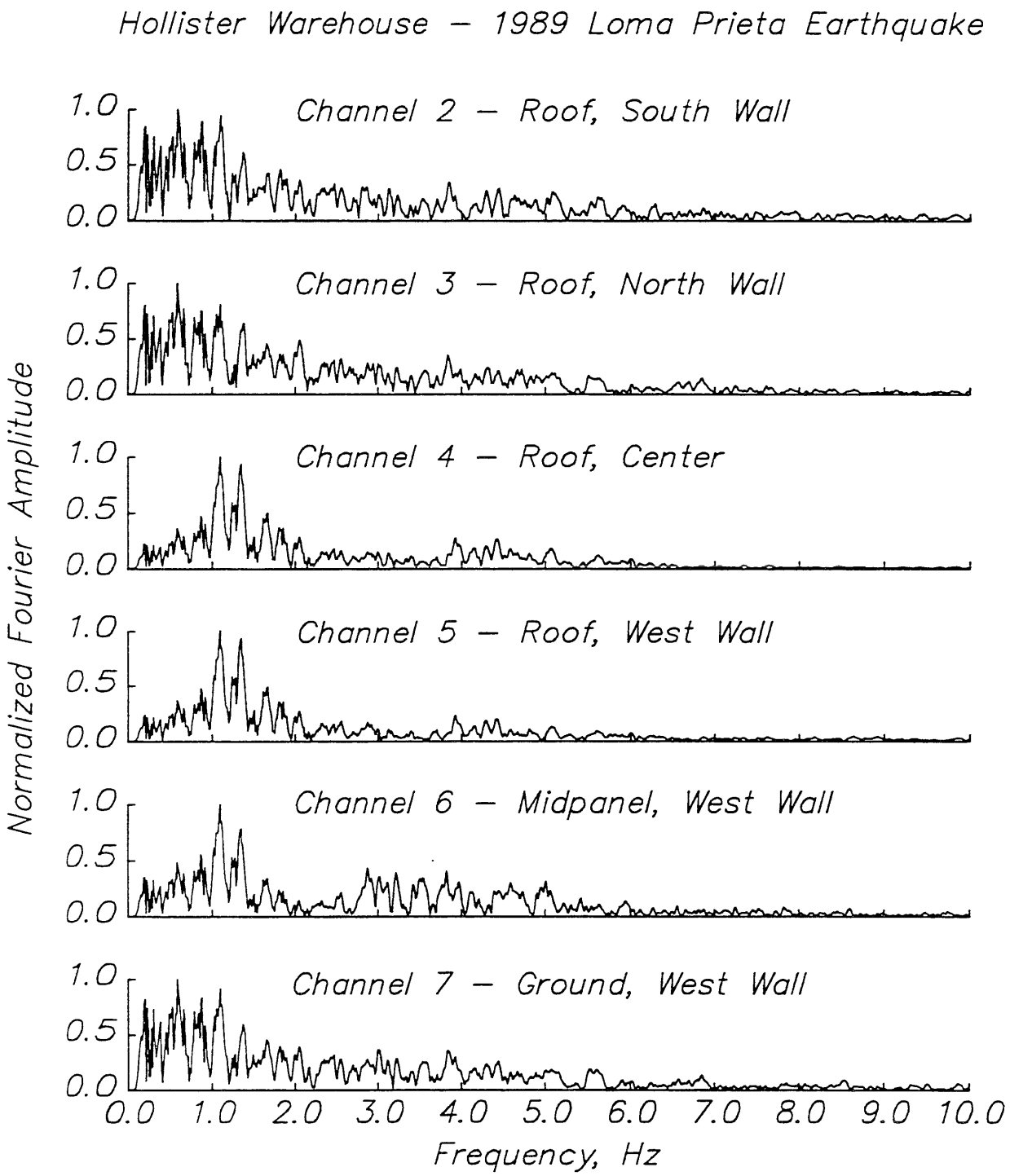

Fig. 5.14 Hollister warehouse – 1989 Loma Prieta earthquake.
(a) Normalized Fourier amplitude spectra of transverse acceleration response.

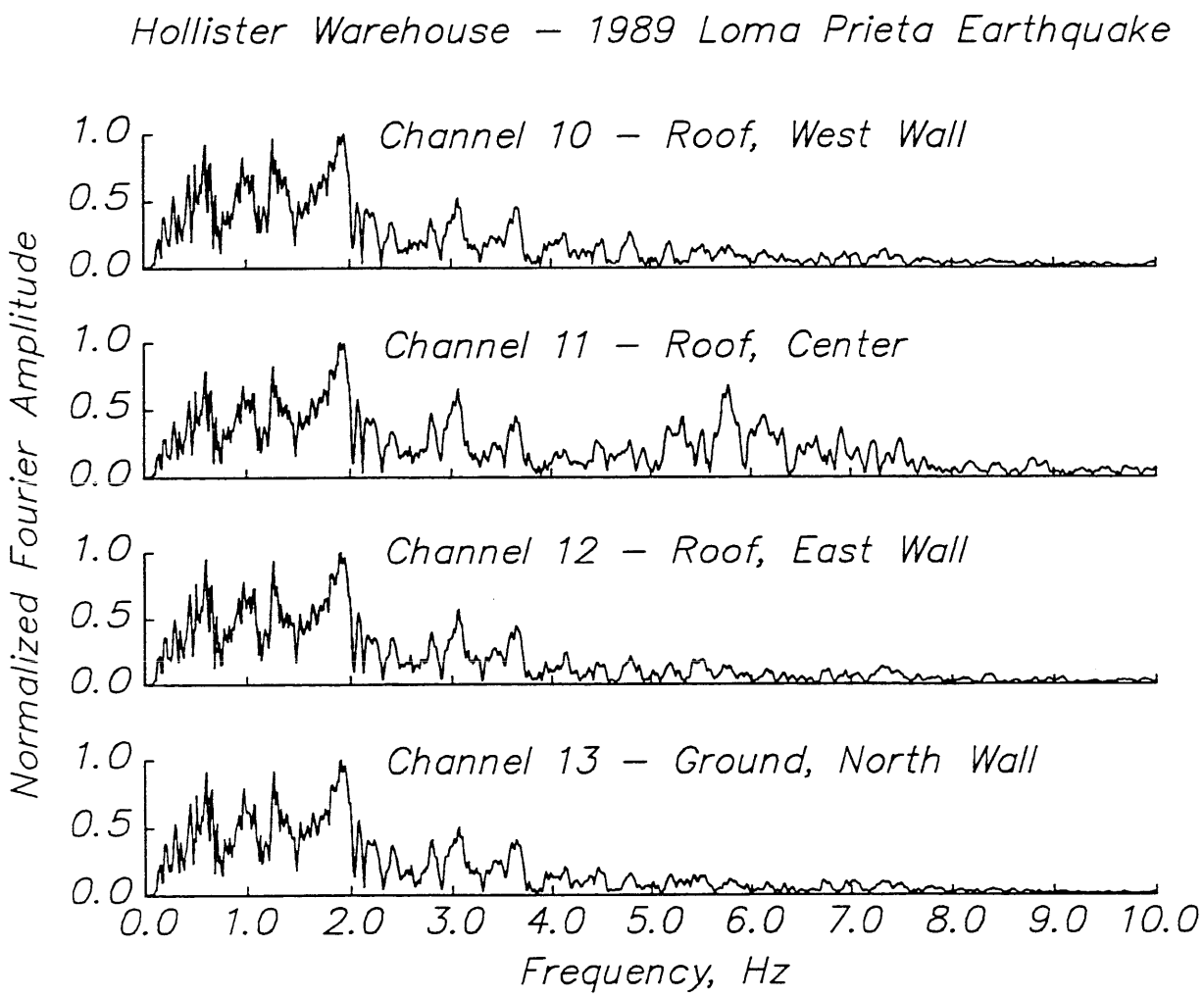

Fig. 5.14 (cont.) Hollister warehouse – 1989 Loma Prieta earthquake.
(b) Normalized Fourier amplitude spectra of longitudinal acceleration response.

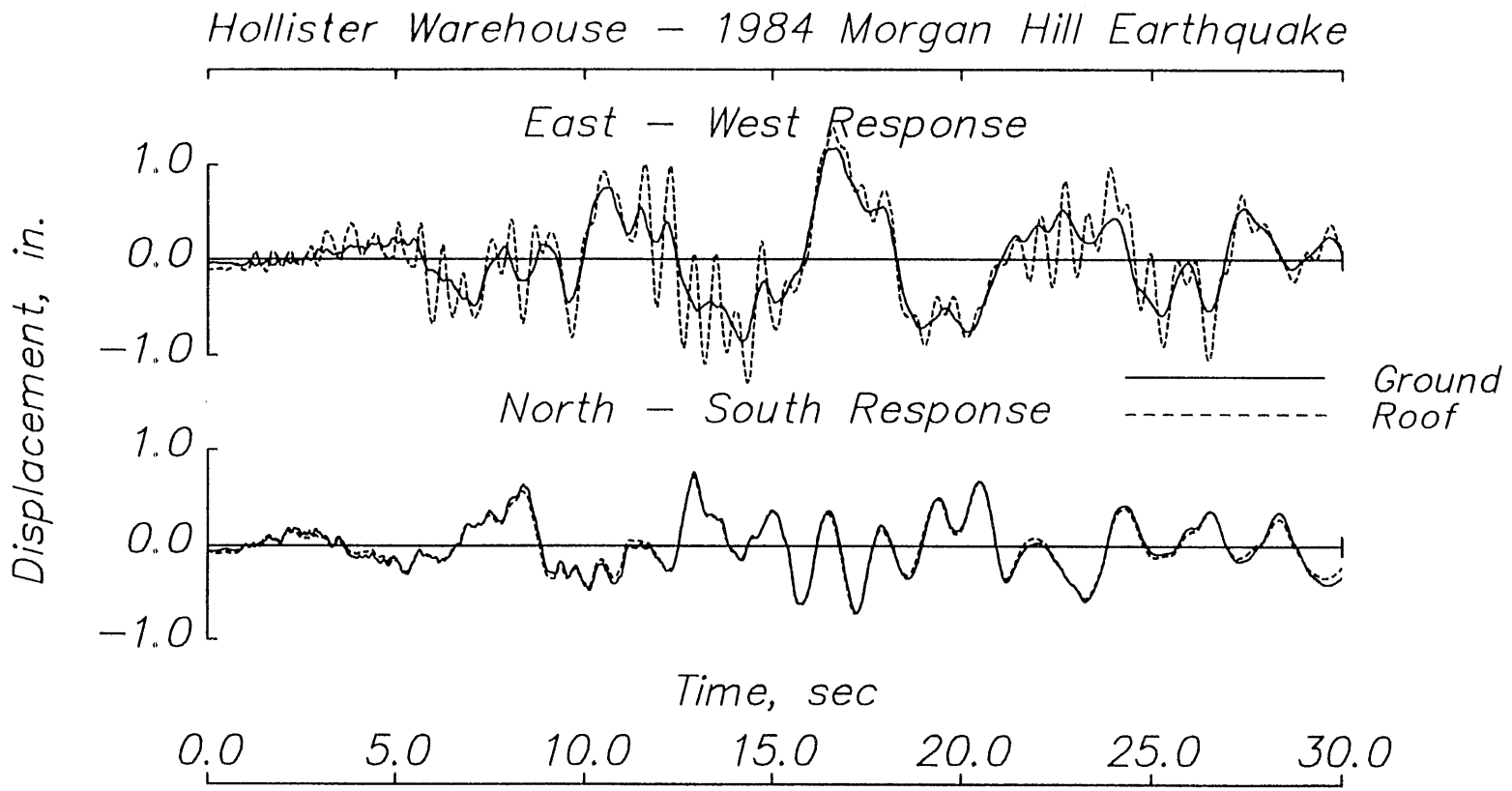

Fig. 5.15 Hollister warehouse – Absolute displacement response.

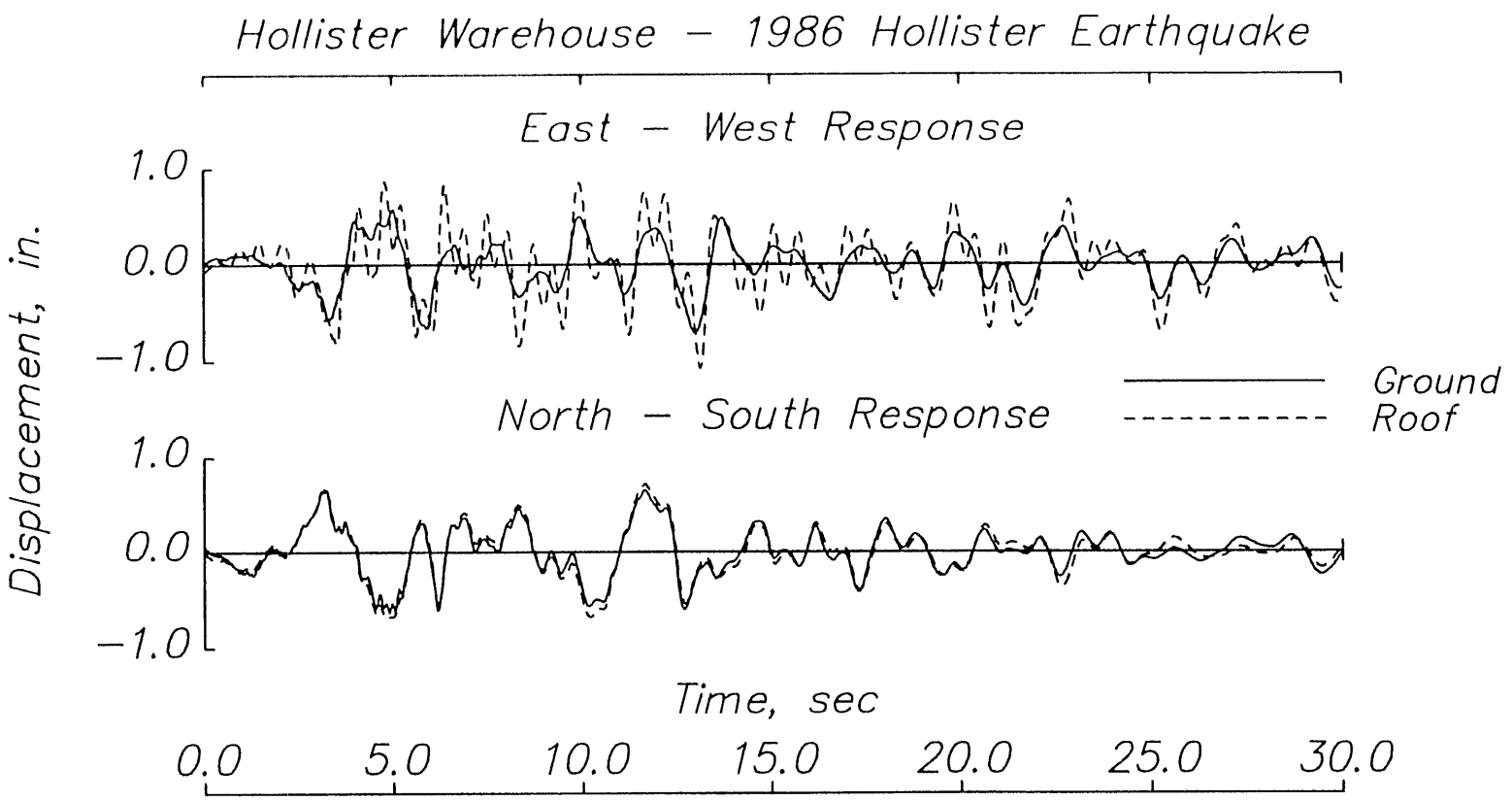

Fig. 5.15 (cont.) Hollister warehouse – Absolute displacement response.

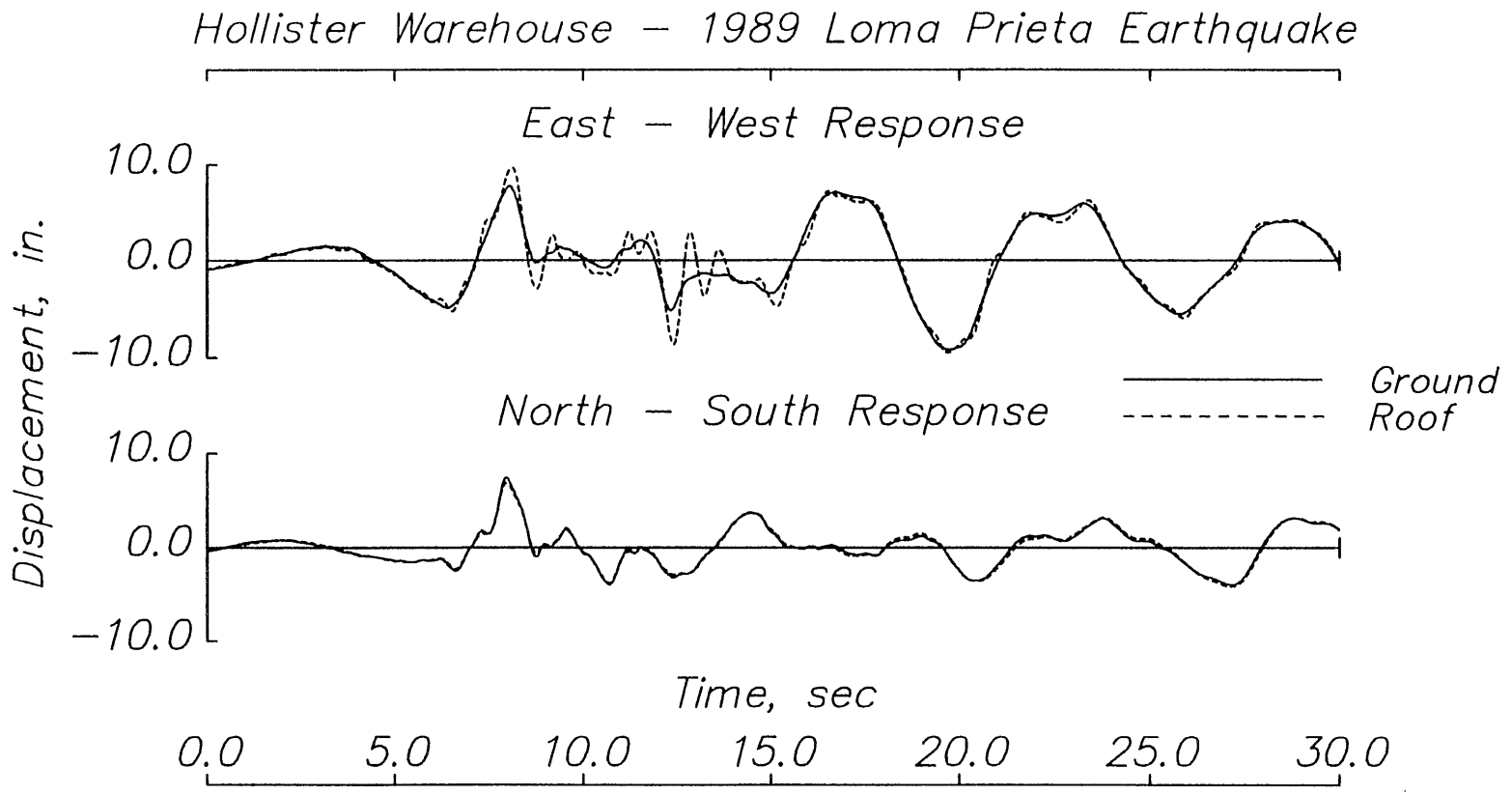

Fig. 5.15 (cont.) Hollister warehouse – Absolute displacement response.

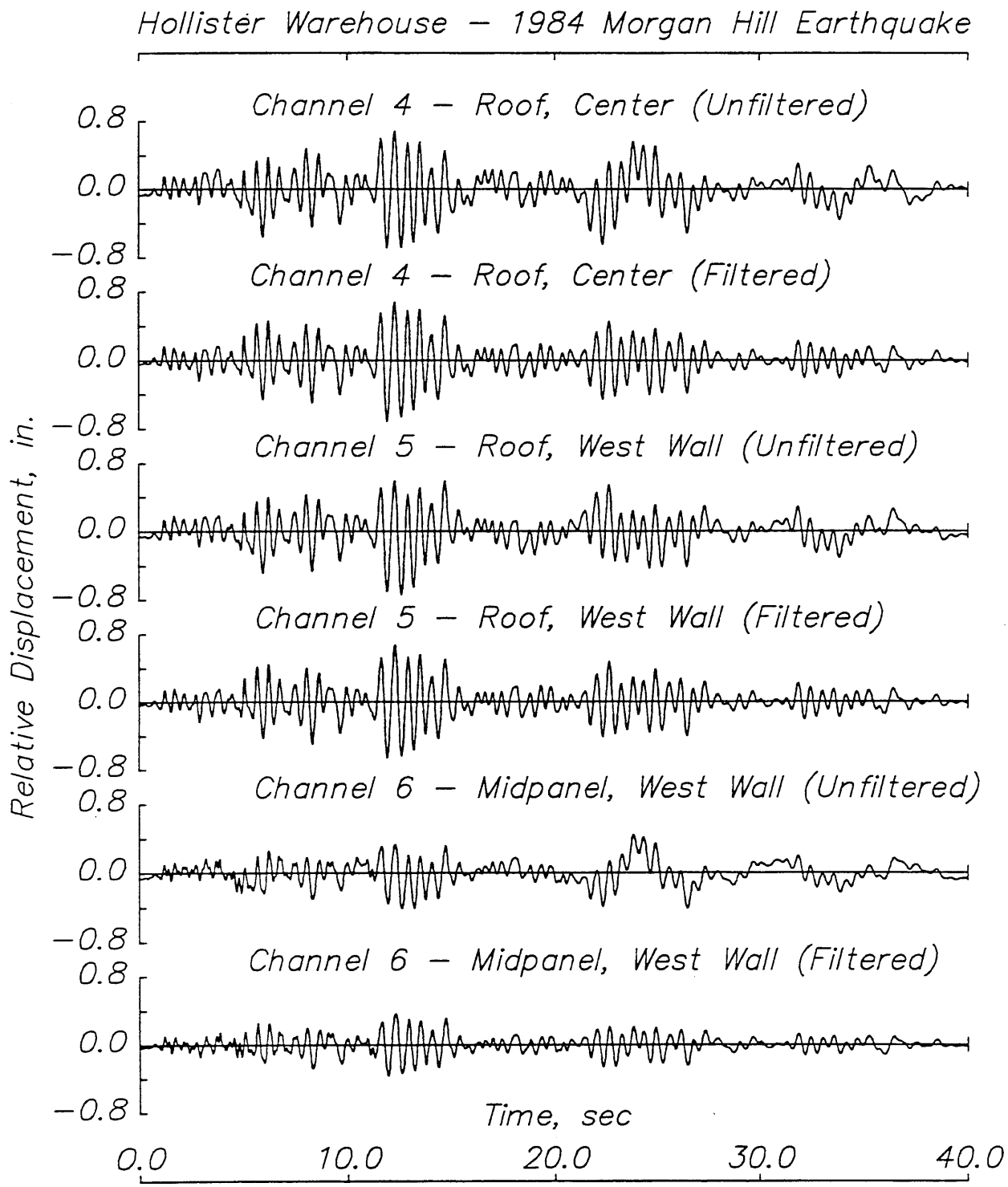

Fig. 5.16 Hollister warehouse – 1984 Morgan Hill earthquake.
(a) Transverse relative displacement response.

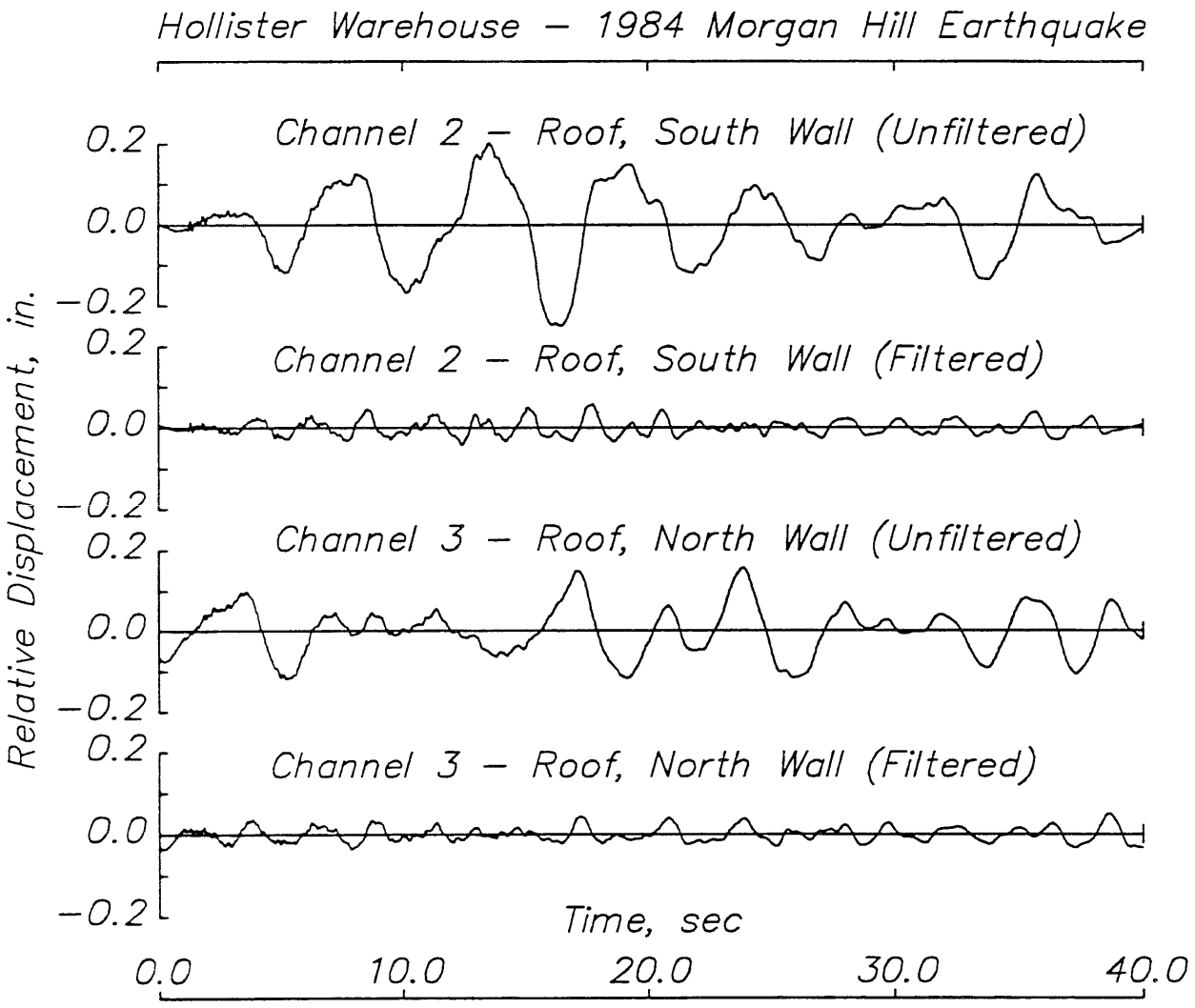

Fig. 5.16 (cont.) Hollister warehouse – 1984 Morgan Hill earthquake.
(b) Transverse relative displacement response.

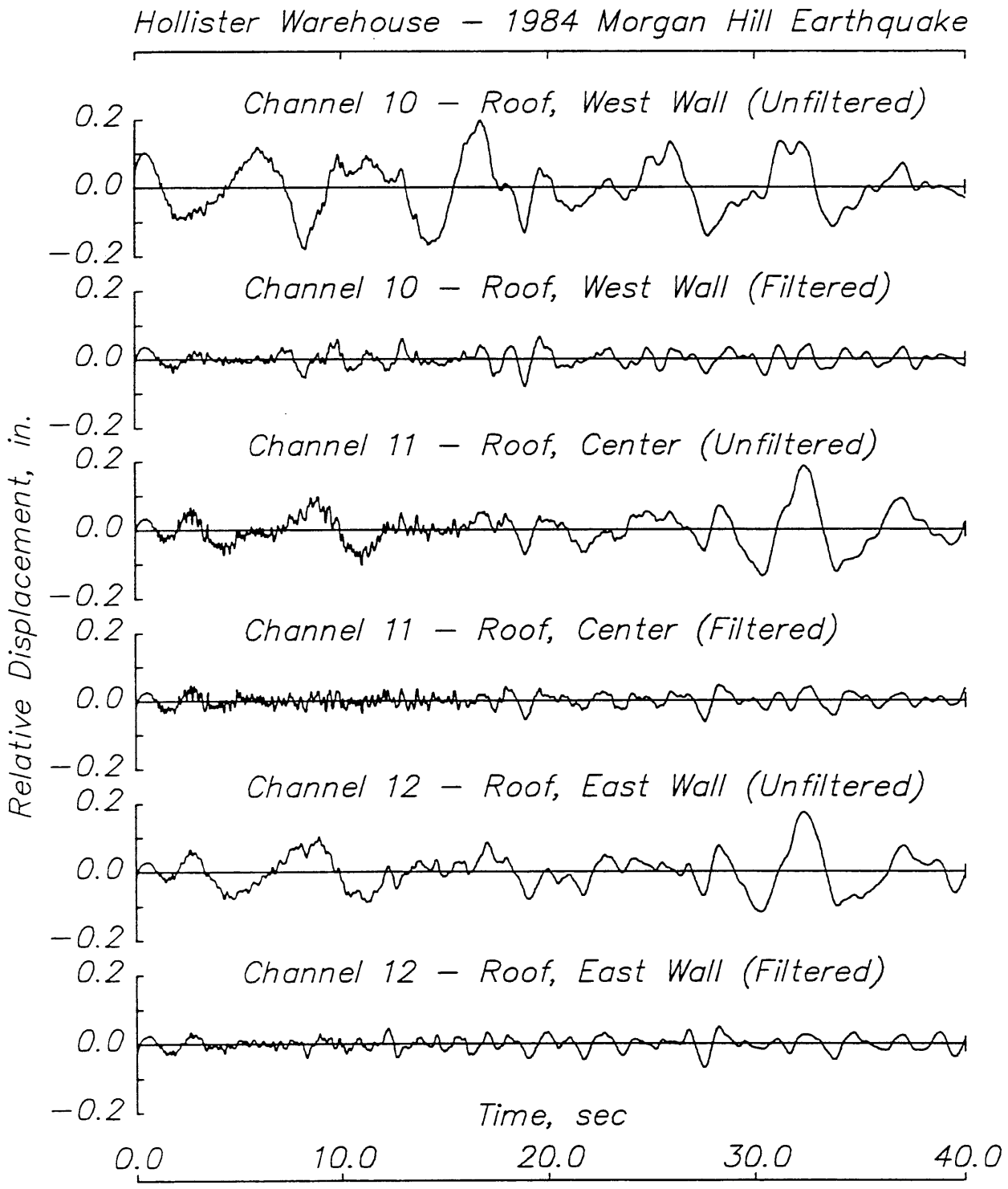

Fig. 5.16 (cont.) Hollister warehouse – 1984 Morgan Hill earthquake.
(b) Transverse relative displacement response.

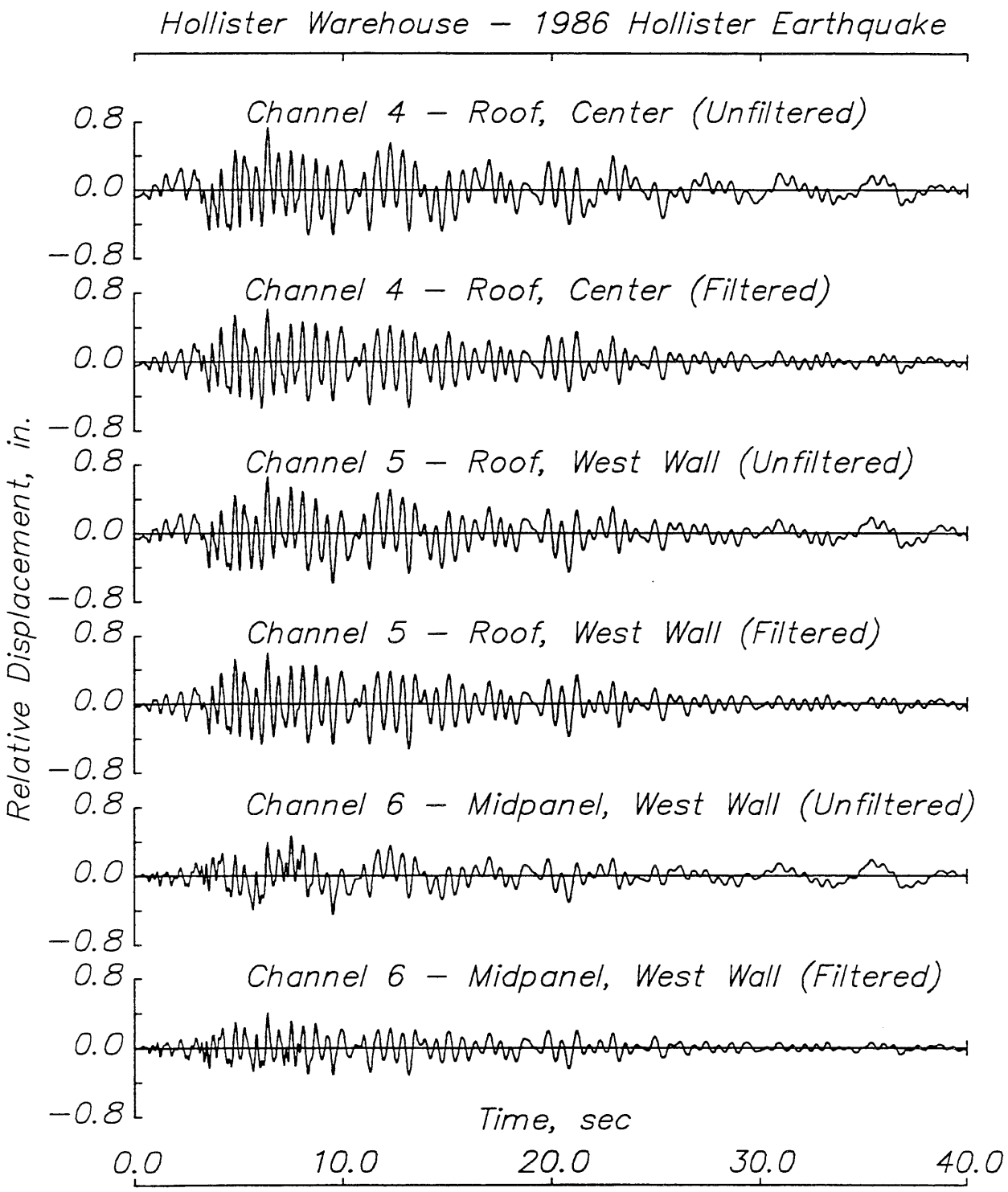

Fig. 5.17 Hollister warehouse – 1986 Hollister earthquake.
(a) Transverse relative displacement response.

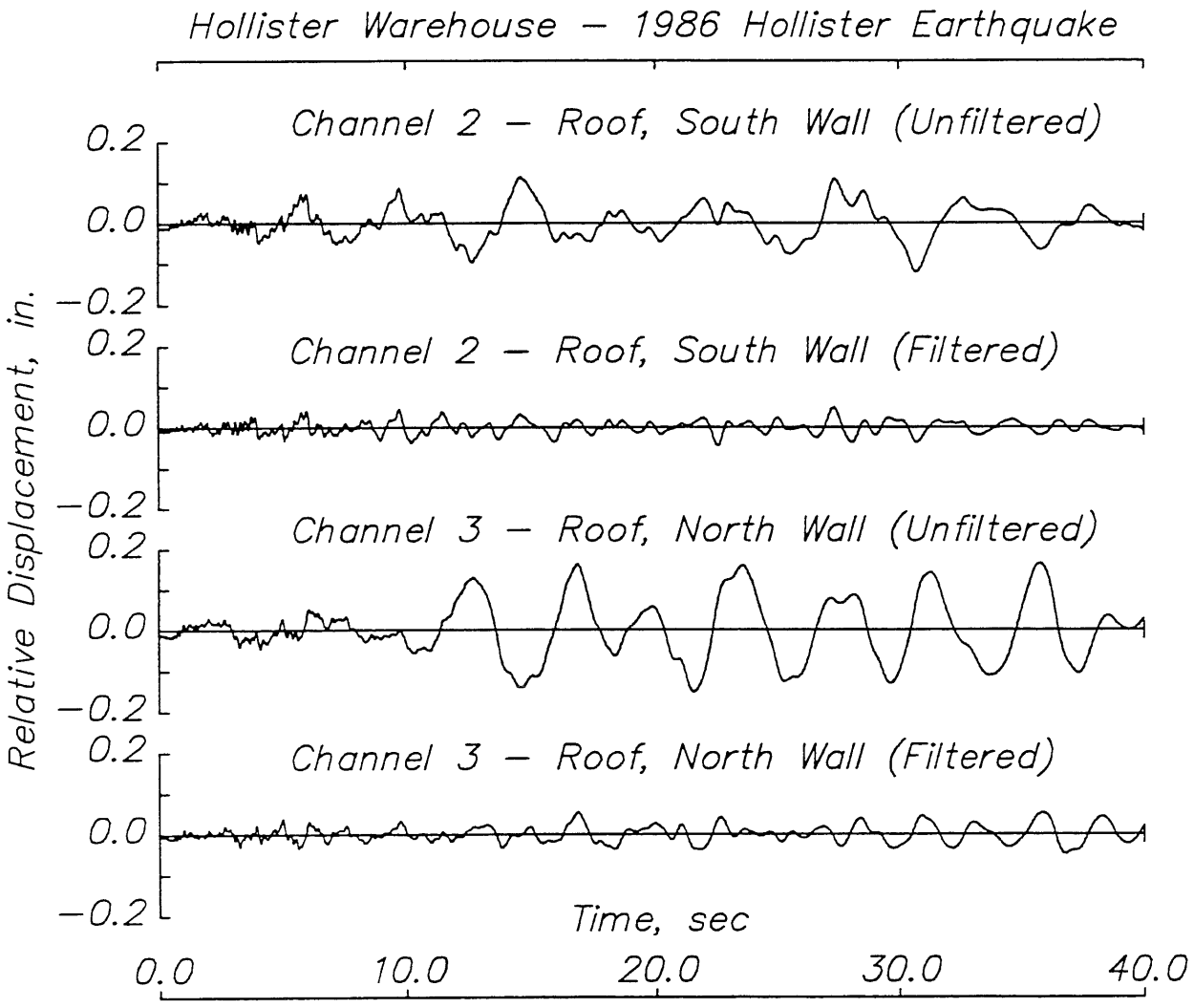

Fig. 5.17 (cont.) Hollister warehouse – 1986 Hollister earthquake.
(a) (cont.) Transverse relative displacement response.

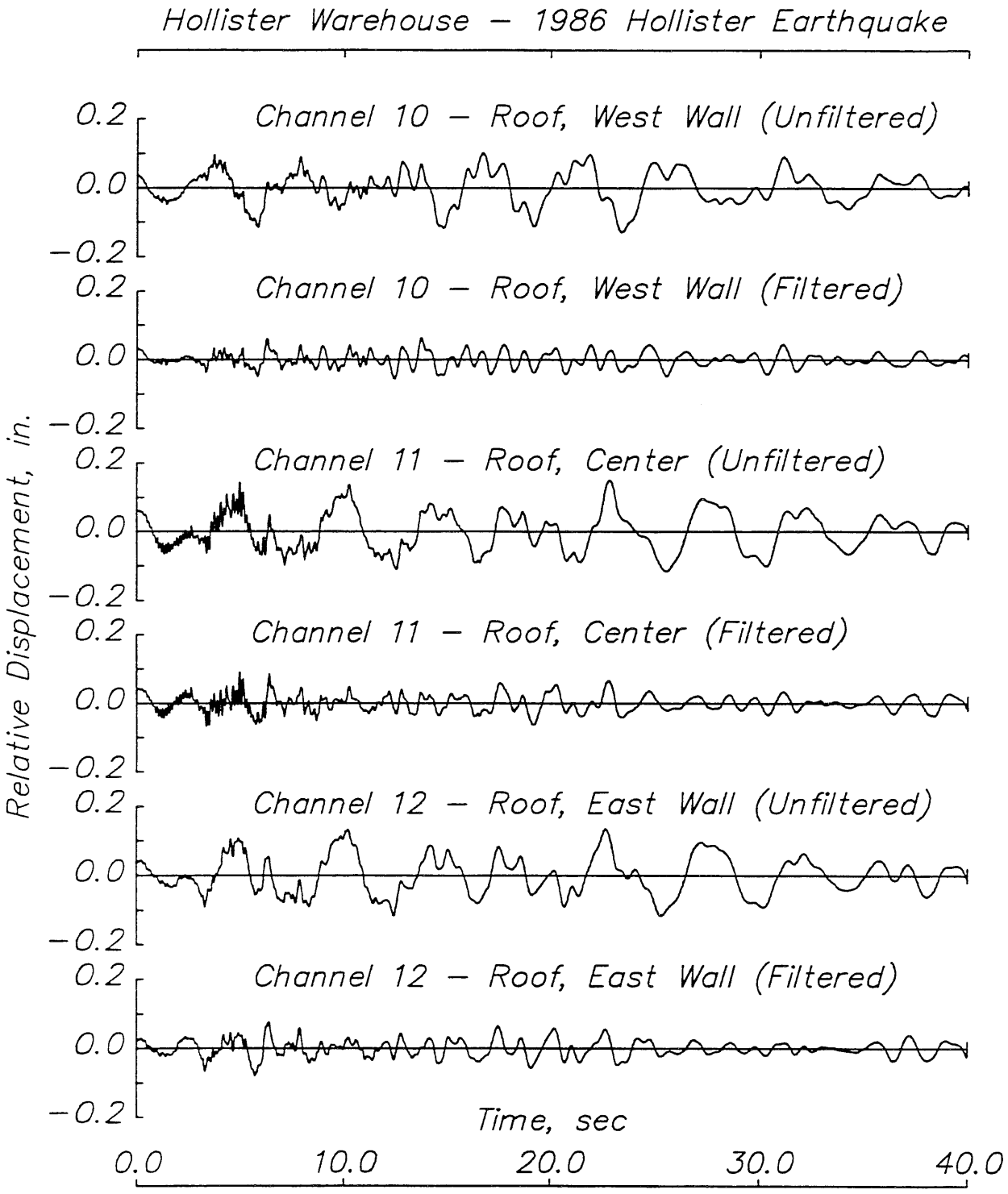

Fig. 5.17 (cont.) Hollister warehouse – 1986 Hollister earthquake.
(b) Longitudinal relative displacement response.

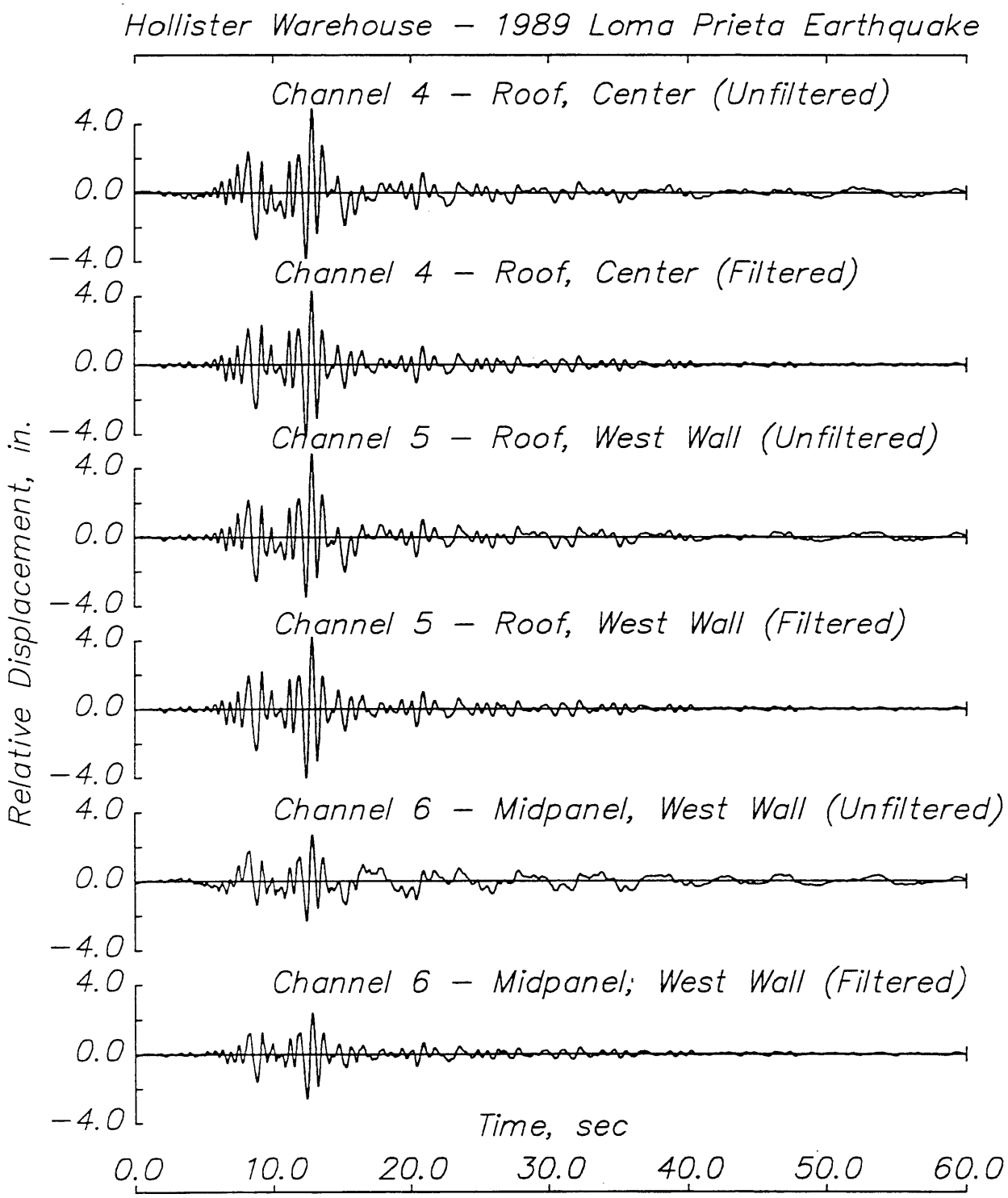

Fig. 5.18 Hollister warehouse – 1989 Loma Prieta earthquake.
(a) Transverse relative displacement response.

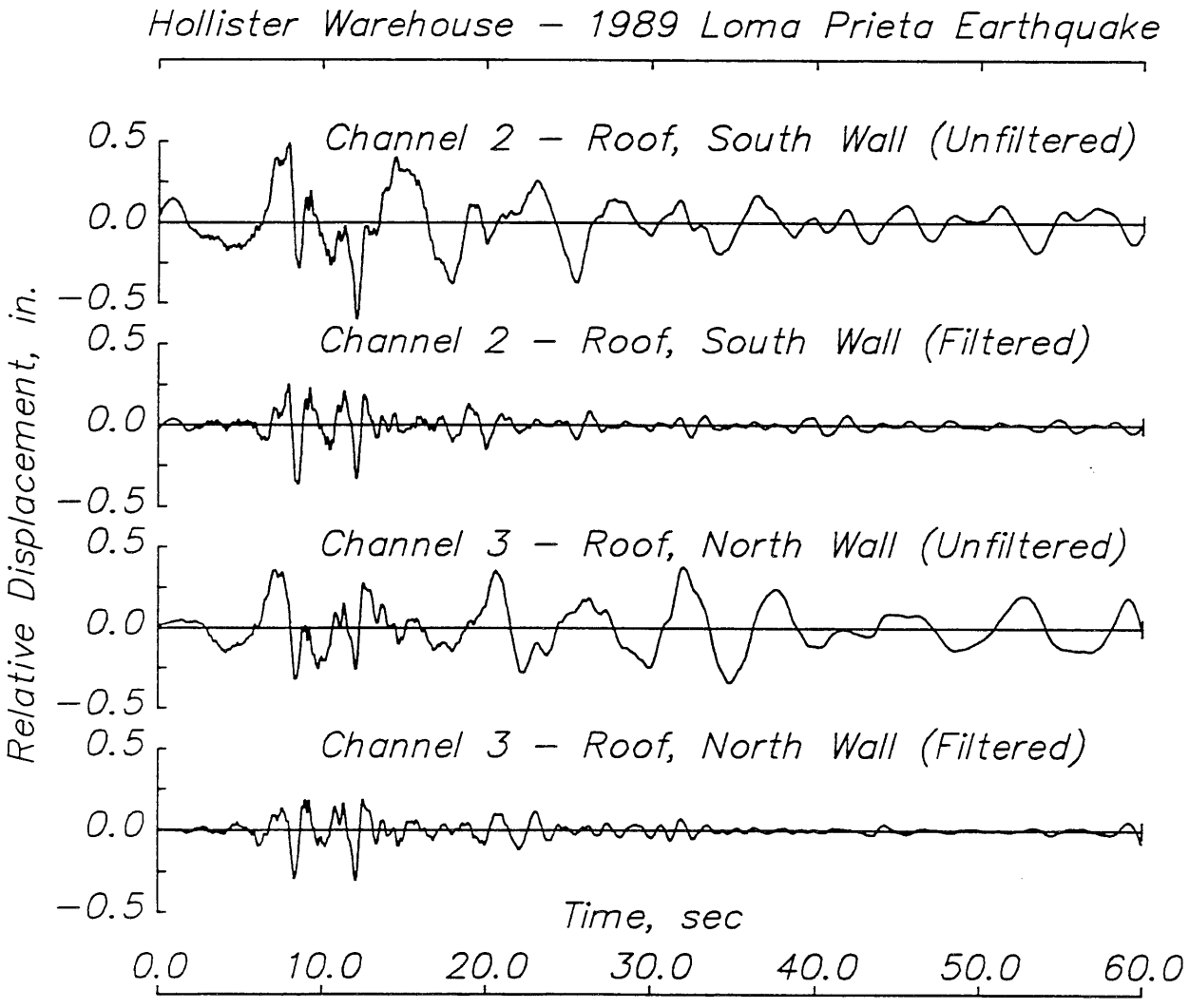

Fig. 5.18 (cont.) Hollister warehouse – 1989 Loma Prieta earthquake.
(a) (cont.) Transverse relative displacement response.

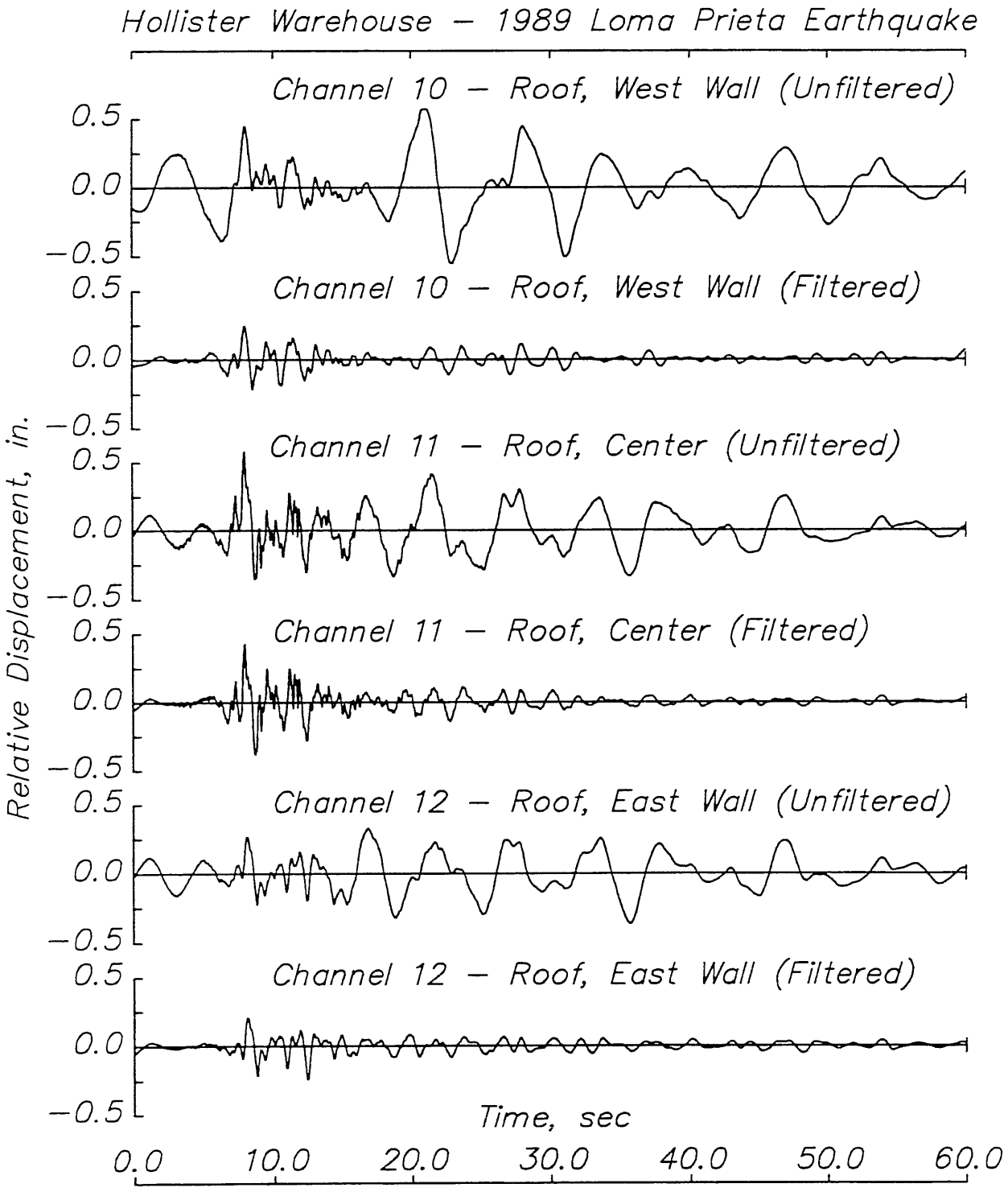

Fig. 5.18 (cont.) Hollister warehouse – 1989 Loma Prieta earthquake.
(b) Longitudinal relative displacement response.

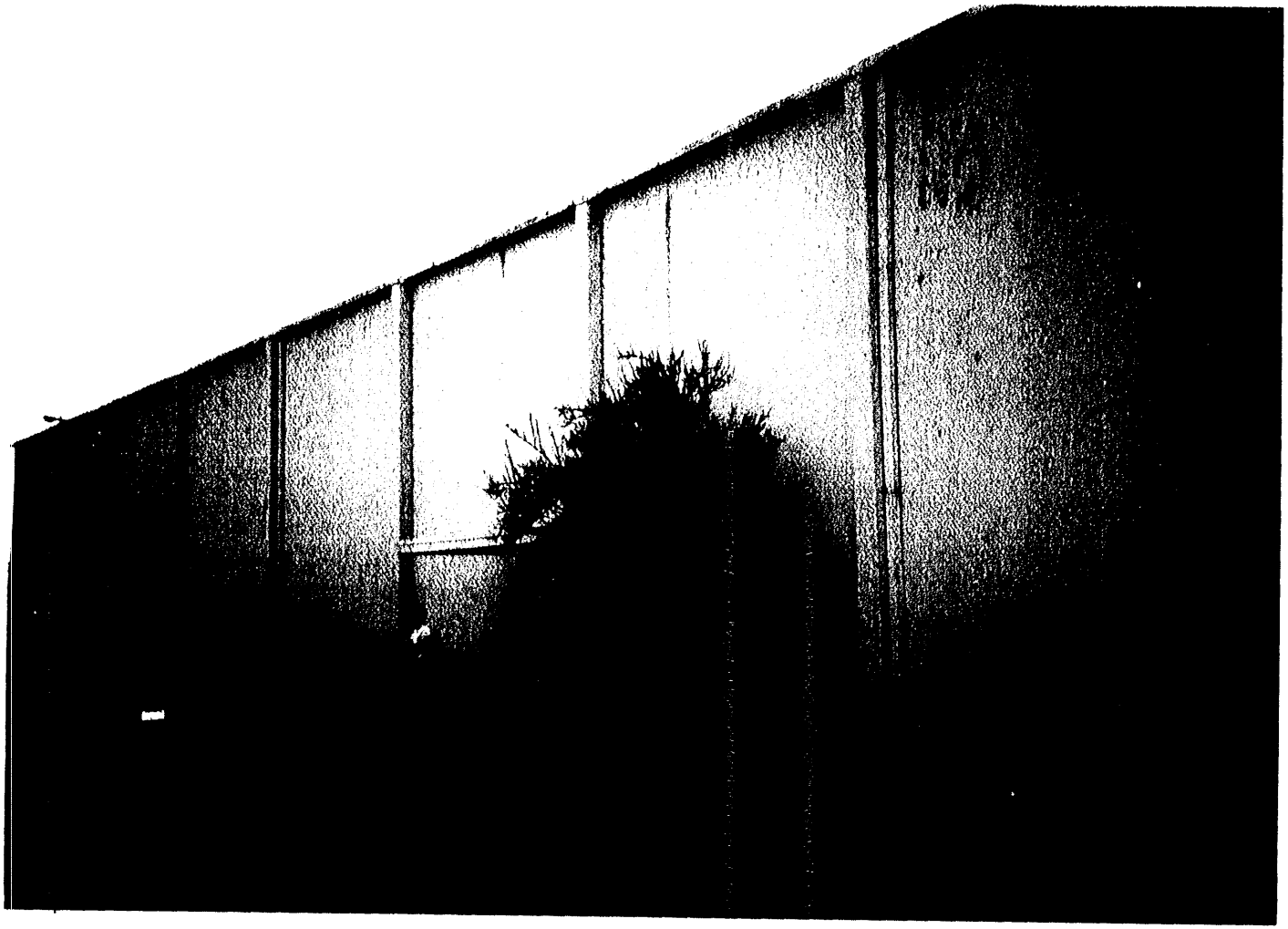

Fig. 5.19 Redlands warehouse.

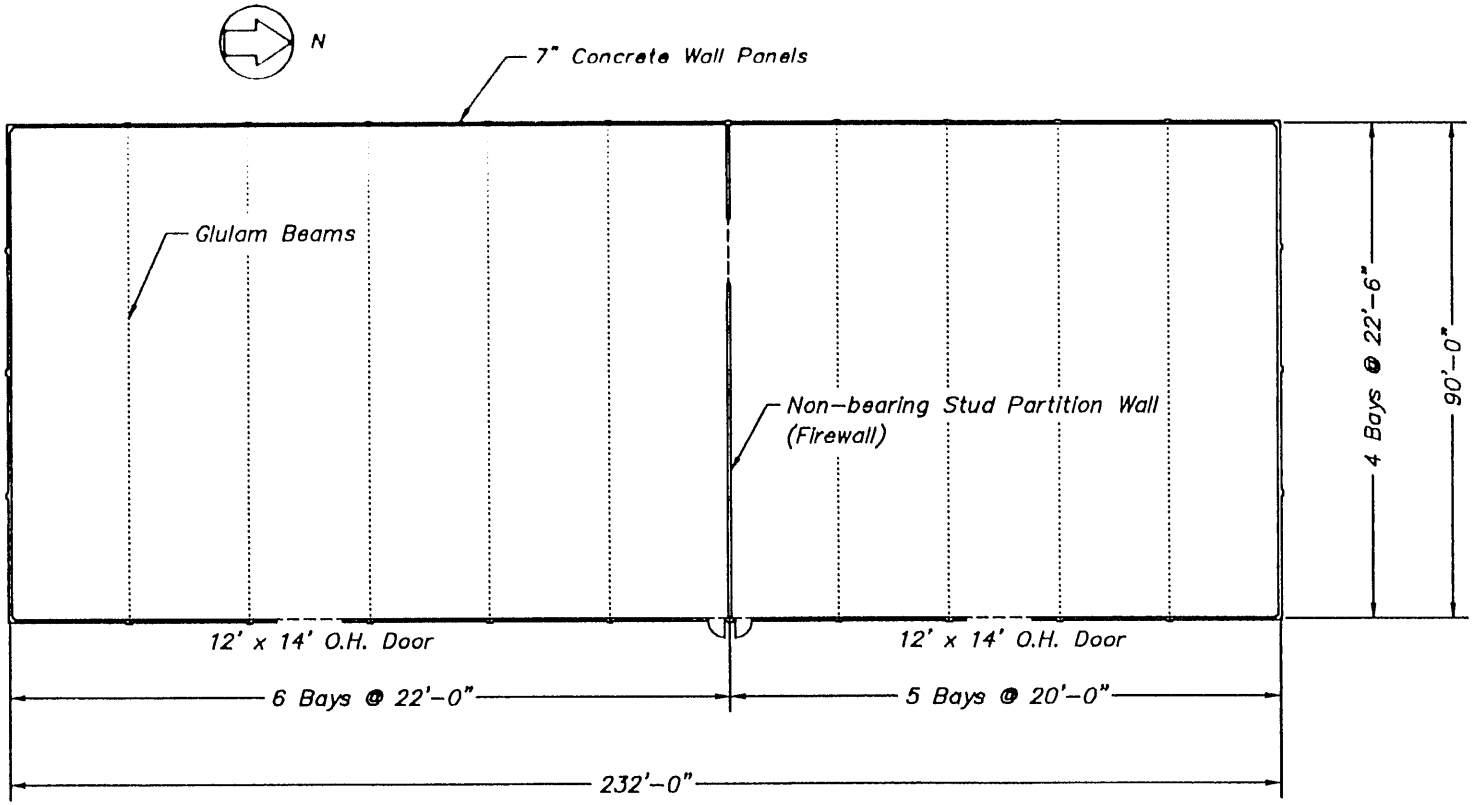

Fig. 5.20 Floor plan – Redlands warehouse.

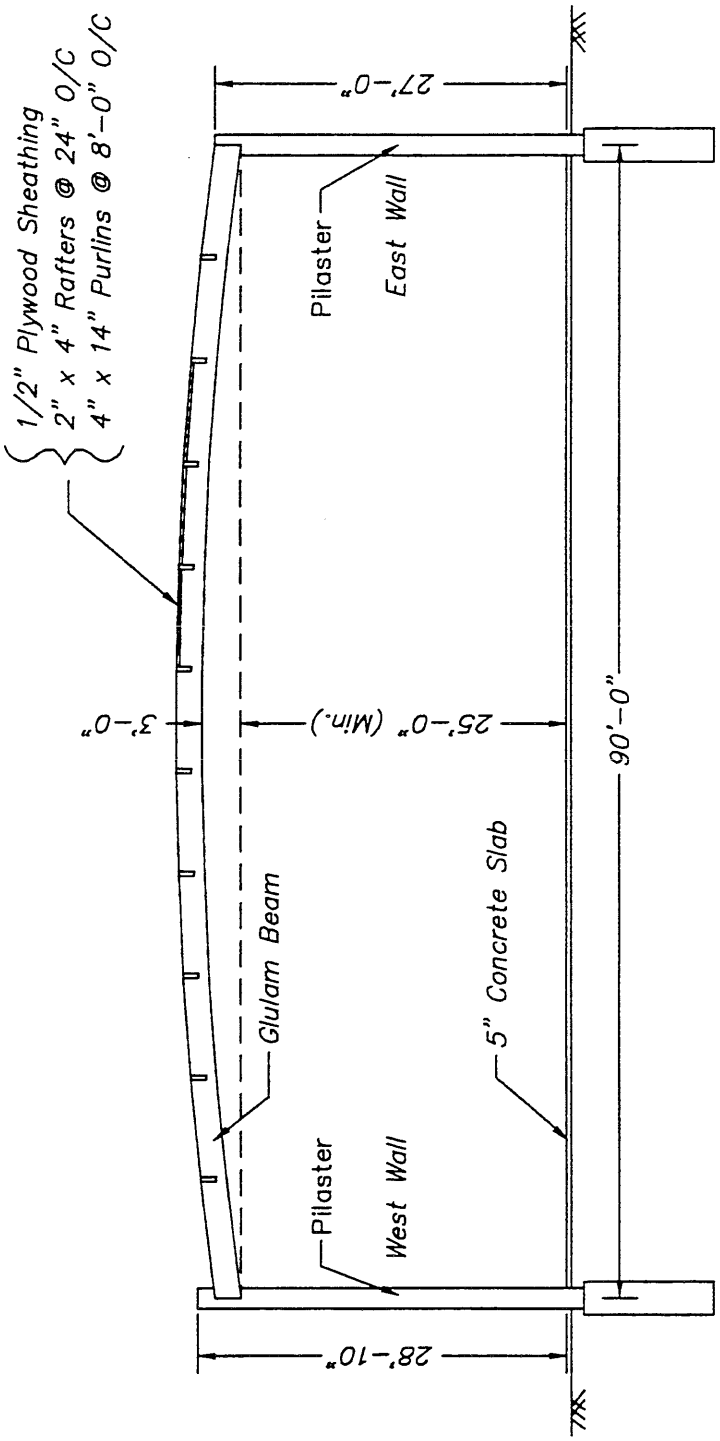

Fig. 5.21 Transverse cross section – Redlands warehouse.

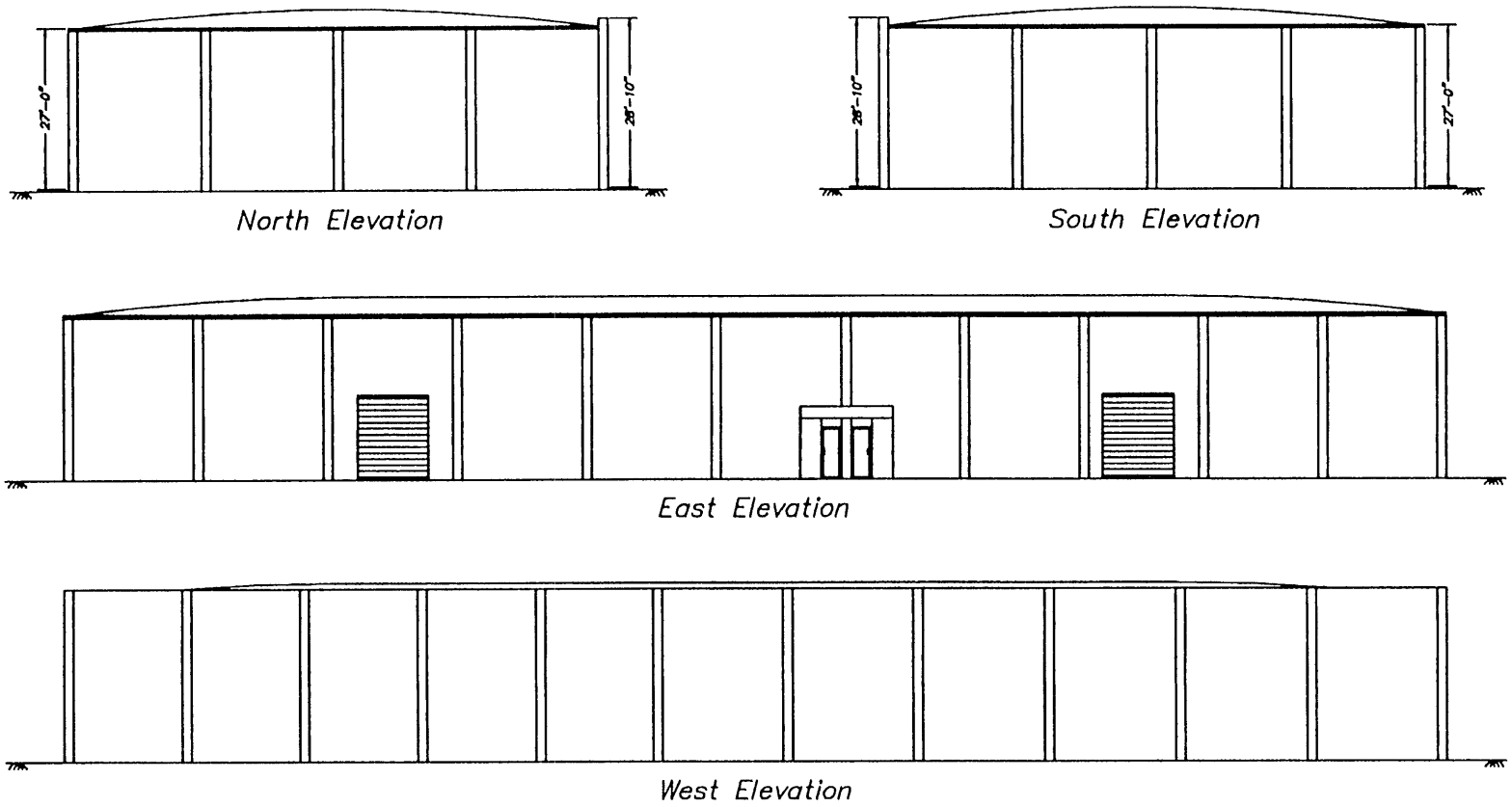

Fig. 5.22 Elevations – Redlands warehouse.

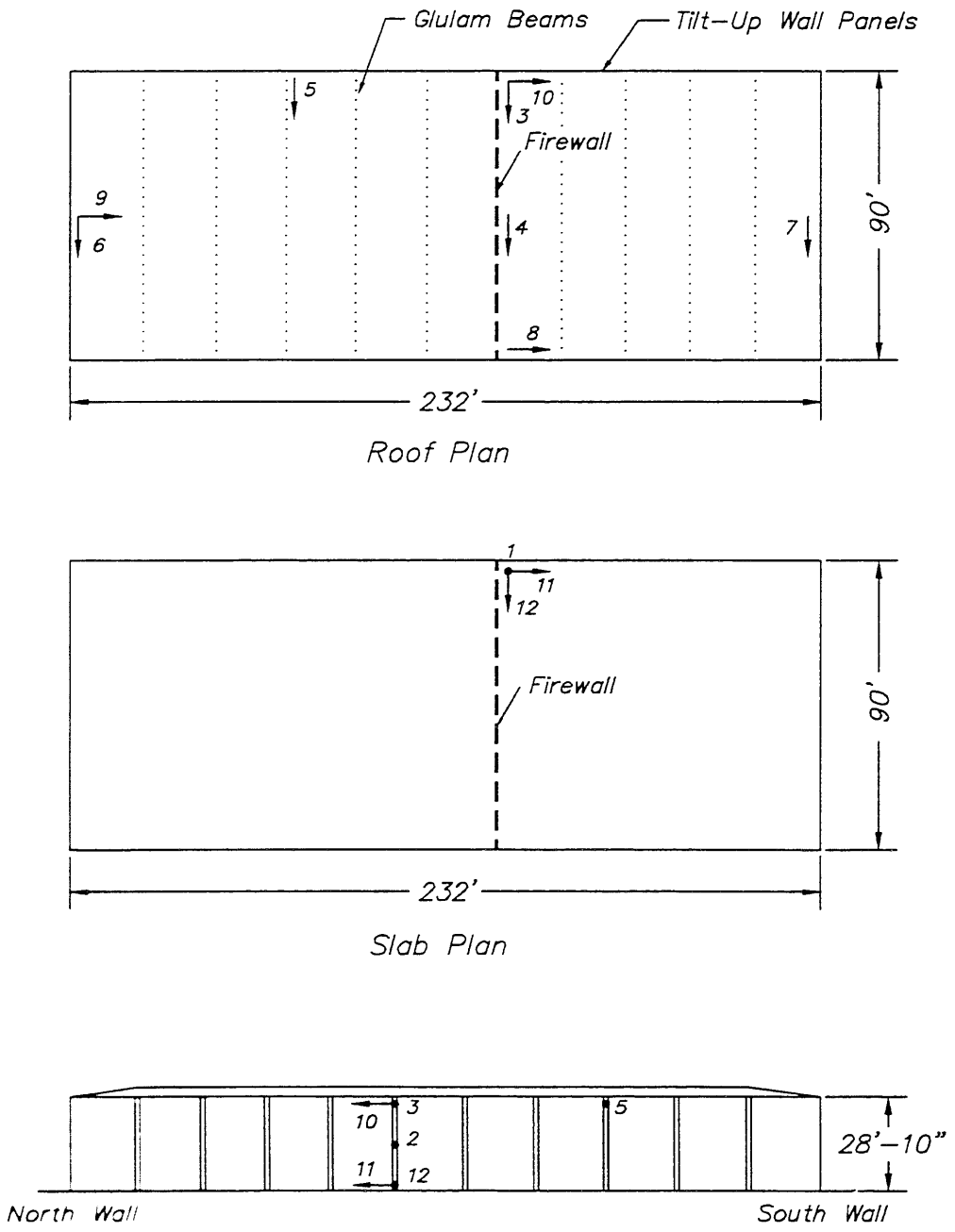

Fig. 5.23 Locations of strong–motion instruments – Redlands warehouse.

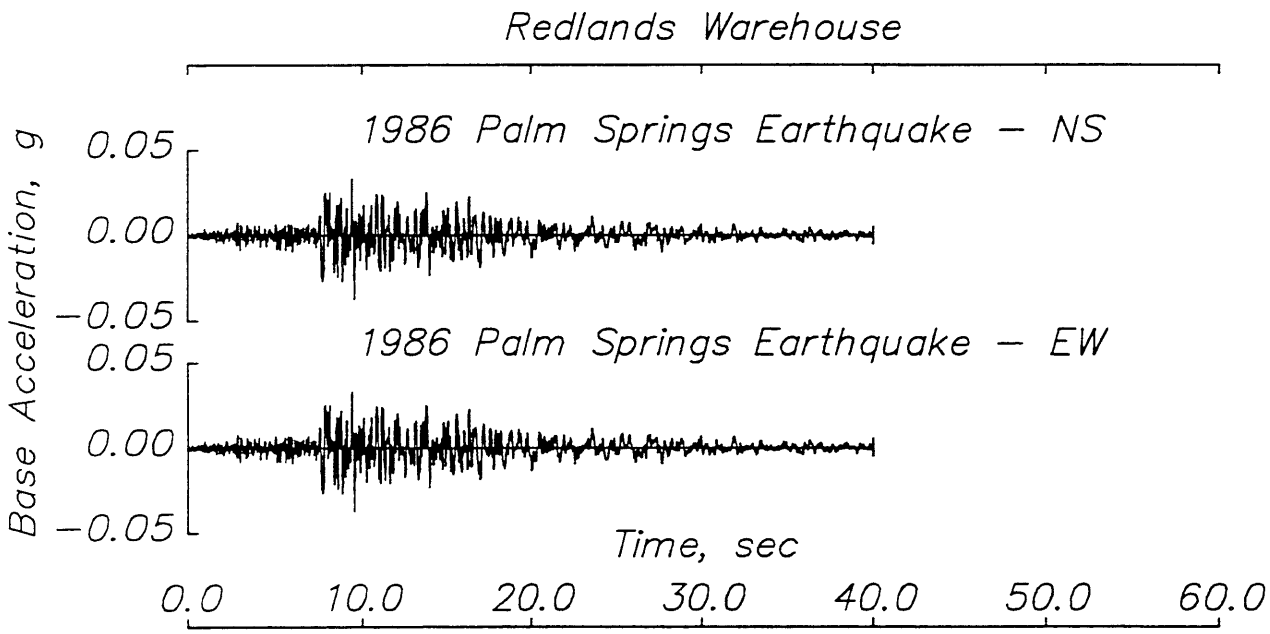

Fig. 5.24 Measured ground accelerations – Redlands warehouse.

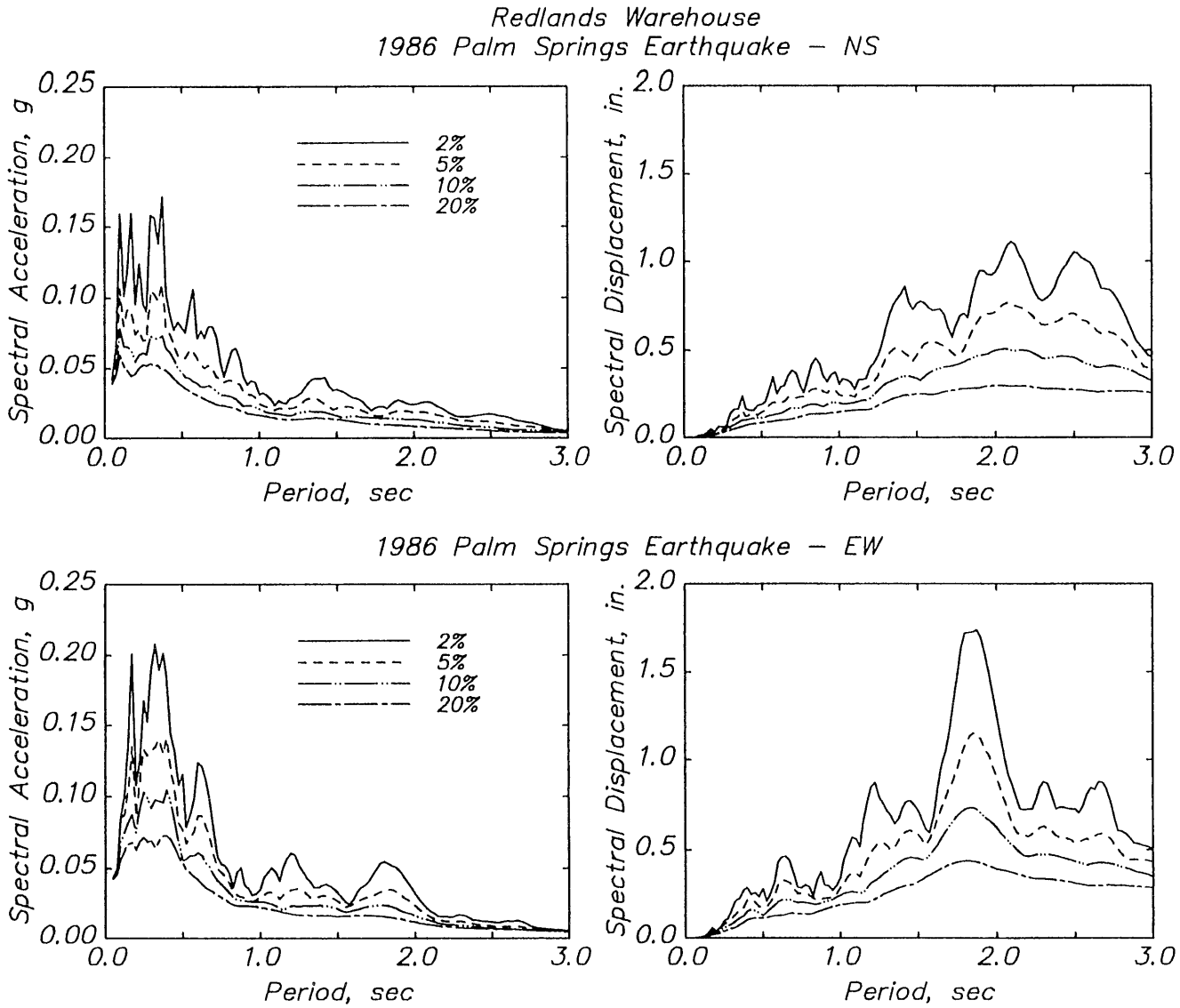

Fig. 5.25 Linear response spectra – Redlands warehouse.

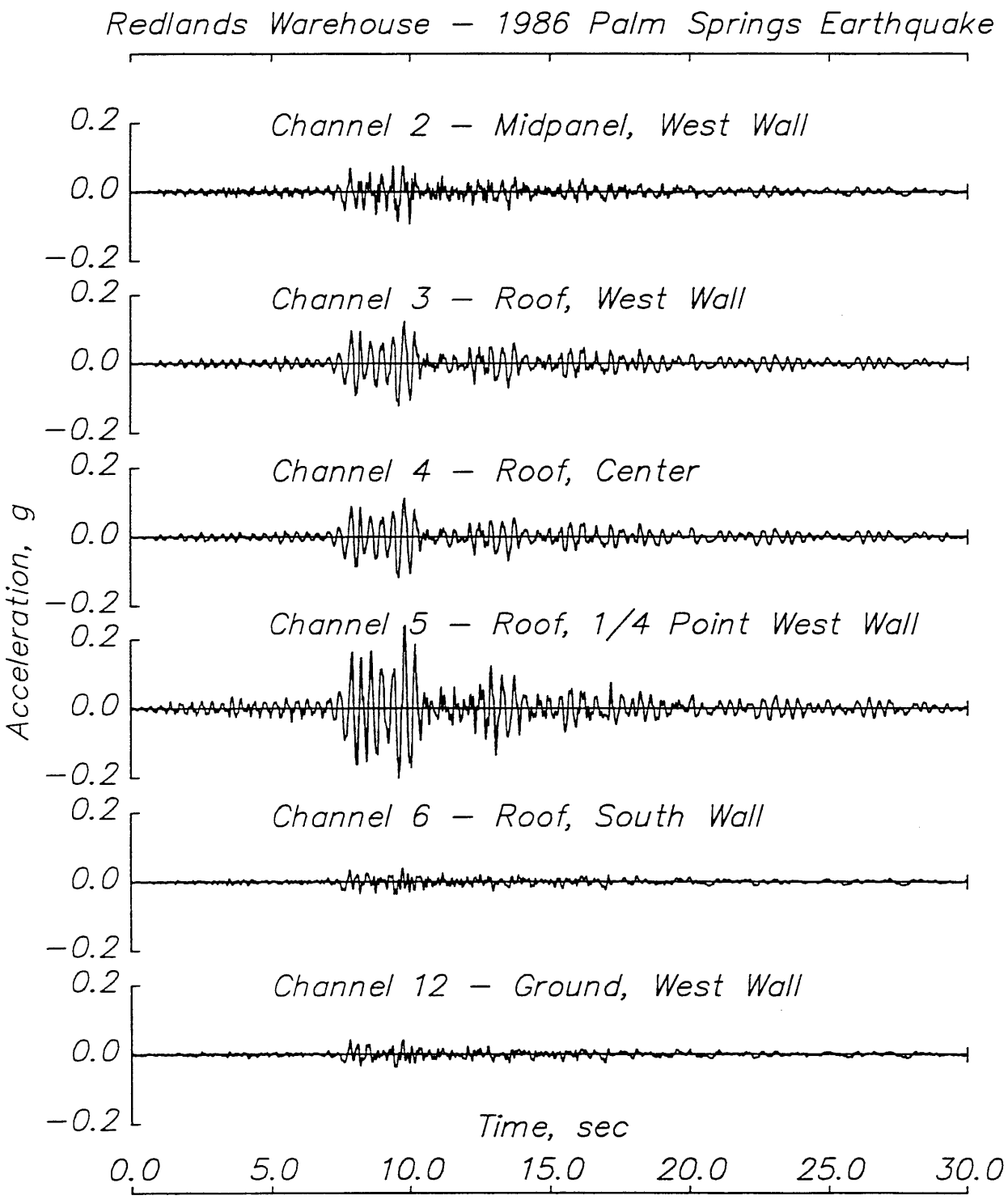

Fig. 5.26 Redlands warehouse – 1986 Palm Springs earthquake.
(a) Transverse acceleration response.

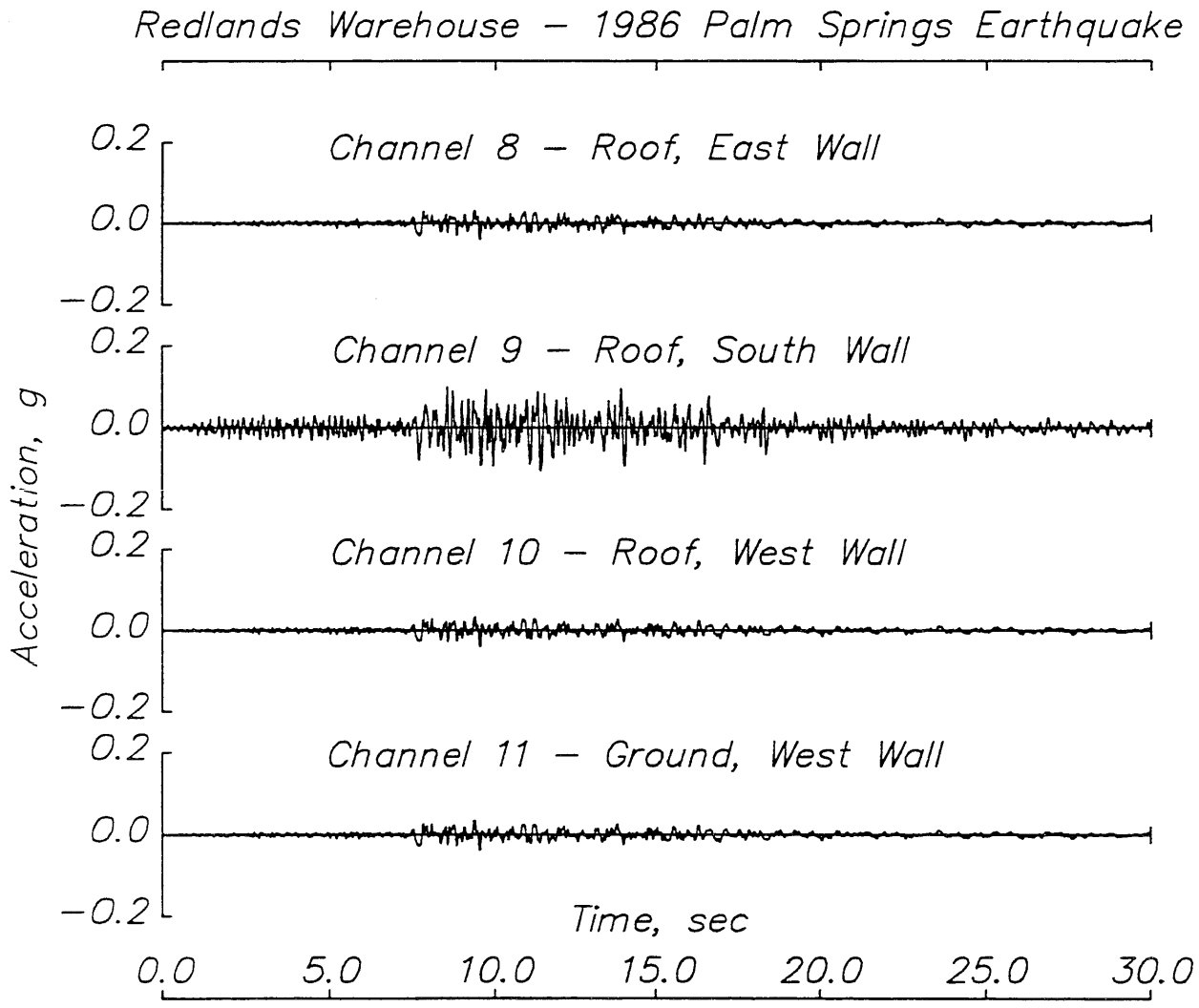

Fig. 5.26 Redlands warehouse – 1986 Palm Springs earthquake.
(b) Longitudinal acceleration response.

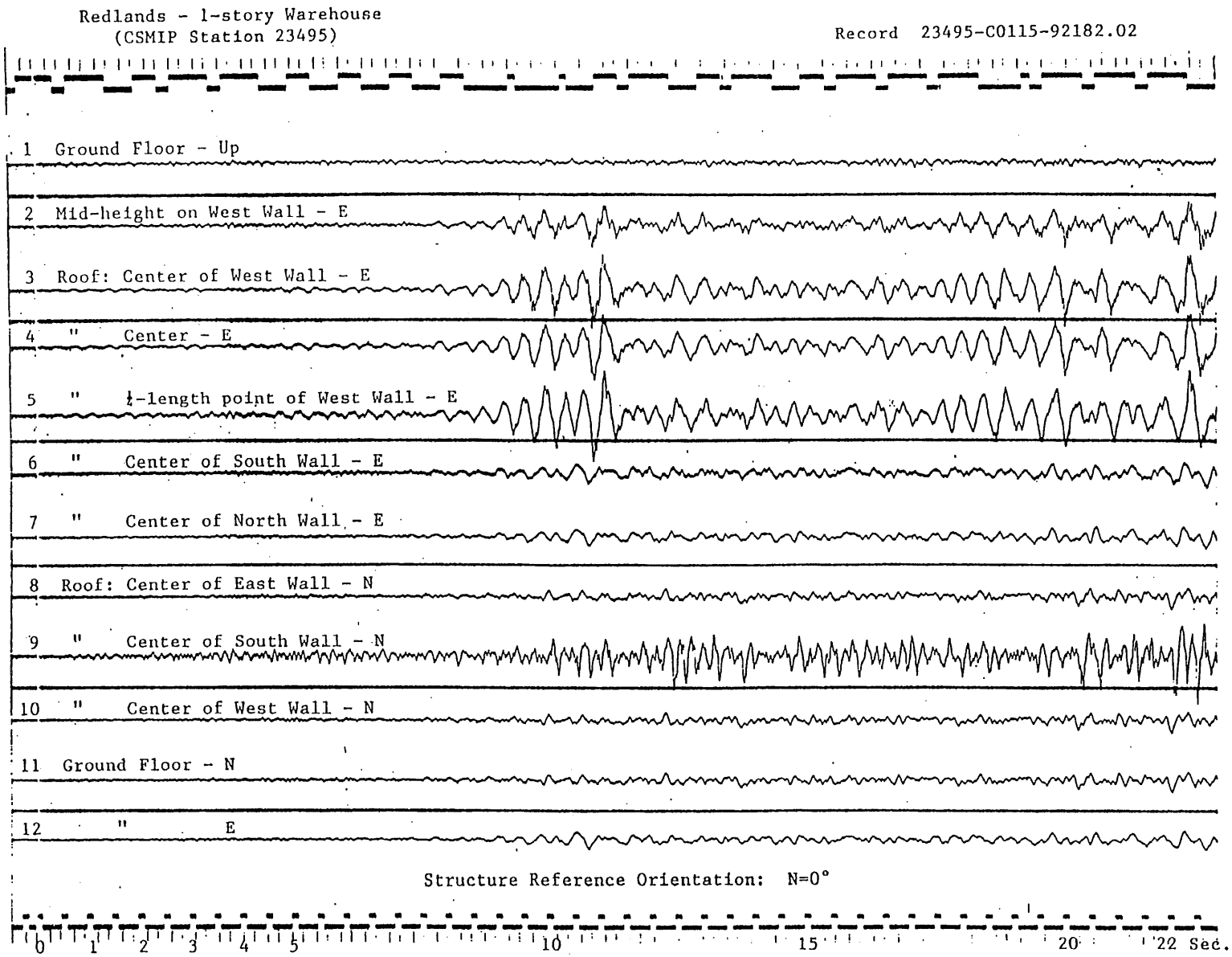

Fig. 5.27 Redlands warehouse – 1992 Landers earthquake [66].

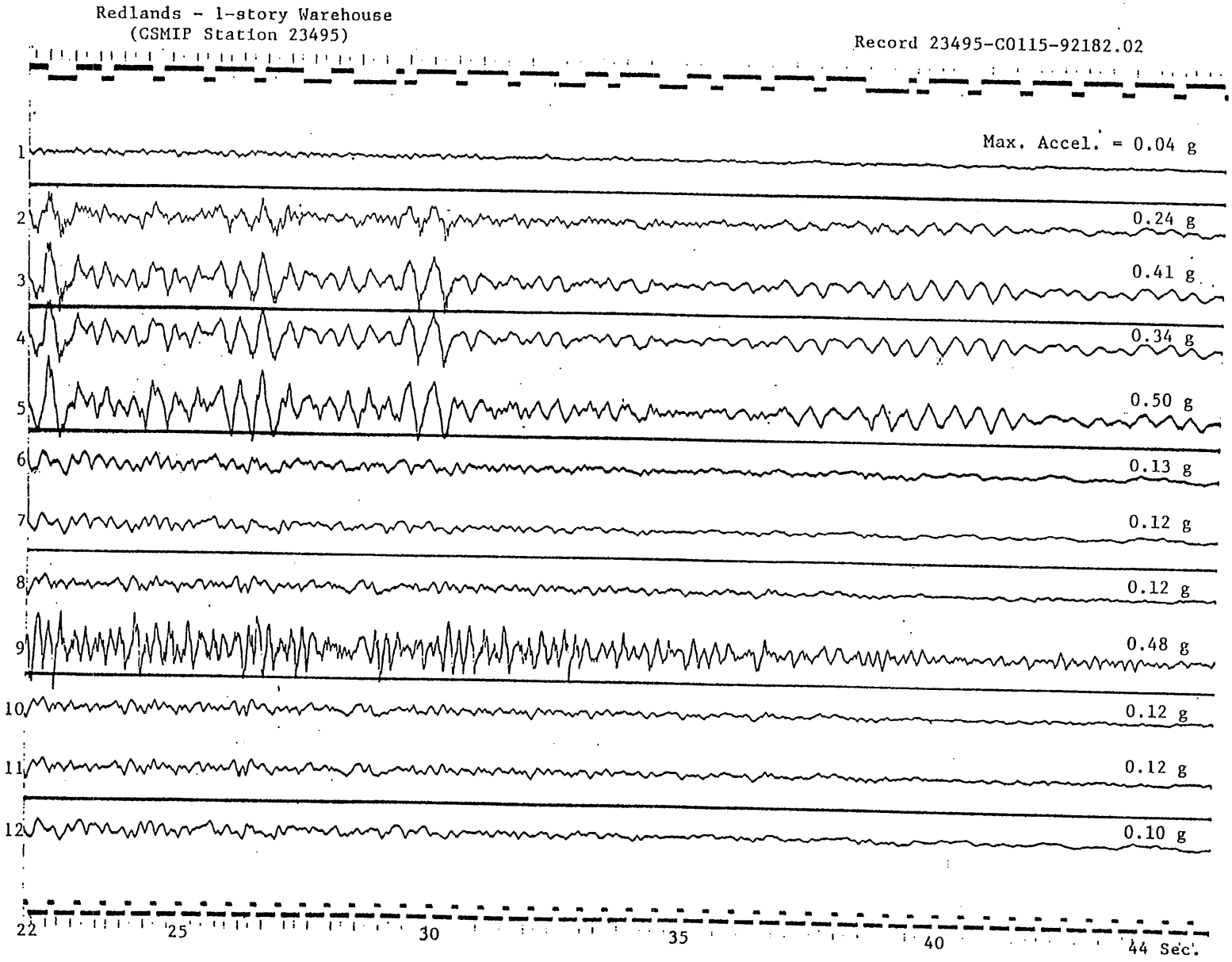

Fig. 5.27 (cont.) Redlands warehouse – 1992 Landers earthquake [66].

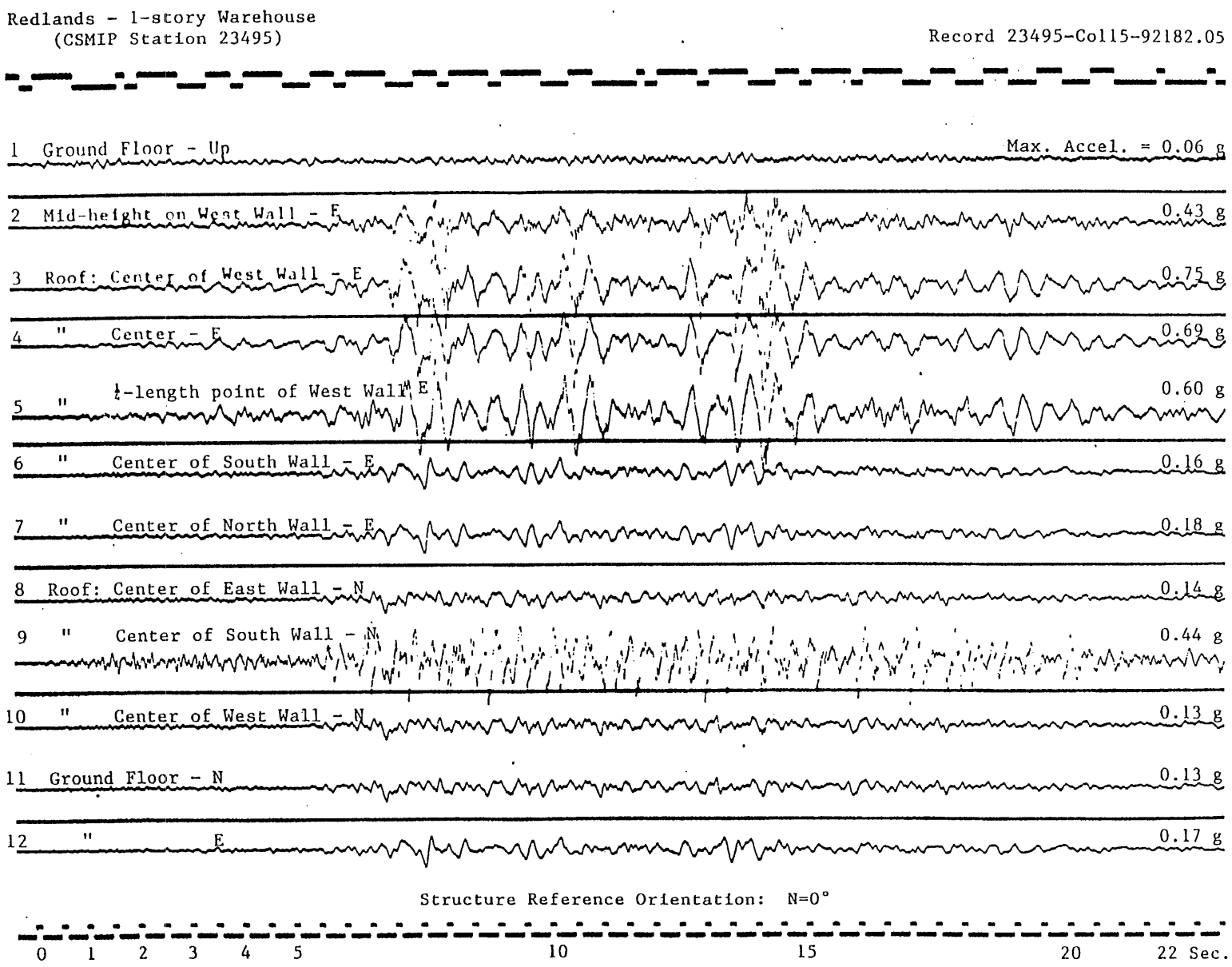

Fig. 5.28 Redlands warehouse – 1992 Big Bear earthquake [37].

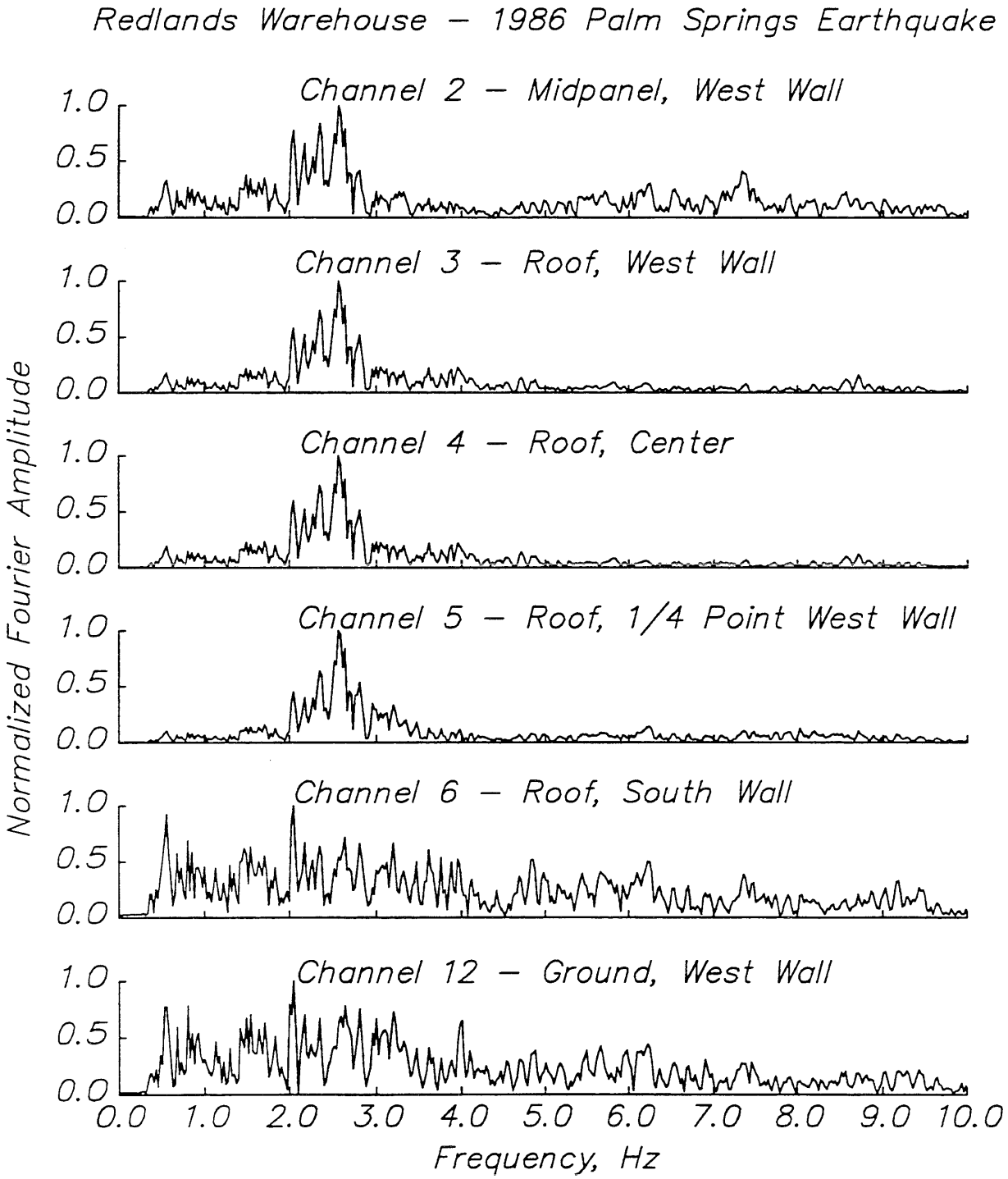

Fig. 5.29 Redlands warehouse – 1986 Palm Springs earthquake.
(a) Normalized Fourier amplitude spectra of transverse acceleration response.

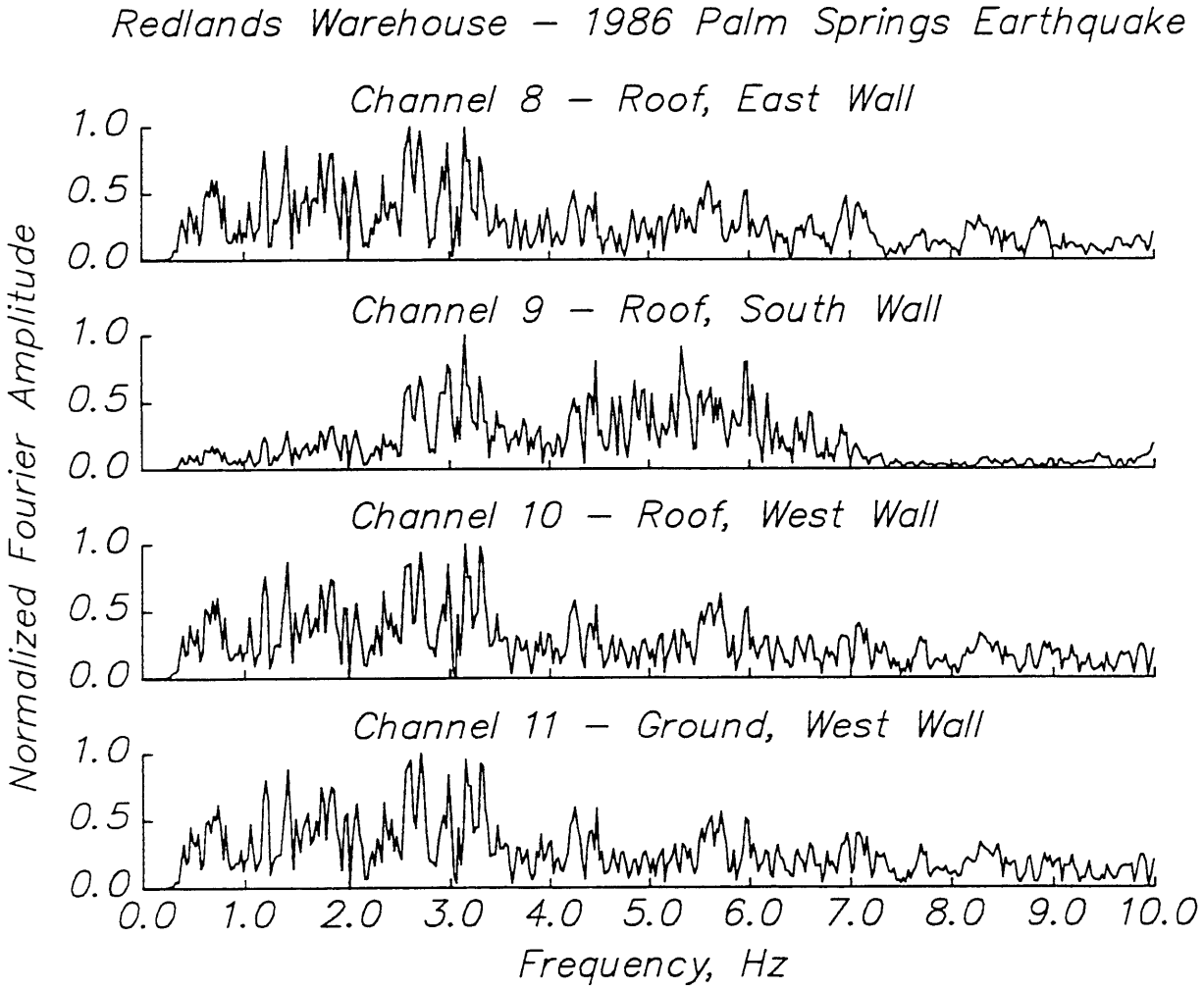

Fig. 5.29 Redlands warehouse – 1986 Palm Springs earthquake.
(b) Normalized Fourier amplitude spectra of longitudinal acceleration response.

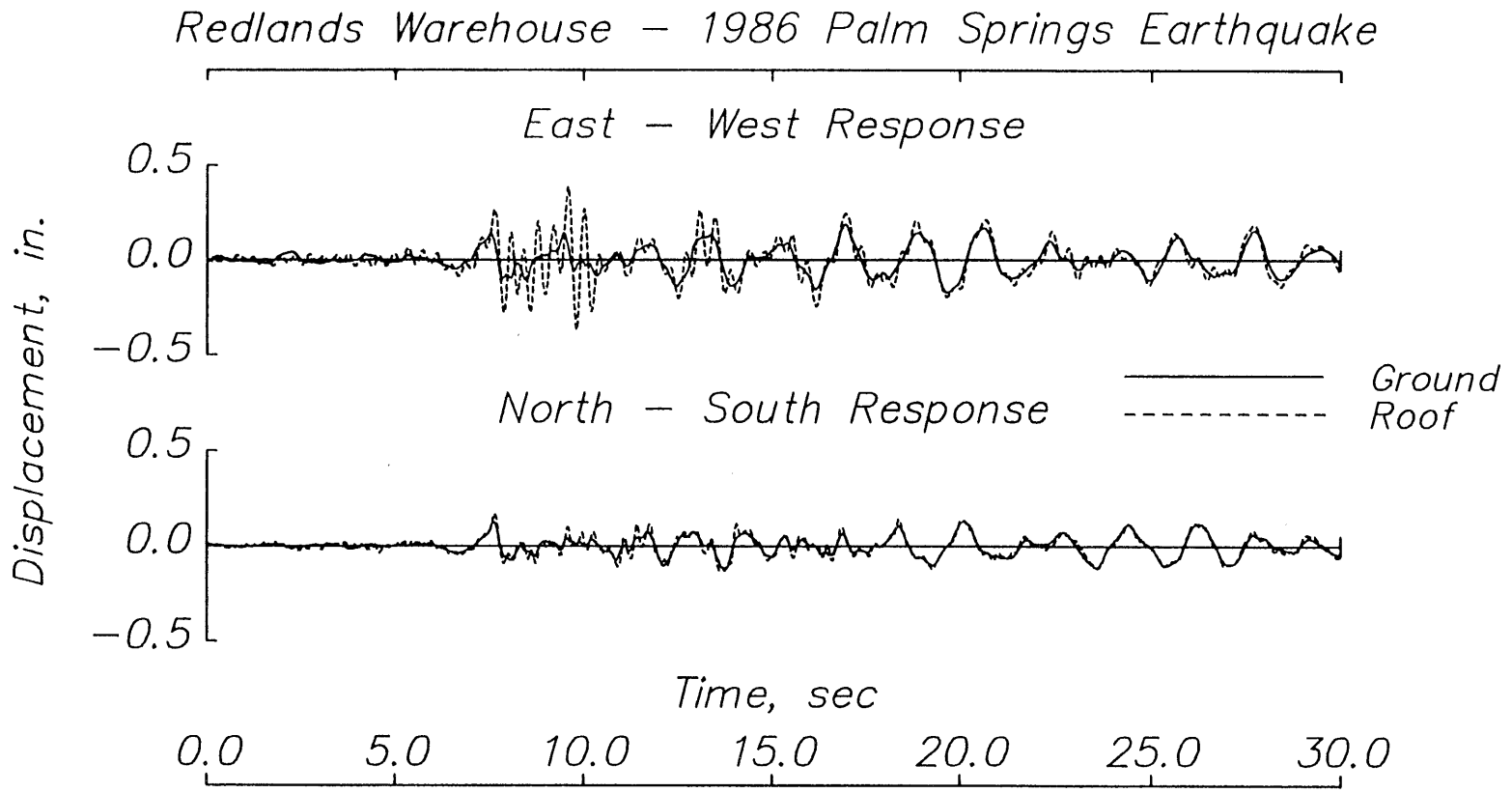

Fig. 5.30 Redlands warehouse – Absolute displacement response.

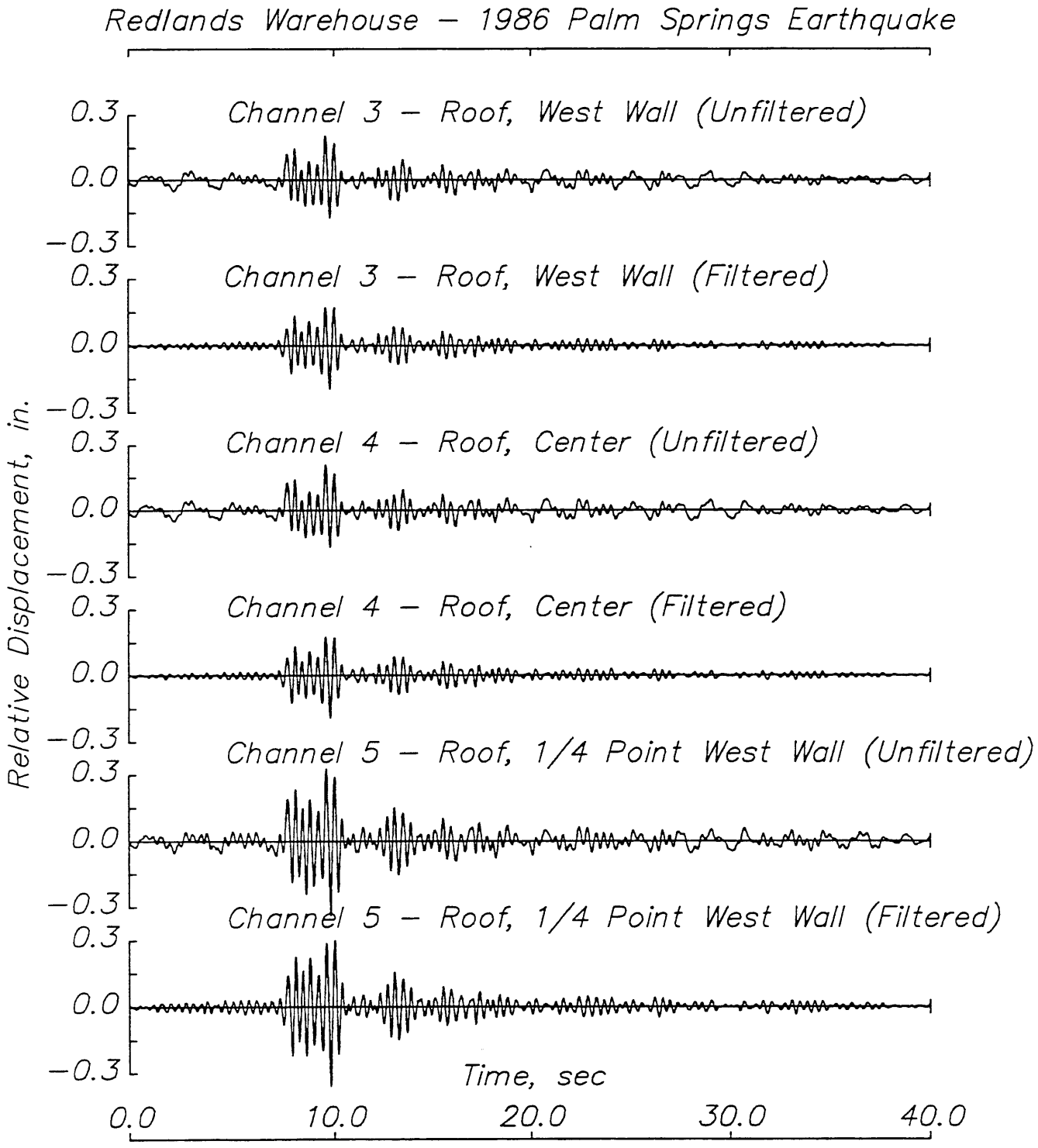

Fig. 5.31 Redlands warehouse – 1986 Palm Springs earthquake.
(a) Transverse relative displacement response.

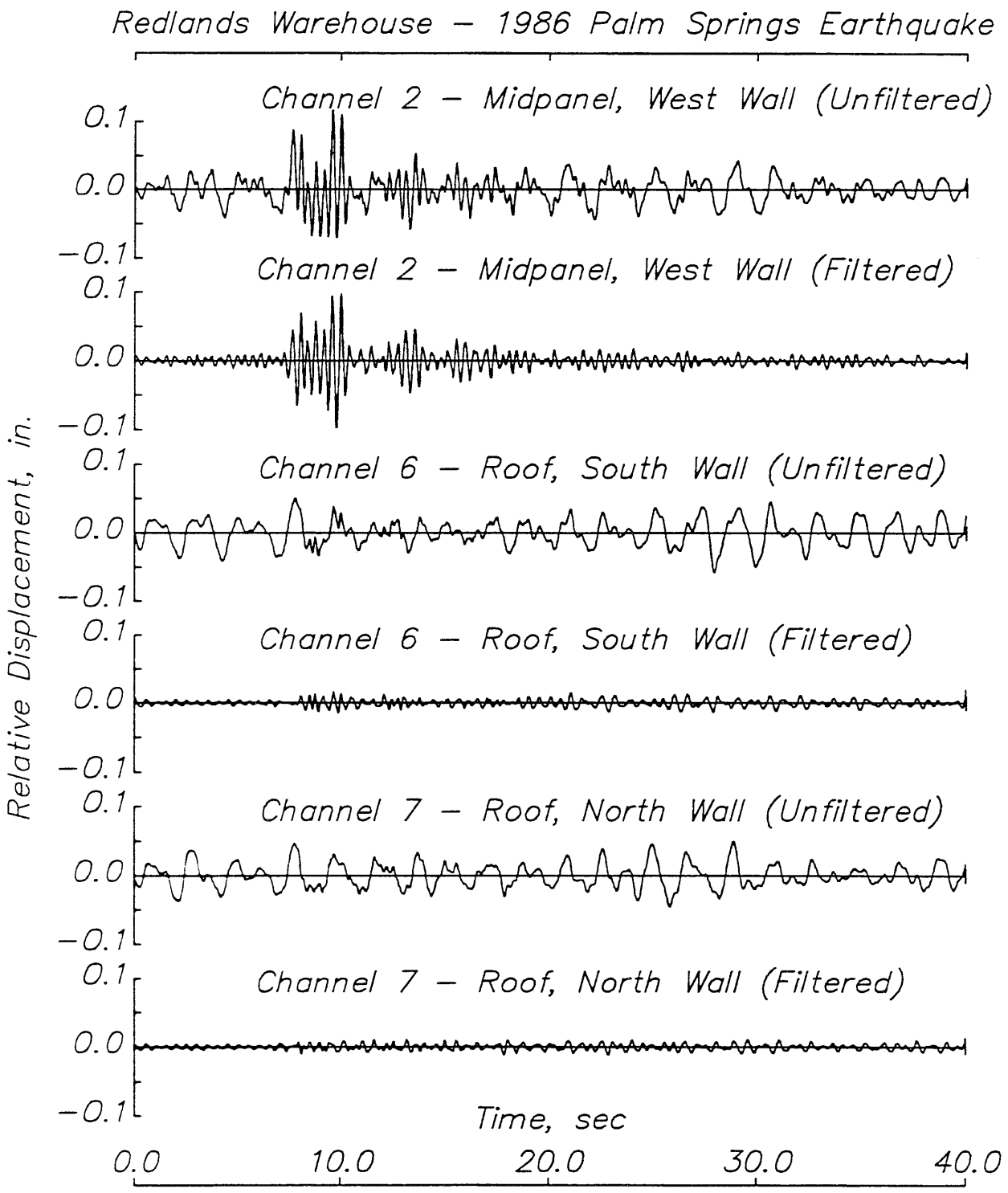

Fig. 5.31 (cont.) Redlands warehouse – 1986 Palm Springs earthquake.
(a) (cont.) Transverse relative displacement response.

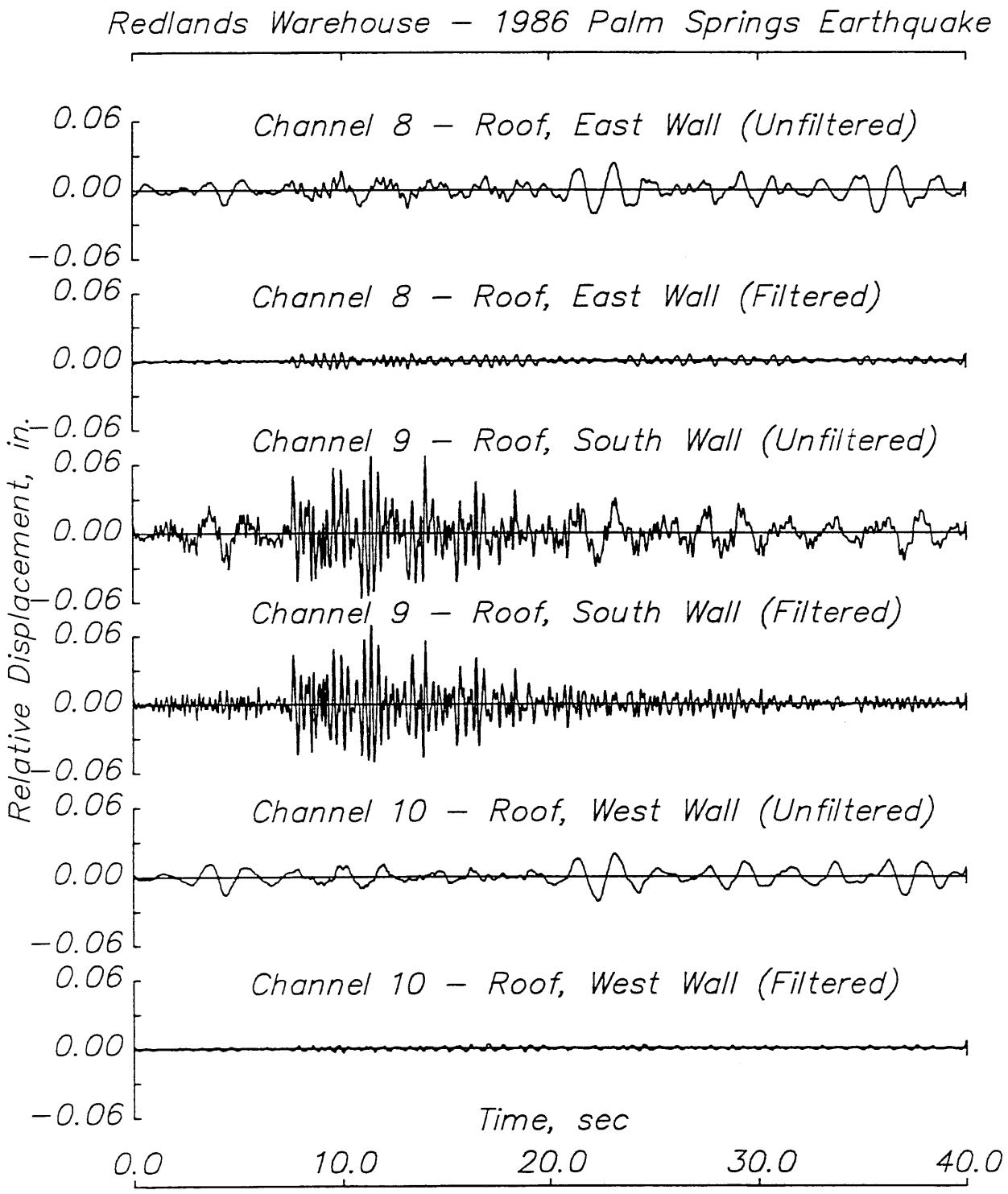

Fig. 5.31 (cont.) Redlands warehouse – 1986 Palm Springs earthquake.
(b) Longitudinal relative displacement response.

Fig. 5.32 Milpitas industrial building.

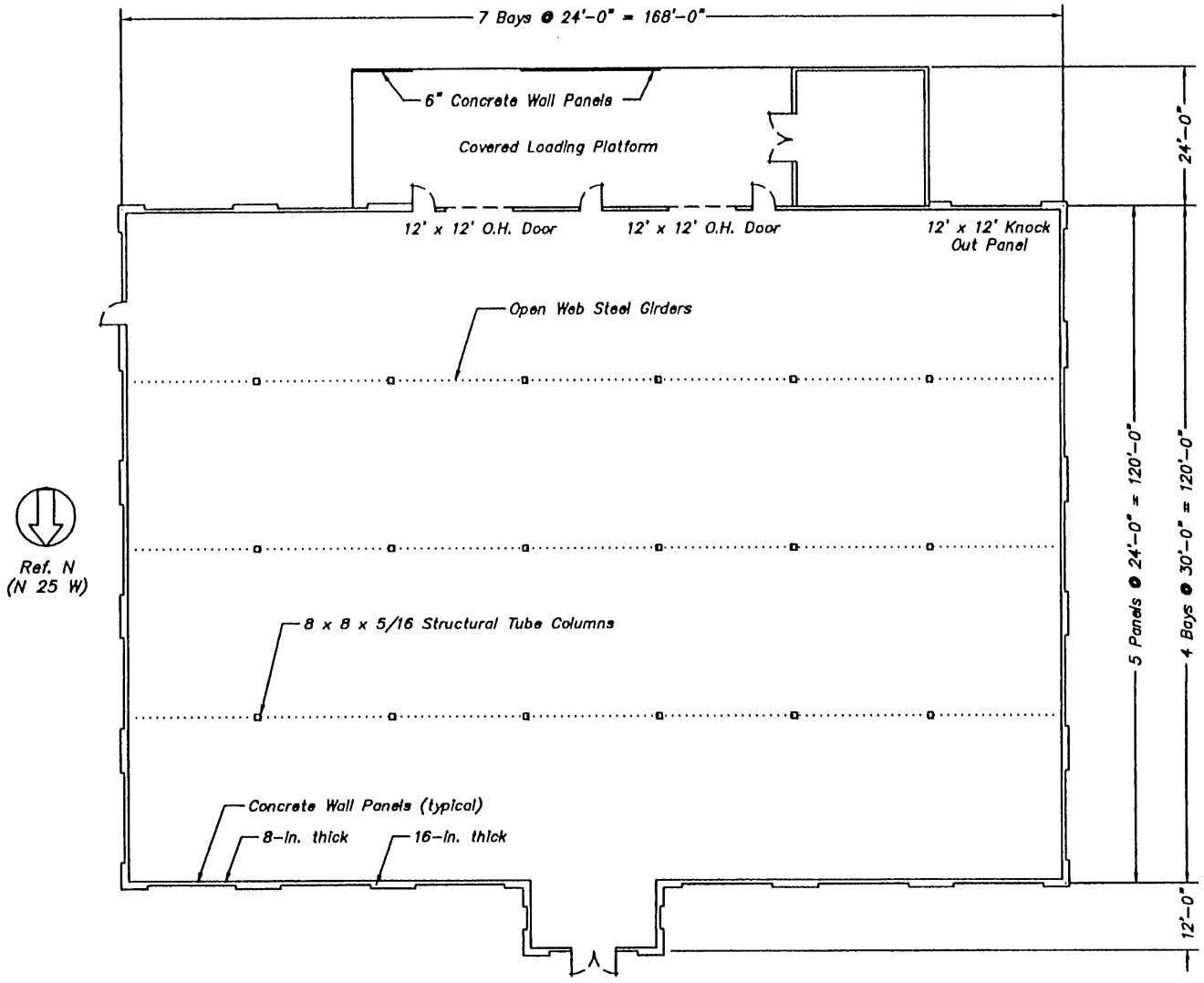

Fig. 5.33 Floor plans – Milpitas industrial building.

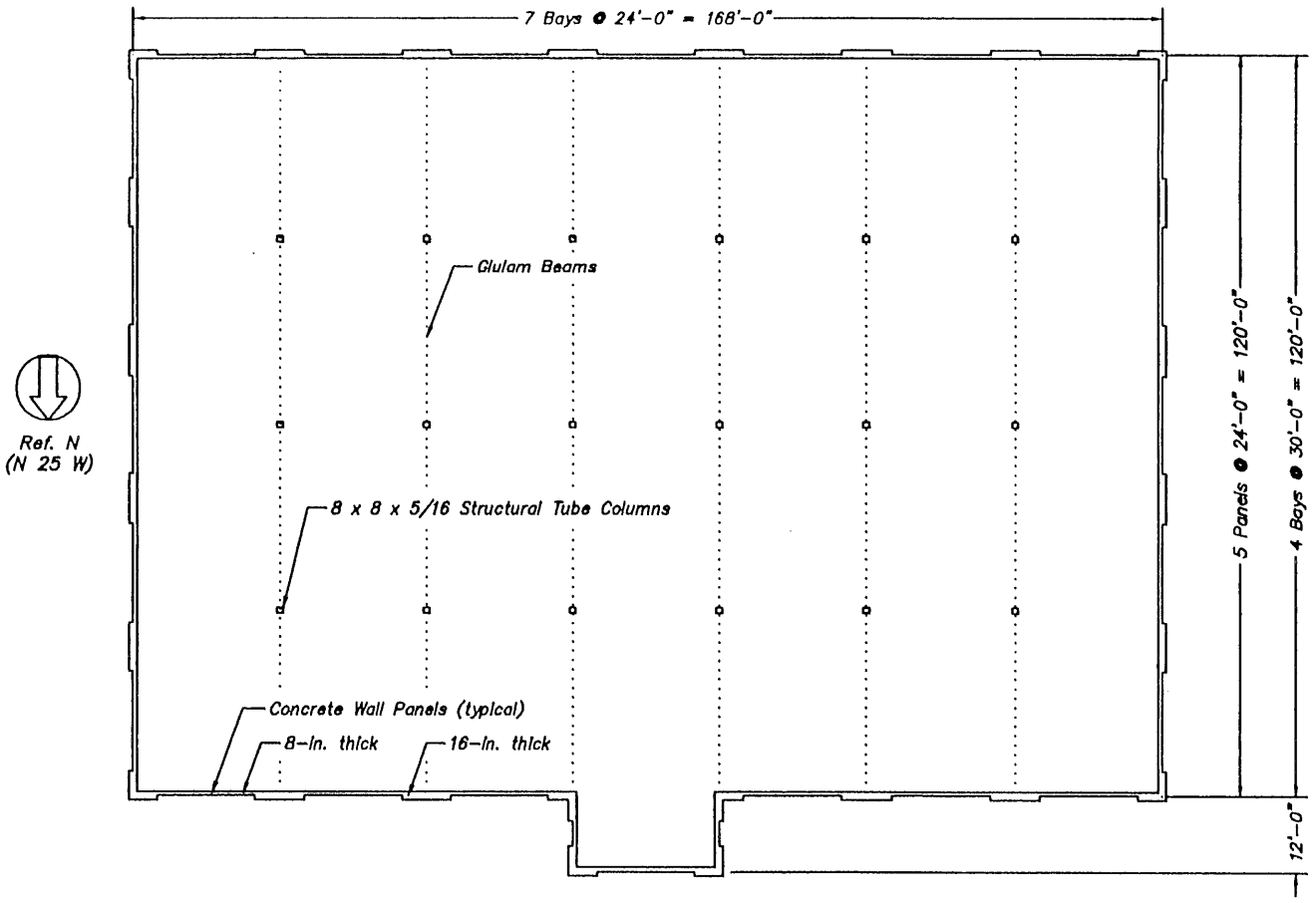

Second-Story Plan – Milpitas Industrial Building

Fig. 5.33 (cont.) Floor plans – Milpitas industrial building.

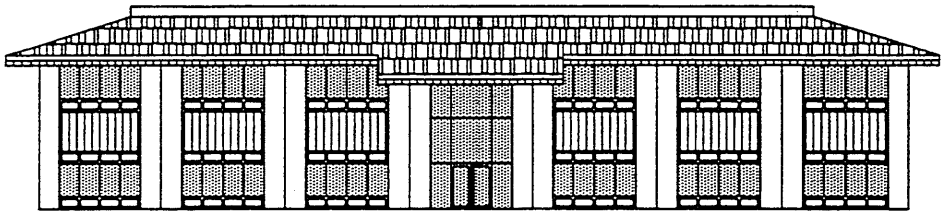

North Elevation

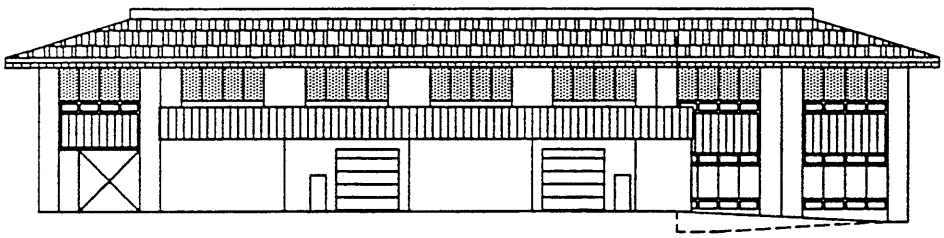

South Elevation

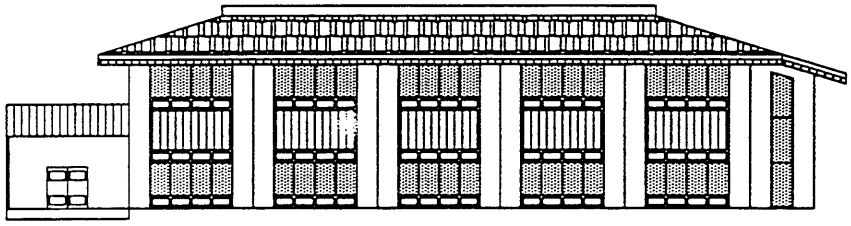

East Elevation

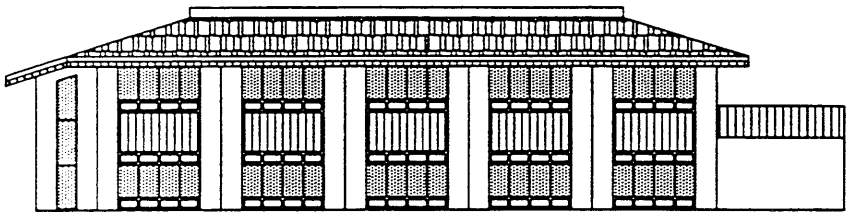

West Elevation

Fig. 5.34 Elevations – Milpitas industrial building.

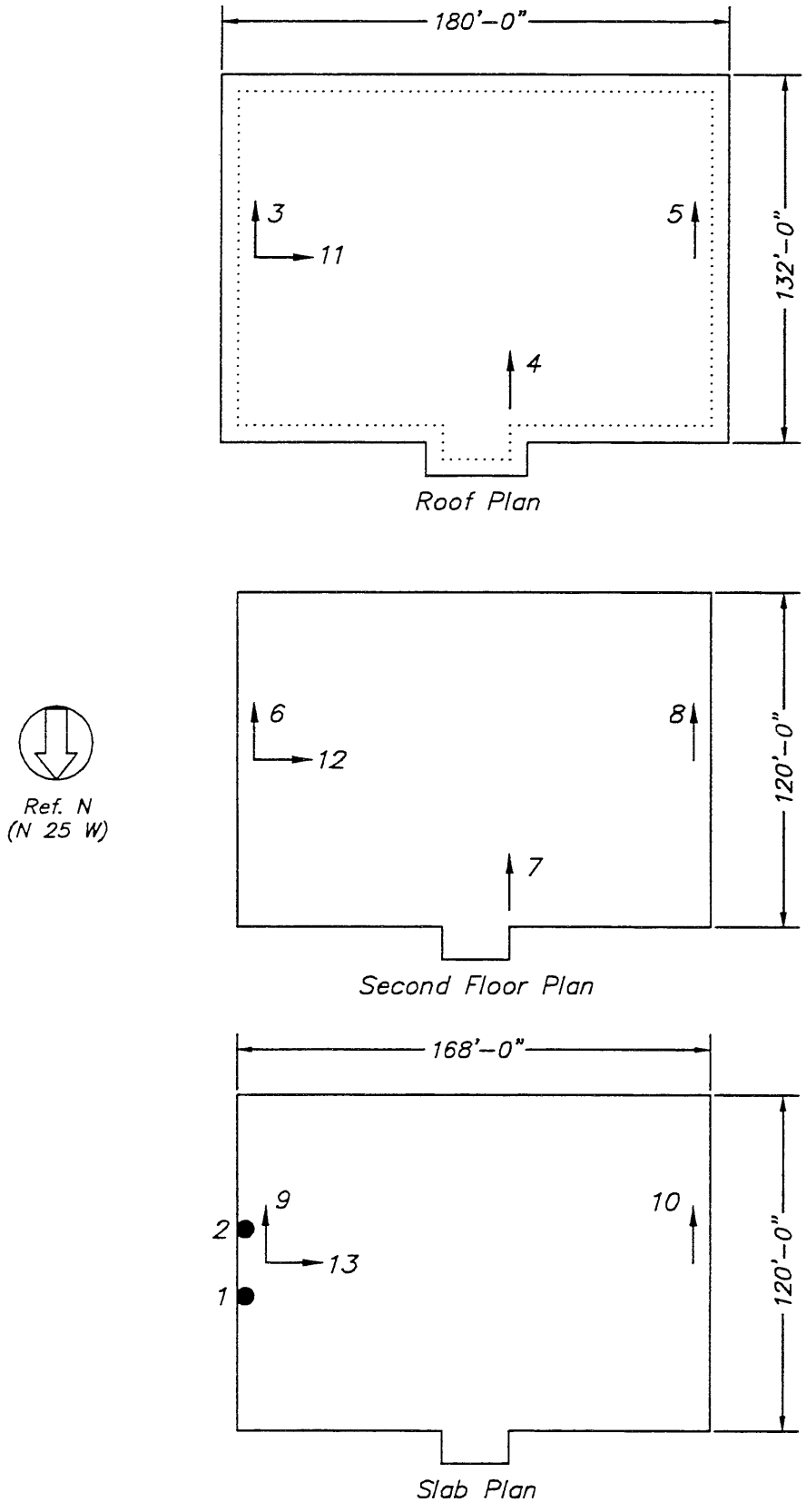

Fig. 5.35 Locations of strong–motion instruments – Milpitas industrial building.

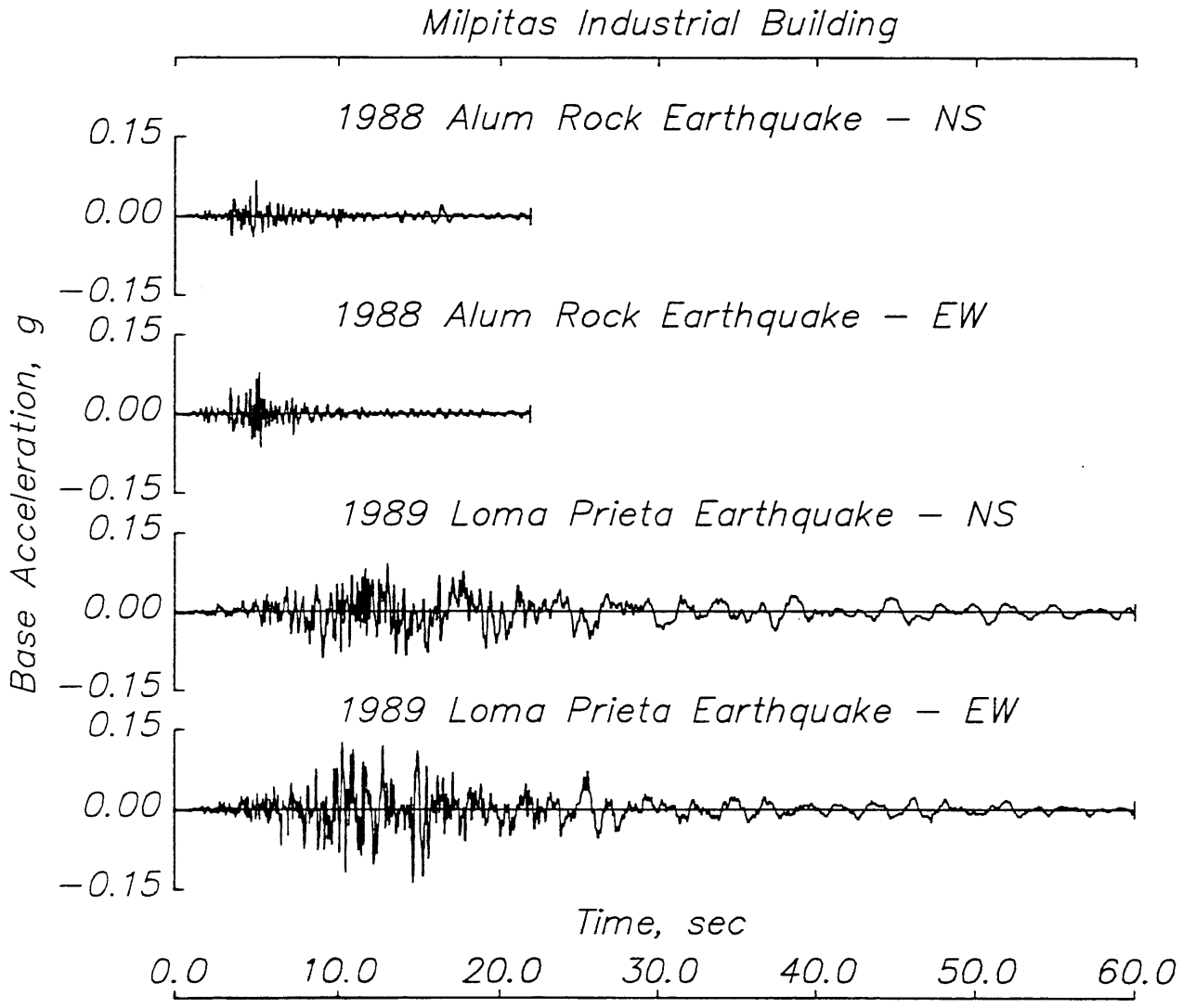

Fig. 5.36 Measured ground accelerations – Milpitas industrial building.

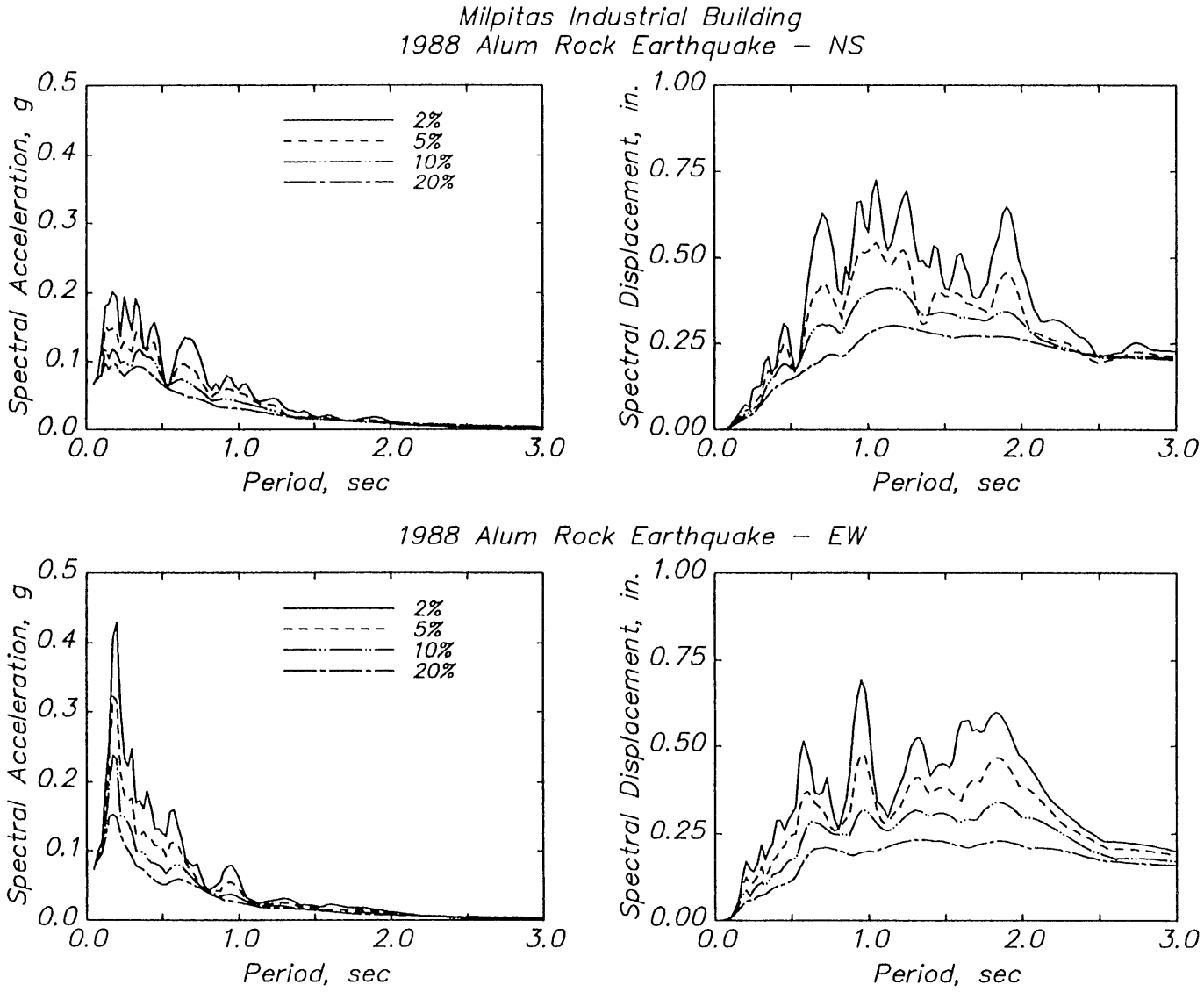

Fig. 5.37 Linear response spectra – Milpitas industrial building.

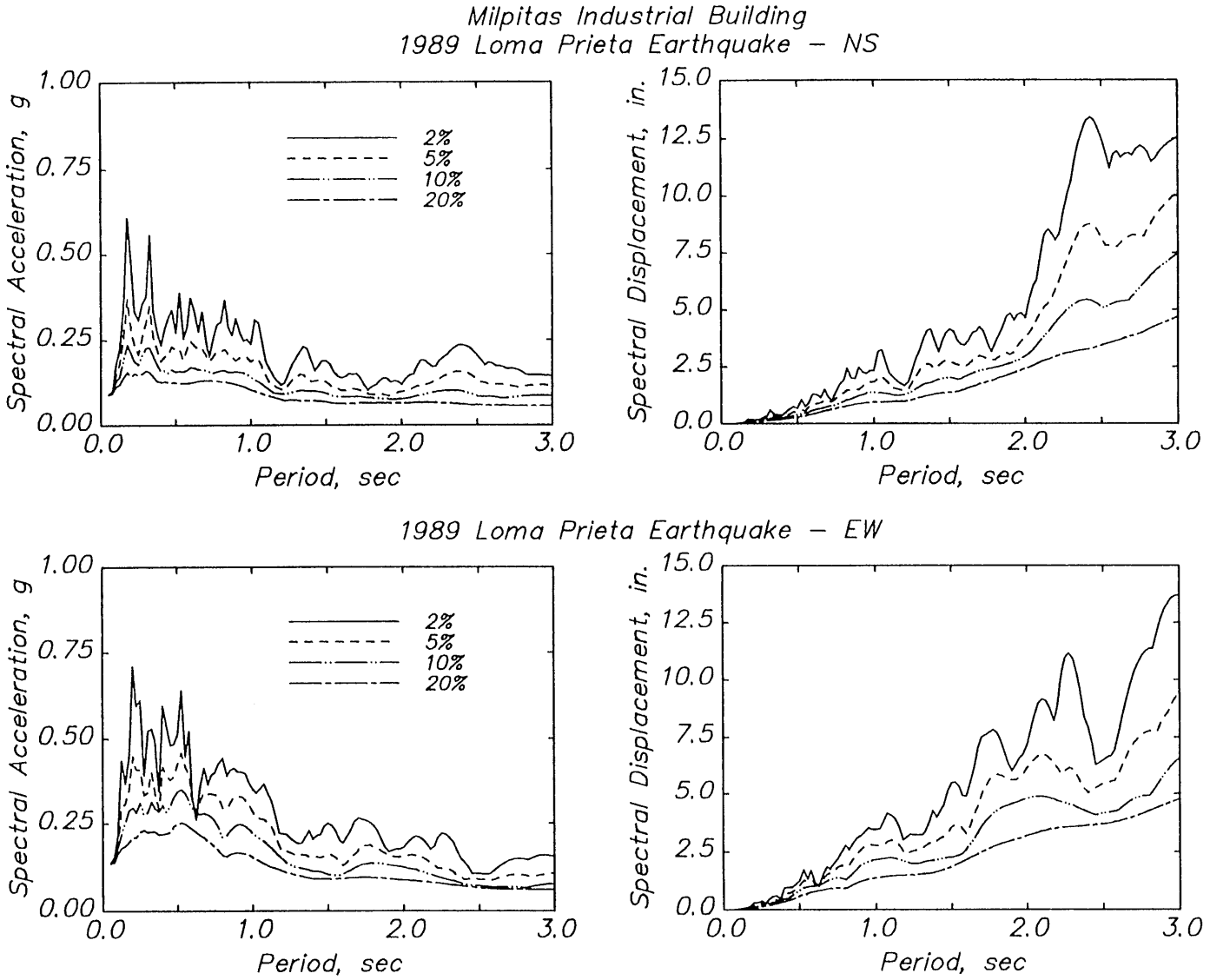

Fig. 5.37 (cont.) Linear response spectra – Milpitas industrial building.

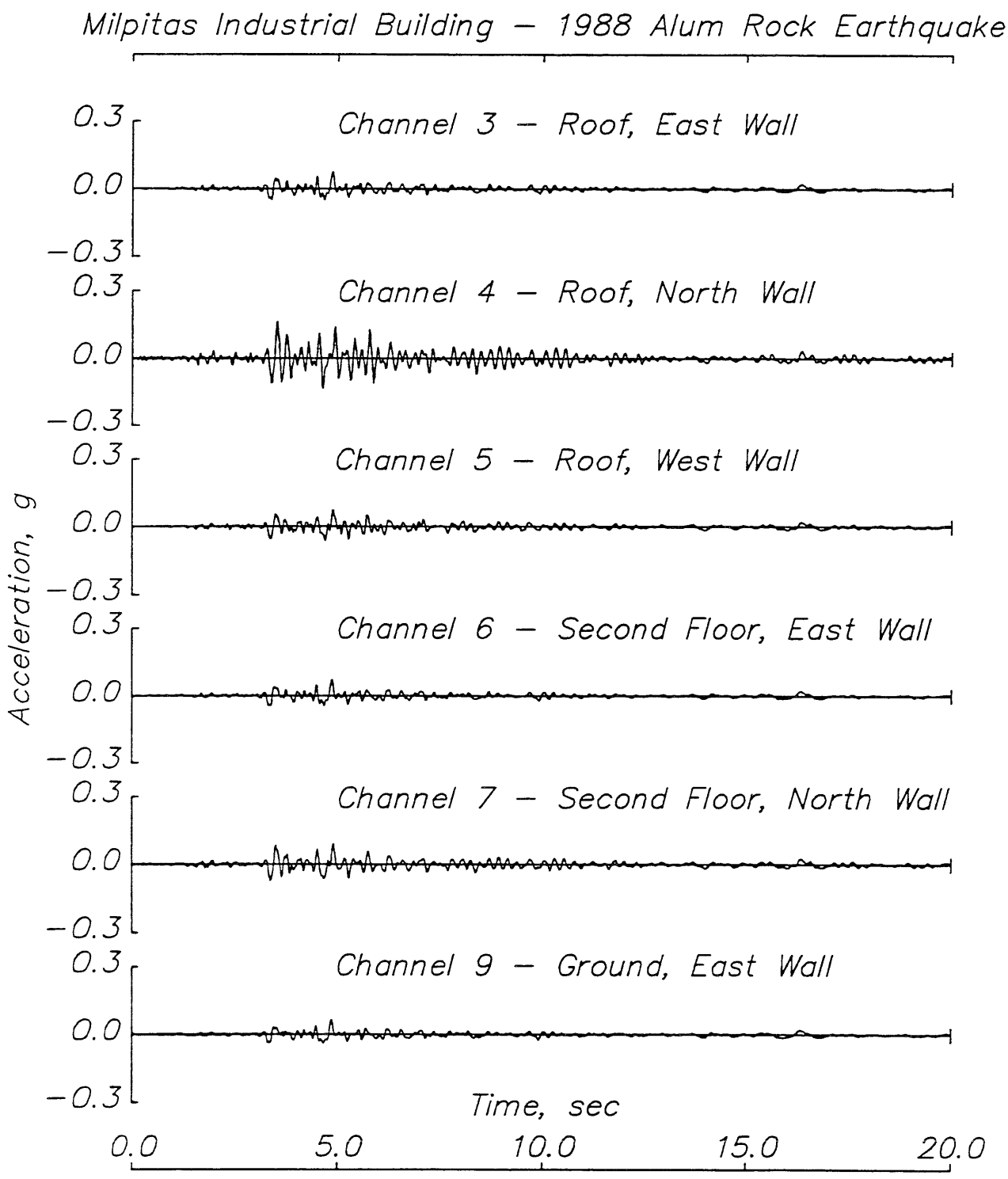

Fig. 5.38 Milpitas industrial building – 1988 Alum Rock earthquake.
(a) Transverse acceleration response.

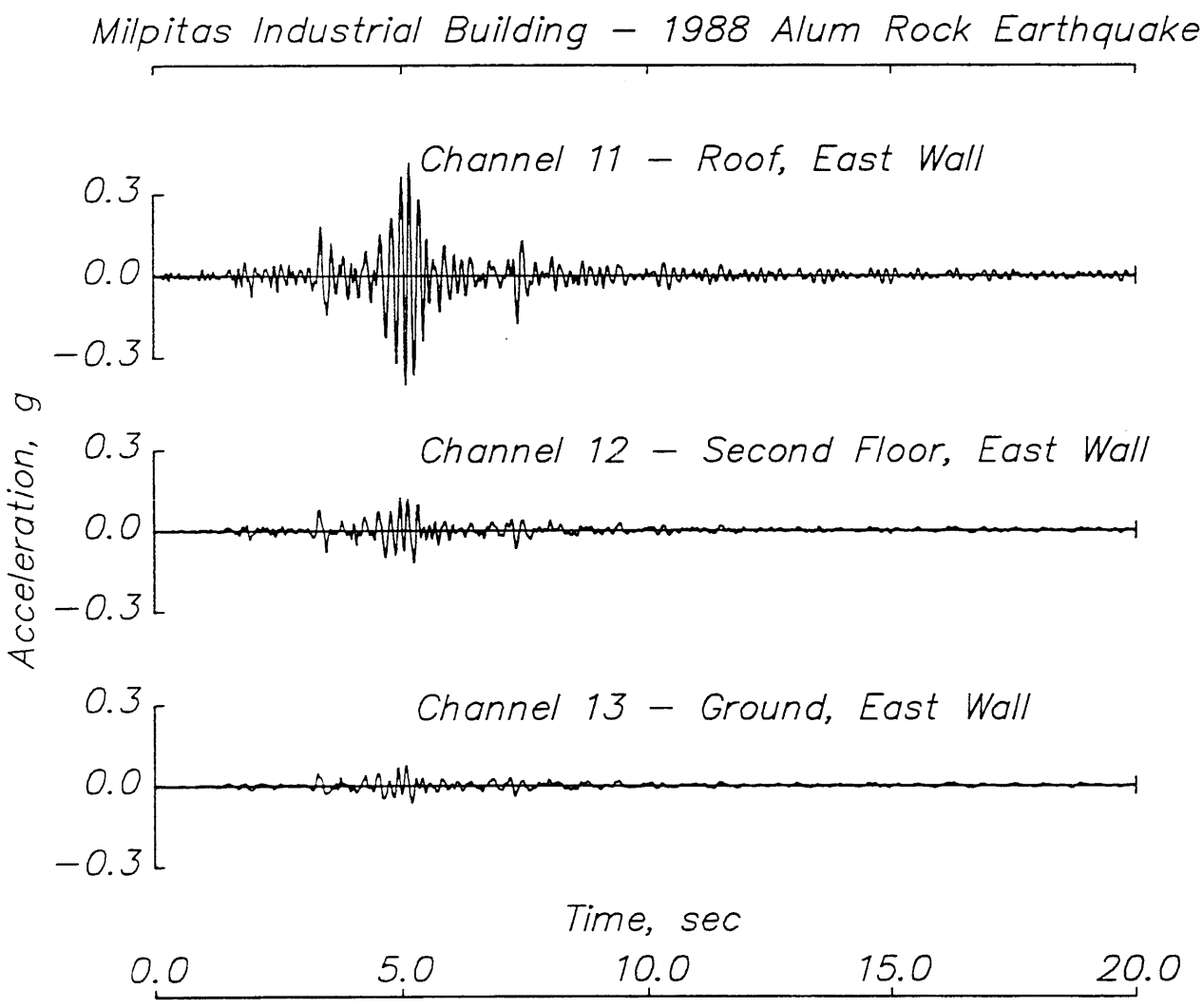

Fig. 5.38 (cont.) Milpitas industrial building – 1988 Alum Rock earthquake.
(b) Longitudinal acceleration response.

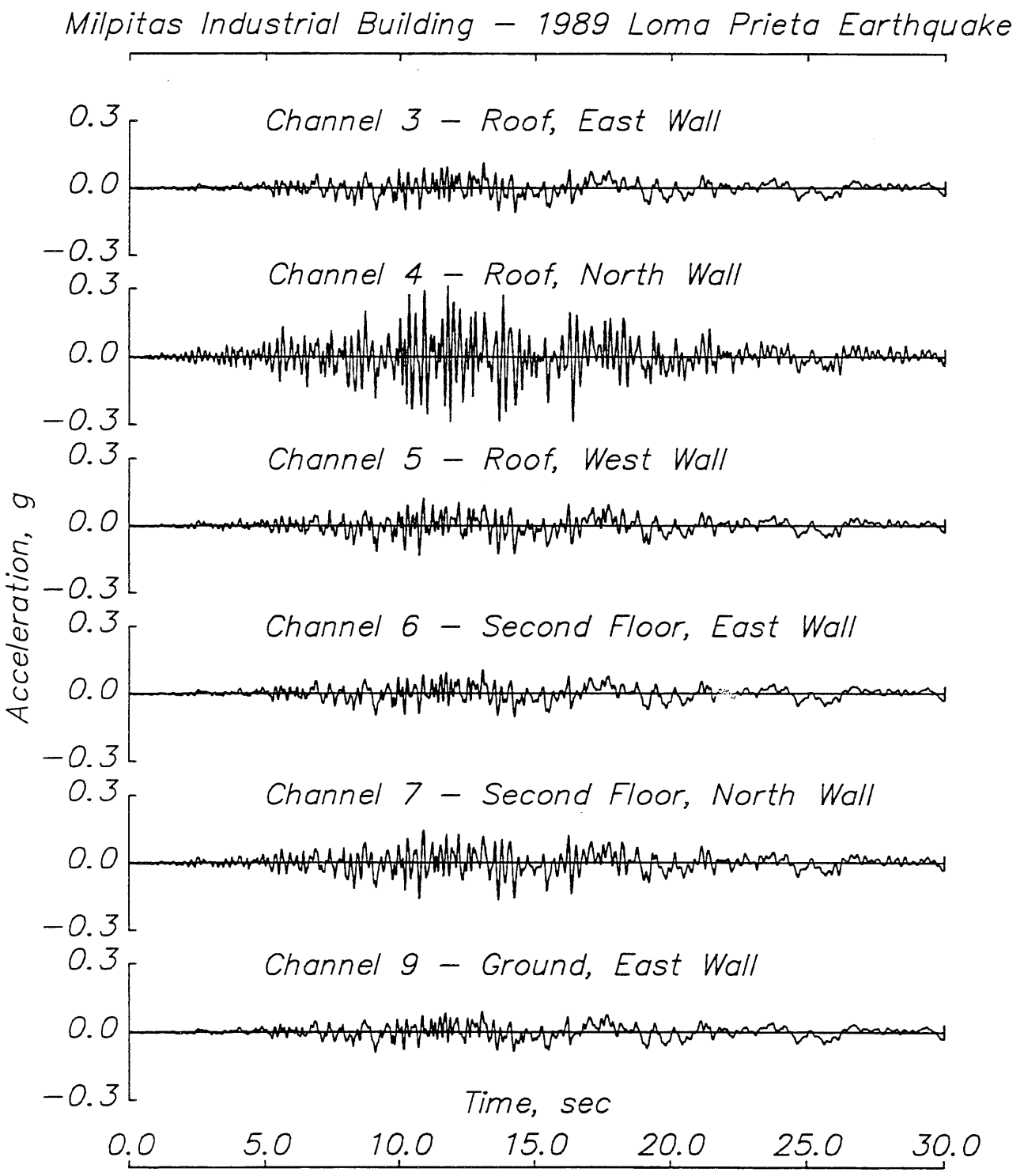

Fig. 5.39 Milpitas industrial building – 1989 Loma Prieta earthquake.
(a) Transverse acceleration response.

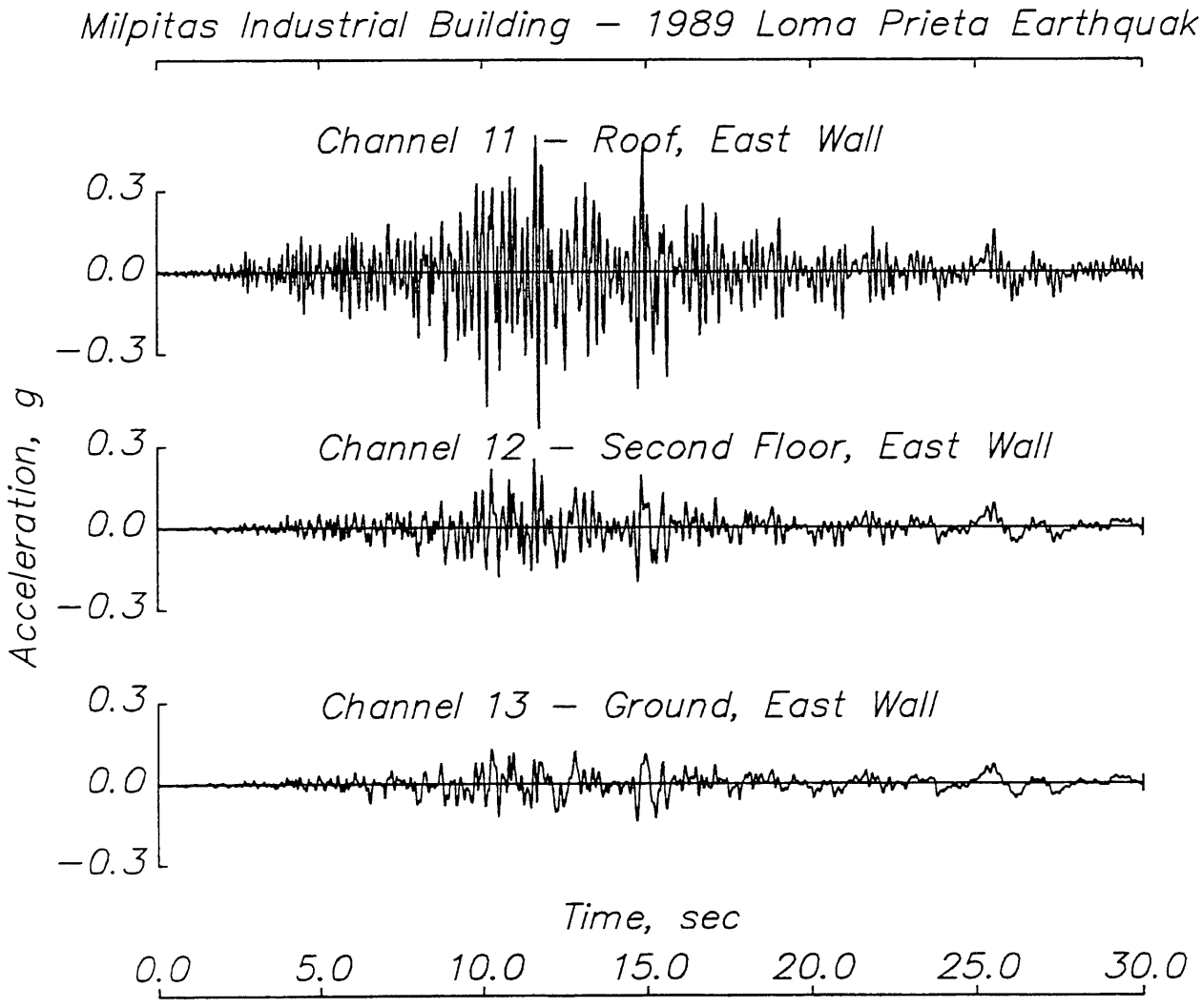

Fig. 5.39 (cont.) Milpitas industrial building – 1989 Loma Prieta earthquake.
(b) Longitudinal acceleration response.

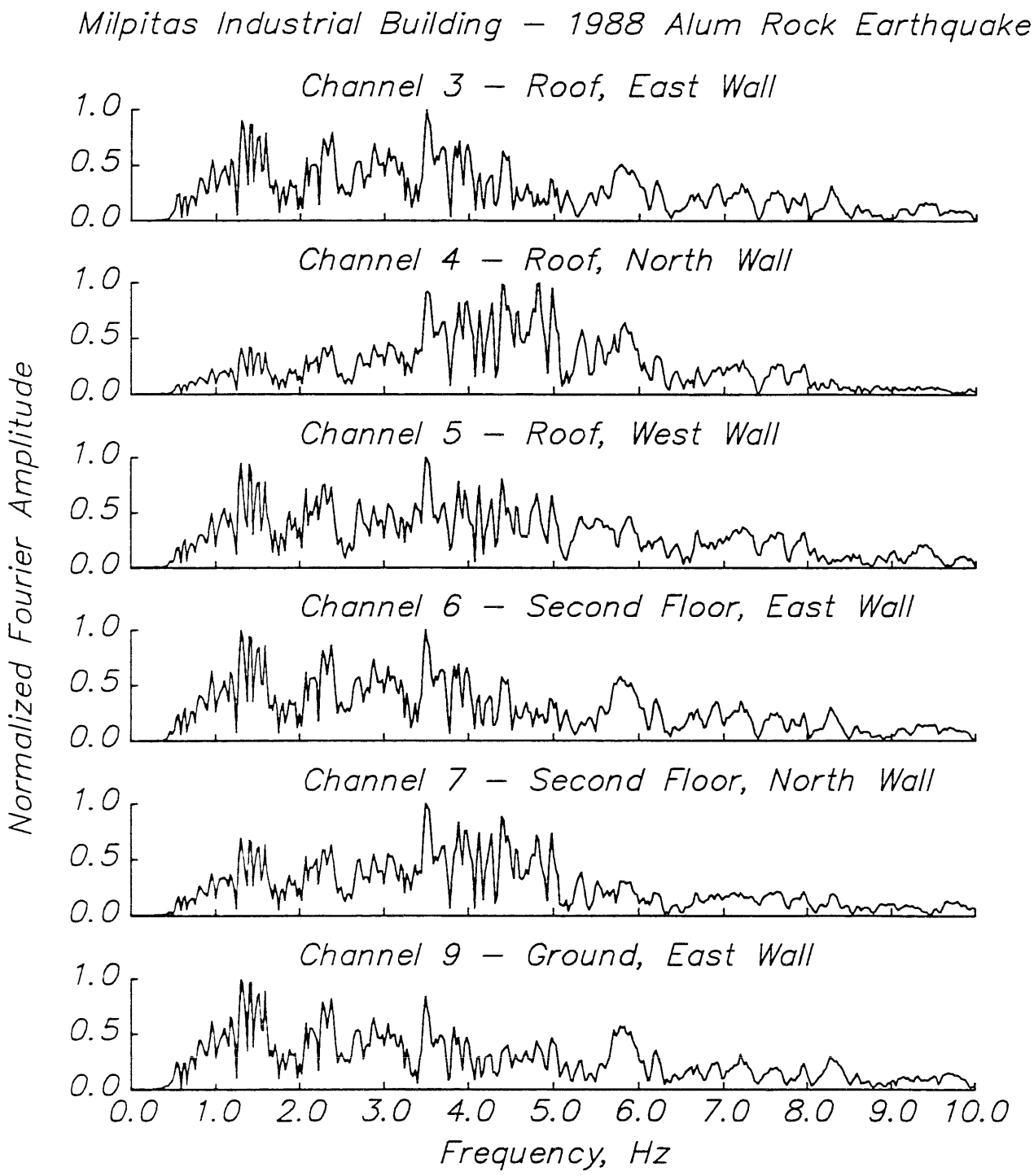

Fig. 5.40 Milpitas industrial building – 1988 Alum Rock earthquake.
(a) Normalized Fourier amplitude spectra of transverse acceleration response.

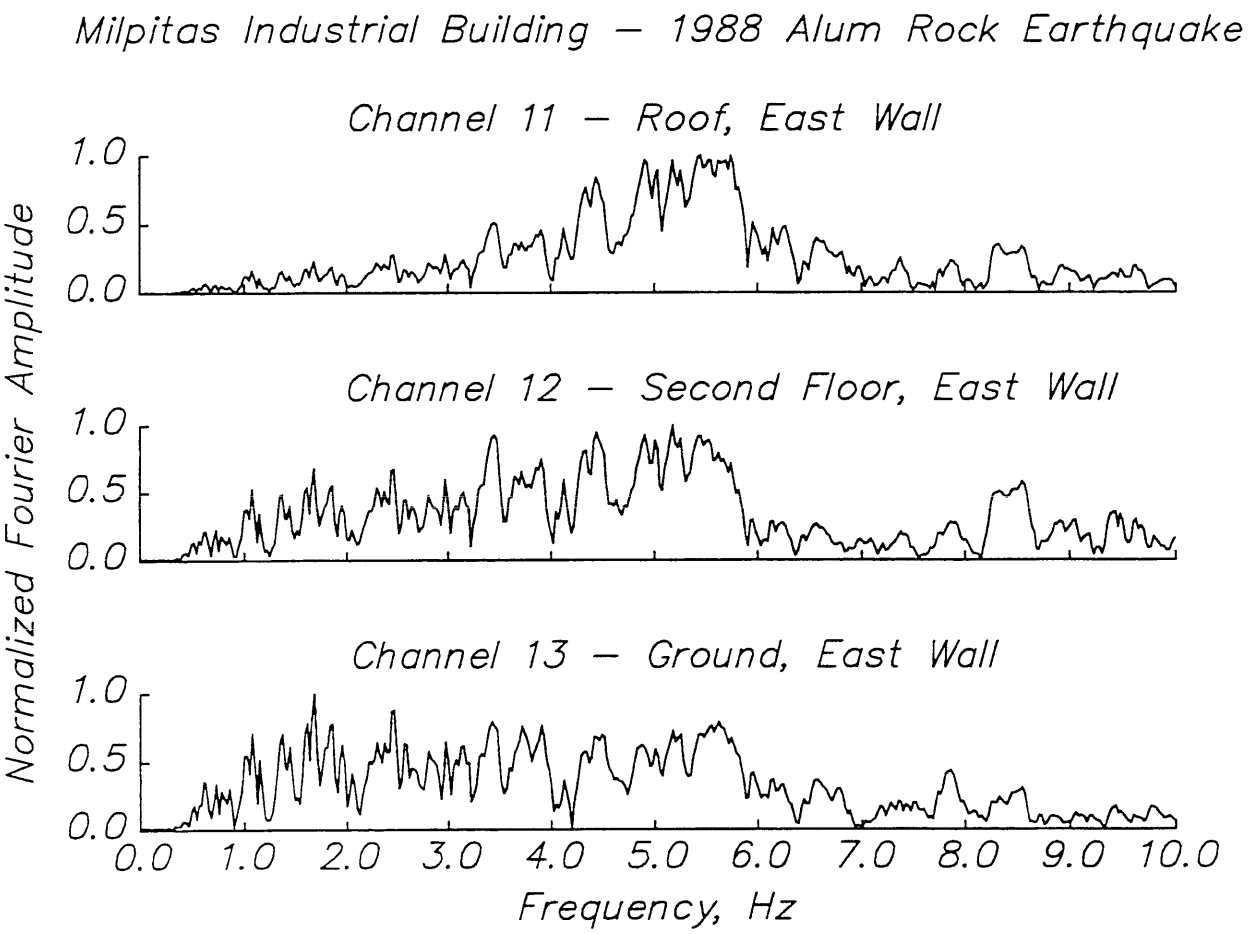

Fig. 5.40 (cont.) Milpitas industrial building – 1988 Alum Rock earthquake.
(b) Normalized Fourier amplitude spectra of longitudinal acceleration response.

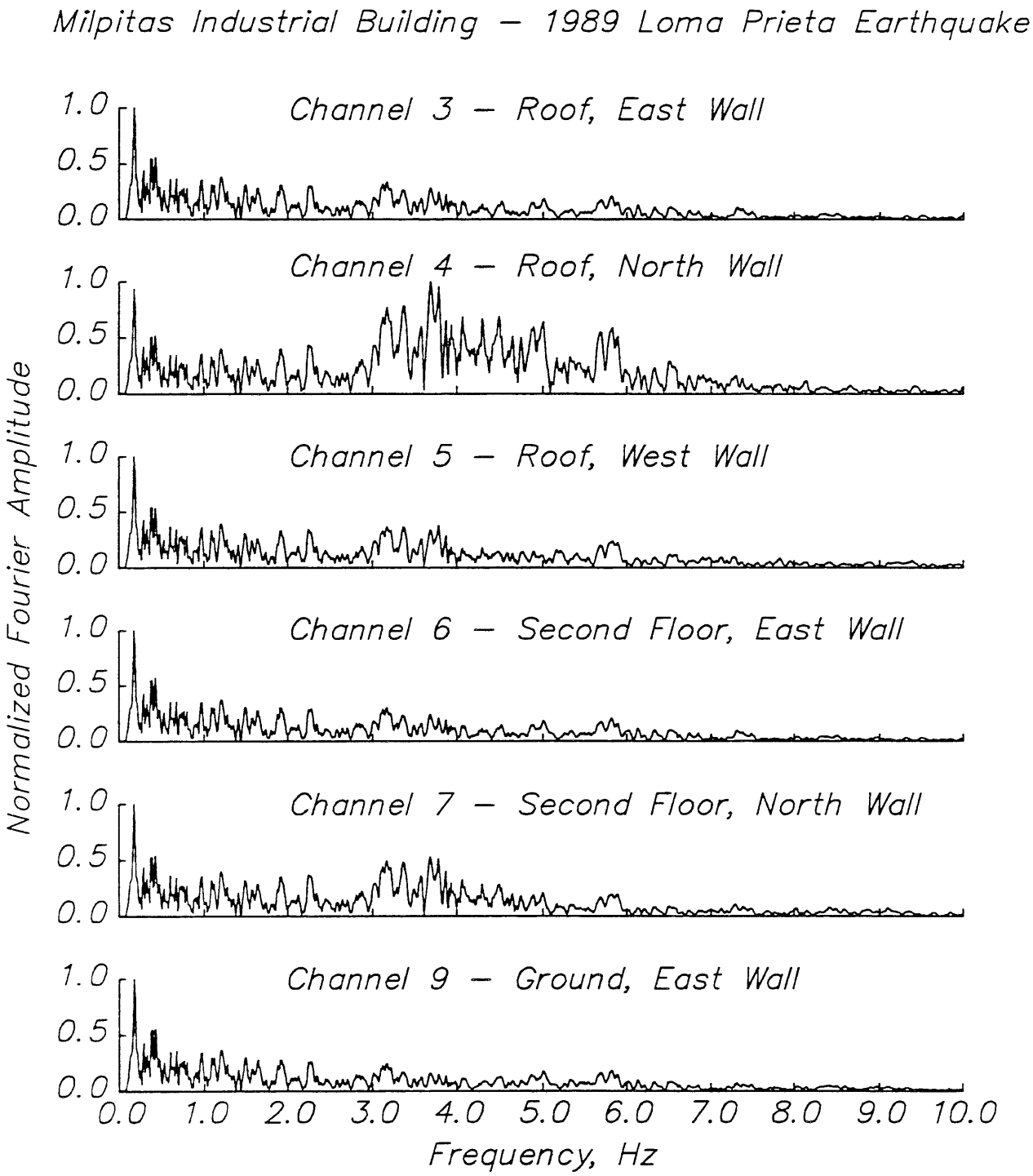

Fig. 5.41 Milpitas industrial building – 1989 Loma Prieta earthquake.
(a) Normalized Fourier amplitude spectra of transverse acceleration response.

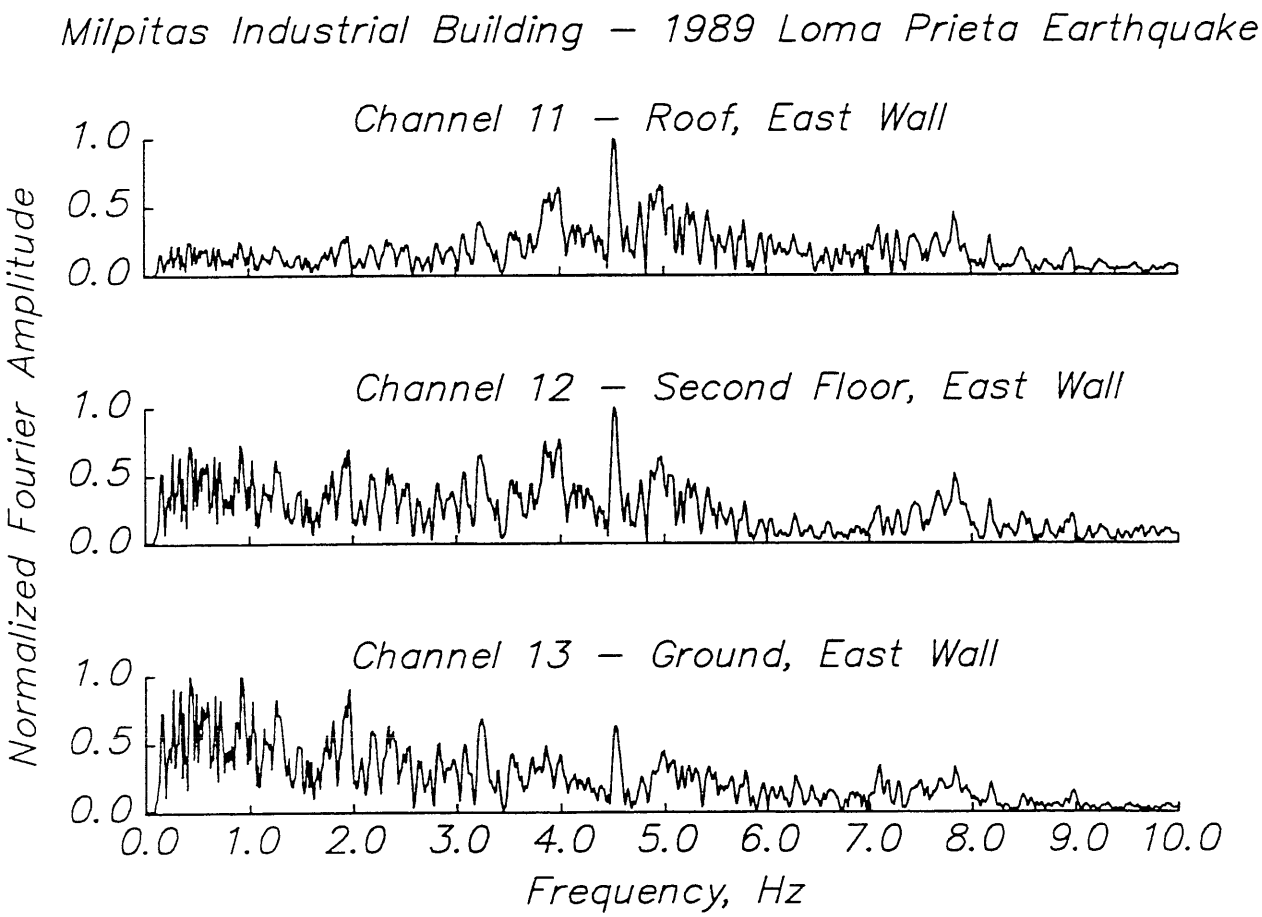

Fig. 5.41 (cont.) Milpitas industrial building – 1989 Loma Prieta earthquake.
(b) Normalized Fourier amplitude spectra of longitudinal acceleration response.

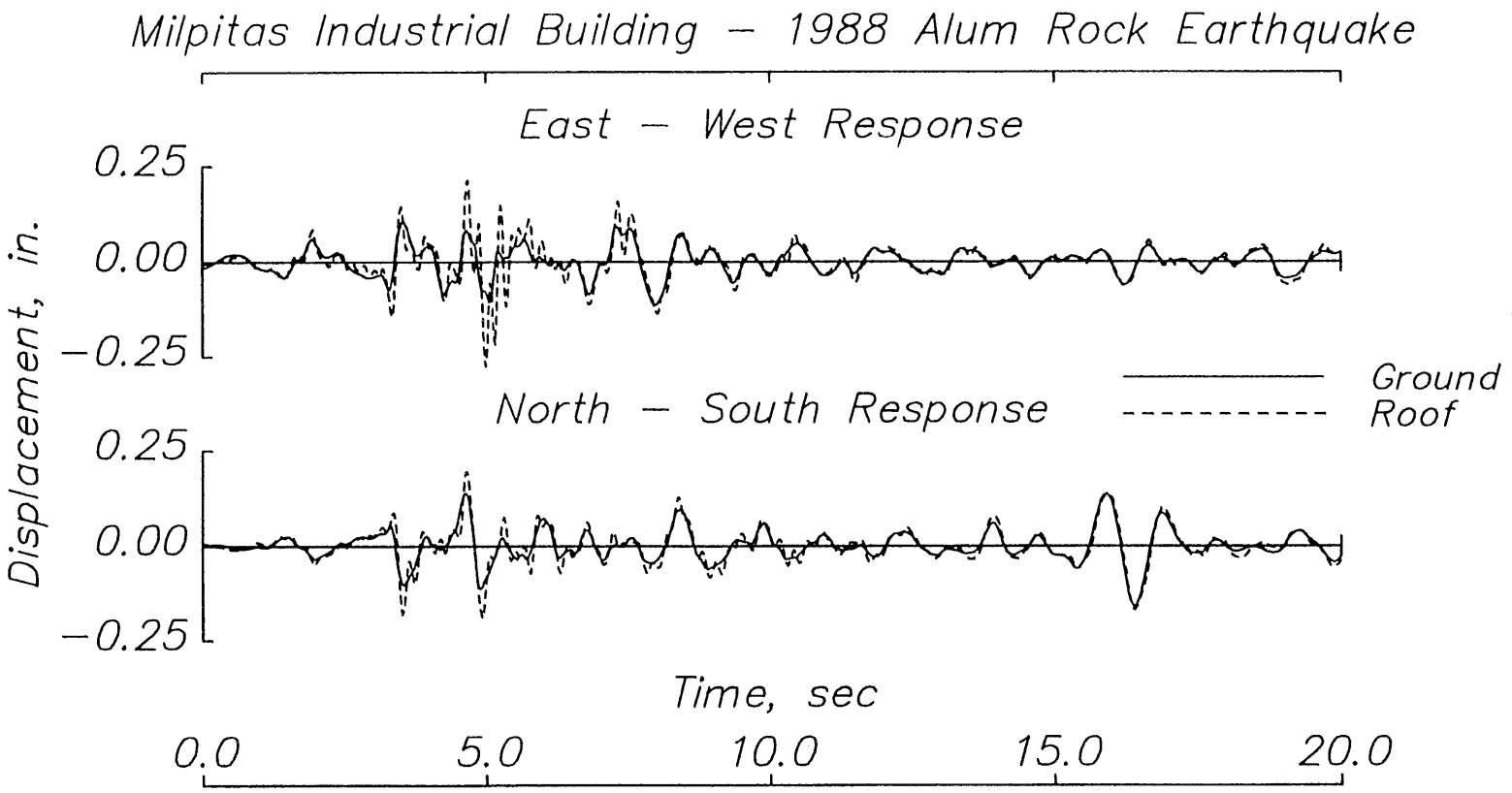

Fig. 5.42 **Milpitas industrial building – Absolute displacement response.**

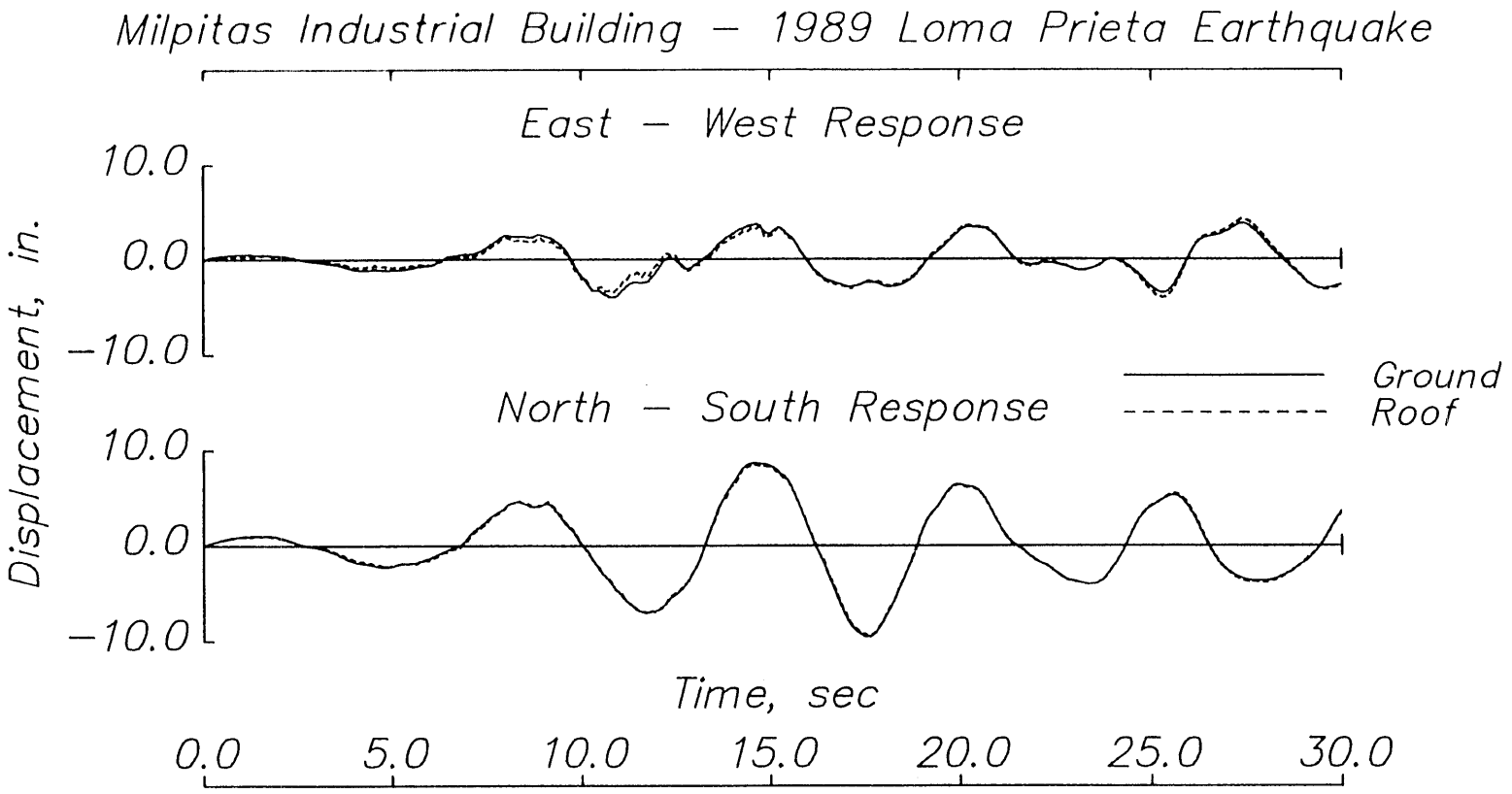

Fig. 5.42 (cont.) Milpitas industrial building – Absolute displacement response.

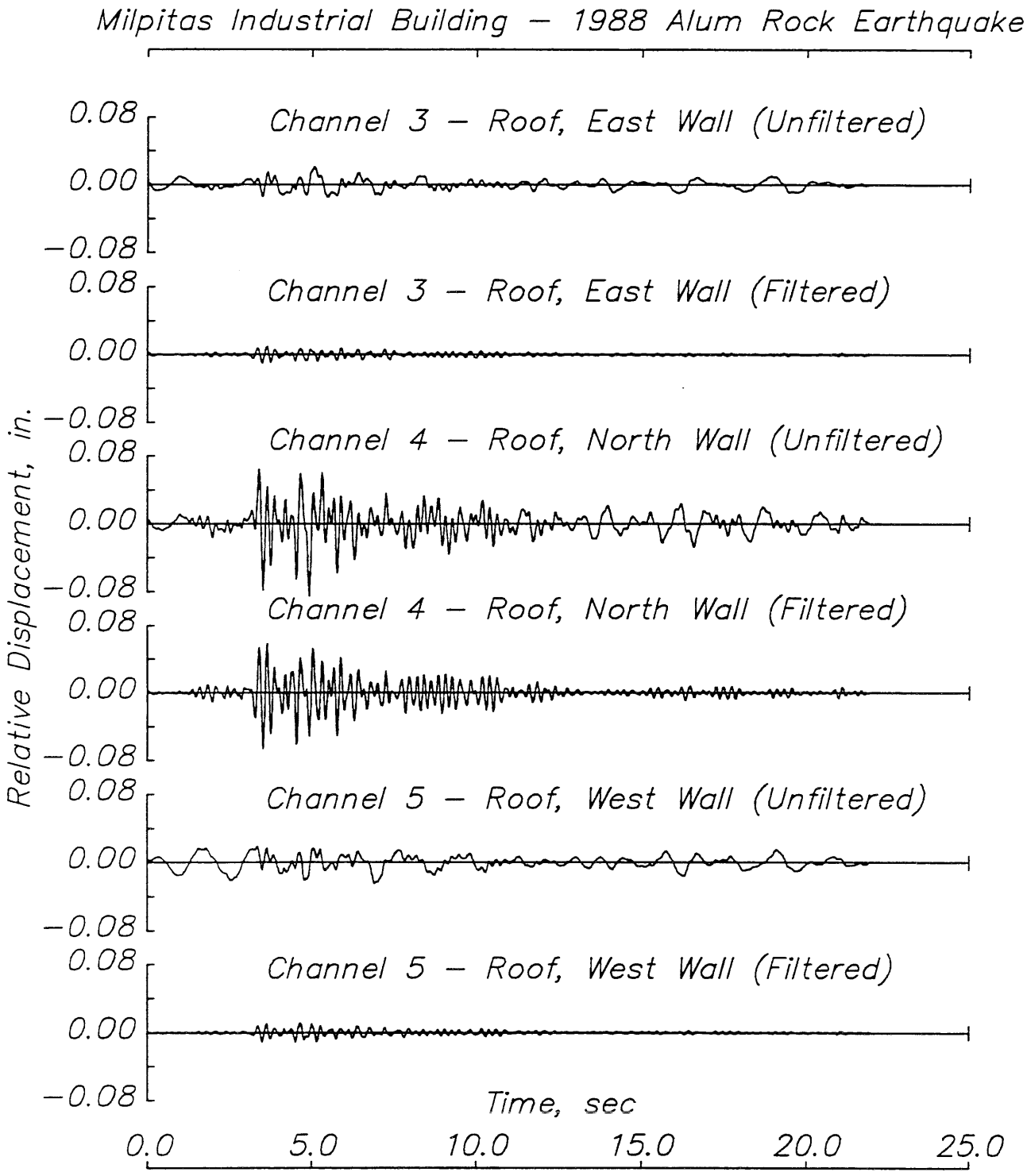

Fig. 5.43 Milpitas industrial building – 1988 Alum Rock earthquake.
(a) Transverse relative displacement response.

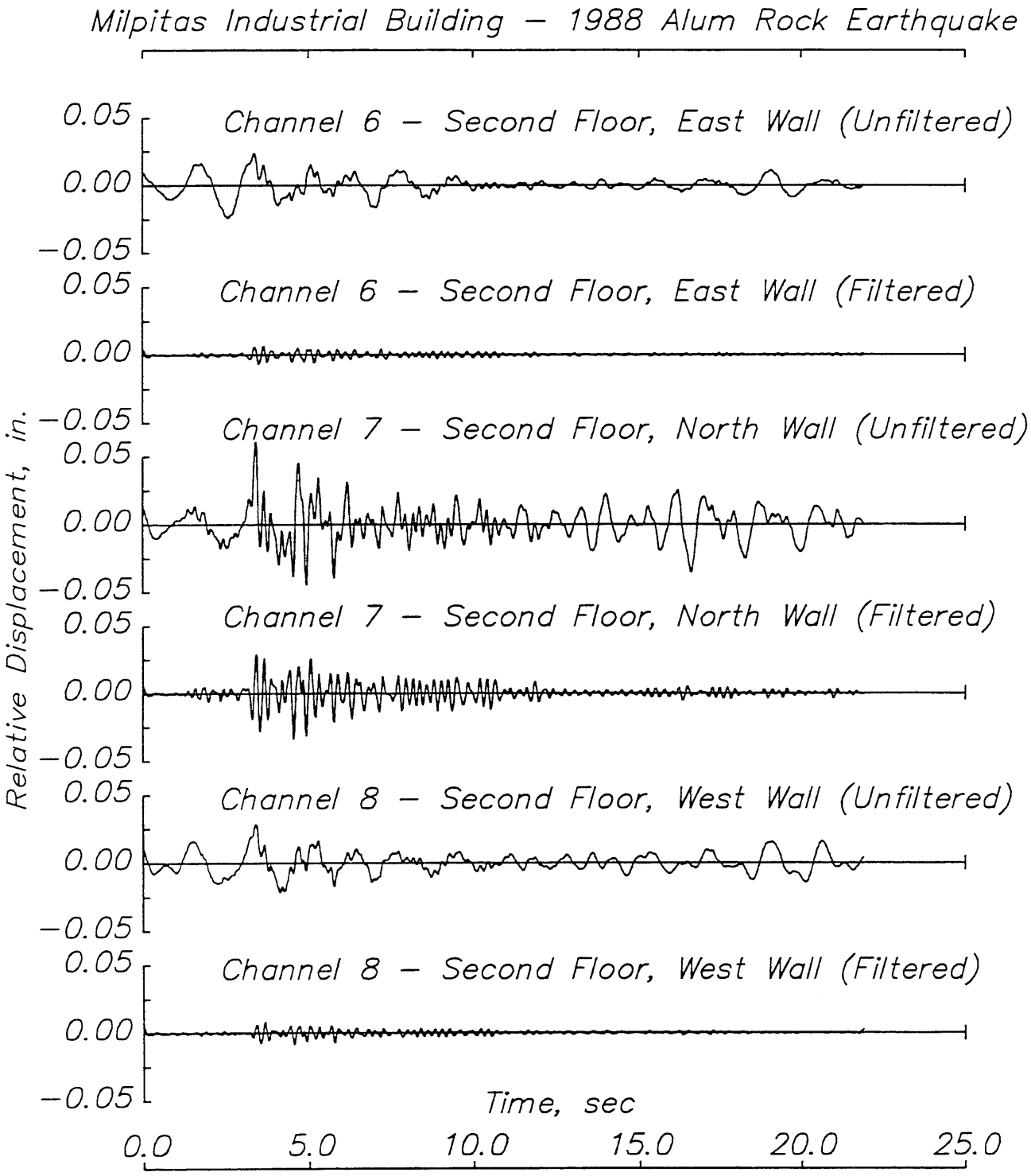

Fig. 5.43 (cont.) Milpitas industrial building – 1988 Alum Rock earthquake.
(a) (cont.) Transverse relative displacement response.

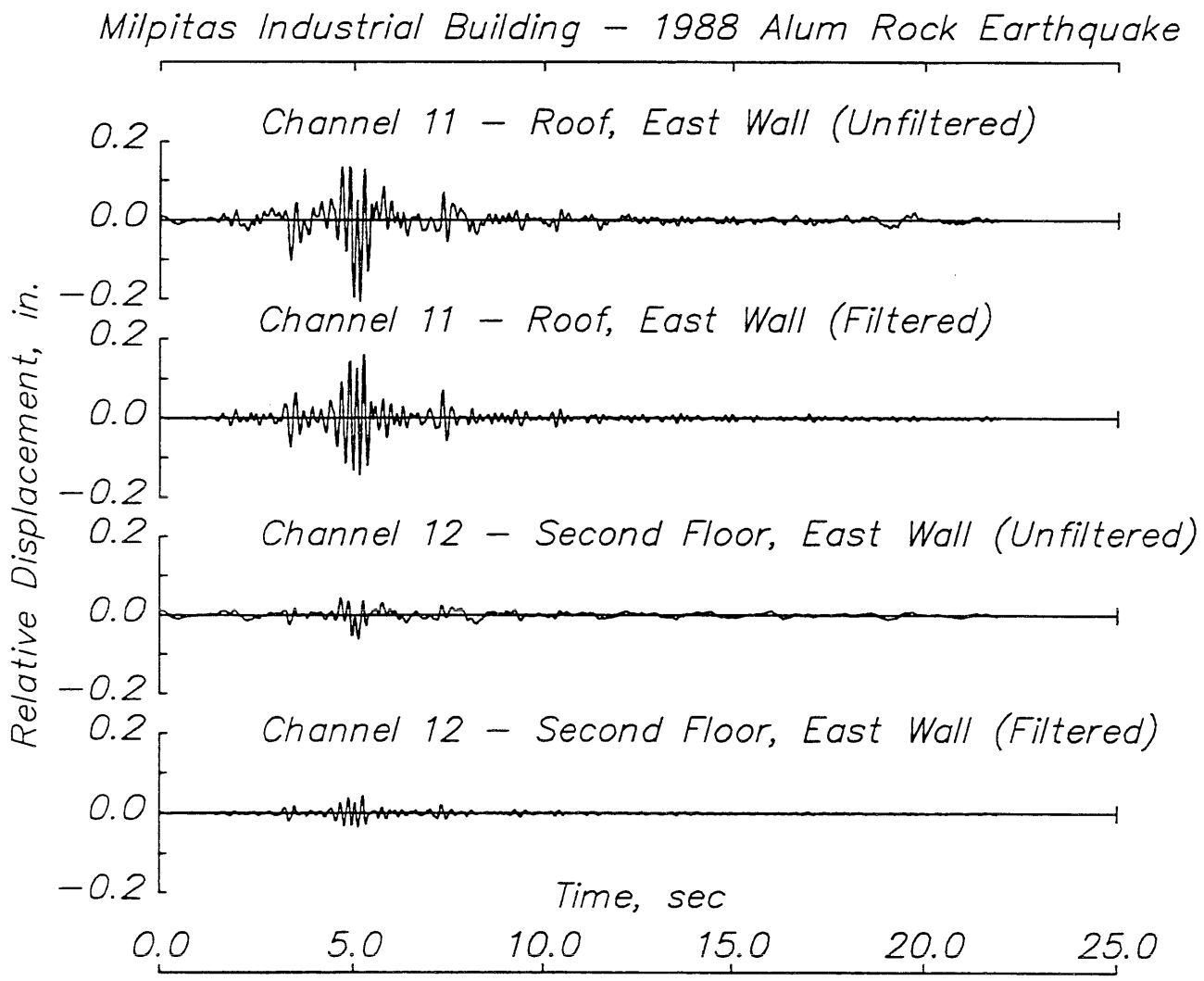

Fig 5.43 (cont.) Milpitas industrial building – 1988 Alum Rock earthquake.
(b) Longitudinal relative displacement response.

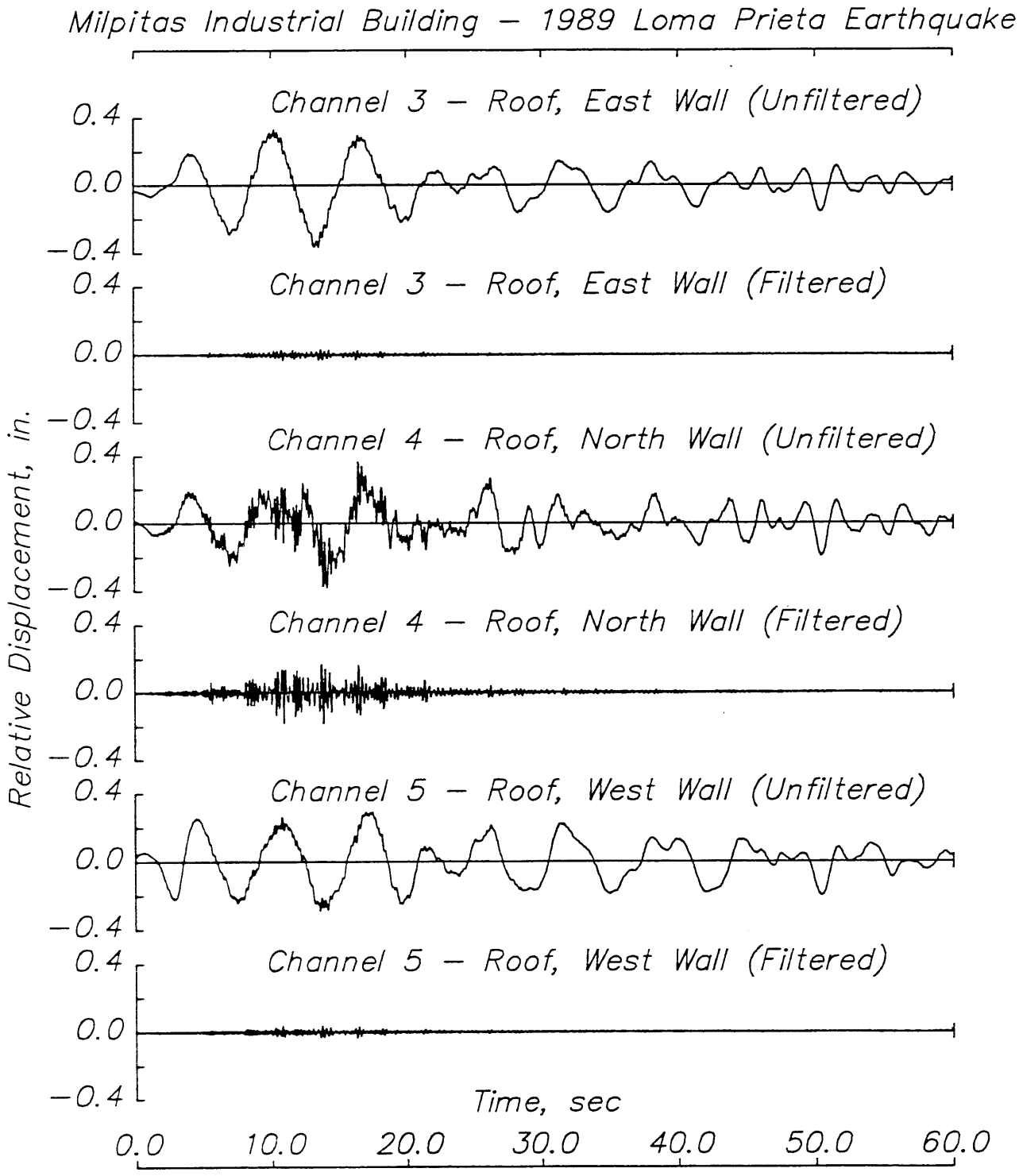

Fig. 5.44 Milpitas industrial building – 1989 Loma Prieta earthquake.
(a) Transverse relative displacement response.

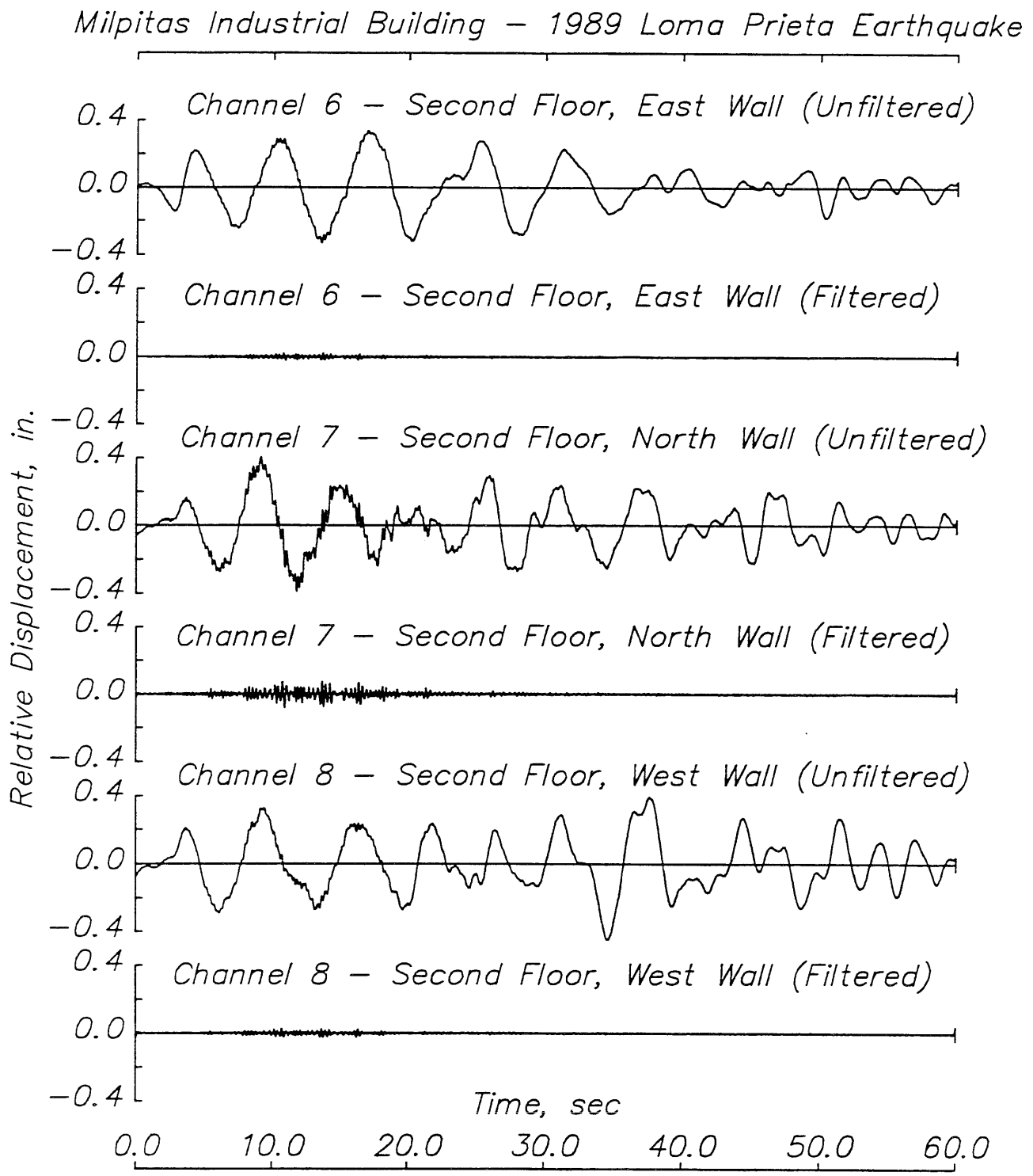

Fig. 5.44 (cont.) Milpitas industrial building – 1989 Loma Prieta earthquake.
(a) (cont.) Transverse relative displacement response.

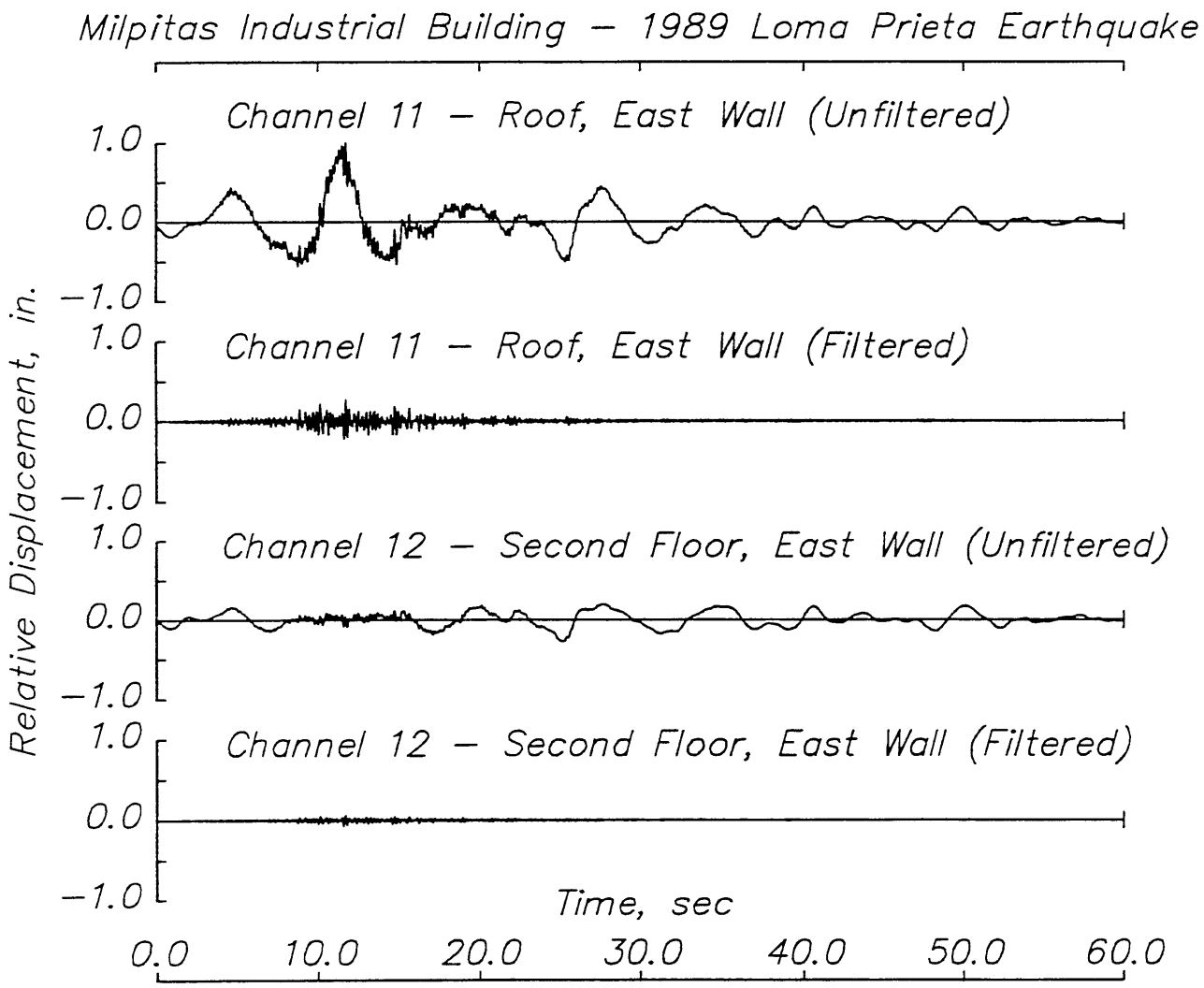

Fig. 5.44 (cont.) Milpitas industrial building – 1989 Loma Prieta earthquake.
(b) Transverse relative displacement response.

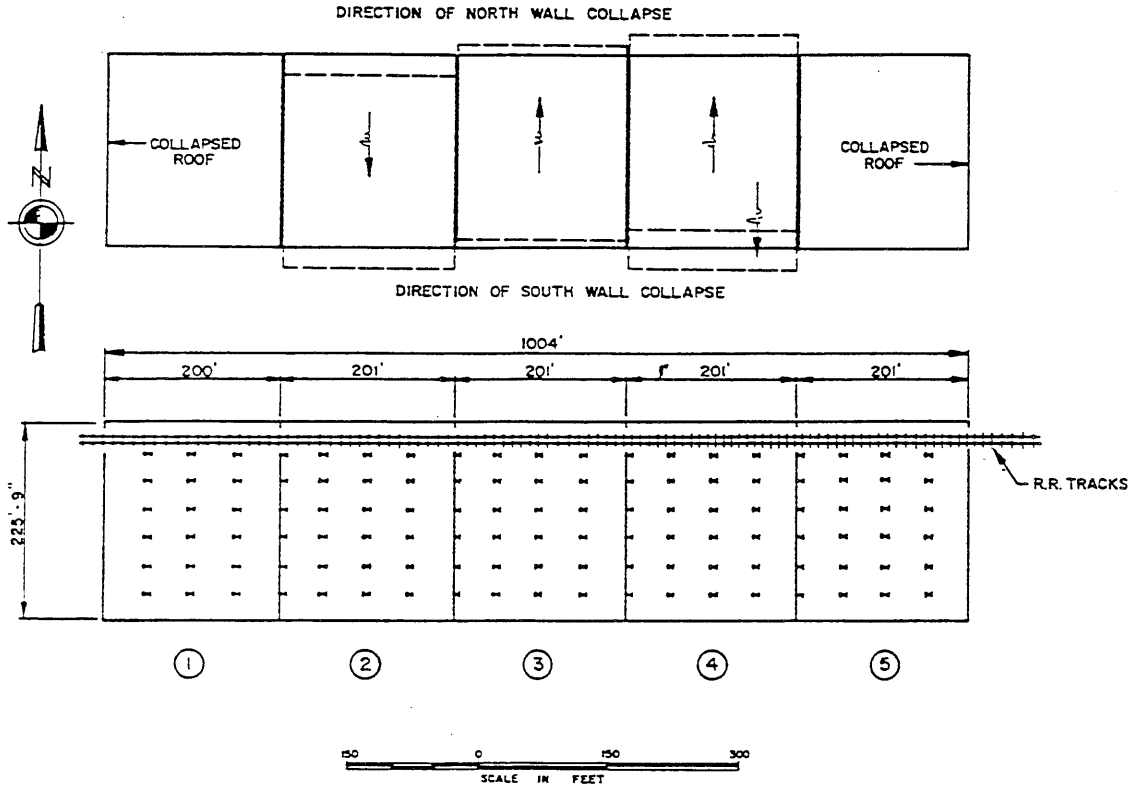

Fig. 6.1 Plan view of Elmendorf Warehouse indicating locations of damage [32].

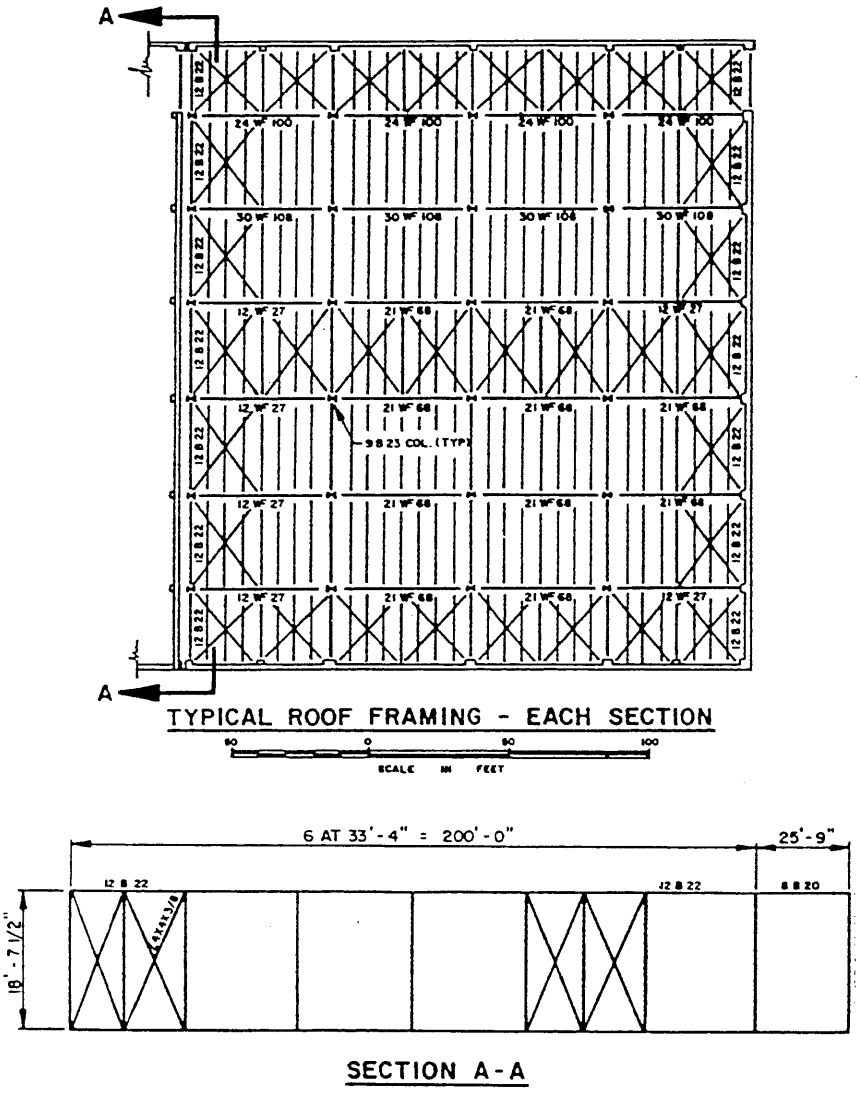

Fig. 6.2 Typical roof framing plan and elevation of fire wall in Elmendorf Warehouse [32].

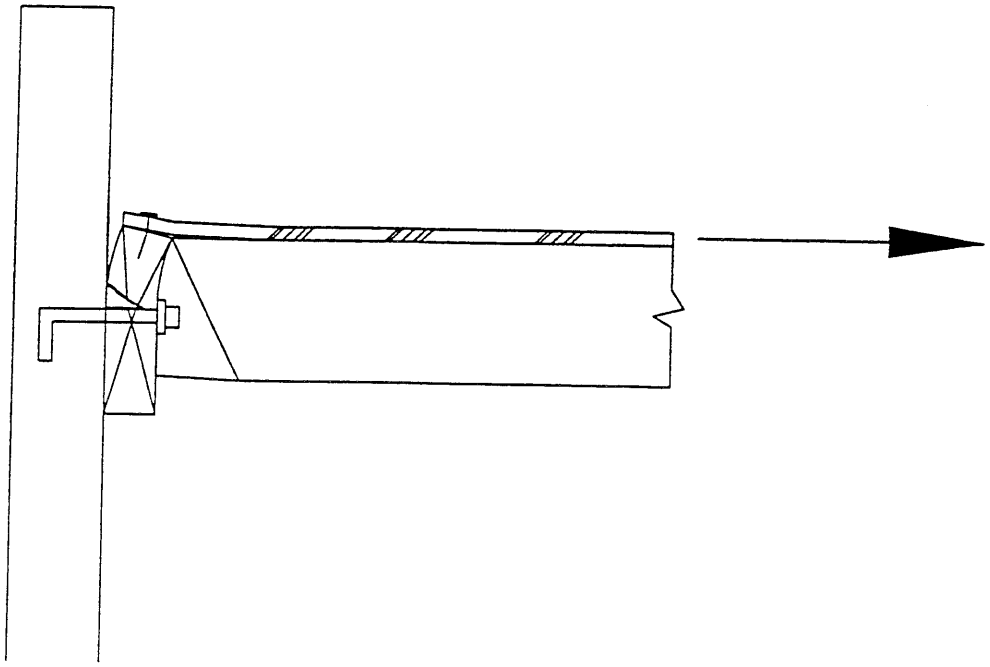

Fig. 6.3 Failure of a wood ledger beam in cross–grain bending.

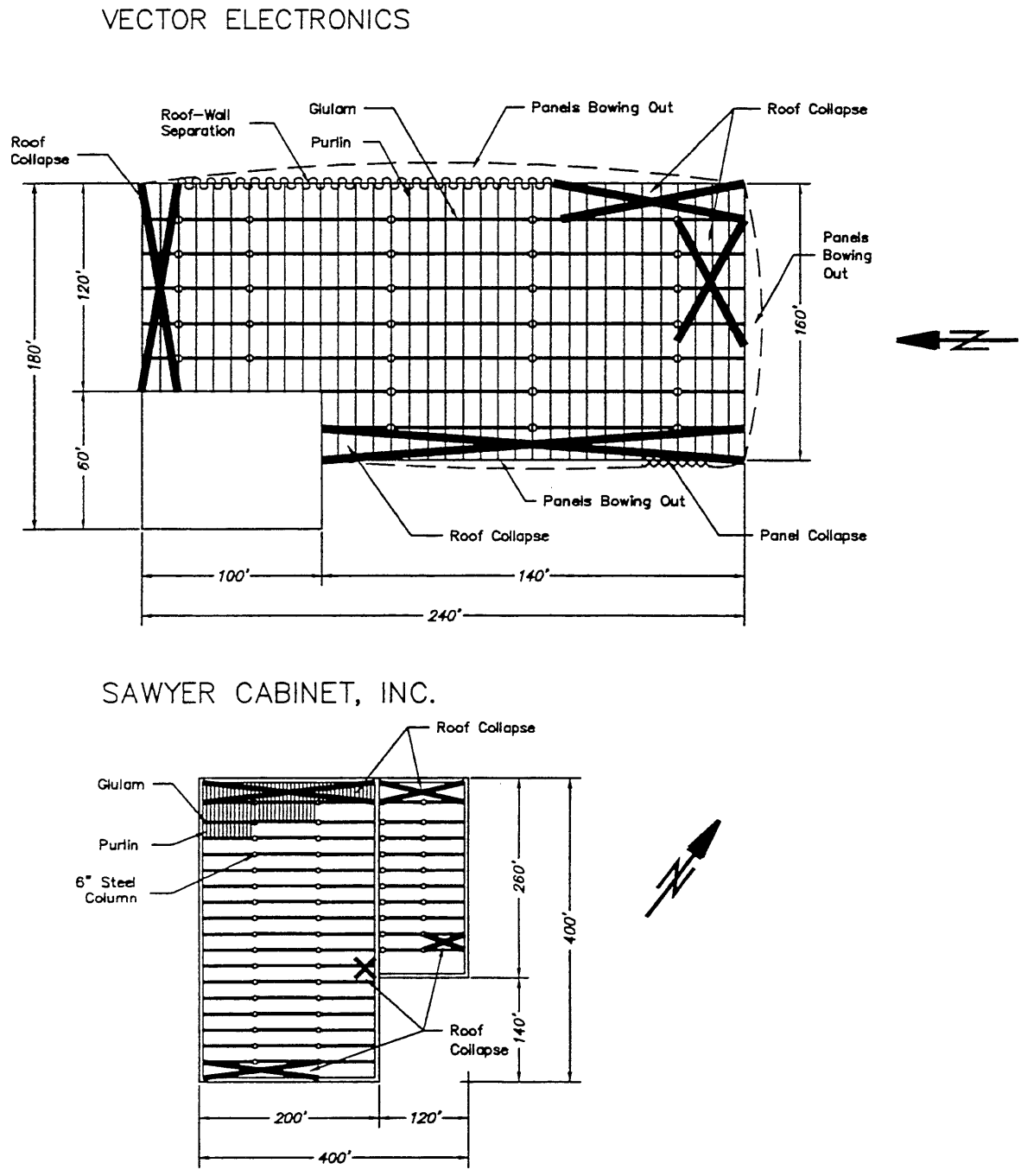

Fig. 6.4 Summary of damage in tilt–up buildings during the 1971 San Fernando earthquake [41,55].

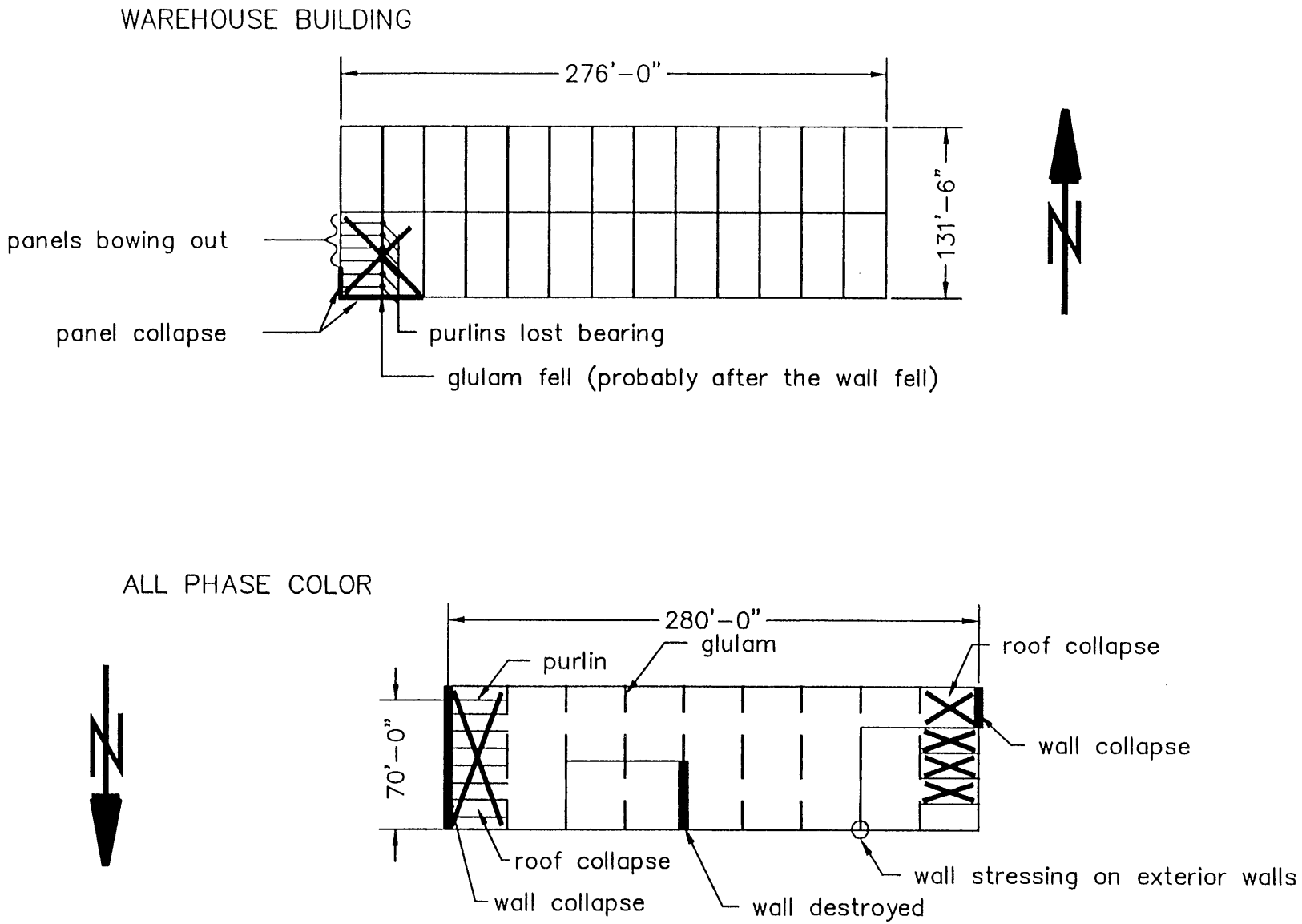

Fig. 6.4 (cont.) Summary of damage in tilt–up buildings during the 1971 San Fernando earthquake [41,55].

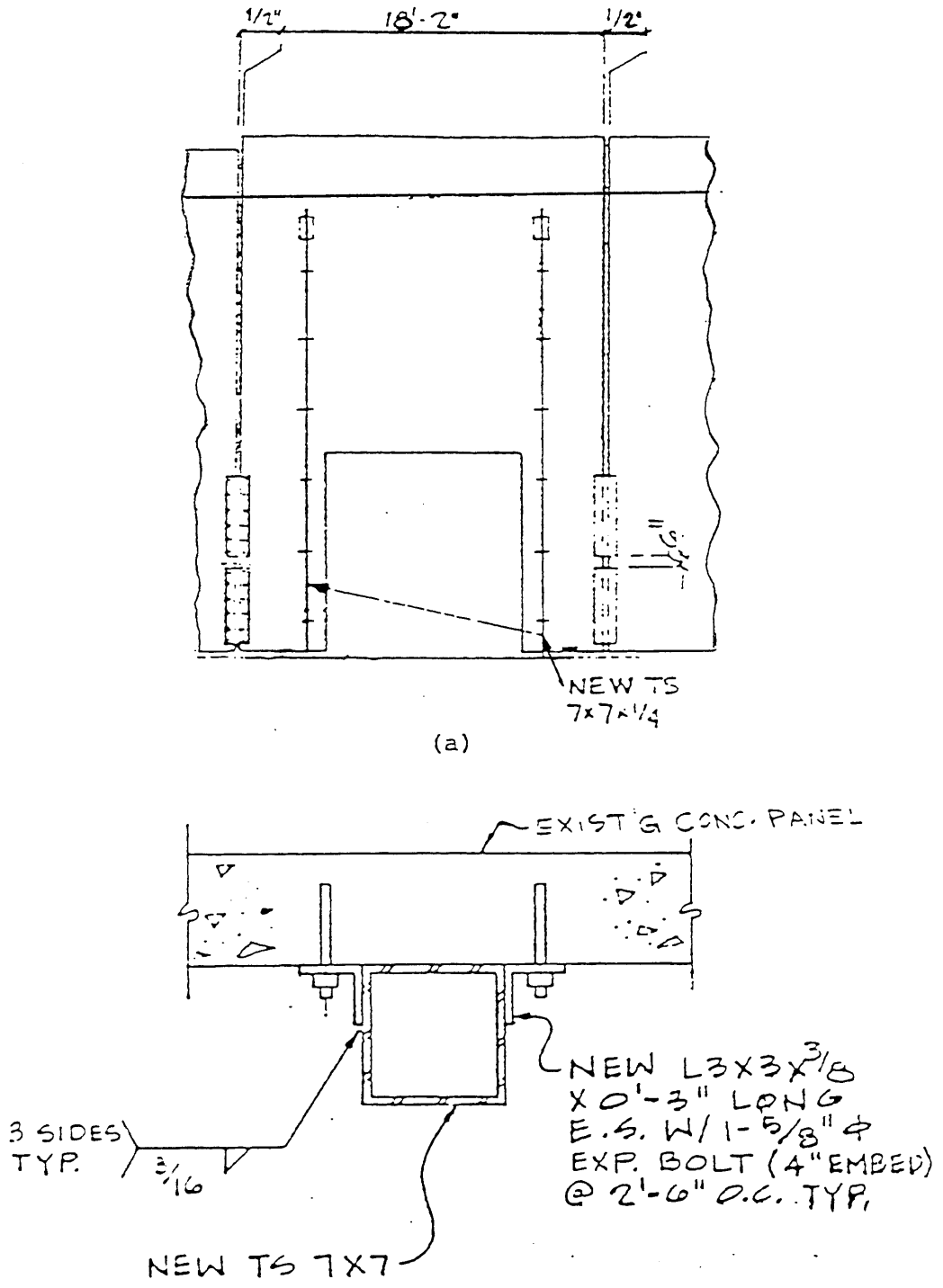

Fig. 6.5 Use of steel kickers to increase the strength and stability of tilt–up panels with large openings [10].

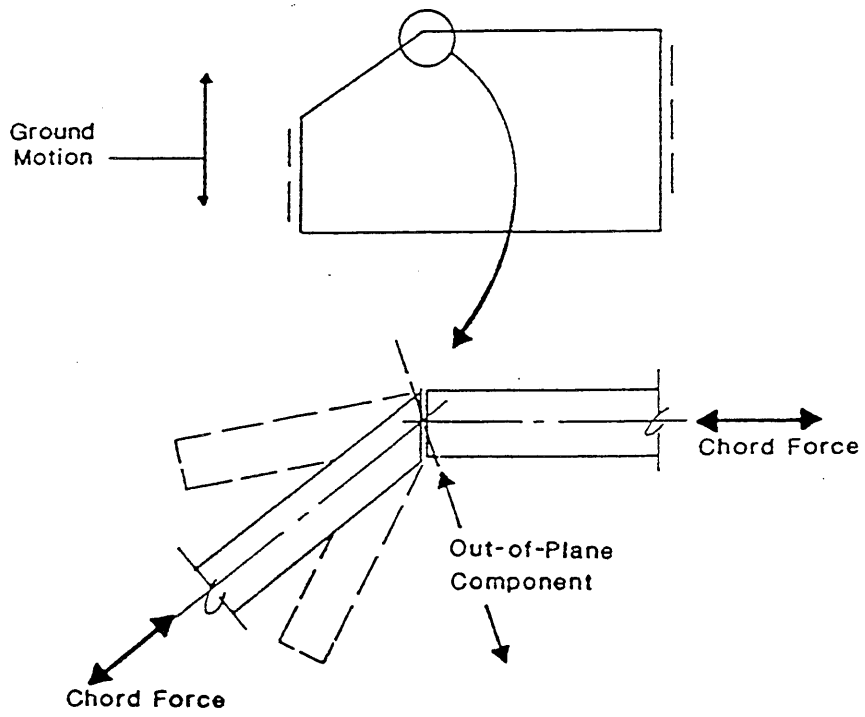

Fig. 6.6 Skewed wall joints [35].

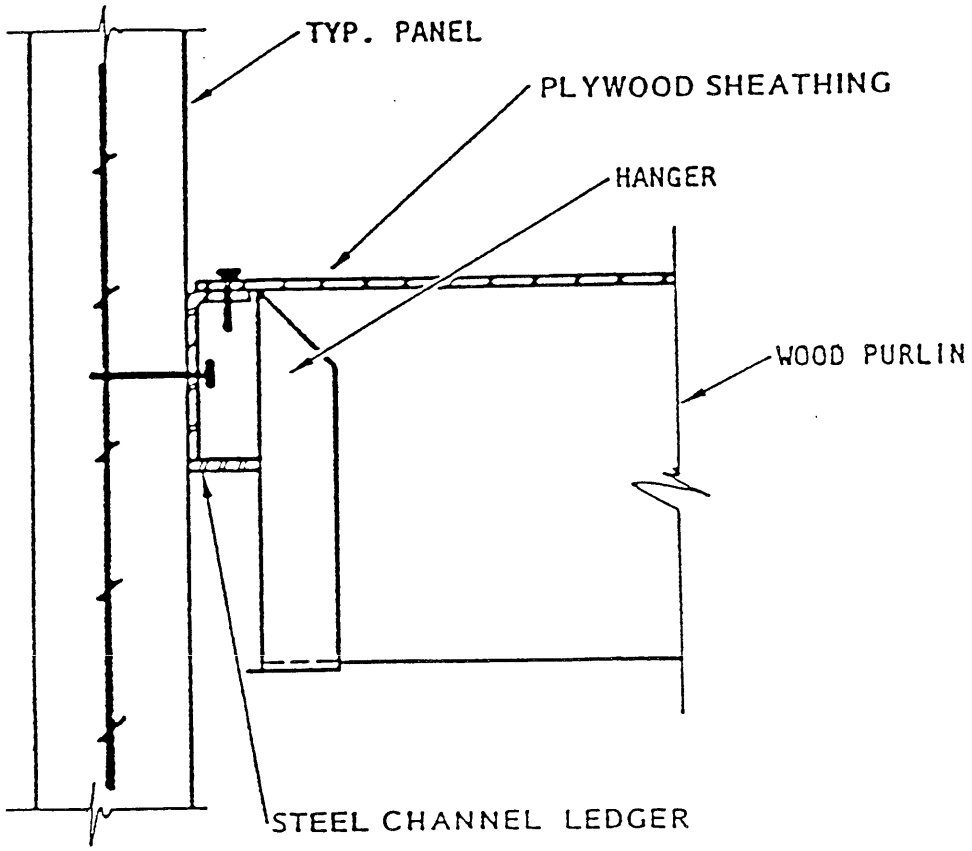

Fig. 6.7 Typical connection between wood purlin and steel ledger [10].

APPENDIX A
SUMMARY OF UBC PROVISIONS

Anchorage of Concrete or Masonry Walls

Sec. 2310. Concrete or masonry walls shall be anchored to all floors and roofs which provide lateral support for the wall. Such anchorage shall provide a positive direct connection capable of resisting the horizontal forces specified in this Chapter or a minimum force of 200 pounds per lineal foot of wall, whichever is greater. Walls shall be designed to resist bending between anchors where the anchor spacing exceeds 4 feet. Required anchors in masonry walls of hollow units or cavity walls shall be embedded in a reinforced grouted structural element of the wall. See Section 2312 (j) 2D and 2312 (j) 3A.

Sec. 2312(j) 2D and 2312(j) 3A

D. **Diaphragms.** Floor and roof diaphragms shall be designed to resist the forces set forth in Table No. 23-J. Diaphragms supporting concrete or masonry walls shall have continuous ties between diaphragm chords to distribute, into the diaphragm, the anchorage forces specified in this Chapter. Added chords may be used to form sub-diaphragms to transmit the anchorage forces to the main cross ties. Diaphragm deformations shall be considered in the design of the supported walls. See Section 2312 (j) 3 A for special anchorage requirements of wood diaphragms.

3. **Special requirements.** A. **Wood diaphragms providing lateral support for concrete or masonry walls.** Where wood diaphragms are used to laterally support concrete or masonry walls the anchorage shall conform to Section 2310. In Zones No. 2, No. 3 and No. 4 anchorage shall not be accomplished by use of toe nails, or nails subjected to withdrawal; nor shall wood framing be used in cross grain bending or cross grain tension.

B. **Pile caps and caissons.** Individual pile caps and caissons of every building or structure shall be interconnected by ties, each of which can carry by tension and compression a minimum horizontal force equal to 10 percent of the larger pile cap or caisson loading, unless it can be demonstrated that equivalent restraint can be provided by other approved methods.

C. **Exterior elements.** Precast, nonbearing, nonshear wall panels or similar elements which are attached to or enclose the exterior, shall accommodate movements of the structure resulting from lateral forces or temperature changes. The concrete panels or other elements shall be supported by means of cast-in-place concrete or by mechanical fasteners in accordance with the following provisions.

Connections and panel joints shall allow for a relative movement between stories of not less than two times story drift caused by wind or (3.0 K) times story drift caused by required seismic forces; or ¼ inch, whichever is greater.

Connections shall have sufficient ductility and rotation capacity so as to preclude fracture of the concrete or brittle failures at or near welds. Inserts in concrete shall be attached to, or hooked around reinforcing steel, or otherwise terminated so as to effectively transfer forces to the reinforcing steel

Connections to permit movement in the plane of the panel for story drift shall be properly designed sliding connections using slotted or oversize holes or may be connections which permit movement by bending of steel or other connections providing equivalent sliding and ductility capacity.

TABLE NO. 23-J—HORIZONTAL FORCE FACTOR "C_p" FOR ELEMENTS OF STRUCTURES

PART OR PORTION OF BUILDINGS	DIRECTION OF FORCE	VALUE OF C_p
1. Exterior bearing and nonbearing walls, interior bearing walls and partitions, interior nonbearing walls and partitions. Masonry or concrete fences	Normal to flat surface	0.20[1]
2. Cantilever parapet	Normal to flat surface	1.00
3. Exterior and interior ornamentations and appendages.	Any direction	1.00
4. When connected to, part of, or housed within a building: a. Towers, tanks, towers and tanks plus contents, chimneys, smokestacks and penthouse	Any direction	0.20[2]
b. Storage racks with the upper storage level at more than 8 feet in height plus contents		0.20[2,3]
c. Equipment or machinery not required for life safety systems or for continued operations of essential facilities		0.20[2,4]
d. Equipment or machinery required for life safety systems or for continued operation of essential facilities		0.50[4,5]
5. When resting on the ground, tank plus effective mass of its contents.	Any direction	0.12
6. Suspended ceiling framing systems (Applies to Seismic Zones Nos. 2, 3 and 4 only)	Any direction	0.20[6]
7. Floors and roofs acting as diaphragms	Any direction	0.12[7]
8. Connections for exterior panels or for elements complying with Section 2312 (j) 3C.	Any direction	2.00
9. Connections for prefabricated structural elements other than walls, with force applied at center of gravity of assembly	Any direction	0.30[8]

[1] See also Section 2309 (b) for minimum load on deflection criteria for interior partitions.

[2] When located in the upper portion of any building where the h_n/D ratio is five-to-one or greater the value shall be increased by 50 percent.

[3] W_p for storage racks shall be the weight of the racks plus contents. The value of C_p for racks over two storage support levels in height shall be 0.16 for the levels below the top two levels. In lieu of the tabulated values steel storage racks may be designed in accordance with U.B.C. Standard No. 27-11.

Where a number of storage rack units are interconnected so that there are a minimum of four vertical elements in each direction on each column line designed to resist horizontal forces, the design coefficients may be as for a building with K values from Table No. 23-I, $CS = 0.20$ for use in the formula $V = ZIKCSW$ and W equal to the total dead load plus 50 percent of the rack rated capacity. Where the design and rack configurations are in accordance with this paragraph the design provisions in U.B.C. Standard No. 27-11 do not apply.

[4] For flexible and flexibly mounted equipment and machinery, the appropriate values of C_p shall be determined with consideration given to both the dynamic properties of the equipment and machinery and to the building or structure in which it is placed but shall not be less than the listed values. The design of the equipment and machinery and their anchorage is an integral part of the design and specification of such equipment and machinery.

[5] For Essential Facilities and life safety systems, the design and detailing of equipment which must remain in place and be functional following a major earthquake shall consider drifts in accordance with Section 2312 (k). The product of IS need not exceed 1.5.

[6] Ceiling weight shall include all light fixtures and other equipment which are laterally supported by the ceiling. For purposes of determining the lateral force, a ceiling weight of not less than 4 pounds per square foot shall be used.

[7] Floors and roofs acting as diaphragms shall be designed for a minimum force resulting from a C_p of 0.12 applied to w_x unless a greater force results from the distribution of lateral forces in accordance with Section 2312 (e).

[8] The W_p shall include 25 percent of the floor live load in storage and warehouse occupancies.

Anchorage of Concrete or Masonry Walls

Sec. 2310. Concrete or masonry walls shall be anchored to all floors, roofs and other structural elements which provide required lateral support for the wall. Such anchorage shall provide a positive direct connection capable of resisting the horizontal forces specified in this chapter or a minimum force of 200 pounds per lineal foot of wall, whichever is greater. Walls shall be designed to resist bending between anchors where the anchor spacing exceeds 4 feet. Required anchors in masonry walls of hollow units or cavity walls shall be embedded in a reinforced grouted structural element of the wall. See Sections 2336, 2337 (b) 8 and 9.

Lateral Force on Elements of Structures and Nonstructural Components Supported by Structures

Sec. 2336. (a) **General.**

(b) **Design for Total Lateral Force.** The total design lateral seismic force, F_p, shall be determined from the following formula:

$$F_p = ZIC_pW_p \qquad (36\text{-}1)$$

The values of Z and I shall be the values used for the building.

EXCEPTIONS: 1. For anchorage of machinery and equipment required for life-safety systems, the value of I shall be taken as 1.5.

2. For the design of tanks and vessels containing sufficient quantities of highly toxic or explosive substances to be hazardous to the safety of the general public if released, the value of I shall be taken as 1.5.

3. The value of I for panel connectors for panels in Section 2337 (b) 4 C shall be 1.0 for the entire connector.

The coefficient C_p is for elements and components and for rigid and rigidly supported equipment. Rigid or rigidly supported equipment is defined as having a fundamental period less than or equal to 0.06 second. Nonrigid or flexibly supported equipment is defined as a system having a fundamental period, including the equipment, greater than 0.06 second.

The lateral forces calculated for nonrigid or flexibly supported equipment supported by a structure and located above grade shall be determined considering the dynamic properties of both the equipment and the structure which supports it, but the value shall not be less than that listed in Table No. 23-P. In the absence of an analysis or empirical data, the value of C_p for nonrigid or flexibly supported equipment located above grade on a structure shall be taken as twice the value listed in Table No. 23-P, but need not exceed 2.0.

EXCEPTION: Piping, ducting and conduit systems which are constructed of ductile materials and connections may use the values of C_p from Table No. 23-P.

The value of C_p for elements, components and equipment laterally self-supported at or below ground level may be two thirds of the value set forth in Table No. 23-P. However, the design lateral forces for an element or component or piece of equipment shall not be less than would be obtained by treating the item as an independent structure and using the provisions of Section 2338.

The design lateral forces determined using Formula (36-1) shall be distributed in proportion to the mass distribution of the element or component.

Forces determined using Formula (36-1) shall be used to design members and connections which transfer these forces to the seismic-resisting systems.

For applicable forces in connectors for exterior panels and diaphragms, refer to Section 2337 (b) 4 and 9.

Forces shall be applied in the horizontal directions, which result in the most critical loadings for design.

(b) **Structural Framing Systems.** 1. **General.** Four types of general building framing systems defined in Section 2333 (f) are recognized in these provisions and shown in Table No. 23-O. Each type is subdivided by the types of vertical elements used to resist lateral seismic forces. Special framing requirements are given in this section and in Chapters 24 through 27.

2. **Detailing for combinations of systems.** For components common to different structural systems, the more restrictive detailing requirements shall be used.

3. **Connections.** Connections which resist seismic forces shall be designed and detailed on the drawings.

4. **Deformation compatibility.** All framing elements not required by design to be part of the lateral force-resisting system shall be investigated and shown to be adequate for vertical load-carrying capacity when displaced $3(R_w/8)$ times the displacements resulting from the required lateral forces. $P\Delta$ effects on such elements shall be accounted for. For designs using working stress methods, this capacity may be determined using an allowable stress increase of 1.7. The rigidity of adjoining rigid and exterior elements shall be considered as follows:

A. **Adjoining rigid elements.** Moment-resistant frames may be enclosed by or adjoined by more rigid elements which would tend to prevent the frame from resisting lateral forces where it can be shown that the action or failure of the more rigid elements will not impair the vertical and lateral load-resisting ability of the frame.

B. **Exterior elements.** Exterior nonbearing, nonshear wall panels or elements which are attached to or enclose the exterior shall be designed to resist the forces per Formula (36-1) and shall accommodate movements of the structure resulting from lateral forces or temperature changes. Such elements shall be supported by means of cast-in-place concrete or by mechanical connections and fasteners in accordance with the following provisions:

(i) Connections and panel joints shall allow for a relative movement between stories of not less than two times story drift caused by wind, $3(R_w/8)$ times the calculated elastic story drift caused by design seismic forces, or $^1/_2$ inch, whichever is greater.

(ii) Connections to permit movement in the plane of the panel for story drift shall be sliding connections using slotted or oversize holes, connections which permit movement by bending of steel, or other connections providing equivalent sliding and ductility capacity.

(iii) Bodies of connections shall have sufficient ductility and rotation capacity so as to preclude fracture of the concrete or brittle failures at or near welds.

(iv) The body of the connection shall be designed for one and one-third times the force determined by Formula (36-1).

(v) All fasteners in the connecting system such as bolts, inserts, welds and dowels shall be designed for four times the forces determined by Formula (36-1).

(vi) Fasteners embedded in concrete shall be attached to, or hooked around, reinforcing steel or otherwise terminated so as to effectively transfer forces to the reinforcing steel.

5. **Ties and continuity.** All parts of a structure shall be interconnected and the connections shall be capable of transmitting the seismic force induced by the parts being connected. As a minimum, any smaller portion of the building shall be tied to the remainder of the building with elements having at least a strength to resist $\frac{Z}{3}$ times the weight of the smaller portion.

A positive connection for resisting a horizontal force acting parallel to the member shall be provided for each beam, girder or truss. This force shall not be less than $\frac{Z}{5}$ times the dead plus live load.

6. **Collector elements.** Collector elements shall be provided which are capable of transferring the seismic forces originating in other portions of the building to the element providing the resistance to those forces.

7. **Concrete frames.** Concrete frames required by design to be part of the lateral force-resisting system shall conform to the following:

A. In Seismic Zones Nos. 3 and 4 they shall be special moment-resisting frames.

B. In Seismic Zone No. 2 they shall, as a minimum, be intermediate moment-resisting frames.

8. **Anchorage of concrete or masonry walls.** Concrete or masonry walls shall be anchored to all floors and roofs which provide lateral support for the wall. The anchorage shall provide a positive direct connection between the wall and floor or roof construction capable of resisting the horizontal forces specified in Section 2336 or Section 2310. Requirements for developing anchorage forces in diaphragms are given in Section 2337 (b) 9 below. Diaphragm deformation shall be considered in the design of the supported walls.

9. **Diaphragms.**

A. The deflection in the plane of the diaphragm shall not exceed the permissible deflection of the attached elements. Permissible deflection shall be that deflection which will permit the attached element to maintain its structural integrity under the individual loading and continue to support the prescribed loads.

B. Floor and roof diaphragms shall be designed to resist the forces determined in accordance with the following formula:

$$F_{px} = \frac{F_t + \sum_{i=x}^{n} F_i}{\sum_{i=x}^{n} w_i} \, w_{px} \qquad (37\text{-}1)$$

The force F_{px} determined from Formula (37-1) need not exceed $0.75\, Z I\, w_{px}$, but shall not be less than $0.35\, Z I\, w_{px}$.

When the diaphragm is required to transfer lateral forces from the vertical resisting elements above the diaphragm to other vertical resisting elements below the diaphragm due to offset in the placement of the elements or to changes in stiffness in the vertical elements, these forces shall be added to those determined from Formula (37-1).

C. Diaphragms supporting concrete or masonry walls shall have continuous ties or struts between diaphragm chords to distribute the anchorage forces specified in Section 2337 (b) 8. Added chords may be used to form subdiaphragms to transmit the anchorage forces to the main crossties.

D. Where wood diaphragms are used to laterally support concrete or masonry walls, the anchorage shall conform to Section 2337 (b) 8 above. In Seismic Zones Nos. 2, 3 and 4 anchorage shall not be accomplished by use of toenails or nails subject to withdrawal, nor shall wood ledgers or framing be used in cross-grain bending or cross-grain tension, and the continuous ties required by Item C above shall be in addition to the diaphragm sheathing.

E. Connections of diaphragms to the vertical elements and to collectors and connections of collectors to the vertical elements in structures in Seismic Zones Nos. 3 and 4, having a plan irregularity of Type A, B, C or D in Table No. 23-N, shall be designed without considering one-third increase usually permitted in allowable stresses for elements resisting earthquake forces.

F. In structures in Seismic Zones Nos. 3 and 4 having a plan irregularity of Type B in Table No. 23-N, diaphragm chords and drag members shall be designed considering independent movement of the projecting wings of the structure. Each of these diaphragm elements shall be designed for the more severe of the following two assumptions:

Motion of the projecting wings in the same direction.

Motion of the projecting wings in opposing directions.

EXCEPTION: This requirement may be deemed satisfied if the procedures of Section 2335 in conjunction with a three-dimensional model have been used to determine the lateral seismic forces for design.

APPENDIX B
FILTERING OF RELATIVE DISPLACEMENT HISTORIES

Corrected absolute acceleration, absolute velocity, and absolute displacement records were provided by the California Office of Strong Motion Studies for each of the tilt–up buildings studied [37,38,59,60,61,66, 67]. Relative displacements are typically used to interpret structural response, because the displacement of a building relative to its foundation is a measure of the distortions within the structure during the earthquake. However, digitizing, filtering, and integrating the measured acceleration records introduces noise [68]. Therefore, reliable values of relative displacement can not be calculated simply by subtracting the absolute displacement of the ground from the absolute displacement of the structure.

In an attempt to quantify the amplitude of the error introduced during the digitization process, Shakal and Ragsdale [68] digitized a straight line as if it were an acceleration trace. The digitized acceleration records were filtered and integrated to obtain absolute velocity and displacement records. The error introduced in the acceleration, velocity, and displacement records is plotted in Fig. B.1 as a function of the long–period filter cut–off period. The results indicate that errors introduced by the digitization process are likely to be on the order of 2 cm/sec^2 for the acceleration records. Errors in velocity and displacement waveforms depend on the frequency of the long–period filter cut–off and increase as the period of the filter cut–off increases. Noise introduced by the recording instrument has been ignored in this process, and the results should be considered to be a lower bound to the amplitude of the actual noise introduced [68].

An Ormsby filter was used during the processing of all the strong–motion data considered in this report [38]. The shape of the filter is shown in Fig. B.2. Frequency cut–offs are summarized in Table B.1 and were determined using an iterative procedure. Progressively shorter long–period filter cut–off periods were used to remove as much noise as possible while retaining as much signal as possible. Given this information, an estimate of the reliability of the displacement records can be made. For example, records measured in the Hollister warehouse during the Loma Prieta earthquake have a useable bandwidth between 0.12 and 23.6 Hz (0.042 and 8.40 sec) [38]. The long–period filter cut–off corresponds to approximately 1 cm or 0.4 in. of processing noise (Fig. B.1).

The procedure used to filter all the relative displacement data will be illustrated using the transverse structural displacement data recorded in the Hollister warehouse during the Loma Prieta earthquake. Channel 4 (located at the center of the roof) is used to represent structural displacements and Channel 7 (located at the center of the west wall) is used to represent the ground movement. Digitized absolute displacement records for the two channels are plotted in Fig. B.3(a) and the Fourier amplitude spectra are shown in Fig. B.3(b). Both plots indicate that the ground motion dominates the absolute displacement response at the roof. The structural vibrations observed between 8 and 16 sec in the structural displacement record correspond to the

peak in the Fourier amplitude spectra at approximately 1.1 Hz. This corresponds to the predominant frequency identified from the acceleration records (Table 5.2). The influence of the Ormsby filter may also be seen in Fig. B.3(b) where it is evident that the long–period response (frequencies less than 1.4 Hz) has been removed from both the ground and structural signals.

The relative displacement signal obtained by subtracting the ground displacement (Channel 7) from the structural displacement (Channel 4) at each time increment is shown in Fig. B.4(a) and the corresponding Fourier amplitude spectra is shown in Fig. B.4(b). Although the predominant frequency in the relative displacement history occurs at 1.1 Hz, it is clear that a significant amount of noise from the ground displacement is present. The long–period oscillations that occur after 30 sec in the relative displacement history also indicate the presence of noise.

A high–pass filter was used to remove the portion of the signal attributable to the ground motion. The shape of the filter is shown in Fig. B.5, and the frequency limits were selected using an iterative approach. The cut–off frequencies were increased until the amplitude of the filtered relative displacement response history tended toward zero at the end of the record. The resulting filtered relative displacement history is shown in Fig. B.6. Cut–off frequencies for the different earthquakes are presented in Table B.1.

As discussed in Chapter 5, the general shape of the unfiltered and filtered relative displacement records did not change appreciably for the transverse displacements measured near the center of the buildings. However, the nature of the filtered and unfiltered longitudinal relative displacements and transverse relative displacements measured at the top of the end walls were considerably different. In most cases, the maximum amplitude of the filtered relative displacements at these locations were of the same magnitude as the amplitude of the expected error shown in Fig. B.1. Therefore, only the transverse relative displacement data measured near the center of the buildings were considered to be reliable.

TABLE B.1 FILTER LIMITS USED TO PROCESS STRONG–MOTION RECORDS

Building and Earthquake	CSMIP Limits for Ormsby Filter (Fig. B.2)				Limits for High–Pass Filter (Fig. B.5)	
	f_{Lt} (Hz)	f_{Lc} (Hz)	f_{Ht} (Hz)	f_{Hc} (Hz)	f_1 (Hz)	f_2 (Hz)
Hollister Warehouse						
1984 Morgan Hill	0.08	0.16	23	25	0.20	0.50
1986 Hollister	0.10	0.20	23	25	0.20	0.50
1989 Loma Prieta	0.07	0.14	23	25	0.20	0.50
Redlands Warehouse						
1986 Palm Springs	0.25	0.50	23	25	1.10	1.25
Milpitas Industrial Building						
1988 Alum Rock	0.30	0.60	23	25	2.0	2.5
1989 Loma Prieta	0.07	0.14	23	25	2.0	2.5

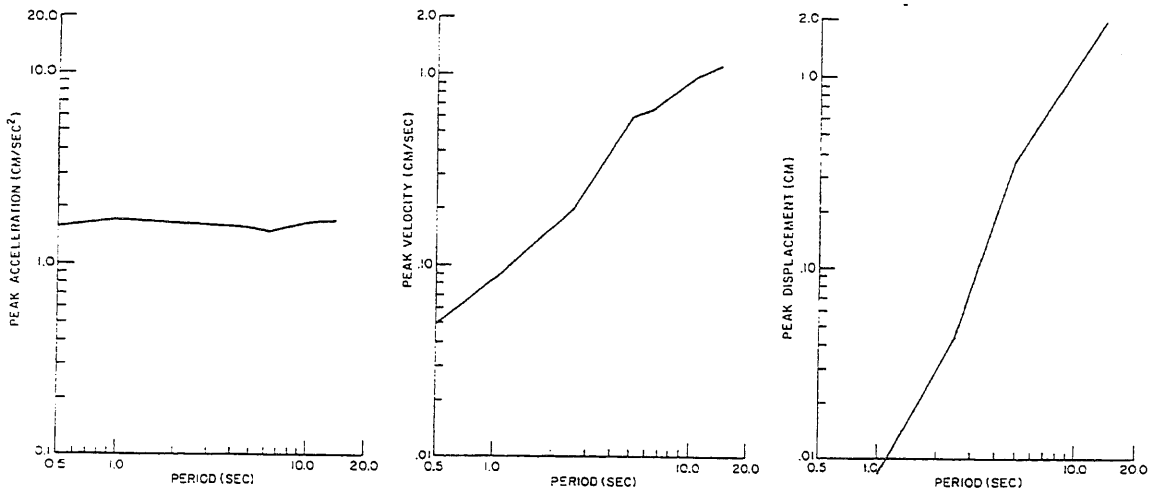

Fig. B.1 Estimate of processing noise present in corrected strong–motion records [68].

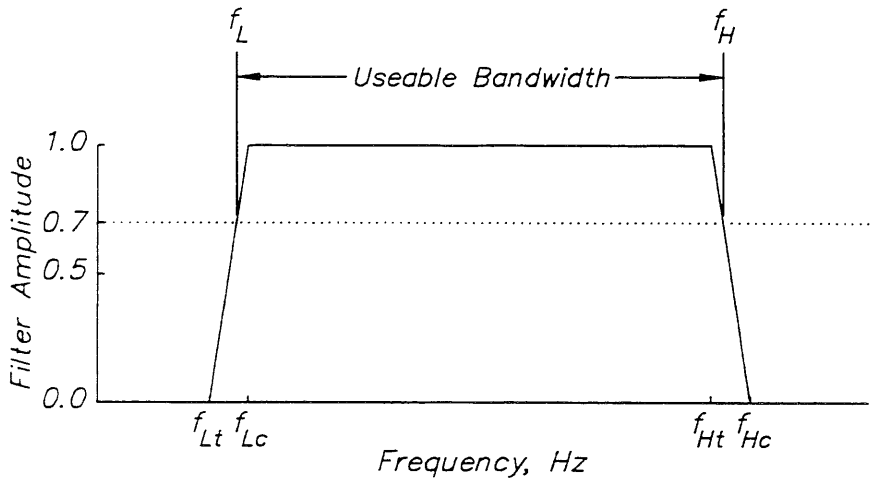

Fig. B.2 Ormsby filter used to process CSMIP records [38].

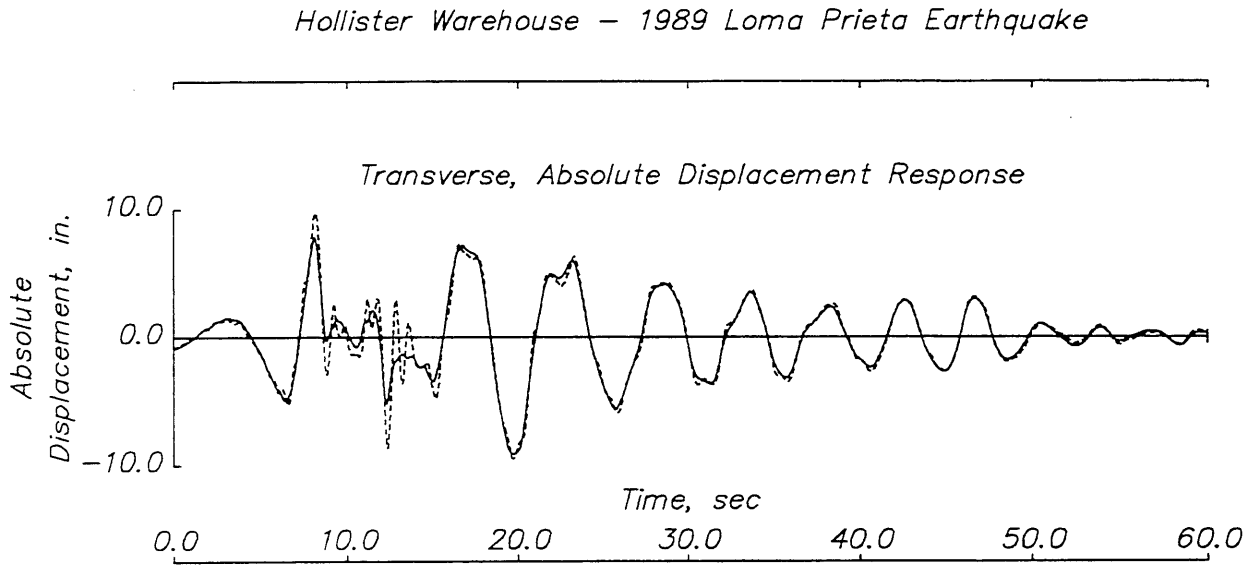

(a) Transverse displacement history.

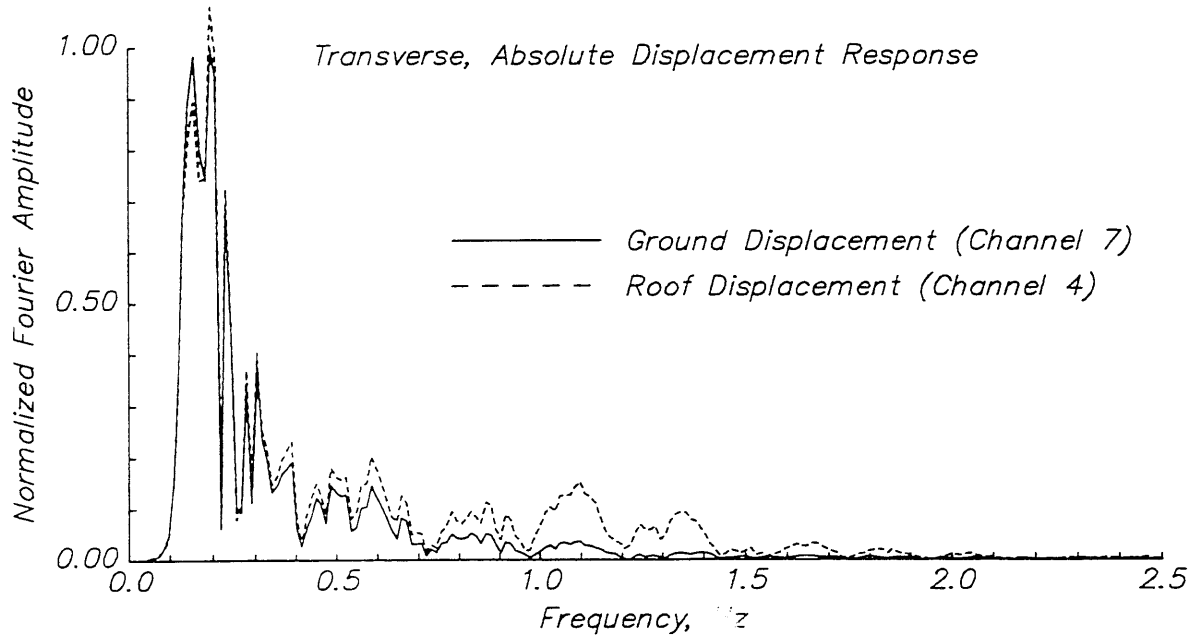

(b) Fourier amplitude spectrum.

Fig. B.3 Absolute displacement response.

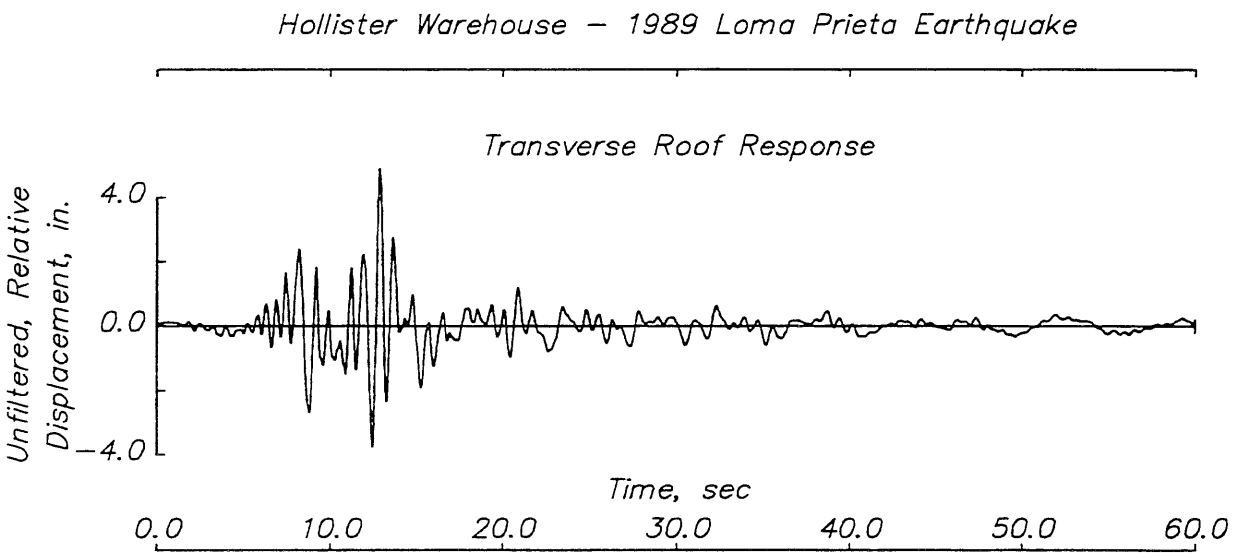

(a) Transverse displacement history.

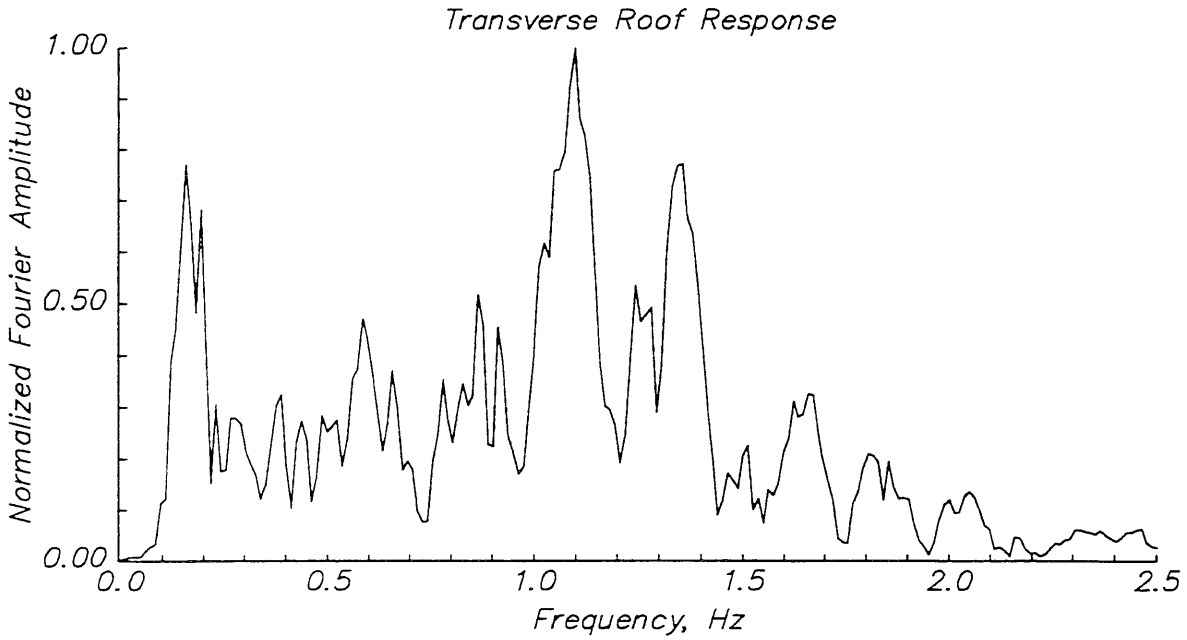

(b) Fourier amplitude spectrum.

Fig. B.4 Unfiltered, relative displacement response at the roof.

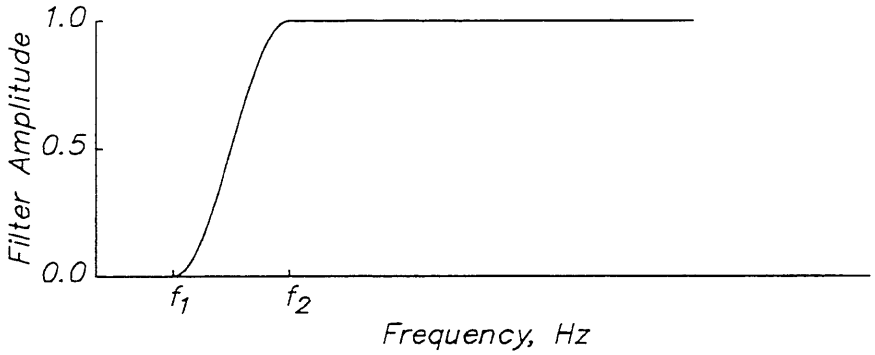

Fig. B.5 High–pass filter used to calculate relative displacement response.

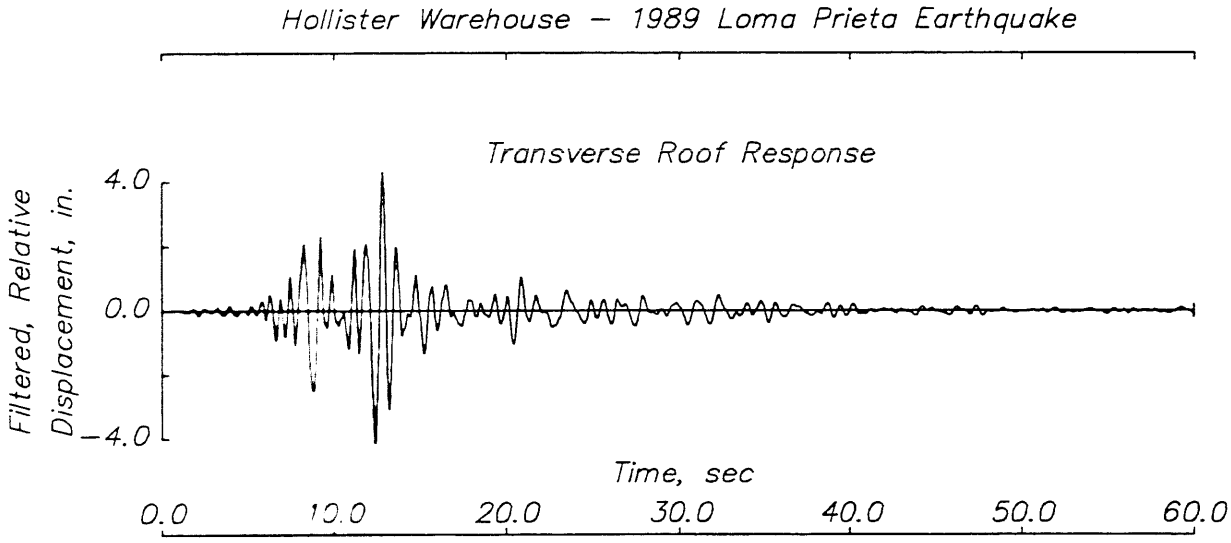

Fig. B.6 Filtered, relative displacement response at the roof.